Selective synthesis of multicomponent crystals using mechanochemistry and sublimation

by Jean Lombard

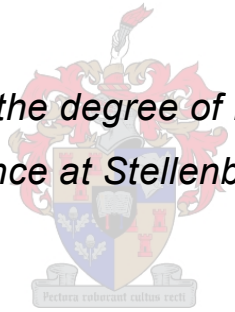

Dissertation presented for the degree of Doctor of Philosophy in the Faculty of Science at Stellenbosch University

Supervisor: Dr Tanya le Roex

Co-supervisor: Prof. Delia A. Haynes

December 2020

Declaration

By submitting this dissertation electronically, I declare that the entirety of the work contained therein is my own, original work, that I am the sole author thereof (save to the extent explicitly otherwise stated), that reproduction and publication thereof by Stellenbosch University will not infringe any third party rights and that I have not previously in its entirety or in part submitted it for obtaining any qualification.

This dissertation includes 3 original unpublished publications. The development and writing of the papers were the principal responsibility of myself and, for each of the cases where this is not the case, a declaration is included in the dissertation indicating the nature and extent of the contributions of co-authors.

Abstract

The aim of this thesis is to demonstrate how careful control of the crystallisation technique used can lead to selective multicomponent crystal formation. Multicomponent materials are often crystallised from solution; however, with this study we were interested in exploring less conventional solid-state and gas-phase methods, such as mechanochemistry and sublimation.

In the first study investigations of two systems are reported: succinic acid with hexamethylene-tetramine, and oxalic acid with 4,4'-bipyridine. Each of these sets of molecules forms both salts and co-crystals. The majority of these multicomponent forms have previously been crystallised from solution, and in this study it was found that they can also be formed mechanochemically, and from the gas phase. The formation of molecular salts by co-sublimation of neutral components was unexpected and has not been reported before. Once formed, these multicomponent crystals could also be re-sublimed so that mixtures of different crystal forms could physically be separated. This work raises important questions about the processes occurring in the gas phase during sublimation – preliminary experiments indicate that ions (or rather clusters of ions) may be present in the gas phase during the sublimation of these salts.

The second study aimed to determine the effect of solvent type and volume on the selectivity between hydrogen- and halogen-bonded co-crystals. A competition study was carried out between four analogous co-crystals containing a ditopic acceptor molecule, 1,2-bis(4-pyridyl)ethane, and either a hydrogen-bond or halogen-bond donor molecule. A number of different crystallisation methods were used, including sonic slurry crystallisation, neat grinding, liquid-assisted grinding, and co-sublimation. We observed a preference for the halogen-bonded co-crystal when polar solvents were used (which was also previously observed), but this selectivity became much less pronounced as the amount of solvent was reduced. Competition experiments carried out by vacuum sublimation exclude all solvent, and it was found that all selectivity for one form over another was eliminated in sublimation co-crystallisation. The amount of solvent used, and not just its polarity, is therefore critical when co-crystallisation is attempted.

The third study describes the formation of a range of multicomponent crystals using mechanochemistry and sublimation, in order to compare these two crystallisation methods and determine the general capability and versatility of co-sublimation. Co-crystals, salts, and their polymorphs are discussed, as well as problems that can arise due to sublimation temperature differences, isomerisation, and degradation. Co-sublimation is shown to be a valuable co-crystallisation technique for the discovery and identification of new multicomponent materials.

In its entirety this thesis demonstrates the important effect that crystallisation technique has on multicomponent crystal formation. In our opinion, a multi-technique approach which includes solid-state and gas-phase techniques is the best course of action when working with complex or problematic systems.

Opsomming

Die doel van hierdie tesis is om te demonstreer hoe noukeurige beheer oor die kristallisasie tegniek wat gebruik word kan lei tot die selektiewe vorming van multikomponent kristalle. Multikomponent materiale word gereeld gekristaliseer vanuit oplossing, maar met hierdie studie het ons daarin belang gestel om minder konvensionele vastestoffase en gasfase metodes, soos meganochemie en sublimasie, te ondersoek.

In die eerste studie word twee sisteme gerapporteer: butanoësuur met heksametieleentetramien, en oksaalsuur met 4,4'-bipiridien. Elkeen van hierdie stelle molekules vorm beide soute en ko-kristalle. Die meerderheid van hierdie multikomponent vorms is voorheen gekristalliseer vanuit oplossing, en in hierdie studie is daar gevind dat hulle ook meganochemies en vanuit die gas fase gevorm kan word. Die vorming van molekulêre soute deur die ko-sublimasie van neutrale komponente was onverwags en is nog nie voorheen gerapporteer nie. As die multikomponent kristalle eers gevorm is, kon hulle ook hersublimeer sodat mengsels van verskillende kristalvorms fisies geskei kon word. Hierdie werk stel belangrike vrae bloot omtrent die prosesse wat plaasvind in die gas fase gedurende sublimasie – voorlopige eksperimente dui aan dat ione (of eerder ioon bondels) dalk in die gas fase voorkom tydens die sublimasie van hierdie soute.

Die tweede studie beoog om te bepaal wat die effek van die tipe en volume oplosmiddel is op die selektiwiteit tussen waterstof- en halogeen-gebinde ko-kristalle. ’n Studie aangaande hierdie kompetisie is uitgevoer tussen vier analoë ko-kristalle wat elk ’n ditopiese akseptor molekule, 1,2-bis(4-piridiel)etaan, bevat asook ’n waterstof-bindende of halogeen-bindende donor molekule. ’n Aantal verskillende kristallisasie metodes is gebruik, insluitende soniese kristallisasie, droë- en vloeistof-vergemaklikde meganochemie en ko-sublimasie. Ons het ’n voorkeer vir halogeen bindings waargeneem wanneer polêre oplosmiddels gebruik word (wat reeds voorheen rapporteer is), maar gevind dat hierdie selektiwiteit veel minder opmerkend is wanneer die hoeveelheid oplosmiddel verminder word. Kompetisie eksperimente wat uitgevoer is deur vakuum sublimasie sluit alle oplosmiddel uit, en daar is gevind dat alle selektiwiteit vir een vorm bo ’n ander dus geëlimineer word

gedurende ko-sublimasie. Die hoeveelheid oplosmiddel wat gebruik word, en nie net die polariteit nie, is dus belangrik wanneer ko-kristallisasie uitgevoer word.

Die derde studie beskryf die vorming van ’n reeks multikomponent kristalle deur gebruik te maak van meganochemie en sublimasie sodat hierdie twee kristallisasiemetodes vergelyk kan word, sodat die algemene bruikbaarheid en veelsydigheid van ko-sublimasie bepaal kan word. Ko-kristalle, soute, en hul polimorfs word bespreek, sowel as probleme wat kan ontstaan na aanleiding van verskille in sublimasie temperature, isomerisasie, en degradasie. Ko-sublimasie is tentoongestel as ’n nuttige ko-kristallisasie tegniek vir die ontdekking en identifikasie van nuwe multikomponent materiale.

As ’n geheel demonstreer hierdie tesis die belangrike effek wat kristallisasie tegniek op multikomponent kristal formasie het. In ons opinie is ’n benadering wat ’n verskeidenheid tegnieke insluit (beide vastestoffase en gasfase tegnieke) die beste plan van aksie wanneer daar met komplekse en problematiese sisteme gewerk word.

Acknowledgements

I would like to thank my supervisors, Dr Tanya le Roex and Prof. Delia Haynes for their complete support throughout this project. I am grateful for your guidance and persistent optimism, and the opportunities you have provided for me to learn and grow.

I would like to extend my gratitude towards the members of the Supramolecular Materials Research Group. To Dr Vincent Smith, Prof. Catharine Esterhuysen, Prof. Len Barbour, Jan Costandius, Thalia Carstens, Oluwatoyin Akerele, Lisa van Wyk, Alan Eaby, and everyone who contributed with incredibly helpful discussions regarding my research. A special thankyou is extended to Dr Isabella Claassens, Dr Monica Clements and Dewald van Heerden for their tremendous support both socially and scientifically. I would also like to thank Heinrich Laker, Marisa Strydom and Dr Nikita Chaudhary for a fun and productive lab environment, and Dr Leigh Loots for keeping the diffraction lab running smoothly and assisting with those difficult crystal structures.

I am grateful for my family and friends for the support, especially for my mother who always made an effort to try and understand why we care about crystals.

Finally, I would like to thank the University of Stellenbosch for providing the necessary facilities and the Wilhelm Frank Scholarship Foundation for funding.

Publications

Not part of this work

Lombard, J.; Loots, L.; Haynes, D. A.; le Roex, T. Polymorphism and Host-Guest Chemistry of a Phenylpyridine-Functionalized Zwitterion, *Cryst. Growth Des.* **2020**, *20* (3), 1503–1511. DOI: 10.1021/acs.cgd.9b01151

Part of this work

Lombard, J.; Smith, V. J.; le Roex, T.; Haynes, D. A. Crystallisation of organic salts by sublimation: salt formation from the gas phase, *Manuscript under review*.

Lombard, J.; le Roex, T.; Haynes, D. A. Competition between hydrogen- and halogen bonds: the effect of solvent volume, *Manuscript under review*.

Lombard, J.; Haynes, D. A.; le Roex, T. Assessment of co-sublimation for the formation of multicomponent crystals, *Manuscript under review*.

Conferences

Indaba 9 – Modelling of Structures and Properties
Skukuza, Kruger National Park, South Africa, 2 – 7 September 2018
Poster and flash oral presentation: *Selective crystallisation of salts and co-crystals using mechanochemistry and sublimation*

CSCR Symposium 2020 – Centre for Supramolecular Chemistry Symposium 2020
University of Cape Town, South Africa, 24 January 2020
Oral presentation: *Selective preparation of multicomponent crystals using mechanochemistry and sublimation*

ISXB4 – 4th International Symposium on Halogen Bonding
Stellenbosch, South Africa, 22 – 27 March 2020 (Conference postponed to 2 – 6 November 2020)
Selected to give an oral presentation: *Selective crystallisation of halogen- and hydrogen-bonded co-crystals: The central role of solvent volume*

Abbreviations

23LUT	2,3-Lutidine
3PIC	3-Picoline
4PP	4-Phenylpyridine
ASU	Asymmetric unit
BA	Benzoic acid
BPY	4,4'-Bipyridine
CAF	Caffeine
CAHB	Charge-assisted hydrogen bond
$CHCl_3$	Chloroform
CIF	Crystallographic Information File
CSD	Cambridge Structural Database
DCM	Dichloromethane
DFT	Density functional theory
DSC	Differential scanning calorimetry
FA	Fumaric acid
GA	Gallic acid
HB	Hydrogen bond
HMT	Hexamethylenetetramine
INAM	Isonicotinamide
LAG	Liquid-assisted grinding
MA	Maleic acid
MS	Mass spectrometry
NA	Nicotinic acid
NAM	Nicotinamide
NMR	Nuclear magnetic resonance
OA	Oxalic acid
PIP	Piperazine
PXRD	Powder X-ray diffraction
PYG	Pyrogallol
PYR	Pyridine
SA	Succinic acid
SCXRD	Single-crystal X-ray diffraction
SS	Sonic slurry
TGA	Thermogravimetric analysis
THE	Theophylline
XB	Halogen bond

Atomic colour key

Carbon

Hydrogen

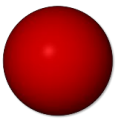

Oxygen

Nitrogen

Iodine

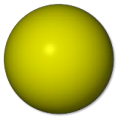

Fluorine

Table of Contents

CHAPTER 1

General Introduction

For the results presented in this thesis to be fully appreciated, it is essential that a number of concepts are introduced, and several terms defined. Furthermore, a study of the recent literature is paramount. The research field of solid-state supramolecular chemistry relies heavily on the study of intermolecular interactions. Among these, hydrogen bonding and halogen bonding play vital roles during the aggregation of organic molecules – these interactions will be discussed in detail. Molecular assembly can lead to the formation of crystals, either containing a single type of molecule, or a variety. The latter, the so-called multicomponent crystals, can be grouped into three main classes, namely co-crystals, salts, and solvates. In these studies, co-crystals and salts take centre stage, and will be discussed at length. Consequently, we will devote significant attention to the ionisation of organic molecules as well as the proton transfer required for this to occur. The focus of our work is not only on the existence of multicomponent crystals, but on the routes of their formation. Therefore, the techniques used for multicomponent crystallisation will be discussed in detail, as well as potential ways of manipulating these methods to obtain control over the crystalline materials formed. Lastly, the aims of this thesis will be stated, followed by an outline of the chapters to follow.

1.1 Solid-state supramolecular chemistry

Supramolecular chemistry is the study of the assembly of molecules. When working in the solid state, the design and assembly of functional crystalline solids is the focus point: a field of research often called crystal engineering.[1] This type of solid-state supramolecular chemistry is about the study of intermolecular interactions and how these interactions govern crystal packing. The resultant three-dimensional structures (and all the forces involved) affect the properties of crystalline solids. Researchers can use knowledge of such structure-property relationships for the directed design of new and tuneable materials and devices. They hope to impart these new materials with specific desired properties; however, that is still easier said than done.[2]

1.2 Intermolecular interactions

Crystal engineering relies on our knowledge of molecular recognition and intermolecular interactions. The energetics, directionality and selectivity of these intermolecular interactions, along with other factors such as the geometry of the molecules and the mechanics of crystal growth, sustain and direct crystal packing. Specific pairwise interactions (i.e. functional groups that interact via a frequently observed intermolecular interaction) are called supramolecular synthons.[3] Synthons can be thought of as common examples of intermolecular interactions which should be kept in mind when trying to predict how molecules will interact in the solid state. Understanding intermolecular interactions means they can be exploited for bottom-up design.

Various types of non-covalent intermolecular interactions exist, differing in strength, depending on the molecules and atoms that are involved. These include van der Waals interactions, hydrogen bonds, ionic interactions, halogen bonds, π-π interactions, cation/anion-π interactions, etc. These interactions are all significantly weaker and less stable than covalent bonds, and so they are reversible. Crystal packing is the result of many weak interactions working together; however, the strongest types of intermolecular interactions between organic molecules, i.e. those that generally direct crystal packing, are hydrogen bonds[4] and halogen bonds.[5]

1.2.1 Hydrogen bonding

The hydrogen bond (HB) is generally considered to be the most common and well-understood type of interaction between molecules. They are abundant in nature, where they can be found in DNA, proteins, and of course in water (Figure 1.1). A hydrogen bond forms when a hydrogen atom (covalently bonded to a more electronegative atom, D) interacts with another atom (A), which is usually a Lewis base (e.g. oxygen, nitrogen, sulphur, phosphorus), or a π system (Figure 1.1).[4,6]

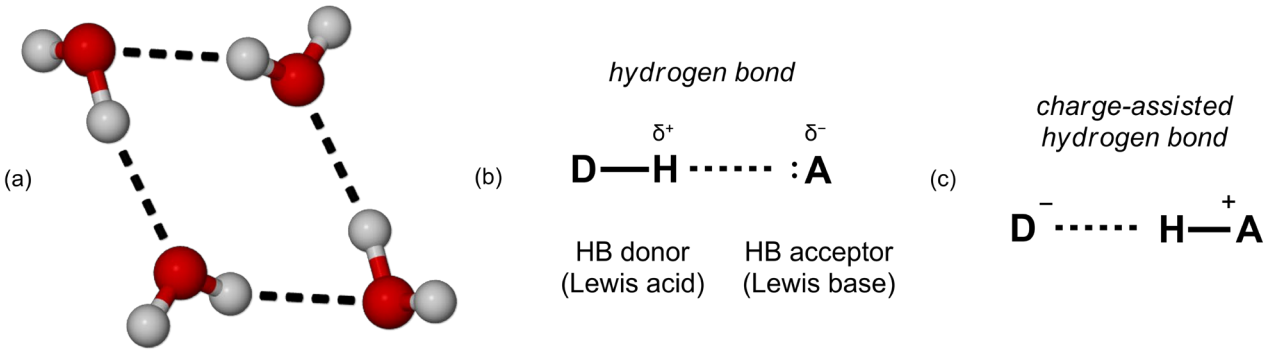

Figure 1.1. Schematic representation of (a) a cluster of four hydrogen-bonded water molecules, (b) a hydrogen bond and (c) a charge-assisted hydrogen bond. Hydrogen bonds are indicated with dashed lines.

Hydrogen bonds can direct molecular association because of their directionality and strength. The most familiar types of hydrogen bonds are O−H···N (~30 kJ mol^{-1}), O−H···O (~20 kJ mol^{-1}) and N−H···N (~15 kJ mol^{-1}) interactions (Figure 1.2). These are of medium strength with distances ranging from about 2.6 Å – to 3.1 Å (from D to A) and angles between approximately 145° and 180° (∠DHA).[7] In some cases, when it is an acid and a base that are interacting, the hydrogen atom is transferred from the acid to the base, which strengthens the interaction. These interactions are specifically called charged-assisted hydrogen bonds (CAHBs) (Figure 1.1). Weaker interactions are also very common. Hydrogen bonds of the type C−H···O, C−H···N and O−H···π are typically 5 – 15 kJ mol^{-1}, are longer than 3 Å, and deviate more from linearity.[8] Very strong hydrogen bonds also exist, such as F−H···F$^-$, but these are not commonly observed in organic molecular crystals.[7]

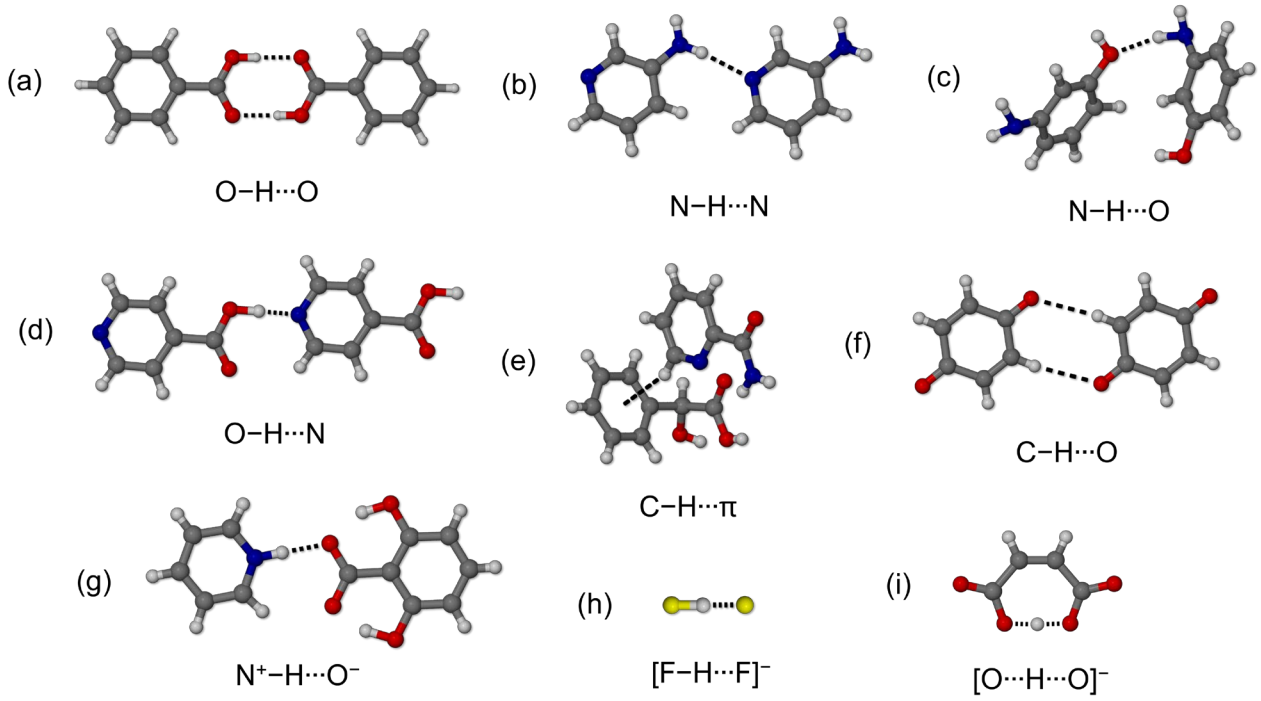

Figure 1.2. Some examples of moderate hydrogen bonds (a – d), weak hydrogen bonds (e – f), a CAHB (g) and very strong hydrogen bonds (h – i), that can be observed in crystal structures deposited in the Cambridge Structural Database (CSD). The CSD reference codes for the structures are as follows: (a) BENZAC01[9], (b) AMIPYR[10], (c) MAMPOL[11], (d) ISNICA[12], (e) HOGGOB[13], (f) BNQCLP[14], (g) LEZJIH[15], (h) DEHSOY[16] and (i) GUXBIL[17].

1.2.2 Halogen bonding

A halogen bond (XB) is an attractive interaction between an electron-rich Lewis base (the XB acceptor atom, A) with the electrophilic region of a halogen atom (the XB donor atom, X).[5] This electrophilic region is called a σ-hole, which is a localised area of decreased electron density opposite

the halogen atom's covalent bond, along the extension of the bond.[18] This area of positive electrostatic potential is what interacts with the basic acceptor atom to form the halogen bond (Figure 1.3).

A halogen atom has both an electrophilic region (σ-hole) and a nucleophilic region (electronegative equatorial belt). Naturally, these regions can attract each other to form halogen-halogen interactions in the solid state (Figure 1.3). Such an X···X interaction where the σ-hole of one halogen atom approaches another side-on is called a type II interaction, which is considered to be a true halogen bond.[19] Another type of X···X interaction is also observed in crystal structures where two halogen atoms approached each other symmetrically. Such type I interactions are not considered true halogen bonds, but dispersion interactions arising from close packing.[20] They are usually associated with crystallographic inversion centres.[19]

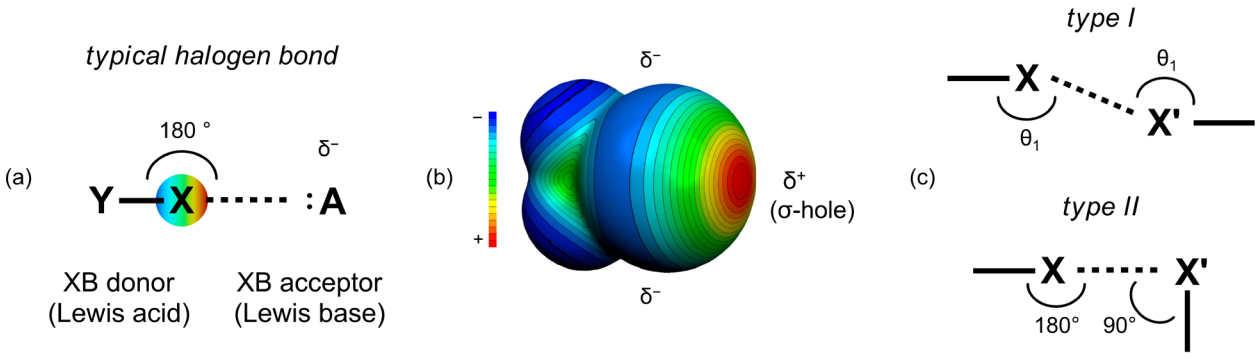

Figure 1.3. (a) Schematic representation of a halogen bond between a halogen atom, X, and an electron-rich Lewis base, A. X = a halogen atom; Y = C, N, O or X; A = N, O, S, Se, Cl^-, Br^-, I^-, etc. (b) The molecular electrostatic potential surface at 0.001 electrons $Bohr^{-3}$ for CF_3I is shown as an example, indicating the position of the σ-hole in red, as well as the electronegative equatorial belt around the atom (blue) (image adapted from Clark *et al.*[21]). (c) Halogen-halogen interactions can be classified as type I or type II interactions (image adapted from Gilday *et al.*)[19]. All angles are approximate values.

In general, halogen bonds are very directional. In fact, XBs tend to be even more directional than HBs because the position of the σ-hole is fixed along the axis of the covalent bond.[18] The interaction forms directly along the line of the Y−X covalent bond and the lone pair of the halogen bond acceptor atom, with the YXA angle being close to 180° (where X is the halogen atom and A is the XB acceptor atom).[22]

There are certain requirements for the formation of halogen bonds that are strong enough to contribute to crystal packing. Specifically, the strength of a halogen bond depends on the XB donor atom, the XB acceptor atom, as well as the surrounding atoms. Larger halogen atoms are more polarizable and so a larger σ-hole can form. Therefore, larger halogen atoms, such as iodine, can form strong halogen bonds, while smaller halogen atoms like fluorine do not participate in these

interactions.[21] The electron-accepting ability of the halogen atom is further improved by nearby (covalently bonded) electron withdrawing groups or atoms, such as fluorine.[23] However, recent work has shown that the sp-hybridisation of the atom covalently bonded to the halogen atom can have an even larger effect.[24] Halogen atoms covalently bonded to an sp^2 or sp carbon atom form stronger XB interactions, with the following trend found in donor ability: C(sp)−X > C(sp^2)−X > C(sp^3)−X. Lastly, the more basic the acceptor atom, the stronger the halogen bond.[25,26] Halogen bonds are therefore very tuneable. When all of the abovementioned conditions are met, very strong halogen bonds are able to form.[27]

Interactions involving halogen atoms are perhaps less well known than classical hydrogen bonding, but halogen bonds are analogous to hydrogen bonds. Both of these interactions form by nucleophilic-electrophilic interaction and can be similar in strength, geometry and directionality. Because these interactions are so similar, they often compete for the same interaction sites during crystallisation – which has led to a number of competition studies.[28–35] In some of these cases the halogen bond was even found to be stronger than the hydrogen bond.[32,33] However, the forces governing the formation of XBs and HBs are not identical. Theoretical studies show that hydrogen bonds are more electrostatic in nature, while halogen bonds have larger dispersive and inductive components.[36,37] Halogen- and hydrogen atoms are also very different in size, which means they can on occasion play different roles in crystal structures without competing with each other. Riel *et al.* recently reported an interesting case of HB and XB cooperativity, which they call hydrogen-bond enhanced halogen bonds.[38,39] In their work they show how an intramolecular hydrogen bond to the electron rich equatorial belt of a halogen atom can further polarise the halogen atom to improve the strength and stability of the halogen bond it forms through its σ-hole (Figure 1.4).

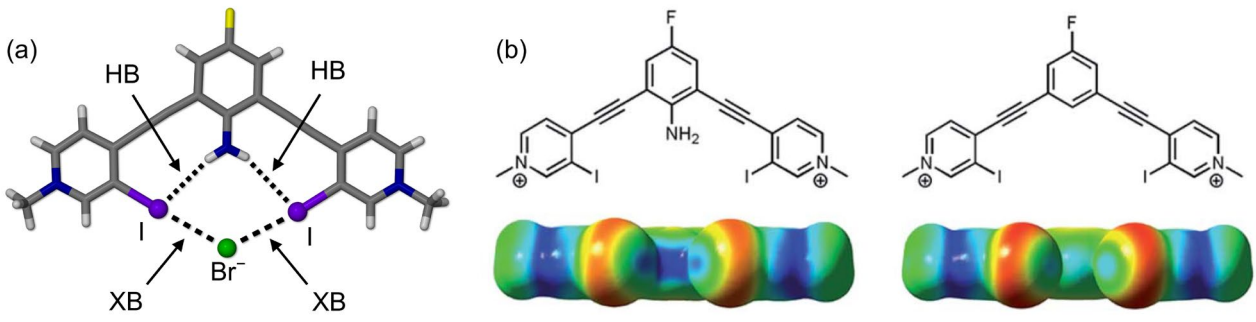

Figure 1.4. (a) A bidentate molecule halogen bonds to a bromide ion with the help of intramolecular hydrogen bonds (CSD Refcode: HIHYIJ[38]). (b) Electrostatic potential (ESP) maps showing the effect that a hydrogen-bonding group has on the potential of a halogen atom at the σ-hole. Blue = electron deficient; red = electron rich. Image adapted from Riel *et al.*[38]

1.3 Crystal growth

When enough molecules interact with each other, they may eventually start to crystallise, i.e. form solid materials with long-range periodic ordering. Intermolecular interactions are the most obvious structure-directing influences; however, crystal growth is a process and not simply a result. Crystal formation depends on synthons and molecular geometry and flexibility, but also on nucleation,[40] and the mechanisms and kinetics of molecular aggregation.[41]

The complexity of the situation becomes even more apparent when considering crystal growth phenomena such as polymorphism. Molecules that are identical in solution can crystallise into different solid-state forms (polymorphs), with different packing or connectivity, and different properties.[42] Furthermore, when dealing with mixtures of molecules these can potentially interact with each other as well, and crystallise together to form a variety of multicomponent crystals.

1.4 Multicomponent crystals

A multicomponent crystal forms when two or more different chemical components are contained in a single crystalline material. Multicomponent crystals are of interest as they can have different physicochemical properties compared to their constituent species. This is partly because each component confers some of its distinctiveness to the material, but also because even slight differences in the 3D arrangement of molecules in solids can change their behaviour. Therefore, crystallising different molecules together can potentially be used to improve the stability and efficacy of solid-state materials such as pharmaceuticals,[43] agrochemicals,[44] pigments,[45] and explosives,[46] without necessarily affecting the activity of these compounds. For example, the stability, solubility, bioavailability and compressibility of drugs can potentially be improved by forming a multicomponent crystal.[43,47–50] Multicomponent crystal formation also affects intellectual property and patent law, as compounds are being modified into new materials.[51] Additionally, on a fundamental level, the study of multicomponent crystals leads to an improved understanding of supramolecular interactions and molecular recognition.[52]

1.4.1 Classification of multicomponent crystals

Multicomponent crystals can contain any type of chemical entity, be it neutral molecules, ions or solvent molecules. Unfortunately, there is still much debate as to the exact naming system that should be used for multicomponent crystals;[53–55] however, an in-depth discussion is not relevant to this thesis. The simple naming conventions to be used will be defined below (Figure 1.5).

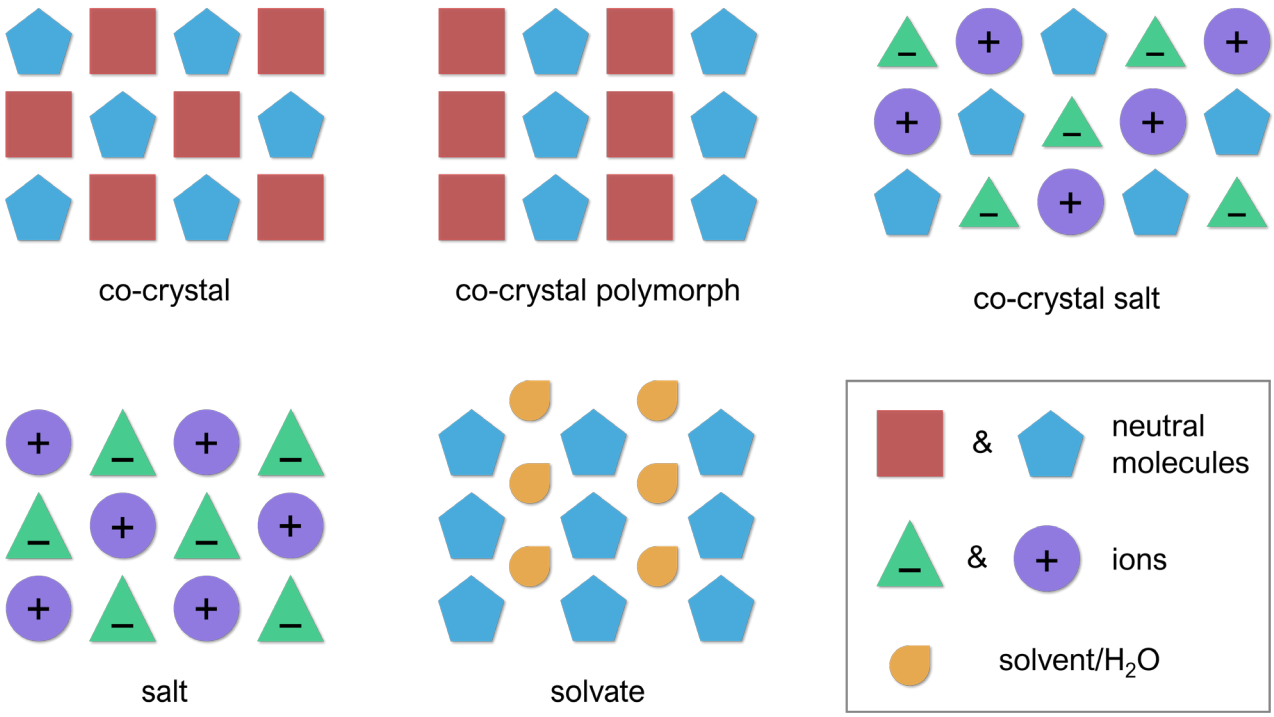

Figure 1.5. Visual representation of the different multicomponent crystals that appear in this thesis. Note that in the case of a co-crystal salt, the neutral molecule and one of the ions are often derivatives of one another, for example succinic acid and succinate.

When two or more neutral (solid) organic molecules are combined into one crystalline material in a definite stoichiometric ratio, they form a co-crystal.[56] The constituents of such a co-crystal are called coformers (co-crystal formers or sometimes co-crystallising agents), and the process called co-crystallisation. Most co-crystals consist of only two different molecules, but ternary and quaternary co-crystals are known to exist as well.[57] Coformers are generally held together by intermolecular interactions, and form when the interactions between different molecules are stronger than the interactions needed to form the homomeric products.[58] It should be noted that a specific combination of coformers can form more than one type of co-crystal, each with distinct packing. These forms can have the same stoichiometry (in which case they are polymorphs), or the stoichiometry can be different.

When the components of a co-crystal are charged, they are called salts. Molecular organic salts are similar to co-crystals, except for the transfer of a hydrogen atom from one molecule to the other (from acid to base), which changes the ionisation states in the system. This means that the number of molecule combinations that are able to form salts when co-crystallised is limited, as they need to have ionisable groups. Co-crystals do not have this requirement, which is why they have recently been receiving more attention. However, the reasons behind wanting to form salts and co-crystals are the same.

Some multicomponent materials contain both neutral and charged molecules. We will use the convention proposed by Grothe *et al.*, which defines a complex containing one or more neutral molecules with two or more ions (but no solvent molecules), a *co-crystal salt* (Figure 1.6).[55] Such mixed complexes have also been called ionic co-crystals;[59] however, some sources use this term exclusively to refer to materials containing inorganic ions,[60] so this phrase will not be used further.

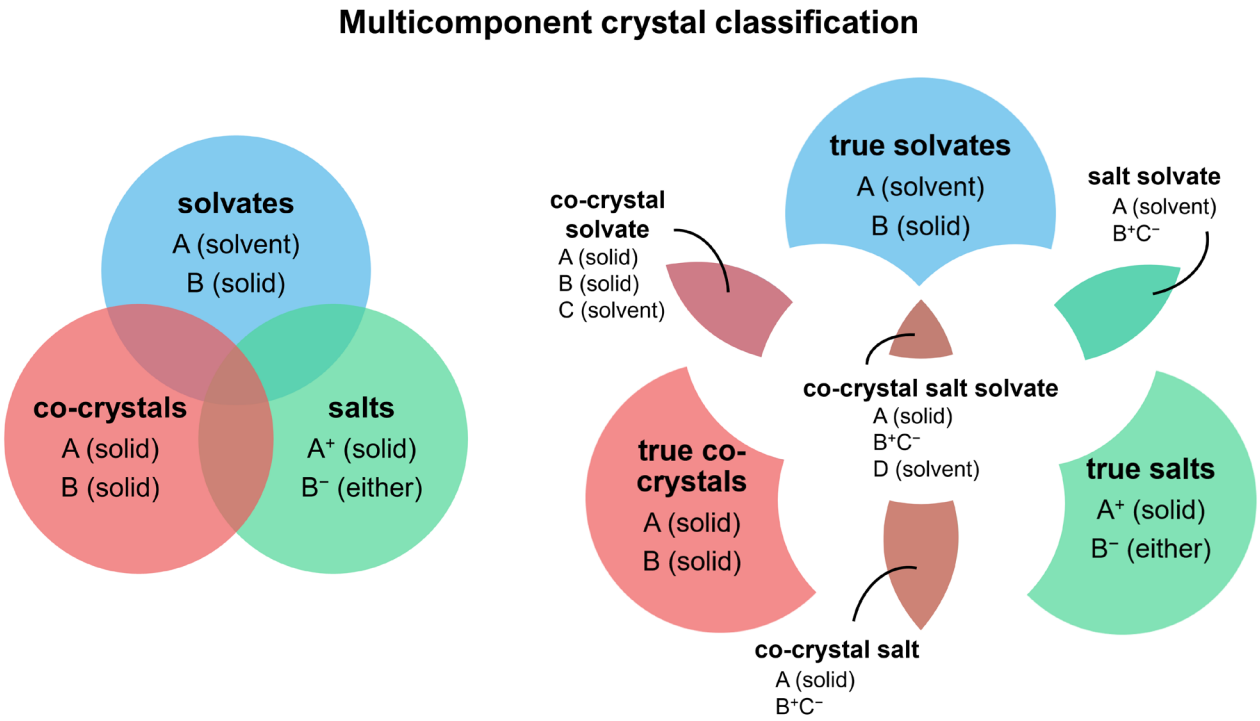

Figure 1.6. The three main classes of multicomponent crystals, co-crystals, salts and solvates form seven subclasses, including co-crystal salts which contain both charged and neutral molecules. Figure reproduced from Grothe *et al.*[55]

Crystals are often formed in the presence of a solvent. These solvent molecules will frequently be included into the crystal to form another type of multicomponent crystal, called a solvate.[61] If such an inclusion complex contains water molecules, the product is instead called a hydrate. Within the crystal structure of a solvate (or hydrate), the solvent molecules (also called guests)[62] usually reside within pockets or channels, where they can potentially form intermolecular interactions with themselves, or with the other molecules. However, these interactions can be very weak, and some solvents are included simply due a size and shape fit.[61] Solvent molecules can be included into molecular materials, co-crystals and salts (Figure 1.6).

1.4.2 Salts versus co-crystals

Some combinations of molecules habitually only form salts, and others only co-crystals. This is often related to the crystalline environment, which includes the acidity and basicity of the coformers. It is, to some extent, possible to predict whether a salt or a co-crystal will form based on pK_a values.[63] The pK_a rule[64] states that molecules with a pK_a difference larger than 4 (ΔpK_a = pK_a[protonated base] – pK_a[acid]) will likely form a salt when combined. When ΔpK_a is smaller than −1, a co-crystal is likely to form. However, in the intermediate range, $-1 < \Delta pK_a < 4$, either a salt or a co-crystal can technically form, and no prediction can be made. The rule is quite simplistic and serves best only as a general guideline – reports have shown it to be inaccurate in some cases.[65–67] The main reason why the pK_a rule sometimes fails is because pK_a values are generally determined in aqueous media, which is often not the medium used for crystallisation. For example, the drug Ephedrine has a pK_a of 9.74 in water, but 8.74 in methanol. On the other hand, acetic acid has a pK_a of 4.76 (in water) or 9.76 (in methanol). When these two molecules are combined they have a pK_a difference of 4.98 or −0.97, depending on the solvent used, which is a large variance.[68] Generally, the pK_a rule works well when the pK_a values of the acid and base are very different so that combinations of molecules clearly fall into the salt or co-crystal category. It is in the intermediate region where ionisation is not so clear cut, and in fact, some combinations of molecules that fall in this region can crystallise as both a salt and a co-crystal.

1.4.3 Does ionisation matter?

Co-crystals and salts have been described as simply being on opposite ends of a continuum of the same class of materials, where the one end of the scale experiences complete proton transfer and the other end, none.[69] Solids can therefore fall anywhere on the continuum, depending on the degree of proton transfer. It has been suggested that the nature of the interaction is not important enough to classify salts and co-crystals as different materials.[54] The difference between a co-crystal and a salt is seemingly only the slight shift of one hydrogen atom (from the acid to the base) and one may expect their crystal structures to be very similar if they contain the same molecules. Steiner *et al.* reports such a case where a salt and a co-crystal can be interconverted by changing the temperature so that the acidic hydrogen atom moves from one molecule to the other (the atom merely shifts by 0.1 Å between 200 K and 20 K).[70] The salt and co-crystal appear to be the same material.

While the distinction between co-crystals and salts may occasionally appear artificial, it is not always the case. The forces exerted by ions are different than those surrounding neutral atoms/molecules, and so they cannot always play exactly the same role in a crystal structure.[71] Co-

crystals and salts (and co-crystal salts) constructed from the same pairs of molecules can pack very differently. Some co-crystals and salts have different stoichiometries, even when they contain the same sets of molecules.[72–75] These forms can therefore also have different properties. A single pair of molecules can even form both a salt and a co-crystal with the same stoichiometry, but which packs differently (salt-co-crystal polymorphs).[76–82] The reason differently-charged multicomponent crystals (containing the same molecules) pack differently can be approached from two sides: either the change in ionisation affects the crystal packing, or the crystalline environment directs the ionisation.

Aakeröy *et al.* describes the first scenario in their 2007 paper.[83] They postulate that when an acidic functional group is ionised (e.g. a carboxylate anion), there is an excess of charge which is often not satisfied by simply forming a single hydrogen bond. Instead, this electron-rich site prefers to interact with an additional hydrogen-bond donor, which naturally affects the crystal packing, and possibly the stoichiometry, of the material. On the other hand, neutral molecules are less prone to do this, and a carboxylic acid group will most likely form just one hydrogen bond (or at least fewer than the anion). Therefore, the electronics in the system can lead to the salt and co-crystal structures being different. Mohamed *et al.* demonstrates such structural differences computationally using crystal structure prediction calculations.[84] They show that a pair of neutral molecules has a different set of predicted crystal structures (in the lattice energy landscape) compared to their charged counterparts.

On the other hand, Kavanagh *et al.*[67] report another plausible idea: maybe the ionisation we observe is just a consequence of how the molecules pack relative to each other. If aggregating molecules approach each other such that there are additional supporting hydrogen-bond donors (such as the type Aakeröy suggests) in the vicinity, such a system can then become charged, as the charge will be stabilised. Either way, the ionisation state of a system is not random, and the charge plays a fundamental role in the stability of the crystal packing.

1.4.4 The transfer of hydrogen atoms

It was previously stated that pK_a values are used to describe proton transfer in aqueous solutions. Proton transfer from an acid to a base is prevalent in aqueous solutions as the water molecules can stabilise the ions that form and thereby reduce the energetic gap between molecules and their ions.[85] Hydrogen atoms are also known to be transferred in other solvents,[86] in the melt,[87] and in the solid state[88] as there are other species readily available in the matrix to stabilise the ions. From a crystallographic perspective, there are reports of salts being formed from proton transfer in solution,[89] melt,[90] and the solid state[91]. However, proton transfer in the gas phase is a much more rarely observed phenomenon. Proton transfer can occur in the gas phase under extreme conditions, such as inside a mass spectrometer where a strong external ionisation source is used,[92] but the high energetic cost

makes it less likely under milder laboratory conditions. Gas-phase deprotonation is very endothermic ($\Delta H >> 0$) and very endergonic ($\Delta G >> 0$).[93] In fact, a number of computational studies have shown that additional surrounding water molecules are needed for proton transfer in the gas phase, as the cation and anion that form need to be stabilised by hydration.[94–96] However, it is also possible (as shown by computational methods) that other species can be used for stabilisation purposes, including the neutral molecules themselves.[97] The difficulty lies in carrying out gas-phase analyses to prove whether proton transfer can occur in the gas phase.

1.5 Crystallisation techniques

There are numerous ways to grow crystals of multicomponent materials. Most crystallisation methods require at least partial dissolution of the constituents in a solvent, but solid-state and gas-phase methods also exist. Some of the methods that have been used for crystallisation include crystallisation from solution, solid-state grinding (mechanochemistry), crystallisation from the melt, hot melt extrusion, apparent spontaneous co-crystallisation, resonant acoustic mixing, slurry conversion, sonication, sublimation, freeze drying, etc.[56,98,99] The list is long, but due to co-crystal commercialisation (especially in the pharmaceutical industry)[100,101] there is a place for newly developed, efficient and environmentally friendly co-crystallisation techniques. Additionally, a better understanding is needed of how to best use and control the existing co-crystallisation methodologies.

1.5.1 Co-crystallisation from solution

Crystallisation is usually carried out in solution as it is often easily achieved and frequently yields good quality crystals. There are a number of ways that such a crystallisation can be carried out, the most common method being crystal growth by slow evaporation of the solvent. In this method the molecules to be crystallised are dissolved in a solvent or solvent mixture (with or without applying heat to aid dissolution). The solution is then left undisturbed so that crystals can form as the solvent evaporates and the solution becomes supersaturated. Crystals can also be grown by slowly cooling such a solution, adding a solvent in which compounds are insoluble, or by layering different solutions where each contains a different coformer. Naturally, each variation of this technique has a number of variables that can be controlled in order to selectively make the desired multicomponent crystals.

The biggest influencing factors for solution crystallisation are the temperature and solvent used. It is well known that solvent choice can influence polymorphism,[102] which includes the formation of polymorphic co-crystals.[103,104] Other seemingly insignificant things, like dissolving coformers separately, or together, can also make a difference.[105] Modifying the solvent used during solution

crystallisation can also be used to control whether a set of molecules crystallises as a salt or a co-crystal (see for example the combination of saccharine and sulfamethazine).[79]

In general, solution crystallisation is able to yield high-quality single crystals for structure elucidation. Unfortunately, solution crystallisation tends to be serendipitous, unpredictable, and often irreproducible. The ratio of starting materials used is often not reflected in the stoichiometry of the product,[106] and crystallisation can be quite slow (taking up to 6 months in some cases).[107] Additionally, the solubility of the coformers, which may be very different, needs to be taken into account, and compatibility issues may arise. The use of large amounts of solvent is also detrimental to the environment. Fortunately, once structural (and bonding) data has been obtained for a particular material, single crystals are not usually necessary, and other crystallisation techniques can be employed to produce bulk material.

1.5.2 Mechanochemical co-crystallisation

Another popular (and more recently developed) crystallisation technique is crystallisation by mechanochemistry. When mechanical energy is used to activate a reaction, it can be classified as a form of mechanochemistry.[108] Mechanochemistry can be used for the formation of multicomponent materials (in powdered form), but also for organic synthesis, catalysis, etc.[109] Mechanochemical co-crystallisation is carried out by grinding coformers together manually using a mortar and pestle, or with a mechanical ball mill. This can be performed without the addition of any solvent (neat/dry co-grinding) or with the addition of small amounts of solvents which has been shown to improve the reaction kinetics and crystallinity of the product. This latter form of grinding is called liquid-assisted grinding (LAG) or alternatively, solvent-drop grinding or kneading. Friščić *et al.* defines the amount of solvent added as η (eta) which can be calculated as the amount of liquid added per milligram of sample (μL mg^{-1}).[110] They suggest that using a solvent amount of $\eta < 1$ μL mg^{-1} can be classified as LAG.[110] When more solvent is used, a slurry forms, which can also lead to the formation of multicomponent materials.

Apart from the amount of solvent used, there are several other variables that can be controlled. Variables include the type of solvent used, the ratio of starting materials, the reaction time, the milling frequency, the type of mill (oscillating or rotating), the milling media (amount, type, and weight of milling balls), the material the milling jars are made of, etc. Recent studies have tried to determine the effect of these variables.[99] For example, there are a number of reports showing the effect that solvent polarity can have on co-crystal polymorphism,[111–113] and how control of both solvent amount and polarity can lead to a variety of co-crystal forms.[114] Additionally, when co-crystal forms differ in terms of stoichiometry, it is usually a very simple matter to control which form is obtained by using

the correct ratio of starting materials.[106] Yuan *et al*. also reports on a very interesting pair of polymorphic theophylline-acesulfame co-crystals.[115] The polymorphic outcome of their mechanochemical co-crystallisations was dependent on whether grinding was carried out by hand or using a mill, as well as the frequency of milling, as this affects the imparted energy. Additionally, they report that the polymorphic identity of the starting materials could affect which form of the co-crystal was obtained, along with grinding time, solvent polarity, starting material stoichiometry, and the use of seed crystals.[115]

Mechanochemical co-crystallisation has been shown to be very successful. Reactions are highly reproducible and give near-quantitative yields.[116] The significantly decreased use of solvent and room temperature reaction conditions also make this a much more environmentally friendly technique compared to solution crystallisation. Mechanochemical co-crystallisation is fast and therefore very useful for carrying out co-crystal screening tests and producing bulk polycrystalline material in a matter of minutes. Additionally, co-crystallisation kinetics can be followed *in situ* (using powder diffraction, Raman spectroscopy, etc.) if a translucent capsule is used, which can lead to the discovery of new intermediate co-crystal forms.[117] However, single crystals are not obtained, and polycrystalline material needs to be recrystallised using a different technique in order to obtain crystals (although once a material is identified, single crystals are generally not needed). Large-scale mechanochemical co-crystallisation for industrial purposes also still presents a challenge.

1.5.3 Co-sublimation

Sublimation is the process whereby a solid material converts directly into a gas. When discussing solid-state chemistry, the subsequent deposition or crystallisation step (from the gas back to a solid) is naturally included in this definition. Many organic molecules can sublime under laboratory conditions of temperature and pressure. For example, heating a simple organic compound such as naphthalene in a beaker with a Bunsen burner will quickly cause sublimation, and pure crystals of naphthalene will subsequently grow on a colder surface. However, it is usually necessary to carry out sublimation under vacuum conditions, so that the sample has a high enough vapour pressure at a specific temperature in order to vaporise. Therefore, small scale laboratory sublimation experiments are often carried out in Schlenk tubes that can be sealed under vacuum and heated at one end. Crystals can then deposit in the cooler end of the tube, somewhere along the temperature gradient, or onto a liquid-cooled cold finger. More complex methods of sublimation have been developed as well, for example: carrying out sublimation inside a precisely-controlled multi-zone heating apparatus under reduced pressure or using a carrier gas,[118] and sublimation between two temperature-controlled glass plates or slides held inside a vacuum oven.[119]

Traditionally, sublimation has been used as a method of purification and crystal growth; however, it has recently been discovered that the simultaneous sublimation of two compounds (co-sublimation) can lead to the formation of co-crystals. Co-crystals containing hydrogen bonds,[120] halogen bonds,[121] and S···S/S···N interactions[122] have been formed in this way, although it is not a commonly used co-crystallisation technique. To date, there have been no studies comparing the formation of these interactions in the gas phase (something which will be addressed in this thesis). Additionally, there are no reports in the literature of salts forming by co-sublimation. As mentioned previously, the proton transfer required for salt formation in the gas phase is not considered to occur readily, but there is one report of an organic salt being able to re-sublime.[10] The distinction between co-sublimation and re-sublimation will be important in this thesis: re-sublimation refers to the sublimation of pre-formed multicomponent material (potentially re-forming upon solidification), while the term co-sublimation is used to describe the sublimation of separate, neutral starting materials.

Co-sublimation and re-sublimation are currently not routinely used for the formation of multicomponent crystals. However, some advantages of using these techniques are evident: solids can be formed relatively quickly, while impurities are excluded. Sublimation can also, on occasion, yield diffraction-quality single crystals, which is a definite improvement compared to other solvent-free methods like mechanochemistry. Crystals of co-crystals have also been obtained from sublimation when no other technique sufficed.[123] However, much about sublimation co-crystallisation, and the variables used to control it, is still unknown. This thesis aims to further explore the co-sublimation technique, so that its usefulness and robustness may be determined.

1.5.4 A multi-technique approach

Generally, it is assumed that co-crystallisation outcome is independent of the method used for crystallisation. This is true in most cases. For example, crystallisation from solution mostly yields the same product as crystallisation by solid-state grinding.[124] However, a number of reports are starting to show that this is not always the case. Some products can, for example, only be obtained mechanochemically and not by traditional solution methods.[125] A number of caffeine-succinic acid solvates have been shown to form by mechanochemistry even though they were not obtained from solution crystallisation.[126] Conversely, when solution crystallisation leads to solvate formation, a solvent-free technique such as sublimation can lead to new solvent-free crystal forms.[127,128] Eddleston *et al.* describes something similar regarding co-crystal polymorphs: in their work a multi-technique approach was needed to obtain all forms of a co-crystal.[129] This is not an isolated case. Crystal growth proceeds differently depending on the technique used, and so the utilisation of new crystallisation techniques can often lead to the identification of new co-crystal polymorphs.[130–133]

Apart from the identification of new crystalline materials, being able to selectively produce a specific crystal form is also of interest, as different crystal types can have different properties. In this thesis we are specifically interested in the selective formation of co-crystals and salts. Recently there has been a report regarding a set of molecules (β-alanine and DL-tartaric acid) that exist as both a salt and a co-crystal, both with a 1:1 stoichiometry. Losev and Boldyreva could control whether the metastable salt or the stable co-crystal was crystallised by using different crystallisation techniques (mechanochemistry and variations of solution crystallisation).[78] Hydrazone and mesaconic acid also crystallise as two multicomponent forms that differ in terms of stoichiometry and ionisation. Using solution crystallisation and neat grinding, Mazur *et al.* could control which form was obtained.[134] Similarly, the combination of ethionamide and salicylic acid forms both a salt and co-crystal. The salt form is produced using LAG, while the co-crystal polymorph is obtained by rapid precipitation from solution.[76] To date, there have been no reports of sublimation being used to selectively form a salt or co-crystal when both can form from the same fundamental components.

1.6 Aims

Multicomponent materials can potentially have improved physicochemical properties compared to the individual molecules that they are composed of. These property changes stem from changes in the crystal structures. Different types of multicomponent crystals formed from the same components pack differently, and so they too can have varied properties. Therefore, it is important to be able to control which multicomponent form is obtained, so that the desired crystal form can be obtained deliberately and selectively. With this study we aim to demonstrate, using model systems, how careful control of the crystallisation technique used can lead to selective formation of a particular multicomponent crystal.

To start out, the aim was to examine pairs of molecules that can crystallise as both a salt and a co-crystal. We wanted to determine whether we were able to control the outcome of a multicomponent crystallisation reaction involving proton transfer. **Chapter 2** examines two such sets of molecules. We set out to use mechanochemistry as a means of crystal formation, and also sublimation, as proton transfer in the gas phase is not known to occur spontaneously. Such a study could provide insight into the formation of co-crystals and salts by sublimation, as well as gas-phase proton transfer, the existence of ions in the gas phase, and the potential for gas-phase hydrogen bonding. The aim was to use sublimation to selectively prepare co-crystals.

Additionally, we aimed to study competitive co-crystallisation, i.e. selective co-crystallisation in the presence of competing coformers. Co-crystal competition experiments are often carried out in

solution,[135] and even in the solid state, but gas-phase techniques have not been used for selectivity purposes before, and were therefore the focus of this part of the study. In particular we wanted to study and compare the formation of hydrogen and halogen bonds by sublimation, in the presence of a mutual acceptor molecule. Additionally, we aimed to explore the role of solvent in mechanochemical co-crystal competition studies for the first time. The results of these competition experiments are presented in **Chapter 3**.

As a whole, this study aims to investigate the value of historically unconventional crystallisation techniques, i.e. sublimation and mechanochemistry, for the selective formation of multicomponent crystals, and point out any advantages over traditional crystallisation techniques, as well as any pitfalls to avoid. **Chapter 4** aims to provide a complete evaluation of the utility of co-sublimation in comparison to mechanochemistry by looking at a large number of multicomponent systems. We will discuss co-crystals, salts, and polymorphs, as well as problems that can arise during the sublimation process. We need to determine whether the examples discussed in chapters 2 and 3 are anomalous, or whether co-sublimation is truly a reliable method of co-crystal formation.

Ultimately, we want to determine whether solid-state and gas-phase co-crystallisation are useful tools for selectively synthesising multicomponent materials.

1.7 References

[1] Desiraju, G. R.; Vittal, J. J.; Ramanan, A. *Crystal Engineering A Textbook*; World Scientific Publishing Co. Pte. Ltd.: Singapore, **2011**.

[2] Steed, J. W.; Turner, D. R.; Wallace, K. *Core Concepts in Supramolecular Chemistry and Nanochemistry*; John Wiley & Sons, Ltd: Chichester, **2007**.

[3] Desiraju, G. R. *Angew. Chem. Int. Ed.* **1995**, *34* (21), 2311–2327.

[4] Arunan, E.; Desiraju, G. R.; Klein, R. A.; Sadlej, J.; Scheiner, S.; Alkorta, I.; Clary, D. C.; Crabtree, R. H.; Dannenberg, J. J.; Hobza, P.; Kjaergaard, H. G.; Legon, A. C.; Mennucci, B.; Nesbitt, D. J. *Pure Appl. Chem.* **2011**, *83* (8), 1–5.

[5] Desiraju, G. R.; Ho, P. S.; Kloo, L.; Legon, A. C.; Marquardt, R.; Metrangolo, P.; Politzer, P.; Resnati, G.; Rissanen, K. *Pure Appl. Chem.* **2013**, *85* (8), 1711–1713.

[6] Gilli, G.; Gilli, P. *The Nature of the Hydrogen Bond*; Oxford University Press: New York, **2009**.

[7] Bishop, R. *CrystEngComm* **2015**, *17* (39), 7448–7460.

[8] Desiraju, G. R.; Steiner, T. *The Weak Hydrogen Bond*; Oxford University Press: Oxford, 1999.

[9] Bruno, G.; Randaccio, L. *Acta Crystallogr. Sect. B* **1980**, *36* (7), 1711–1712.

[10] Chao, M.; Schemp, E.; Rosenstein, R. D. *Acta Crystallogr. Sect. B* **1975**, *31* (12), 2924–2926.

[11] Allen, F. H.; Hoy, V. J.; Howard, J. A. K.; Thalladi, V. R.; Desiraju, G. R.; Wilson, C. C.; McIntyre, G. J. *J. Am. Chem. Soc.* **1997**, *119* (15), 3477–3480.

[12] Takusagawa, F.; Shimada, A. *Acta Crystallogr. Sect. B* **1976**, *32* (6), 1925–1927.

[13] Chan, H. C. S.; Woollam, G. R.; Wagner, T.; Schmidt, M. U.; Lewis, R. A. *CrystEngComm* **2014**, *16* (21), 4365–4368.

[14] Shipley, G. G.; Wallwork, S. C. *Acta Crystallogr.* **1967**, *22* (4), 593–601.

[15] Gdaniec, M.; Gilski, M.; Denisov, G. S. *Acta Crystallogr. Sect. C* **1994**, *50* (10), 1622–1626.

[16] Boenigk, D.; Mootz, D. *J. Am. Chem. Soc.* **1988**, *110* (7), 2135–2139.

[17] Guven, K.; Bakir, G. *Z. Kristallogr. NCS* **2010**, *225*, 197–198.

[18] Politzer, P.; Murray, J. S.; Clark, T.; Resnati, G. *Phys. Chem. Chem. Phys.* **2017**, *19* (48), 32166–32178.

[19] Gilday, L. C.; Robinson, S. W.; Barendt, T. A.; Langton, M. J.; Mullaney, B. R.; Beer, P. D. *Chem. Rev.* **2015**, *115* (15), 7118–7195.

[20] Mukherjee, A.; Tothadi, S.; Desiraju, G. R. *Acc. Chem. Res.* **2014**, *47* (8), 2514–2524.

[21] Clark, T.; Hennemann, M.; Murray, J. S.; Politzer, P. *J. Mol. Model.* **2007**, *13* (2), 291–296.

[22] Huber, S. M.; Scanlon, J. D.; Jimenez-Izal, E.; Ugalde, J. M.; Infante, I. *Phys. Chem. Chem. Phys.* **2013**, *15* (25), 10350–10357.

[23] Riley, K. E.; Murray, J. S.; Fanfrlík, J.; Řezáč, J.; Solá, R. J.; Concha, M. C.; Ramos, F. M.; Politzer, P. *J. Mol. Model.* **2011**, *17* (12), 3309–3318.

[24] Bosch, E. *Cryst. Growth Des.* **2014**, *14* (1), 126–130.

[25] Borley, W.; Watson, B.; Nizhnik, Y. P.; Zeller, M.; Rosokha, S. V. *J. Phys. Chem. A* **2019**, *123* (32), 7113–7123.

[26] Lu, Y.-X.; Zou, J.-W.; Wang, Y.-H.; Jiang, Y.-J.; Yu, Q.-S. *J. Phys. Chem. A* **2007**, *111* (42), 10781–10788.

[27] Aakeröy, C. B.; Wijethunga, T. K.; Desper, J.; Đaković, M. *Cryst. Growth Des.* **2015**, *15* (8), 3853–3861.

[28] Aakeröy, C. B.; Fasulo, M.; Schultheiss, N.; Desper, J.; Moore, C. *J. Am. Chem. Soc.* **2007**, *129* (45), 13772–13773.

[29] Gamekkanda, J. C.; Sinha, A. S.; Desper, J.; Đaković, M.; Aakeröy, C. B. *New J. Chem.* **2018**, *42* (13), 10539–10547.

[30] Alkorta, I.; Blanco, F.; Solimannejad, M.; Elguero, J. *J. Phys. Chem. A* **2008**, *112* (43), 10856–10863.

[31] Takemura, A.; McAllister, L. J.; Karadakov, P. B.; Pridmore, N. E.; Whitwood, A. C.; Bruce,

D. W. *CrystEngComm* **2014**, *16* (20), 4254–4264.

[32] Corradi, E.; Meille, S. V.; Messina, M. T.; Metrangolo, P.; Resnati, G. *Angew. Chem. Int. Ed.* **2000**, *39* (10), 1782–1786.

[33] Li, C.; Chai, Y.; Zhou, X.; Shen, Z.; Ma, B.; Chen, B.; Huang, R.; Chen, H.; Li, W.; He, Y. *CrystEngComm* **2018**, *20* (22), 3006–3010.

[34] Awwadi, F. F.; Taher, D.; Haddad, S. F.; Turnbull, M. M. *Cryst. Growth Des.* **2014**, *14* (4), 1961–1971.

[35] Nagels, N.; Geboes, Y.; Pinter, B.; De Proft, F.; Herrebout, W. A. *Chem. Eur. J.* **2014**, *20* (27), 8433–8443.

[36] Riley, K. E.; Řezáč, J.; Hobza, P. *J. Mol. Model.* **2013**, *19* (7), 2879–2883.

[37] Wu, J.; Zhang, J.; Wang, Z.; Cao, W. *J. Chem. Theory Comput.* **2007**, *3* (1), 95–102.

[38] Riel, A. M. S.; Decato, D. A.; Sun, J.; Massena, C. J.; Jessop, M. J.; Berryman, O. B. *Chem. Sci.* **2018**, *9* (26), 5828–5836.

[39] Riel, A. M. S.; Rowe, R. K.; Ho, E. N.; Carlsson, A.-C. C.; Rappé, A. K.; Berryman, O. B.; Ho, P. S. *Acc. Chem. Res.* **2019**, *52* (10), 2870–2880.

[40] Davey, R. J.; Schroeder, S. L. M.; ter Horst, J. H. *Angew. Chem. Int. Ed.* **2013**, *52* (8), 2166–2179.

[41] Tsarfati, Y.; Rosenne, S.; Weissman, H.; Shimon, L. J. W.; Gur, D.; Palmer, B. A.; Rybtchinski, B. *ACS Cent. Sci.* **2018**, *4* (8), 1031–1036.

[42] *Polymorphism in Molecular Crystals*; Bernstein, J., Ed.; Oxford: Clarendon Press: New York, **2002**.

[43] Berry, D. J.; Steed, J. W. *Adv. Drug Deliv. Rev.* **2017**, *117*, 3–24.

[44] Casali, L.; Mazzei, L.; Shemchuk, O.; Sharma, L.; Honer, K.; Grepioni, F.; Ciurli, S.; Braga, D.; Baltrusaitis, J. *ACS Sustain. Chem. Eng.* **2019**, *7* (2), 2852–2859.

[45] Bučar, D.-K.; Filip, S.; Arhangelskis, M.; Lloyd, G. O.; Jones, W. *CrystEngComm* **2013**, *15* (32), 6289.

[46] Aakeröy, C. B.; Wijethunga, T. K.; Desper, J. *Chem. Eur. J.* **2015**, *21* (31), 11029–11037.

[47] Kuminek, G.; Cao, F.; Bahia de Oliveira da Rocha, A.; Gonçalves Cardoso, S.; Rodríguez-Hornedo, N. *Adv. Drug Deliv. Rev.* **2016**, *101*, 143–166.

[48] Duggirala, N. K.; Perry, M. L.; Almarsson, Ö.; Zaworotko, M. J. *Chem. Commun.* **2016**, *52* (4), 640–655.

[49] Bak, A.; Gore, A.; Yanez, E.; Stanton, M.; Tufekcic, S.; Syed, R.; Akrami, A.; Rose, M.; Surapaneni, S.; Bostick, T.; King, A.; Neervannan, S.; Ostovic, D.; Koparkar, A. *J. Pharm. Sci.* **2008**, *97* (9), 3942–3956.

[50] Mannava, M. K. C.; Dandela, R.; Tothadi, S.; Solomon, K. A.; Nangia, A. K. *Cryst. Growth Des.* **2020**, *20* (5), 3064–3076.

[51] Almarsson, Ö.; Peterson, M. L.; Zaworotko, M. *Pharm. Pat. Anal.* **2012**, *1* (3), 313–327.

[52] Gunawardana, C. A.; Aakeröy, C. B. *Chem. Commun.* **2018**, *54* (100), 14047–14060.

[53] Zhang, C.; Xiong, Y.; Jiao, F.; Wang, M.; Li, H. *Cryst. Growth Des.* **2019**, *19* (3), 1471–1478.

[54] Aitipamula, S.; Banerjee, R.; Bansal, A. K.; Biradha, K.; Cheney, M. L.; Choudhury, A. R.; Desiraju, G. R.; Dikundwar, A. G.; Dubey, R.; Duggirala, N.; Ghogale, P. P.; Ghosh, S.; Goswami, P. K.; Goud, N. R.; Jetti, R. R. K. R.; Karpinski, P.; Kaushik, P.; Kumar, D.; Kumar, V.; Moulton, B.; Mukherjee, A.; Mukherjee, G.; Myerson, A. S.; Puri, V.; Ramanan, A.; Rajamannar, T.; Reddy, C. M.; Rodriguez-Hornedo, N.; Rogers, R. D.; Row, T. N. G.; Sanphui, P.; Shan, N.; Shete, G.; Singh, A.; Sun, C. C.; Swift, J. A.; Thaimattam, R.; Thakur, T. S.; Kumar Thaper, R.; Thomas, S. P.; Tothadi, S.; Vangala, V. R.; Variankaval, N.; Vishweshwar, P.; Weyna, D. R.; Zaworotko, M. J. *Cryst. Growth Des.* **2012**, *12* (5), 2147–2152.

[55] Grothe, E.; Meekes, H.; Vlieg, E.; ter Horst, J. H.; de Gelder, R. *Cryst. Growth Des.* **2016**, *16* (6), 3237–3243.

[56] Karimi-Jafari, M.; Padrela, L.; Walker, G. M.; Croker, D. M. *Cryst. Growth Des.* **2018**, *18* (10), 6370–6387.

[57] Mir, N. A.; Dubey, R.; Desiraju, G. R. *Acc. Chem. Res.* **2019**, *52* (8), 2210–2220.

[58] Aakeröy, C. B.; Salmon, D. J. *CrystEngComm* **2005**, *72* (7), 439–448.

[59] Braga, D.; Grepioni, F.; Maini, L.; Prosperi, S.; Gobetto, R.; Chierotti, M. R. *Chem. Commun.* **2010**, *46* (41), 7715–7717.

[60] Pindelska, E.; Sokal, A.; Kolodziejski, W. *Adv. Drug Deliv. Rev.* **2017**, *117*, 111–146.

[61] Boothroyd, S.; Kerridge, A.; Broo, A.; Buttar, D.; Anwar, J. *Cryst. Growth Des.* **2018**, *18* (3), 1903–1908.

[62] Nassimbeni, L. R. *Acc. Chem. Res.* **2003**, *36* (8), 631–637.

[63] Lemmerer, A.; Govindraju, S.; Johnston, M.; Motloung, X.; Savig, K. L. *CrystEngComm* **2015**, *17* (19), 3591–3595.

[64] Cruz-Cabeza, A. J. *CrystEngComm* **2012**, *14* (20), 6362–6365.

[65] Childs, S. L.; Stahly, G. P.; Park, A. *Mol. Pharm.* **2007**, *4* (3), 323–328.

[66] Stahly, G. P. *Cryst. Growth Des.* **2007**, *7* (6), 1007–1026.

[67] Kavanagh, O. N.; Walker, G.; Lusi, M. *Cryst. Growth Des.* **2019**, *19* (9), 5308–5313.

[68] Black, S. N.; Collier, E. A.; Davey, R. J.; Roberts, R. J. *J. Pharm. Sci.* **2007**, *96* (5), 1053–1068.

[69] Childs, S. L.; Stahly, G. P.; Park, A. *Mol. Pharm.* **2007**, *4* (3), 323–338.

[70] Steiner, T.; Majerz, I.; Wilson, C. C. *Angew. Chem. Int. Ed.* **2001**, *40* (14), 2651–2654.

[71] Kelley, S. P.; Narita, A.; Holbrey, J. D.; Green, K. D.; Reichert, W. M.; Rogers, R. D. *Cryst. Growth Des.* **2013**, *13* (3), 965–975.

[72] Pratik, S. M.; Datta, A. *J. Phys. Chem. B* **2016**, *120* (30), 7606–7613.

[73] Haynes, D. A.; Jones, W.; Motherwell, W. D. S. *CrystEngComm* **2006**, *8* (11), 830–840.

[74] Nangia, A.; Gunnam, A.; Suresh, K. *Cryst. Growth Des.* **2018**, *18* (5), 2824–2835.

[75] Roselló, Y.; Benito, M.; Bagués, N.; Martínez, N.; Moradell, A.; Mata, I.; Galcerà, J.; Barceló-Oliver, M.; Frontera, A.; Molins, E. *Cryst. Growth Des.* **2020**, *20* (5), 2985–2997.

[76] Bernasconi, D.; Bordignon, S.; Rossi, F.; Priola, E.; Nervi, C.; Gobetto, R.; Voinovich, D.; Hasa, D.; Duong, N. T.; Nishiyama, Y.; Chierotti, M. R. *Cryst. Growth Des.* **2020**, *20* (2), 906–915.

[77] Stainton, P.; Grecu, T.; McCabe, J.; Munshi, T.; Nauha, E.; Scowen, I. J.; Blagden, N. *Cryst. Growth Des.* **2018**, *18* (7), 4150–4159.

[78] Losev, E. A.; Boldyreva, E. V. *CrystEngComm* **2018**, *20* (16), 2299–2305.

[79] Perumalla, S. R.; Wang, C.; Guo, Y.; Shi, L.; Sun, C. C. *CrystEngComm* **2019**, *21* (13), 2089–2096.

[80] Jones, C. L.; Skelton, J. M.; Parker, S. C.; Raithby, P. R.; Walsh, A.; Wilson, C. C.; Thomas, L. H. *CrystEngComm* **2019**, *21* (10), 1626–1634.

[81] Fu, X.; Li, J.; Wang, L.; Wu, B.; Xu, X.; Deng, Z.; Zhang, H. *RSC Adv.* **2016**, *6* (31), 26474–26478.

[82] Losev, E.; Boldyreva, E. *Acta Crystallogr. Sect. C* **2018**, *74* (2), 177–185.

[83] Aakeröy, C. B.; Fasulo, M. E.; Desper, J. *Mol. Pharm.* **2007**, *4* (3), 317–322.

[84] Mohamed, S.; Tocher, D. A.; Price, S. L. *Int. J. Pharm.* **2011**, *418* (2), 187–198.

[85] Mohammed, O. F. *Science* **2005**, *310* (5745), 83–86.

[86] Kim, H.; Gao, J.; Burgess, D. J. *Int. J. Pharm.* **2009**, *377* (1–2), 105–111.

[87] Li, Y.-J.; Luo, Y.-H.; Wang, J.-W.; Chen, C.; Sun, B.-W. *J. Mol. Struct.* **2018**, *1153*, 96–105.

[88] Sheth, A. R.; Lubach, J. W.; Munson, E. J.; Muller, F. X.; Grant, D. J. W. *J. Am. Chem. Soc.* **2005**, *127* (18), 6641–6651.

[89] Wang, T.; Stevens, J. S.; Vetter, T.; Whitehead, G. F. S.; Vitorica-Yrezabal, I. J.; Hao, H.; Cruz-Cabeza, A. J. *Cryst. Growth Des.* **2018**, *18* (11), 6973–6983.

[90] Lee, H. L.; Vasoya, J. M.; Cirqueira, M. de L.; Yeh, K. L.; Lee, T.; Serajuddin, A. T. M. *Mol. Pharm.* **2017**, *14* (4), 1278–1291.

[91] Trask, A. V.; Haynes, D. A.; Motherwell, W. D. S.; Jones, W. *Chem. Commun.* **2006**, No. 1,

51–53.

[92] Prazeller, P.; Palmer, P. T.; Boscaini, E.; Jobson, T.; Alexander, M. *Rapid Commun. Mass Spectrom.* **2003**, *17* (14), 1593–1599.

[93] Raczynska, E. D.; Gal, J.; Maria, P.; Szelag, M. *Croat. Chem. Acta* **2009**, *82* (1), 87–103.

[94] Cazar, R.; Jamka, A.; Tao, F.-M. *Chem. Phys. Lett.* **1998**, *287* (5–6), 549–552.

[95] Boda, M.; Naresh Patwari, G. *Phys. Chem. Chem. Phys.* **2017**, *19* (11), 7461–7464.

[96] Vargas-Caamal, A.; Cabellos, J. L.; Ortiz-Chi, F.; Rzepa, H. S.; Restrepo, A.; Merino, G. *Chem. Eur. J.* **2016**, *22* (8), 2812–2818.

[97] Li, R.-J.; Li, Z.-R.; Wu, D.; Chen, W.; Li, Y.; Wang, B.-Q.; Sun, C.-C. *J. Phys. Chem. A* **2005**, *109* (4), 629–634.

[98] Douroumis, D.; Ross, S. A.; Nokhodchi, A. *Adv. Drug Deliv. Rev.* **2017**, *117*, 178–195.

[99] Hasa, D.; Jones, W. *Adv. Drug Deliv. Rev.* **2017**, *117*, 147–161.

[100] Hun, A. J.; Won, J. K.; Ho, P. M.; Jin, L. C. Patent: WO2019KR02079 20190220, **2020**.

[101] Hammock, B. D.; Hwang, S. H.; Wagner, K. M.; Mcreynolds, C. B. Patent: WO2020010244, **2020**.

[102] Lombard, J.; Haynes, D. A.; le Roex, T. *Cryst. Growth Des.* **2017**, *17* (12), 6625–6633.

[103] Bevill, M. J.; Vlahova, P. I.; Smit, J. P. *Cryst. Growth Des.* **2014**, *14* (3), 1438–1448.

[104] Ueto, T.; Takata, N.; Muroyama, N.; Nedu, A.; Sasaki, A.; Tanida, S.; Terada, K. *Cryst. Growth Des.* **2012**, *12* (1), 485–494.

[105] Surov, A. O.; Manin, A. N.; Voronin, A. P.; Churakov, A. V.; Perlovich, G. L.; Vener, M. V. *Cryst. Growth Des.* **2017**, *17* (3), 1425–1437.

[106] Karki, S.; Friščić, T.; Jones, W. *CrystEngComm* **2009**, *11* (3), 470–481.

[107] Duggirala, N. K.; Smith, A. J.; Wojtas, Ł.; Shytle, R. D.; Zaworotko, M. J. *Cryst. Growth Des.* **2014**, *14* (11), 6135–6142.

[108] Baláž, P.; Achimovičová, M.; Baláž, M.; Billik, P.; Cherkezova-Zheleva, Z.; Criado, J. M.; Delogu, F.; Dutková, E.; Gaffet, E.; Gotor, F. J.; Kumar, R.; Mitov, I.; Rojac, T.; Senna, M.; Streletskii, A.; Wieczorek-Ciurowa, K. *Chem. Soc. Rev.* **2013**, *42* (18), 7571–7637.

[109] Do, J.-L.; Friščić, T. *ACS Cent. Sci.* **2017**, *3* (1), 13–19.

[110] Friščić, T.; Childs, S. L.; Rizvi, S. A. A.; Jones, W. *CrystEngComm* **2009**, *11* (3), 418–426.

[111] Aitipamula, S.; Chow, P. S.; Tan, R. B. H. *CrystEngComm* **2010**, *12* (11), 3691–3697.

[112] Trask, A. V.; Motherwell, W. D. S.; Jones, W. *Chem. Commun.* **2004**, No. 7, 890–891.

[113] Fischer, F.; Heidrich, A.; Greiser, S.; Benemann, S.; Rademann, K.; Emmerling, F. *Cryst. Growth Des.* **2016**, *16* (3), 1701–1707.

[114] Hasa, D.; Miniussi, E.; Jones, W. *Cryst. Growth Des.* **2016**, *16* (8), 4582–4588.

[115] Yuan, Y.; Wang, L.; Li, D.; Deng, Z.; Zhang, H. *Cryst. Growth Des.* **2018**, *18* (12), 7244–7247.

[116] Aitipamula, S.; Chow, P. S.; Tan, R. B. H. *CrystEngComm* **2014**, *16* (17), 3451–3465.

[117] Kulla, H.; Greiser, S.; Benemann, S.; Rademann, K.; Emmerling, F. *Cryst. Growth Des.* **2017**, *17* (3), 1190–1196.

[118] Jeon, H.-G.; Inoue, M.; Hiramatsu, N.; Ichikawa, M.; Taniguchi, Y. *Org. Electron.* **2008**, *9* (5), 903–905.

[119] Karpinska, J.; Erxleben, A.; McArdle, P. *Cryst. Growth Des.* **2013**, *13* (3), 1122–1130.

[120] Zhang, T.; Yu, Q.; Li, X.; Ma, X. *J. Cryst. Growth* **2017**, *469*, 114–118.

[121] Szell, P. M. J.; Gabriel, S. A.; Caron-Poulin, E.; Jeannin, O.; Fourmigué, M.; Bryce, D. L. *Cryst. Growth Des.* **2018**, *18* (10), 6227–6238.

[122] Robinson, S. W.; Haynes, D. A.; Rawson, J. M. *CrystEngComm* **2013**, *15* (47), 10205–10211.

[123] O'Malley, C.; Erxleben, A.; Kellehan, S.; McArdle, P. *Chem. Commun.* **2020**, 4–7.

[124] Weyna, D. R.; Shattock, T.; Vishweshwar, P.; Zaworotko, M. J. *Cryst. Growth Des.* **2009**, *9* (2), 1106–1123.

[125] Trask, A. V.; van de Streek, J.; Motherwell, W. D. S.; Jones, W. *Cryst. Growth Des.* **2005**, *5* (6), 2233–2241.

[126] Friščić, T.; Trask, A. V.; Jones, W.; Motherwell, W. D. S. *Angew. Chem. Int. Ed.* **2006**, *45* (45), 7546–7550.

[127] Spisak, S. N.; Wei, Z.; Darzi, E.; Jasti, R.; Petrukhina, M. A. *Chem. Commun.* **2018**, *54* (56), 7818–7821.

[128] Karpinska, J.; Erxleben, A.; McArdle, P. *Cryst. Growth Des.* **2011**, *11* (7), 2829–2838.

[129] Eddleston, M. D.; Sivachelvam, S.; Jones, W. *CrystEngComm* **2013**, *15* (1), 175–181.

[130] Losev, E. A.; Mikhailenko, M. A.; Achkasov, A. F.; Boldyreva, E. V. *New J. Chem.* **2013**, *37* (7), 1973.

[131] Grossjohann, C.; Serrano, D. R.; Paluch, K. J.; O'Connell, P.; Vella-Zarb, L.; Manesiotis, P.; McCabe, T.; Tajber, L.; Corrigan, O. I.; Healy, A. M. *J. Pharm. Sci.* **2015**, *104* (4), 1385–1398.

[132] Porter, W. W.; Elie, S. C.; Matzger, A. J. *Cryst. Growth Des.* **2008**, *8* (1), 14–16.

[133] Wang, J.; Ding, L.; Yang, C. *CrystEngComm* **2007**, *9* (7), 591–594.

[134] Mazur, L.; Materek, I.; Bond, A. D.; Jones, W. *Cryst. Growth Des.* **2019**, *19* (5), 2663–2678.

[135] Robertson, C. C.; Wright, J. S.; Carrington, E. J.; Perutz, R. N.; Hunter, C. A.; Brammer, L. *Chem. Sci.* **2017**, *8* (8), 5392–5398.

CHAPTER 2

Crystallisation of organic salts by sublimation: salt formation from the gas phase

---

2.1 Article submitted to Chemical Communications (unpublished)

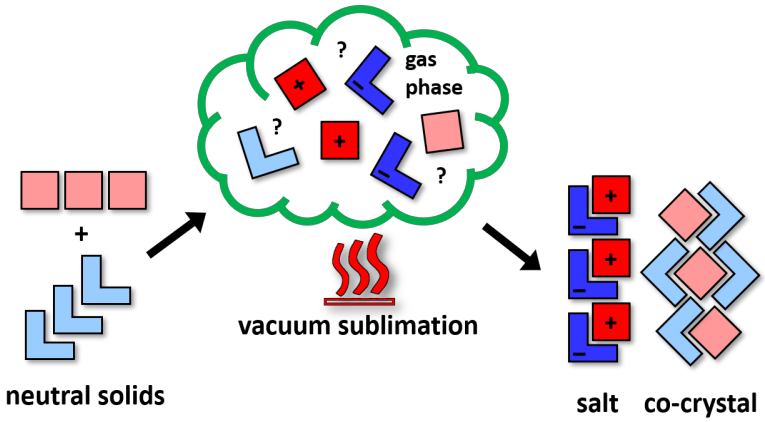

Contributions of the author:

- Design of project with co-authors
- Preparation of all salts and co-crystals
- Re-sublimation experiments
- Collection of single-crystal X-ray data
- Solution and refinement of single-crystal X-ray structures
- Recording of PXRD patterns
- Recording of TGA and DSC thermograms
- Recording of FTIR spectra
- Gas-cell experiments with Dr Isabella E. Claassens
- Interpretation of results with co-authors
- Writing the first draft of the article

COMMUNICATION

Crystallisation of organic salts by sublimation: salt formation from the gas phase

Jean Lombard,[a] Vincent J. Smith,[b] Tanya le Roex[a] and Delia A. Haynes*[a]

Received 00th January 20xx,
Accepted 00th January 20xx

DOI: 10.1039/x0xx00000x

Crystals of organic salts and co-crystals have been grown by co-sublimation of neutral components in two systems: succinic acid with hexamethylenetetramine, and oxalic acid with 4,4'-bipyridine. Additionally, salts and co-crystals can be re-sublimed once formed. Preliminary experiments indicate that ion pairs may be present in the gas phase during sublimation.

Organic multicomponent crystals, such as co-crystals and salts, are of interest in various industries[1–4] due to the possibility that they will have improved physicochemical properties compared to their constituent species.[5] Co-crystals consist of two or more neutral molecules, whereas molecular salts contain ions, usually resulting from simple transfer of a hydrogen atom from one molecule to the other. Species containing both charged and neutral molecules also exist, often called co-crystals of salts.[6,7] While organic salts and co-crystals technically only differ by a change in the position of a hydrogen atom, they are distinct crystal forms,[1] often with different stoichiometries[8] and distinct physicochemical properties. It is important that these different forms can be prepared selectively in order to take advantage of whichever form has the more favourable properties. The use of different preparative techniques is one way of controlling the product of a crystallisation. Herein we demonstrate that organic salts and co-crystals can be selectively prepared, recrystallised and separated by sublimation.

Reports of sublimation of organic salts are rare, with only one paper mentioning re-sublimation of a molecular salt.[9] (When pre-formed multicomponent materials are sublimed to re-crystallise the material, so that the same material is re-formed, we shall use the term re-sublimation, to distinguish this from subliming the individual molecular components together in order to form a multicomponent material, which we have called co-sublimation.) In fact, salt formation has been used to prevent the sublimation of volatile compounds (for example the salt of mirtazapine[10]). Sublimation of salts generally involves high temperatures, and the material degrades or dissociates in the process.[11–13]

There are no previous reports of crystallisation of organic salts from neutral starting materials by co-sublimation. It is known that proton transfer in the dilute gas phase is not favorable,[14] and isolated ions are not stable in the gas phase, so formation of salts from the gas phase by co-sublimation of neutral components is not anticipated. It has been reported that co-crystals can be formed by co-sublimation,[15–18] with one recent report from our group,[19] although this technique is not commonly used (see for example ref. 20, a review on preparative methods for co-crystals that does not mention sublimation). The re-sublimation of co-crystals is also rarely mentioned in the literature: the first report of this is a 2019 paper by Ye *et al.*[21] It is clear that the use of sublimation to prepare multicomponent organic crystals has not been well explored.

We therefore set out to investigate sublimation as a method to selectively form organic salts or co-crystals. We hypothesised that, due to the absence of solvation, neutral molecules would be more stable in the gas phase, leading to preferential formation of co-crystals by co-sublimation. As proof of concept, we selected two systems known to form multicomponent crystals: the combination of succinic acid (SA) with hexamethylenetetramine (HMT), and oxalic acid (OA) with 4,4'-bipyridine (BPY) (Chart 1). The ΔpK_a in both systems suggests that either a salt or a co-crystal could form in both cases.[22] The combination of SA and HMT gave a salt (**1a**) and three co-crystals (**1b**, **1c** and **1d**), while the combination of OA and BPY gave one salt (**2a**), and one co-crystal (**2b**) (Table 1). The

[a] Department of Chemistry and Polymer Science, Stellenbosch University, P. Bag X1, Matieland, 7602, Stellenbosch, Republic of South Africa. Email: dhaynes@sun.ac.za
[b] Department of Chemistry, Rhodes University, PO Box 94, Grahamstown, 6140, Republic of South Africa.

† Electronic Supplementary Information (ESI) available: Crystallisation procedures; mechanochemical conversions; re-sublimation procedures; crystal structure descriptions and crystallographic tables; hydrogen-bonding tables; crystallographic data for gas cell experiments; instrumental characterisation and analysis for all compounds (PXRD, TGA, DSC, FTIR) and TOF-MS data for **1a**. CCDC 1970253–1970262. For ESI and crystallographic data in CIF format see DOI: 10.1039/x0xx00000x

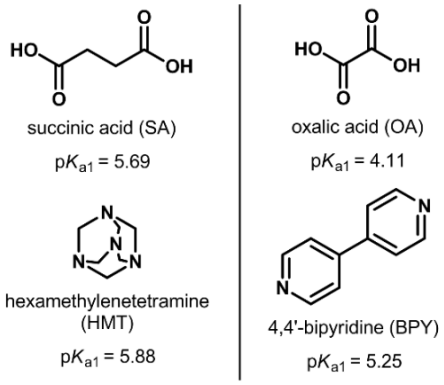

Chart 1 Molecules used in this study with predicted pK_a values for the first ionisation.[23]

structures of **1b**, **2a**, and **2b** have been reported previously (CSD refcodes: TOZTIN01[24], EZECOC[25] & XEZDIQ[26]). All crystal structures were re-determined for this study in order to confirm the position of the acidic hydrogen atom, i.e. to confirm whether the material is a salt or a co-crystal. All details, as well as descriptions of the crystal structures, are given in the Supplementary Information.

Table 1 Summary of the stoichiometry of the multicomponent crystals investigated in this study.*

	Salt or co-crystal?	Stoichiometry (acid:base)
1a	salt	2:1
1b	co-crystal	1:1
1c	co-crystal	1:2
1d	co-crystal	1:2
2a	salt	2:1
2b	co-crystal	1:1

*All multicomponent crystals can be made from solution, mechanochemically and by sublimation, with the exception of **1d**, which can only be made mechanochemically.

Co-crystallisation of both acid-base combinations was attempted from solution, by mechanochemical grinding using a ball mill and via vacuum sublimation. Products were identified using a combination of single-crystal and powder X-ray diffraction.

Crystalline **1a**, **1b** and **1c** could all be formed from both solution crystallisation and mechanochemistry, although solution crystallisations did not give predictable products. Mechanochemistry could be used to convert between **1a**, **1b** and **1c** by adding the extra equivalents of acid or base to give the required stoichiometry and continuing the milling process.[15,27–29] An additional kinetic form, co-crystal **1d**, was obtained by mechanochemistry only.

Sublimation of a 1:1 mixture of SA and HMT at 90 °C yielded crystals of the co-crystal **1b**. At higher temperatures (110 °C) the salt **1a** also started to crystallise in a thin band below the co-crystal. Careful observation of sublimations of HMT and SA at 110 °C (Fig. 1) revealed that only HMT crystallised initially (it has the higher vapour pressure). As the glass heated up, the HMT crystals re-sublimed higher up the sublimation tube, and the co-crystal **1b** started to crystallise in a separate band. After about

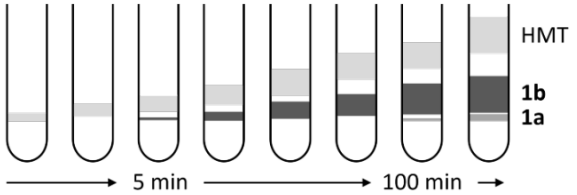

Fig. 1 Product distribution on the sides of the tube during the co-sublimation of succinic acid with HMT at 110 °C.

2 hours, crystals of HMT and the co-crystal had shifted further up the tube, and crystals of the salt started to form in a third band. The clear separation of crystallisation zones allows separate collection of the products. Pure **1b** can be collected if the experiment is stopped before **1a** starts to sublime.

Solution crystallisation experiments and mechanochemistry could be used to form **2a** and **2b**, with co-crystal **2b** crystallising less often from solution. Again, solution crystallisation was unpredictable in terms of the stoichiometry of the product obtained. Formation of **2b** mechanochemically did not go to completion and a small amount **2a** always formed concomitantly. Salt **2a**, the seemingly less stable form, could be converted to co-crystal **2b** by milling with an additional equivalent of BPY, while **2b** only partially converted to **2a** upon milling with additional oxalic acid.

Sublimation of a mixture of OA and BPY at temperatures between 125 °C and 180 °C lead to crystallisation of both multi-component materials in separate bands, allowing crystals to be collected separately to obtain pure **2a** and pure **2b**. Despite testing several temperatures, it was not possible to obtain either only **2a** or only **2b** by sublimation. Once again, crystals of BPY were always observed to form in the higher, cooler parts of the tube (Fig. S2).

The unexpected formation of salts by co-sublimation in both systems investigated led us to question when proton transfer between acid and base is occurring. A mixture of SA and HMT was heated together in the bottom of a test tube at ambient pressure. No multicomponent crystals were observed to from under these conditions, suggesting that multicomponent crystal formation occurs after the molecules enter the gas phase. In a separate series of experiments, solid HMT and SA were kept physically separate from one another during sublimation. Both **1a** and **1b** were observed to crystallise, even though the starting materials were not in physical contact with one another. In these experiments, the two coformers could only encounter one another in the gas phase, and crystals of the salt were observed to form, suggesting that proton transfer is either occurring in the gas phase, or after the neutral components crystallise in an arrangement analogous to that observed in **1a**. Such a 'neutral' form of **1a** would be a co-crystal of different stoichiometry to **1b**, not observed under any other conditions.

Heating OA and BPY together in a test tube at atmospheric pressure, at either 125 or 150 °C, resulted in formation of a mixture of **2a** and **2b**, showing that in this case both the salt and co-crystal form in the solid state before sublimation. However,

both **2a** and **2b** could also be crystallised by vacuum sublimation when the starting materials were not in physical contact with one another, confirming that formation of both the salt and the co-crystal from the gas phase is occurring (as with **1a** and **1b**). These experiments also show that, in the case of **2a** and **2b**, the multicomponent materials can be formed by heating and then re-sublimed. This led us to investigate the re-sublimation of all six multicomponent crystals.

Re-sublimation experiments were carried out in a similar manner to the original sublimation experiments, i.e. in a Schlenk tube heated in an oil bath, *in vacuo* (~0.6 mbar). We found that most of the multicomponent crystals in this study (with the exception of **1c** and **1d**) can be re-sublimed (Scheme S1).

Both **1a** and **1b** re-sublime at 90 °C, but the salt does so to a lesser extent, after a longer time and will only re-sublime optimally at higher temperatures than the co-crystal (i.e. 110 °C). In fact, the co-crystal **1b** can be isolated from a mixture of **1a** and **1b** by re-sublimation at 90 or 110 °C if the apparatus is removed from heat after 2 hours (i.e. before **1a** starts to crystallise). If one or three additional equivalents of HMT are added to **1a** in a Schlenk and the mixture heated under vacuum (to 90 or 110 °C), crystals of **1b** are isolated (along with unreacted HMT). This conversion of **1a** to **1b** requires proton transfer. Conversely, when an extra equivalent of SA or HMT is added to **1b** and the mixture heated under vacuum, no conversion to **1a** is observed, and **1b** crystallises. During re-sublimation, co-crystals **1c** and **1d** convert to **1b**. This is probably because **1b** is the favoured product (it is also observed to form preferentially during co-sublimation). Adding extra succinic acid to **1a** during re-sublimation leads to this salt re-crystallising in larger amounts, with very small amounts of HMT crystallising separately, making this the preferred method for crystallising pure **1a**. The product obtained appears to be, to some extent, dependent on the relative amounts of conformer present in the gas phase.

Salt **2a** and co-crystal **2b** can both be re-sublimed at the same temperature (for example 170 °C), but in all experiments crystals of both forms recrystallise, irrespective of whether **2a** or **2b** is present initially. The same physical distribution of products is observed as with direct co-sublimation, i.e. a band of **2b** above a band of **2a**. The two products can easily be separated due to this difference in deposition region.

It is clear that salts can be formed by co-sublimation of the neutral components, and also that salts are able to re-sublime. This is contrary to our original hypothesis that sublimation would selectively produce co-crystals, because ions are not stable in the gas phase. It is also clear that proton transfer reactions are occurring in both co- and re-sublimation. During co-sublimation, our experiments clearly indicate that this proton transfer occurs *after* the molecules enter the gas phase. One possibility is that during co-sublimation, neutral molecules are entering the gas phase and crystallising as a co-crystal, and that the hydrogen atom transfer to form the salt is only occurring in the solid state after the product has crystallised. Similarly, during re-sublimation, it is possible that heating a salt causes this same shift of the acidic hydrogen atom before the neutral molecules enter the gas phase. It is known that proton migration can occur in a strongly hydrogen-bonded co-crystal on changes in temperature.[30] To explore this possibility in system **1**, a salt re-sublimation experiment was carried out inside an environmental gas cell[31] mounted on a single-crystal diffractometer. Our aim was to determine the crystal structure of the bulk material as it is heated under vacuum, to confirm that no shift in the hydrogen atom position is observed before sublimation. A crystal of salt **1a** was placed under static vacuum (~0.9 mbar) inside a glass capillary on a gas cell, which was mounted on a diffractometer. The temperature was gradually increased from room temperature, and the structure was determined *in vacuo* at 20° intervals. The structural data collected at 90 °C show that the salt has remained essentially unchanged on heating, and that the acidic hydrogen atoms remain attached to the HMT cations (Table S3, S4). Hydrogen atoms were placed on peaks in the electron density map that were clearly evident, and their positions were not fixed in any way (Fig. S28-S31). Further heating of the crystal above 90 °C caused it to re-sublime. These results show that it is unlikely that a bulk neutral co-crystal similar to **1a** exists right before re-sublimation, although it is possible that proton transfer occurs on the surface of the crystal to yield small numbers of neutral molecules which then sublime, and then de-sublime, after which proton transfer once again occurs to yield the salt.

It is also possible that material enters the gas phase as ion pairs or clusters that have an overall neutral charge. This may also be relevant during co-sublimation: hydrogen-bonded clusters of molecules in the gas phase may allow for proton transfer to occur prior to de-sublimation if a stable ion pair is formed as a result. It has been reported that gas-phase proton transfer can take place in the gas phase for strong Bronsted acids and bases where the product of the reaction is an ion-pair complex,[32] and experimental evidence for the existence of such ion pairs in the gas phase has been reported.[33] Other reports have shown that a cluster of molecules is needed for proton transfer to occur.[34,35]

In order to investigate the possible existence of clusters in the gas phase, we turned to mass spectrometry. Attempts were made to carry out measurements on solid samples vaporised using an Atmospheric Solids Analysis Probe (ASAP), however samples degraded before sublimation as a vacuum could not be applied. Similar experiments were carried out under vacuum using an in-house-assembled mass spectrometer. However, crystals of the salt or co-crystal deposited inside the cooler instrument tubing, as heat could not be applied uniformly throughout the instrument. Finally, crystals of salt **1a** were dissolved in methanol and analysed using time-of-flight mass spectrometry. A peak was observed at m/z 257 (Fig. S32), indicating the presence of a hydrogen-bonded adduct of HMT and SA. Although not a replication of the conditions in the sublimation experiment, this does indicate the stability of such hydrogen-bonded adducts.

In conclusion, we have shown that both salts and co-crystals of organic components can be crystallised from the gas phase by co-sublimation. The re-sublimation of both salts and co-crystals was also observed. Preliminary gas-cell and TOF-MS experiments indicate the possibility that ionised molecules are entering the gas phase on re-sublimation, probably as neutral

ion pairs or clusters. During co-sublimation, we have shown that proton transfer to form the salt takes place after the neutral coformers enter the gas phase. It is possible that the formation of small clusters of molecules in the gas phase allows proton transfer to take place, resulting in a stable ion pair or cluster. This may explain why salts are only observed to crystallise from sublimation at higher temperatures: at higher temperatures there are more molecules in the gas phase, and clusters are more likely to form. However, it is also possible that proton transfer occurs in the solid state after deposition of neutral molecules, and only neutral molecules are present in the gas phase. In this case it is unclear why both a salt and a co-crystal should form from sublimation. Investigations to probe both possibilities are ongoing.

In contrast to solution crystallisation, the outcome of sublimation crystallisation is predictable and can be controlled with temperature and time. Mechanochemical co-crystallisation is arguably more predictable, but does not result in single crystals. Co-sublimation results in the crystallisation of multiple products in distinct bands, which can be separated to obtain pure material. The efficacy of re-sublimation for the separation of mixtures of multicomponent crystals was also demonstrated. Sublimation can thus be used to selectively prepare salts or co-crystals.

It is clear from this work that sublimation is a powerful tool for the controlled crystallisation of both organic co-crystals and salts. We hope that this report, highlighting the ease with which organic salts can be prepared by sublimation, will result in increased interest in this surprisingly versatile technique.

The authors would like to thank the National Research Foundation, the Wilhelm Frank Scholarship Fund and Stellenbosch University for funding, as well as Isabella E. Claassens for help with the gas cell experiment. VJS thanks Rhodes University and the Sandisa Imbewu fund. TOF-MS measurements were carried out by the Central Analytical Facility at Stellenbosch University.

Conflicts of interest

There are no conflicts to declare.

Notes and references

1 S. R. Byrn, G. Zografi and X. Chen, *Solid State Properties of Pharmaceutical Materials,* John Wiley & Sons, Inc., Hoboken, 2017.
2 L. Casali, L. Mazzei, O. Shemchuk, L. Sharma, K. Honer, F. Grepioni, S. Ciurli, D. Braga and J. Baltrusaitis, *ACS Sustain. Chem. Eng.*, 2019, **7**, 2852.
3 R. V. Kent, R. A. Wiscons, P. Sharon, D. Grinstein, A. A. Frimer and A. J. Matzger, *Cryst. Growth Des.*, 2018, **18**, 219.
4 M. Li, Z. Li, Q. Zhang, B. Peng, B. Zhu, J. Wang, L. Liu and X. Mei, *Cryst. Growth Des.*, 2018, **18**, 6123.
5 C. Aakeröy, *Acta Crystallogr. Sect. B Struct. Sci. Cryst. Eng. Mater.*, 2015, **71**, 387.
6 E. Grothe, H. Meekes, E. Vlieg, J. H. ter Horst and R. de Gelder, *Cryst. Growth Des.*, 2016, **16**, 3237.
7 In this work, any crystal containing ions is classified as a salt.
8 C. B. Aakeröy, M. E. Fasulo and J. Desper, *Mol. Pharm.*, 2007, **4**, 317.
9 N. B. Báthori, P. Bombicz, S. A. Bourne and G. A. Venter, *New J. Chem.*, 2010, **34**, 405.
10 B. Sarma, R. Thakuria, N. K. Nath and A. Nangia, *CrystEngComm*, 2011, **13**, 3232.
11 R. S. Zhu, J. H. Wang and M. C. Lin, *J. Phys. Chem. C*, 2007, **111**, 13831.
12 R. Zhu and M. C. Lin, *J. Phys. Chem. C*, 2008, **112**, 14481.
13 S. Blairs, *J. Chem. Thermodyn.*, 2006, **38**, 1484.
14 E. D. Raczyńska, J.-F. Gal, P.-C. Maria and M. Szeląg, *Croat. Chem. Acta*, 2009, **82**, 87.
15 P. M. J. Szell, S. A. Gabriel, E. Caron-Poulin, O. Jeannin, M. Fourmigué and D. L. Bryce, *Cryst. Growth Des.*, 2018, **18**, 6227.
16 X. Fang, X. Yang and D. Yan, *J. Mater. Chem. C*, 2017, **5**, 1632.
17 T. Zhang, Q. Yu, X. Li and X. Ma, *J. Cryst. Growth*, 2017, **469**, 114.
18 S. W. Robinson, D. A. Haynes and J. M. Rawson, *CrystEngComm*, 2013, **15**, 10205.
19 T. Carstens, D. A. Haynes and V. J. Smith, *Cryst. Growth Des.*, 2020, **20**, 1139.
20 M. Karimi-Jafari, L. Padrela, G. M. Walker and D. M. Croker, *Cryst. Growth Des.*, 2018, **18**, 6370.
21 X. Ye, Y. Liu, Q. Guo, Q. Han, C. Ge, S. Cui, L. Zhang and X. Tao, *Nat. Commun.*, 2019, **10**, 761.
22 A. J. Cruz-Cabeza, *CrystEngComm*, 2012, **14**, 6362.
23 MarvinSketch 19.8 pK_a calculator plugin; ChemAxon, http://www.chemaxon.com, 2019.
24 L. Androš, P. Planinić and M. Jurić, *Acta Crystallogr. Sect. C Cryst. Struct. Commun.*, 2011, **67**, o337.
25 J. A. Cowan, J. A. K. Howard, H. Puschmann and I. D. Williams, *Acta Crystallogr. Sect. E Struct. Reports Online*, 2007, **63**, o1240.
26 R. Padmavathy, N. Karthikeyan, D. Sathya, R. Jagan, R. Mohan Kumar and K. Sivakumar, *RSC Adv.*, 2016, **6**, 68468.
27 D. Braga, F. Grepioni and G. I. Lampronti, *CrystEngComm*, 2011, **13**, 3122.
28 L. Loots, H. Wahl, L. van der Westhuizen, D. A. Haynes and T. le Roex, *Chem. Commun.*, 2012, **48**, 11507.
29 S. Karki, T. Friščić and W. Jones, *CrystEngComm*, 2008, **11**, 470.
30 J. A. Cowan, J. A.K. Howard, G. J. M. McIntyre, S. M. Lo and I. D. Williams, *Acta Cryst*. 2003, **B59**, 794.
31 T. Jacobs, G. O. Lloyd, J. -A. Gertenbach, K. K. Müller-Nedebock, C. Esterhuysen and L. J. Barbour, *Angew. Chem. Int. Ed.*, 2012, **51**, 4913.
32 P. Burk, I. Koppel, A. Trummal, and I. A. Koppel, *J. Phys. Org. Chem.* 2008, **21**, 571.
33 A. C. Legon, *Chem. Soc. Rev*, 1993, **22**, 153.
34 S. Sen, M. Boda, V. Lata and G. N. Patwari, *Phys. Chem. Chem. Phys.*, 2016, **18**, 16730.
35 M. Boda and G. N. Patwari, *Phys. Chem. Chem. Phys.*, 2017, **19**, 7461.

2.2 Supporting information

Materials and methods

All chemicals and solvents were obtained from Sigma Aldrich South Africa and used without further purification.

Solution crystallisation

Solution crystallisation experiments were carried out in small 10 ml vials using the slow-evaporation method. Starting materials were dissolved in the appropriate solvent or solvent system, with heating, and the resultant solution left to crystallise at room temperature in the capped vial. Crystals formed within a few days.

Mechanochemistry

Mechanochemical milling experiments were carried out using a FTS1000 Shaker Mill from Form-tech Scientific. Samples were loaded into 15 ml steel SmartSnap^{TM} grinding jars containing two 6 mm steel grinding balls (~900 mg each). Samples were milled for 20 minutes at a frequency of 20 Hz (1200 rpm). A total sample mass of roughly 100 mg was used with solvent volume (where applicable for LAG) corresponding to $\eta = 0.25$ µl mg^{-1} (approximately 25 µl).

Sublimation

Sublimation experiments were carried out in thin Schlenk tubes under either static or dynamic vacuum (0.6 mbar line pressure). Tubes were inserted in an oil bath pre-heated to the desired temperature, and sublimation took place onto the sides of the tube within a few hours. For comparison, these experiments were also carried out in a larger Schlenk tube fitted with a water-cooled cold finger as crystallisation surface. To determine the role played by the heat applied during sublimation, select experiments were repeated in a test tube with similar dimensions as a thin Schlenk tube. Here the starting materials were heated in an oil bath and the powder tested to determine how the composition changes due to heat. Finally, sublimation experiments were also carried out in a flat-bottomed Schlenk tube fitted with a cold finger which allowed placement of the starting materials into separate cut-off glass vials. This was done to ensure the starting materials would not come into contact with each other while in the solid state (Figure S1).

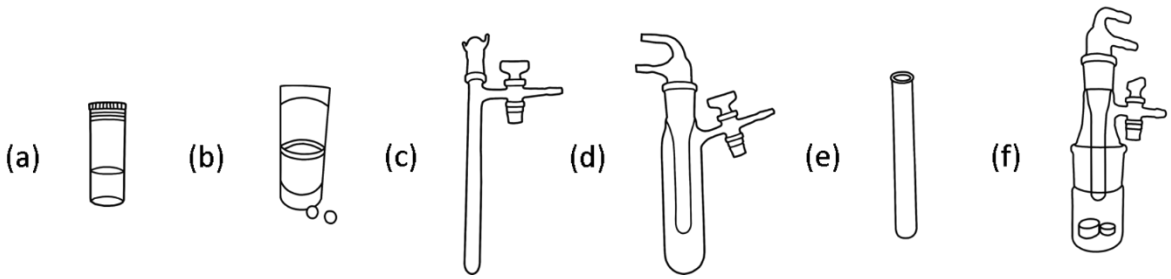

Figure S1. Visual representation of the methods/glassware used in this study. Photographs have been converted to line drawings for clarity, but the images are accurate representations. The methods used include (a) solution crystallisation in small vials, (b) mechanochemistry using a mechanical mill (the grinding jar is shown here), (c) sublimation in a thin Schlenk tube, (d) sublimation in a thick Schlenk tube equipped with a cold finger, (e) heating the starting materials in a test tube, and (f) sublimation without the starting materials being in contact.

Characterisation

Single-crystal X-ray Diffraction (SCXRD) was carried out using a Bruker DUO Apex II CCD area detector diffractometer. The instrument is equipped with an Incoatec IμS microsource coupled with a multilayer mirror optics monochromator. Mo$K\alpha$ radiation of wavelength 0.71073 Å was used for data collections. An Oxford Cryosystems Cryostat (700 Series Cryostream Plus) was used for low temperature data collections at 100 K.

Gas cell SCXRD experiments were carried out using a Bruker D8 Venture diffractometer with a Photon II CPAD detector. The instrument is equipped with an Incoatec IμS microsource coupled with a multilayer mirror optics monochromator. Mo$K\alpha$ radiation of wavelength 0.71073 Å was used for data collections. An Oxford Cryosystems Cryostream 800 series was used for data collections at elevated temperatures and reduced pressure (0.9 mbar).

Data collection and data reduction were carried out using the Bruker software package SAINT[1] through the Apex3 software. This was followed by an absorption correction using SADABS,[2,3] which also corrects for other systematic errors. SHELXT-18,[4] operated through the graphical user interface X-Seed,[5,6] was used to solve the structures using direct methods. The structures obtained were subsequently refined using SHELXL-18.[7] Hydrogen atoms on sp^3- and sp^2-hybridised carbon atoms were placed in calculated positions using riding models, while O–H and N–H hydrogen atoms were placed on maxima in the electron density difference maps. Images were created using POV-ray,[8] as visualised using X-Seed,[5,6] except for the images of the electron density difference maps ($F_{obs} - F_{calc}$; level of detail: 0.118 $Å^{-3}$) (Figure S27 – S30), which were created using Olex2.[9]

Powder X-ray diffraction (PXRD) data were collected on a Bruker D2 Phaser benchtop powder diffractometer equipped with a copper source (1.54183 Å radiation). Data were collected from 2θ = 4 to 40° at a speed of 0.5 seconds per scan (0.016° step size).

Thermogravimetric analysis (TGA) was carried out using a TA Q500 instrument. Samples of roughly 5 – 10 mg were placed in an aluminium pan and heated at 10 °C min^{-1} until after decomposition, and the mass loss recorded. The samples were kept under a constant flow of nitrogen gas (50 ml min^{-1}) to purge decomposition products.

Differential Scanning Calorimetry (DSC) was carried out using a TA Q20 instrument. Powdered samples (3 – 10 mg) were placed in closed aluminium pans vented with a pinhole. An empty reference pan was prepared in the same way. Heat flow in the sample and reference pans were measured as they were heated under a flow of nitrogen gas (50 ml min^{-1}) until just before decomposition, and subsequently cooled to −20 °C. This cycle was repeated once to determine the reproducibility of any observed phenomena.

Fourier Transform Infrared spectroscopy (FTIR) was carried out on powdered samples using a Bruker Alpha P spectrometer with a Platinum ATR attachment.

Mass spectrometric measurements were carried out using a Waters Synapt G2 Time-of-Flight (TOF) MS instrument equipped with an ESI probe, operated in negative ion mode with a cone Voltage of 15 V. The sample was dissolved in methanol before analysis.

Crystallisation of succinic acid with hexamethylenetetramine (1a, 1b, 1c, 1d)

The 2:1 salt of succinic acid and hexamethylenetetramine (**1a**) was formed by combining succinic acid (0.063 g, 0.53 mmol) with hexamethylenetetramine (0.037 g, 0.26 mmol) in 7 ml acetone and stirring them together at 55 °C until the components had completely dissolved. The vial was then capped and left on a shelf to crystallise at room temperature. Colourless plate-like crystals formed after a few hours. A powder of this salt could also be obtained by grinding a 2:1 molar ratio of the two components together for 20 minutes in a ball mill (neat or with the addition of MeOH, THF or water).

The 1:1 co-crystal of succinic acid and hexamethylenetetramine (**1b**) was formed by combining succinic acid (0.045 g, 0.38 mmol) with hexamethylenetetramine (0.053 g, 0.38 mmol) in 7 ml acetone and stirring them together at 55 °C until the components had completely dissolved. The vial was then capped and left on a shelf to crystallise at room temperature. Colourless plate-like crystals formed within a few hours. A powder of this co-crystal could also be obtained by grinding a 1:1 molar ratio of the two components together for 20 minutes in a ball mill (neat or with the addition of MeOH, THF or water).

The 1:2 co-crystal of succinic acid and hexamethylenetetramine (**1c**) was made by combining succinic acid (0.030 g, 0.25 mmol) with hexamethylenetetramine (0.071 g, 0.51 mmol) in 8 ml acetone and stirring them together at 55 °C until the components had completely dissolved. The

vial was then capped and left on a shelf to crystallise at room temperature. Colourless plate-like crystals formed after a day. A powder of this co-crystal could also be obtained by grinding a 1:2 molar ratio of the two components together for 20 minutes in a ball mill (neat or with the addition of MeOH, THF or water). Grinding for shorter amounts of time (e.g. 5 – 15 minutes) lead to formation of the intermediate co-crystal, **1d**, which converts to **1c** upon further grinding. Co-crystal **1d** is therefore suspected to be a kinetic form. No single crystals of **1d** could be obtained, but the FTIR pattern is identical to that of **1c**, indicating that it is also a co-crystal (Figure S26).

Crystals of both **1a** and **1b** were also formed by sublimation. The co-crystal **1b** was made by subliming a 1:1, 2:1 or 3:1 molar ratio of the starting materials at 90 °C under dynamic vacuum for 2 hours, followed by heating for 16 hours under static vacuum. **1b** was also made by subliming a 1:1, 2:1, 1:2 or 1:3 molar ratio of the starting materials at 110 °C under dynamic vacuum for 2 hours. When sublimation was continued for two more hours under static vacuum, **1a** started to form in a band underneath **1b**. All sublimation experiments were carried out at least three times to ensure reproducibility. The co-crystals **1c** and **1d** were never obtained by sublimation, even when component ratios and temperatures were varied.

Crystallisation of oxalic acid with 4,4'-bipyridine (2a, 2b)

The 2:1 salt of oxalic acid and 4,4'-bipyridine (**2a**) was made by combining oxalic acid dihydrate (0.030 g, 0.24 mmol) with 4,4'-bipyridine (0.037 g, 0.24 mmol) in 5 ml water and 5 ml ethanol and stirring them together at 75 °C until the components had completely dissolved (about 30 minutes). The vial was then capped and left on a shelf to crystallise at room temperature. Small, colourless plate-like crystals formed after a day. A powder of this salt could also be obtained by grinding a 2:1 molar ratio of the two components together for 20 minutes in a ball mill (neat or with a few drops of MeOH, THF or water).

The 1:1 co-crystal of oxalic acid and 4,4'-bipyridine (**2b**) was made by combining oxalic acid dihydrate (0.030 g, 0.24 mmol) with 4,4'-bipyridine (0.037 g, 0.24 mmol) in 8 ml water and 6 ml methanol and stirring them together at 60 °C until the components had completely dissolved (about 30 minutes). The vial was then capped and left on a shelf to crystallise at room temperature. Large, striated crystals formed within 24 hours. A powder of this co-crystal could also be obtained by grinding a 1:1 molar ratio of the two components together for 20 minutes in a ball mill (neat or with a few drops of MeOH, THF or water), although some **2a** is also formed concomitantly, so that a pure sample is never obtained.

Both **2a** and **2b** could also be formed by sublimation of a 1:1 molar ratio of the starting materials. Oxalic acid dihydrate (0.030 g, 0.24 mmol) and 4,4'-bipyridine (0.037 g, 0.24 mmol) were added

to a thin Schlenk and heated in a 125 °C oil bath for 1 hour under dynamic vacuum, followed by heating for 3 hours under static vacuum. Co-crystal **2b** formed a band of polycrystalline material, while salt **2a** formed crystals in a band below that, right above the oil line. Crystals of BPY were also formed much higher up in the tube (Figure S2). A variety of sublimation experiments were carried out where conditions were varied, but the outcome remained the same.

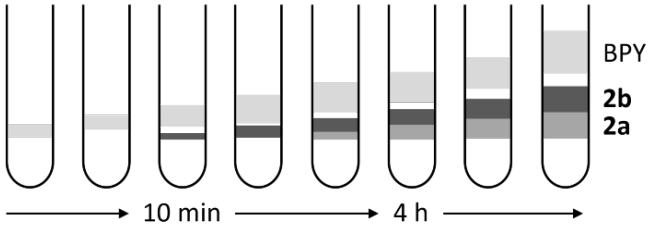

Figure S2. Product distribution on the sides of the tube during the co-sublimation of oxalic acid with BPY.

Crystal structures

Crystal structures for six different multicomponent crystals were obtained. All structural data were collected both at room temperature and at 100 K because temperature has been known to change the ionisation state of molecules, affecting whether a material is a salt or a co-crystal.[9] No major changes in the structures due to temperature were observed, but minor variations will be indicated where applicable. Although the structures of **1b, 2a** and **2b** have been reported previously (CSD refcodes: TOZTIN01[10], EZECOC[11] & XEZDIQ[12]), their structures were re-determined as the position of the acidic hydrogen atom is central to this study. In all cases, IR spectroscopy was used in combination with careful assessment of the C−O bond lengths in order to confirm whether a particular structure is a salt or a co-crystal. It was difficult to determine whether **2b** is a salt or a co-crystal. Acidic hydrogen atoms were placed according to the difference map. The IR indicates this material may contain carboxylate groups. However, carbon-oxygen bond lengths, as well as angles at the heterocyclic nitrogen atom, indicate that this material is a co-crystal, and hydrogen atoms have therefore been placed accordingly in the structure. This results in some long N−H bonds due to very strong hydrogen bonds between the acid and the base.

Crystallographic data are summarised in Table S1 and hydrogen-bond distances and angles in Table S2.

Structures from HMT and SA

Salt **1a** crystallises in the triclinic space group $P\bar{1}$, with one singly protonated HMT cation, one molecule of hydrogen succinate, and two half molecules of neutral succinic acid in the asymmetric unit (ASU) (Figure S3). The succinic acid molecules and succinate ions hydrogen bond to one

another to form grid-like layers (Figure S4). Each grid has alternating rows of R4,4(28) and R8,8(44) hydrogen-bonded motifs. The larger of the two hydrogen-bonded rings is filled by two HMT cations that are hydrogen bonded to the carboxylate groups of hydrogen succinate. The layers stack on top of each other in an offset manner to form a close-packed 3D structure (Figure S4), such that the smaller hydrogen-bonded rings are covered at the top and bottom by HMT molecules of adjacent layers.

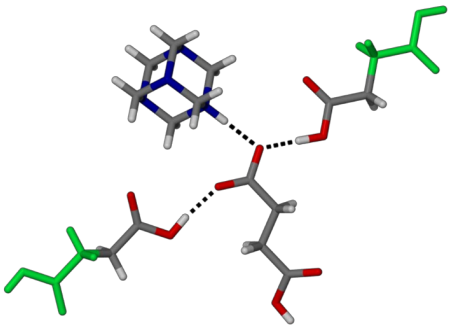

Figure S3. Asymmetric unit of **1a**. Atoms highlighted in green are symmetry generated, (–x, 1–y, 1–z) and (–x, –y–1, –z), and not part of the ASU.

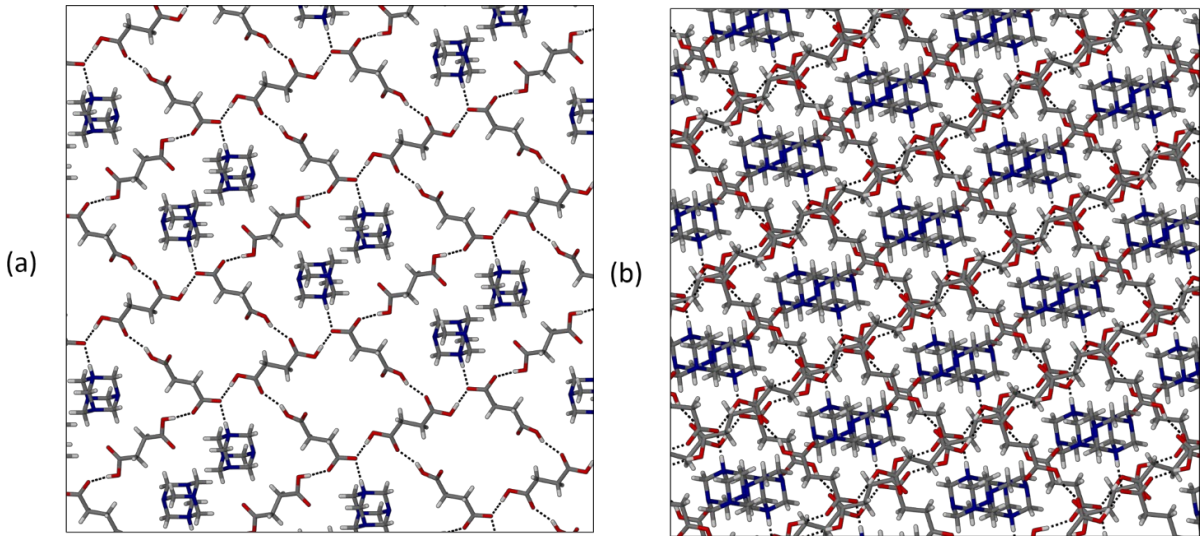

Figure S4. (a) A single hydrogen-bonded layer of **1a** viewed perpendicular to (001). (b) Packing diagram for **1a** viewed along [0−11].

The co-crystal **1b** has been reported previously.[10] It crystallises in the monoclinic space group $P2_1/c$ with one molecule of succinic acid and one molecule of HMT in the ASU. At 100 K, the succinic acid backbone is disordered over two positions in an approximately 50:50 ratio due to rotation in the C–C chain, but the atoms involved in hydrogen bonding are on the same positions for both parts, so the overall packing and hydrogen bonding network is not affected. At room temperature the disorder ratio shifts to 60:40, and the conformation of the whole molecule changes slightly, but again, this does not greatly affect the overall packing. Succinic acid molecules are hydrogen bonded

to HMT molecules, resulting in zig-zag acid-base-acid-base hydrogen-bonded chains running along the *b*-axis (Figure S5a). Chains pack next to each other to form layers, which stack directly on top of one another along [100] (Figure S5b).

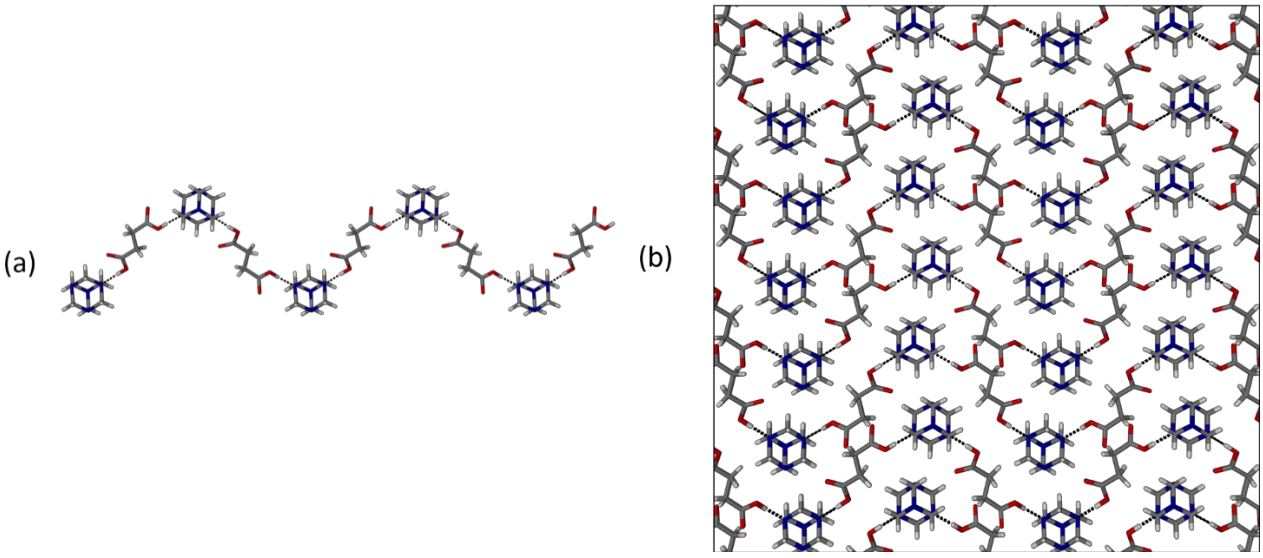

Figure S5. (a) Hydrogen-bonded chain in **1b** viewed along [001], and (b) the packing diagram of **1b** viewed along [100]. The disorder has been omitted in both images for clarity.

Co-crystal **1c** crystallises in the monoclinic space group *C*2/*c* with one molecule of succinic acid and two molecules of HMT in the ASU. The succinic acid backbone is disordered over two positions in an approximately 50:50 ratio due to rotation in the C–C chain, similar to the disorder observed in **1a**. Each molecule of acid hydrogen bonds to two molecules of base so that base-acid-base trimers are formed (Figure S6a). Pairs of trimers pack together in a brick wall pattern, which can be seen when viewed along [010] (Figure S6b).

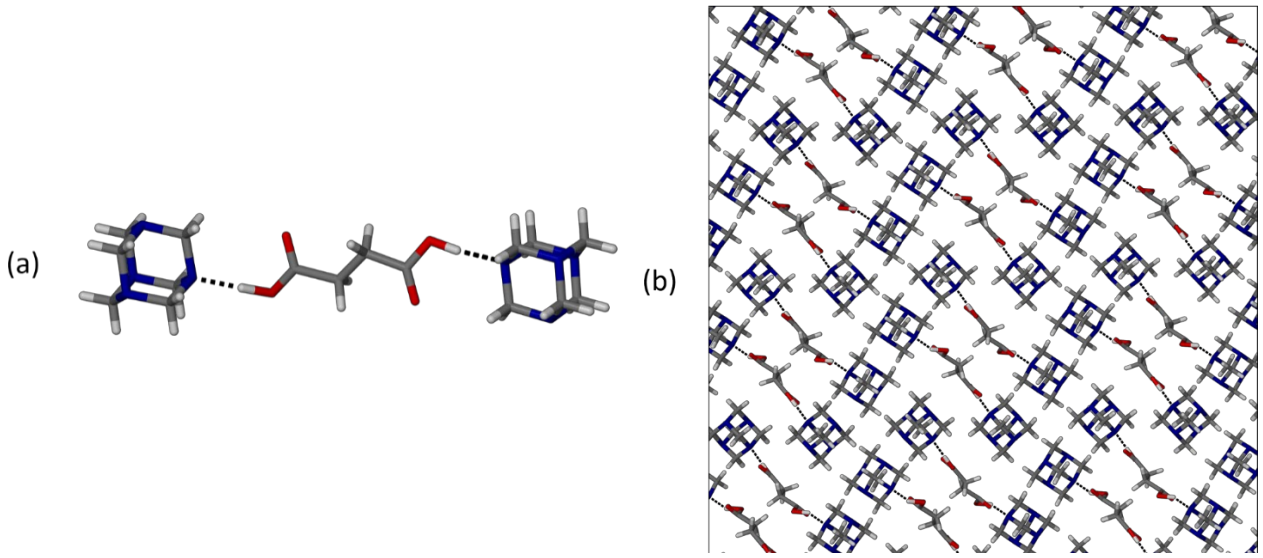

Figure S6. (a) Hydrogen-bonded trimer of **1c**, and (b) the packing diagram viewed along [010]. Disordered parts of SA have been omitted for clarity.

Structures from BPY and OA

The previously-reported salt[11] **2a** crystallises in the triclinic space group $P\bar{1}$ with one molecule of hydrogen oxalate and half a molecule of 4,4'-bipyridinium in the ASU. Two hydrogen oxalate anions hydrogen bond to one another to form an R2,2(10) ring motif (Figure S6). The carboxylate group of each of anion forms an additional hydrogen bond to the NH^+ of 4,4'-bipyridinium, resulting in chains where each molecule of BPY is separated by a pair of anions. Chains stack to form the 3D structure (Figure S7), with offset face-to-face π-π interactions between the BPY aromatic rings (centroid to centroid distance of 3.3146(9) Å).

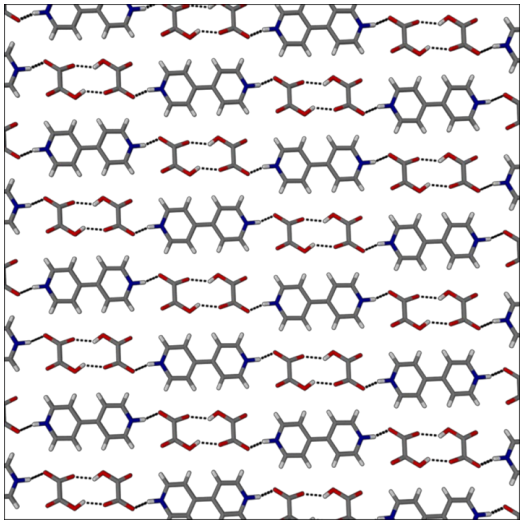

Figure S7. Packing diagram for **2a** viewed along [100].

Co-crystal **2b** crystallises in the triclinic space group $P\bar{1}$ with two molecules of oxalic acid and two molecules of 4,4'-bipyridine in the ASU (Figure S8a). The hydrogen bonds in **2b** are all relatively short (Table S2). The FTIR spectrum we obtained for **2b** has C=O stretching frequencies corresponding to both carboxylic acid and carboxylate groups, indicating that it is a salt (Figure S27), however, the C–O bond lengths and angles between the interacting groups indicate that this is indeed a co-crystal. The peak seemingly indicating a carboxylate group could be due to some **2a** contaminating the sample (Figure S14).

The structure of **2b** is based on acid-base-acid-base chains formed *via* hydrogen bonds. There are two types of hydrogen-bonded chains, type 1 and type 2 (Figure S8a). The BPY molecules in the latter deviate more from planarity; the angle between the planes formed by the two aromatic rings is 22.25(5)° in type 2 chains, while the deviation is only 9.00(4)° in chains of type 1. Chains pack alongside one another to form sheets of either Type 1 or Type 2 chains. Sheets stack on top of each other to give a bilayer-type 3D structure (Figure S8b).

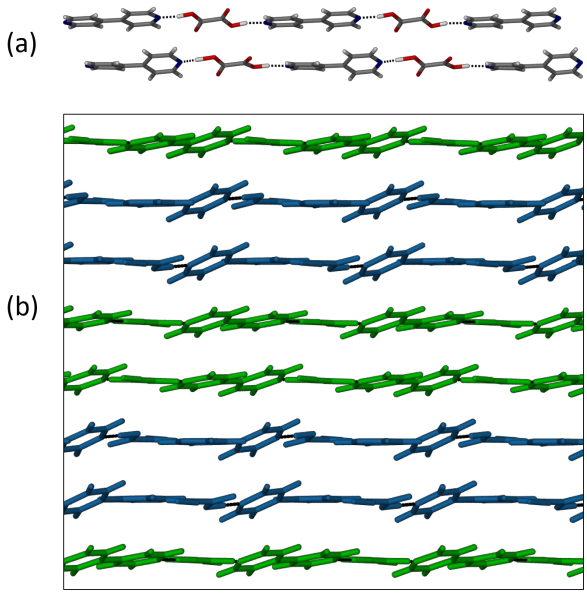

Figure S8. (a) Hydrogen-bonded chains of type 1 (top), and type 2 (bottom), of co-crystal **2b** showing the slight changes in angles. (b) The packing diagram for **2b** viewed along [100] showing how the two types of chains stack (blue = type 1, green = type 2).

Further details regarding re-sublimation

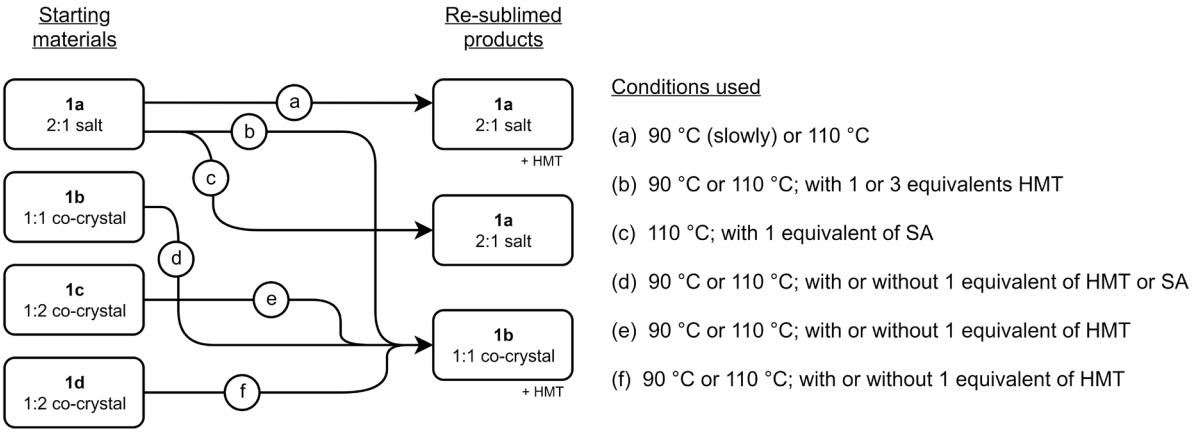

Scheme S1. Summary of the main re-sublimation pathways for crystals consisting of HMT and SA. All experiments were carried out for roughly 18 hours, the first two hours under dynamic vacuum, and the remainder under static vacuum. Starting the experiments using dynamic vacuum allowed for better separation of the different bands of products inside the tube.

A powdered sample of **1a,** obtained from mechanochemical co-crystallisation, was added to a thin Schlenk and heated in a 110 °C oil bath for 2 hours under dynamic vacuum, followed by heating under static vacuum for a further 6 hours. Single-crystal diffraction-quality, colourless crystals of **1a** were obtained, as well as crystals of HMT, which formed higher up in the Schlenk.

A powdered sample of **1a** and one equivalent of HMT was added to a thin Schlenk and heated in a 110 °C oil bath for 2 hours under dynamic vacuum, followed by heating under static vacuum for a further 4 hours. Single-crystal diffraction-quality, colourless crystals of **1b** were obtained, as well as crystals of HMT, which formed higher up in the Schlenk.

A powdered sample of **1a** and one equivalent of SA was added to a thin Schlenk and heated in a 110 °C oil bath for 2 hours under dynamic vacuum, followed by heating under static vacuum for a further 4 hours. Single-crystal diffraction-quality, colourless crystals of **1a** were obtained.

A powdered sample of **1b** was added to a thin Schlenk and heated in a 90 °C oil bath for 2 hours under dynamic vacuum, followed by heating under static vacuum for a further 3 hours. Polycrystalline material of **1b** formed in a band above the oil line, as well as crystals of HMT, which formed higher up in the Schlenk.

A powdered sample of **1c** was added to a thin Schlenk and heated in a 90 °C oil bath for 2 hours under dynamic vacuum, followed by heating under static vacuum for a further 24 hours. Polycrystalline material of **1b** formed in a band above the oil line, as well as crystals of HMT, which formed higher up in the Schlenk.

Similarly, a powdered sample of **1d** was added to a thin Schlenk and heated in a 90 °C oil bath for 2 hours under dynamic vacuum, followed by heating under static vacuum for a further 24 hours. Polycrystalline material of **1b** formed in a band above the oil line, as well as crystals of HMT, which formed higher up in the Schlenk.

The co-crystal **1b** was isolated from a mixture (12 mg **1a** + 12 mg **1b**). The mixture was added to a thin Schlenk and heated in a 110 °C oil bath for 2 hours under dynamic vacuum. Polycrystalline material of **1b** formed in a band above the oil line, as well as crystals of HMT, which formed higher up in the Schlenk.

A powdered sample of **2a** or **2b** was added to a thin Schlenk and heated in a 170 °C oil bath for 4 hours under static vacuum. Crystals of BPY formed high up in the Schlenk, followed by polycrystalline **2a** below that and then **2b** in a band of powder right at the bottom.

Crystallographic tables

Table S1. Crystallographic data for the salts **1a** and **2a**, and the co-crystals **1b**, **1c**, and **2b** (at room temperature and 100 K).

Structure	**1a**		**1b**		**1c**		**2a**		**2b**	
Chemical formula	$C_{14}H_{24}N_4O_8$		$C_{10}H_{18}N_4O_4$		$C_{16}H_{30}N_8O_4$		$C_{14}H_{12}N_2O_8$		$C_{24}H_{20}N_4O_8$	
Formula weight /g mol^{-1}	376.37		258.28		398.48		336.26		492.44	
Crystal system	triclinic		monoclinic		monoclinic		triclinic		triclinic	
Space group	$P\bar{1}$		$P2_1/c$		$C2/c$		$P\bar{1}$		$P\bar{1}$	
Temperature /K	298(2)	100(2)	298(2)	100(2)	298(2)	100(2)	298(2)	100(2)	298(2)	100(2)
a /Å	9.6812(2)	9.6037(4)	6.017(1)	5.8215(8)	21.847(1)	21.654(3)	3.7614(3)	3.6795(7)	8.7731(5)	8.740(1)
b /Å	9.8923(2)	9.8432(4)	18.340(3)	18.363(2)	6.9981(4)	6.948(1)	9.8932(7)	9.855(2)	9.8652(5)	9.849(1)
c /Å	10.3777(3)	10.2613(4)	11.778(2)	11.592(2)	26.359(2)	25.748(4)	10.4498(7)	10.425(2)	13.9929(7)	13.663(2)
α /°	70.346(1)	68.903(1)	90	90	90	90	116.121(1)	116.097(2)	73.741(2)	73.285(2)
β /°	83.328(1)	83.980(1)	99.387(3)	100.266(2)	102.170(1)	101.148(2)	96.721(1)	97.436(2)	72.890(2)	72.292(2)
γ /°	67.442(1)	68.045(1)	90	90	90	90	98.409(1)	97.188(2)	72.483(2)	72.343(2)
Calc. density /g cm^{-3}	1.446	1.490	1.338	1.401	1.344	1.393	1.651	1.694	1.515	1.569
Volume /Å^3	864.26(4)	838.87(6)	1282.3(4)	1219.3(3)	3939.4(4)	3800.7(1)	338.11(4)	329.5(1)	1079.2(1)	1042.5(2)
Z	2	2	4	4	8	8	1	1	2	2
Independent reflections	4299	3442	3199	3017	4898	4758	1679	1630	5389	5192
R_{int}	0.0379	0.0213	0.0286	0.0256	0.0344	0.0276	0.0177	0.0292	0.0744	0.0244
R_1 [I > 2σ(I)]	0.0526	0.0329	0.0718	0.0414	0.0533	0.0473	0.0409	0.0360	0.0936	0.0605

Table S2. Hydrogen bond lengths and angles for **1** and **2** at 100 K.

Structure	D–H···A	D—H /Å	H···A /Å	D···A /Å	D—H···A /°	Symmetry codes
1a	O1–H1···O14	0.87 (2)	1.85 (2)	2.668 (1)	157 (2)	x+1, y−1, z
	O13–H13···O8	0.97 (2)	1.58 (2)	2.544 (1)	178 (2)	
	O9–H9···O7	0.88 (2)	1.73 (2)	2.607 (1)	173 (2)	
	N23–H23···O8	0.94 (2)	1.80 (2)	2.728 (1)	174 (2)	
1b	O1–H1···N9	0.95 (2)	1.73 (2)	2.678 (1)	176 (2)	
	O7A–H7···N13	1.00 (3)	1.73 (3)	2.701 (6)	163 (2)	−x+1, y−1/2, −z+1/2
	O7B–H7···N13	0.96 (3)	1.73 (3)	2.652 (6)	161 (2)	−x+1, y−1/2, −z+1/2
	C5B–H5B2···O8B	0.99	1.72	2.649 (3)	155.3	−x+1, −y+1, −z
1c	O1A–H1···N19	0.99 (2)	1.75 (2)	2.743 (2)	175 (5)	−x+1, −y, −z+1
	O1B–H1···N19	0.93 (2)	1.756 (2)	2.675 (2)	167 (5)	−x+1, −y, −z+1
	O7B–H7B···N9	0.92 (3)	1.82 (3)	2.737 (3)	177 (6)	−x+1/2, −y+3/2, −z+1
	O7A–H7A···N9	0.92 (3)	1.72 (3)	2.634 (2)	171 (5)	−x+1/2, −y+3/2, −z+1
2a	O1–H1···O5	0.92 (2)	2.21 (2)	2.694 (1)	112 (2)	
	O1–H1···O5	0.92 (2)	1.82 (2)	2.594 (1)	141 (2)	−x+2, −y+2, −z+1
	N7–H7···O6	1.03 (2)	1.64 (2)	2.638 (1)	161 (2)	
2b	O1–H1···N16	1.34 (4)	1.24 (4)	2.579 (1)	179 (4)	x+1, y+1, z
	O6–H6···N7	1.10 (3)	1.46 (3)	2.543 (1)	166 (3)	
	O24–H24···N25	1.07 (4)	1.48 (4)	2.535 (1)	167 (4)	
	O19–H19···N34	1.07 (4)	1.50 (4)	2.559 (1)	169 (4)	x−1, y−1, z

Gas cell experiments

Table S3. Crystallographic data for **1a** compared to data collected under vacuum conditions using the gas cell.

Structure	**1a**	**1a_RT_vac**	**1a_323K_vac**	**1a_343K_vac**	**1a_363K_vac**
Temperature /K	298(2)	297(2)	323(2)	343(2)	363(2)
Pressure /mbar	atmospheric	0.9	0.9	0.9	0.9
a /Å	9.6812(2)	9.6855(5)	9.6936(3)	9.7001(3)	9.709(2)
b /Å	9.8923(2)	9.8968(5)	9.9012(2)	9.9056(3)	9.907(1)
c /Å	10.3777(3)	10.3851(5)	10.3959(3)	10.4083(4)	10.410(2)
α /°	70.346(1)	70.349(2)	70.525(1)	70.699(1)	70.848(5)
β /°	83.328(1)	83.366(2)	83.312(1)	83.300(1)	83.298(5)
γ /°	67.442(1)	67.454(2)	67.369(1)	67.299(1)	67.240(5)
Calc. density /g cm^{-3}	1.446	1.444	1.440	1.436	1.433
Volume /Å^3	864.26(4)	865.74(8)	868.18(4)	870.69(5)	872.2(2)
Z	2	2	2	2	2
Independent reflections	4299	4106	4266	4269	4338
R_{int}	0.0379	0.0341	0.0241	0.0255	0.0358
R_1 [I > 2σ(I)]	0.0526	0.0557	0.0526	0.0544	0.0526

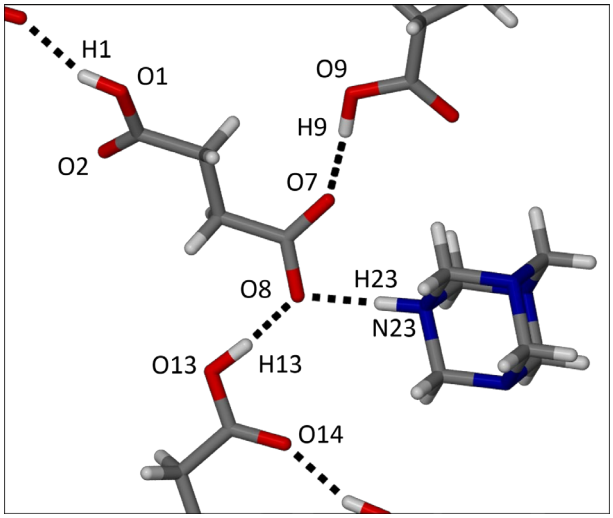

Figure S9. Labels for atoms of **1a** that are involved in hydrogen bonding.

Table S4. Hydrogen bond lengths and angles for **1a** at elevated temperatures under vacuum conditions.

Temperature	D–H···A	D—H /Å	H···A /Å	D···A /Å	D—H···A /°	Symmetry codes
297 K	**N23–H23···O8**	**0.94 (3)**	**1.79 (3)**	**2.731 (2)**	**173 (2)**	
	O1–H1···O14	0.87 (3)	1.87 (3)	2.694 (2)	158 (2)	x−1, y+1, z
	O13–H13···O8	0.96 (3)	1.60 (3)	2.548 (2)	173 (3)	
	O9–H9···O7	0.91 (3)	1.69 (3)	2.595 (2)	176 (3)	
323 K	**N23–H23···O8**	**0.91 (2)**	**1.83 (2)**	**2.731 (2)**	**172 (2)**	
	O1—H1···O14	0.83 (3)	1.91 (3)	2.695 (2)	156 (2)	x−1, y+1, z
	O13–H13···O8	0.94 (3)	1.61 (3)	2.551 (2)	175 (2)	
	O9–H9···O7	0.92 (3)	1.68 (3)	2.593 (2)	171 (3)	
343 K	**N23–H23···O8**	**0.89 (2)**	**1.85 (2)**	**2.731 (2)**	**171 (2)**	
	O1—H1···O14	0.84 (3)	1.90 (3)	2.696 (2)	157 (2)	x−1, y+1, z
	O13–H13···O8	0.93 (3)	1.62 (3)	2.551 (2)	175 (2)	
	O9–H9···O7	0.92 (3)	1.68 (3)	2.591 (2)	171 (3)	
363 K	**N23–H23···O8**	**0.89 (2)**	**1.85 (2)**	**2.733 (2)**	**171 (2)**	
	O1—H1···O14	0.84 (3)	1.90 (3)	2.696 (2)	158 (2)	x−1, y+1, z
	O13–H13···O8	0.93 (3)	1.62 (3)	2.552 (2)	175 (2)	
	O9–H9···O7	0.93 (3)	1.68 (3)	2.589 (2)	168 (3)	

Powder X-Ray diffraction patterns

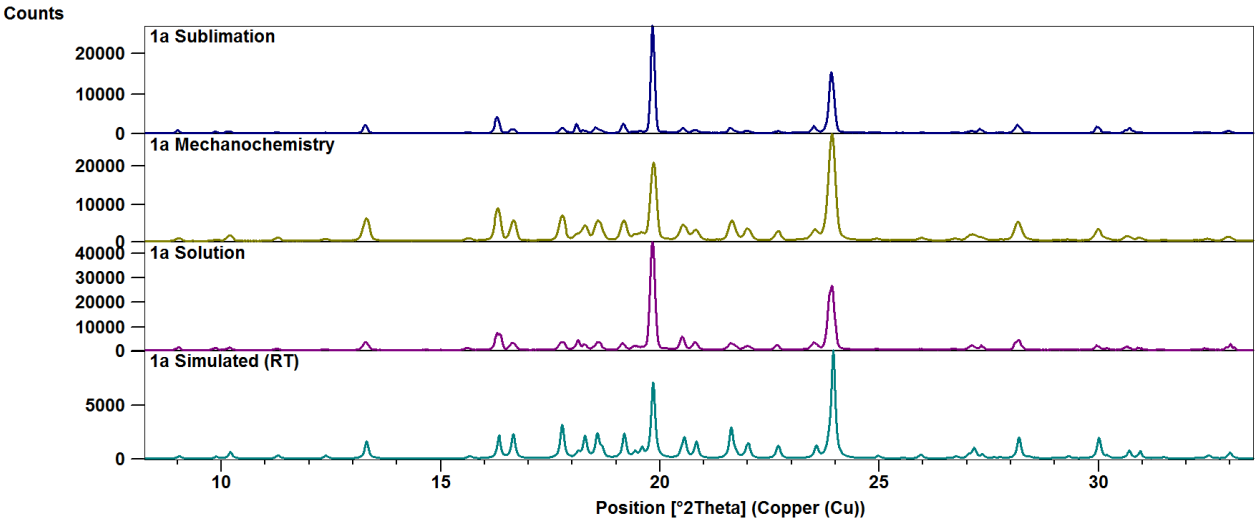

Figure S10. Comparison of the experimental powder patterns of **1a** (obtained from sublimation, LAG using THF, and solution) to the pattern simulated from single-crystal data collected at room temperature.

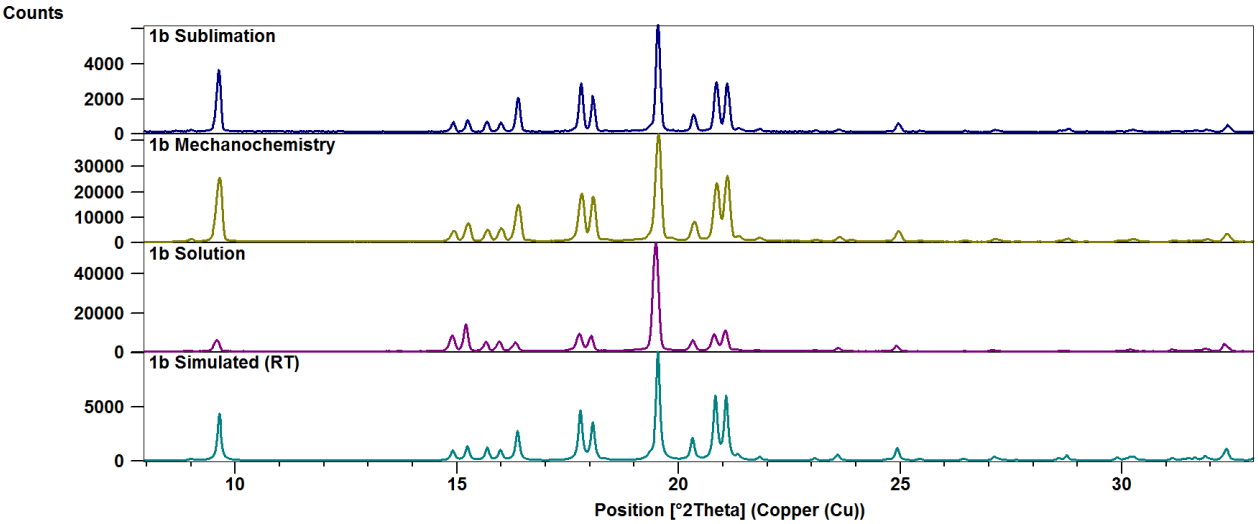

Figure S11. Comparison of the experimental powder patterns of **1b** (obtained from sublimation, LAG using THF, and solution) to the pattern simulated from single-crystal data collected at room temperature.

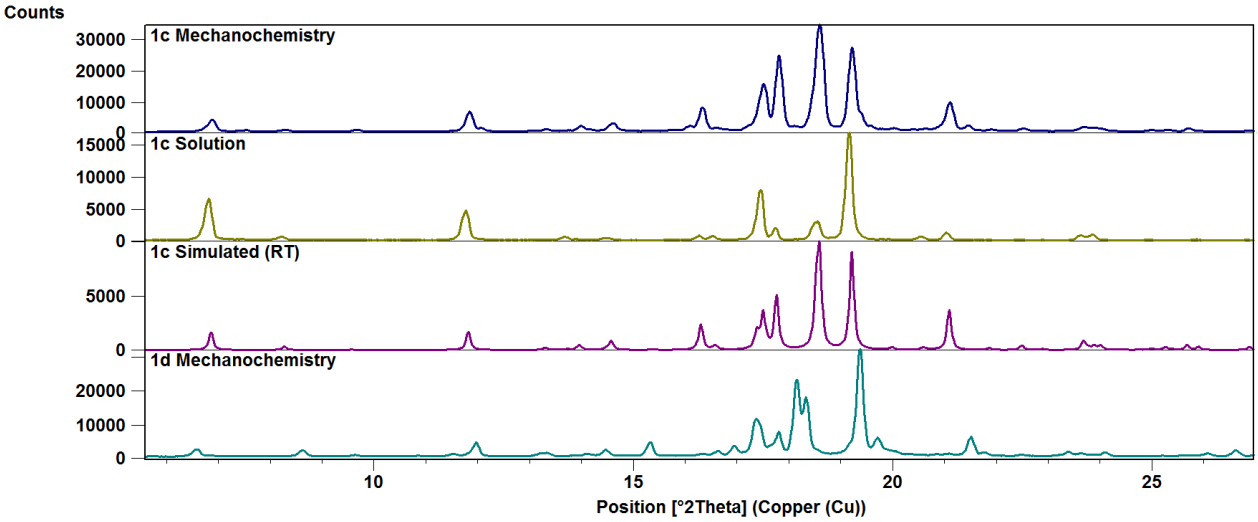

Figure S12. Comparison of the experimental powder patterns of **1c** (obtained from LAG using THF and solution) to the pattern simulated from single-crystal data collected at room temperature. These patterns are also compared to the experimentally obtained pattern for **1d**, which clearly differs from **1c**.

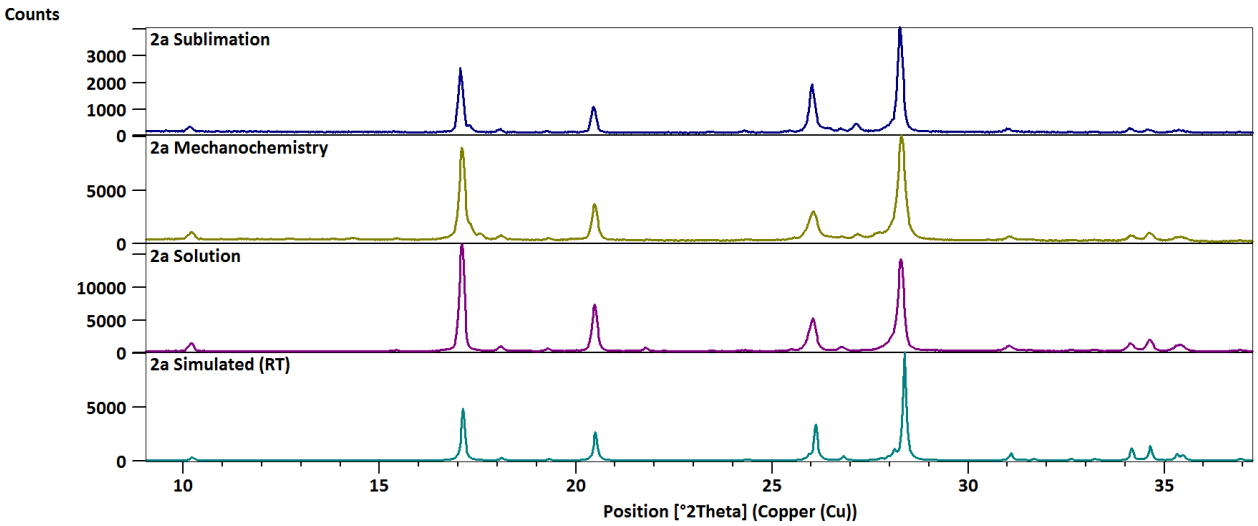

Figure S13. Comparison of the experimental powder patterns of **2a** (obtained from sublimation, LAG using THF, and solution) to the pattern simulated from single-crystal data collected at room temperature.

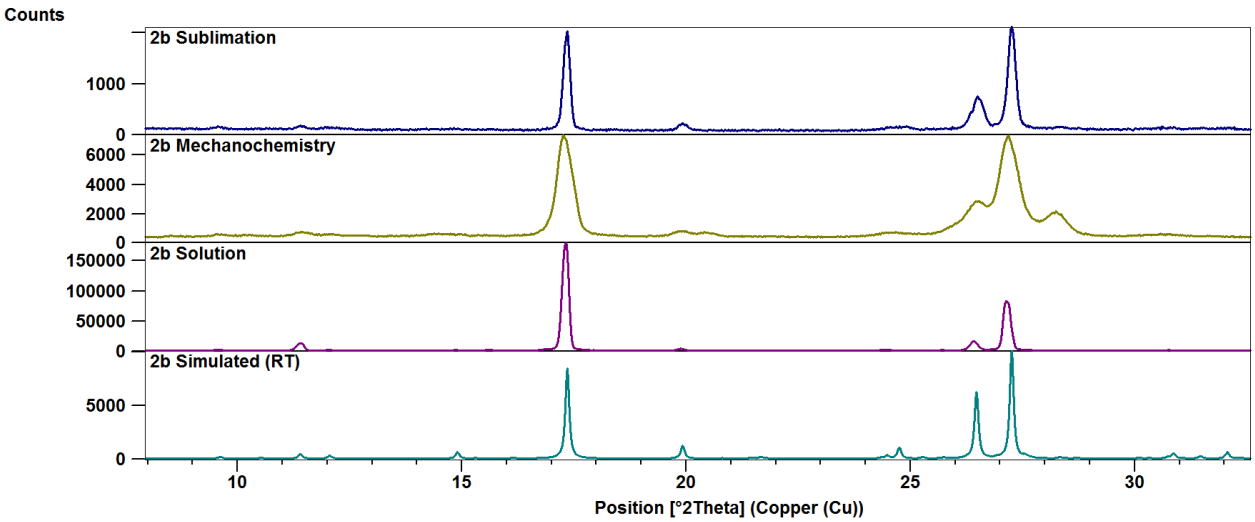

Figure S14. Comparison of the experimental powder patterns of **2b** (obtained from sublimation, LAG using THF, and solution) to the pattern simulated from single-crystal data collected at room temperature. The extra peaks in the mechanochemistry pattern (around 20.5 and 28.2°) are from **2a** forming concomitantly.

Interconversions between stoichiometries by grinding

All the different forms can be interconverted by grinding each with extra equivalents of starting material for 20 minutes in a ball mill (with 20 µl of MeOH; $\eta = 0.25$ µl mg^{-1}). A summary of the results follows:

- **1a** (58 mg, 0.15 mmol) + 1 equivalent HMT (22 mg, 0.16 mmol) gives **1b** (Figure S15)
- **1a** (38 mg, 0.10 mmol) + 3 equivalents HMT (42 mg, 0.30 mmol) gives **1d** (converts to **1c** upon longer grinding) (Figure S16)
- **1b** (55 mg, 0.21 mmol) + 1 equivalent SA (25 mg, 0.21 mmol) gives **1a** (Figure S17)
- **1b** (52 mg, 0.20 mmol) + 1 equivalent HMT (28 mg, 0.20 mmol) gives **1d** (converts to **1c** upon longer grinding) (Figure S16)
- **1c** (62 mg, 0.16 mmol) + 1 equivalent SA (18 mg, 0.15 mmol) gives **1b** (Figure S17)
- **1c** (39 mg, 0.098 mmol) + 3 equivalents SA (35 mg, 0.30 mmol) gives **1a** (Figure S17)
- **2a** (54 mg, 0.16 mmol) + 1 equivalent BPY (25 mg, 0.16 mmol) gives **2b** (Figure S18)
- **2b** (64 mg, 0.13 mmol) + 1 equivalent OA·2H$_2$O (16 mg, 0.13 mmol) gives a mixture of **2a** and **2b**, even when milled for 60 minutes (Figure S18)

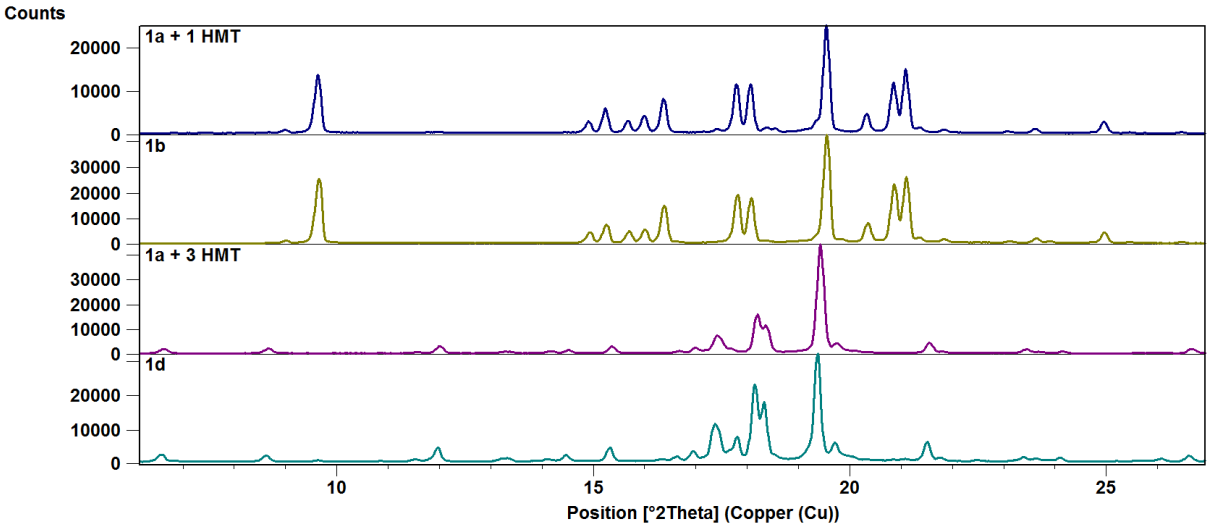

Figure S15. Salt **1a** can be converted to co-crystal **1b** when milled with an additional equivalent of HMT, and to **1d** when milled with three extra equivalents of HMT. The reference patterns for **1b** and **1d** shown here were obtained from previous mechanochemistry experiments and can be used to identify the products obtained.

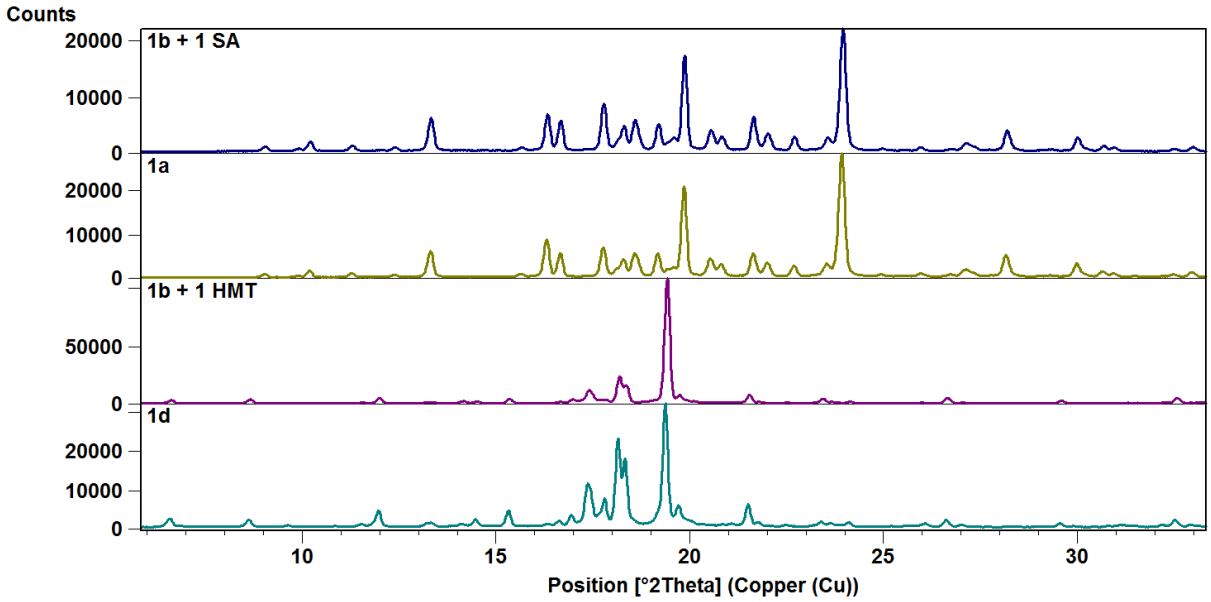

Figure S16. Co-crystal **1b** can be converted to salt **1a** when milled with an additional equivalent of SA, and to **1d** when milled with an extra equivalent of HMT. The reference patterns for **1a** and **1d** shown here were obtained from previous mechanochemistry experiments and can be used to identify the products obtained.

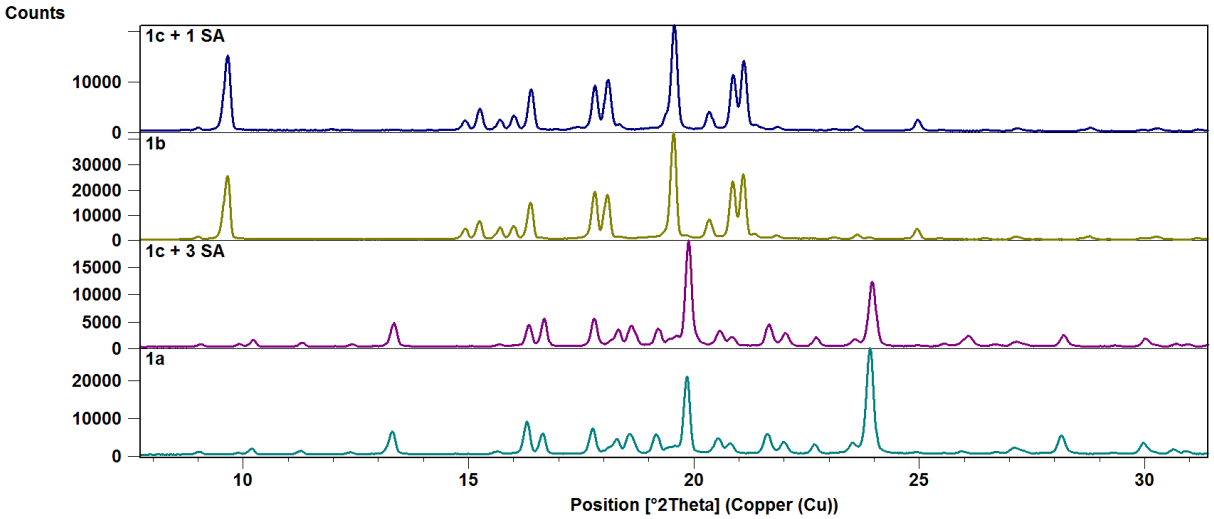

Figure S17. Co-crystal **1c** can be converted to co-crystal **1b** when milled with an additional equivalent of SA, and to **1a** when milled with three extra equivalents of SA. The reference patterns for **1b** and **1a** shown here were obtained from previous mechanochemistry experiments and can be used to identify the products obtained.

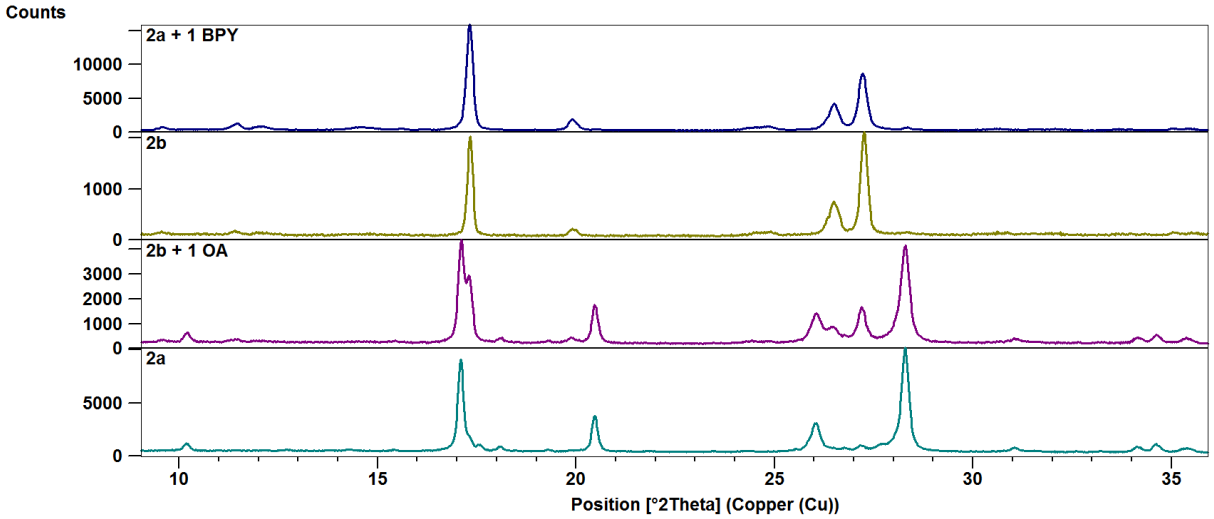

Figure S18. Salt **2a** can be converted to **2b** when milled with an additional equivalent of BPY. On the other hand, when co-crystal **2b** is milled with an extra equivalent of OA, it only partially converts to **2a**, while some **2b** remains. The reference patterns for **2b** and **2a** shown here were obtained from previous mechanochemistry experiments and can be used to identify the products obtained.

Test tube heating experiments

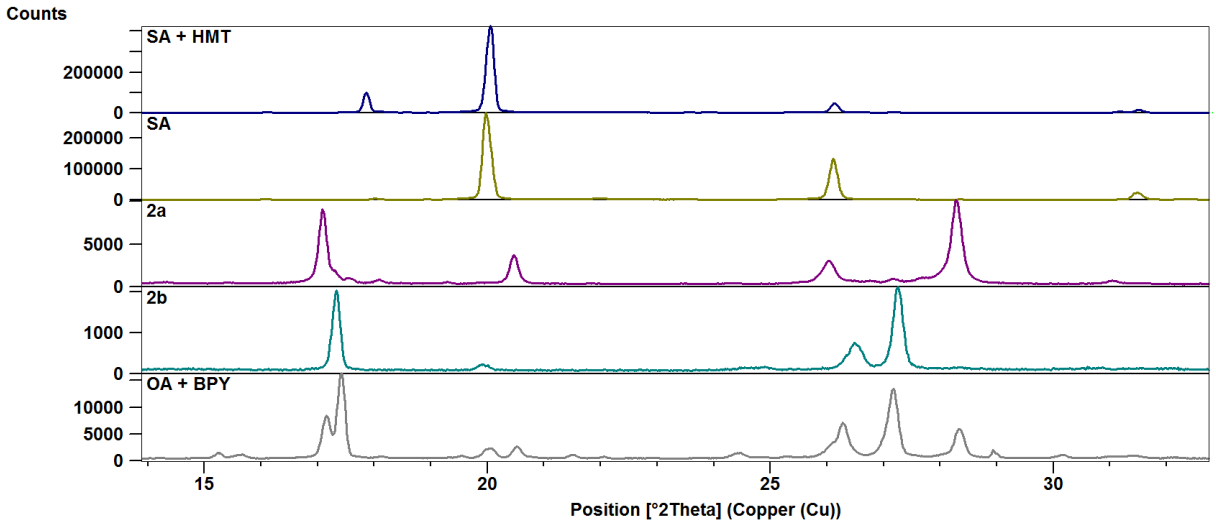

Figure S19. When SA and HMT are heated together under ambient conditions (top pattern), HMT sublimes, leaving only succinic acid. On the other hand, OA and BPY combine to form both **2a** and **2b** when heated together under ambient conditions (bottom pattern).

Thermal analysis (TGA and DSC)

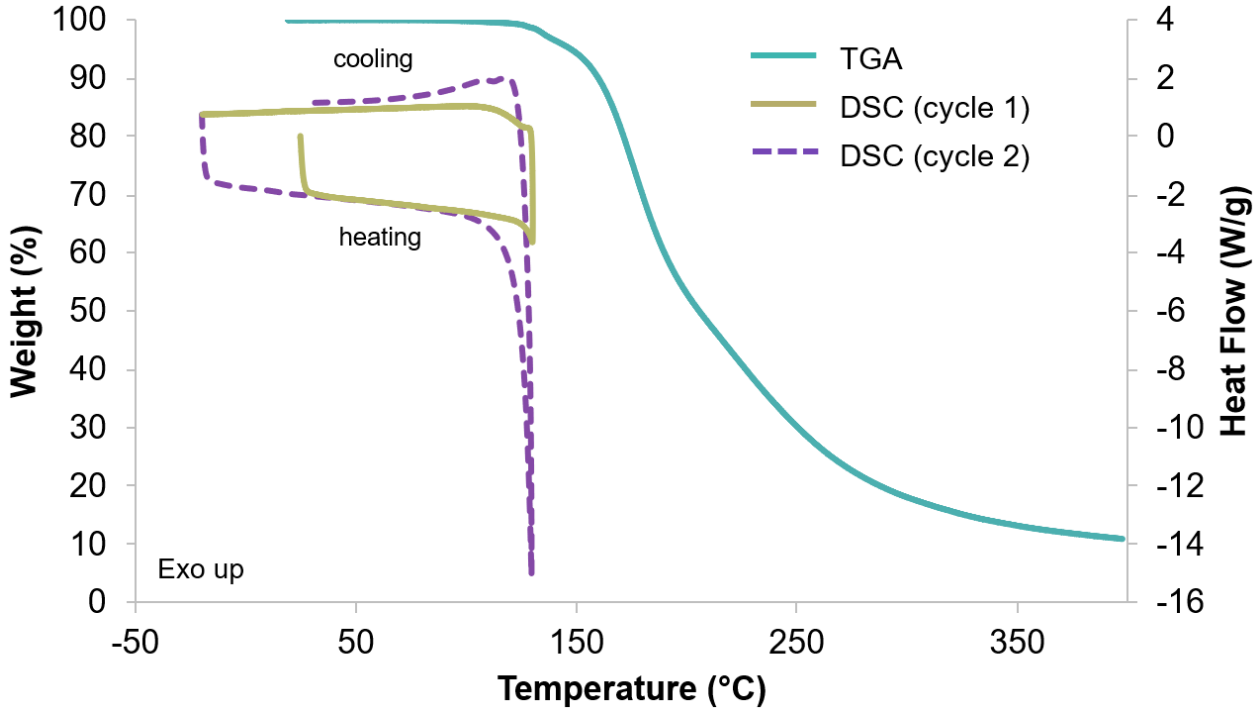

Figure S20. Thermal analysis results for **1a**. TGA trace shown in blue and DSC traces in yellow (cycle 1) and purple dashes (cycle 2).

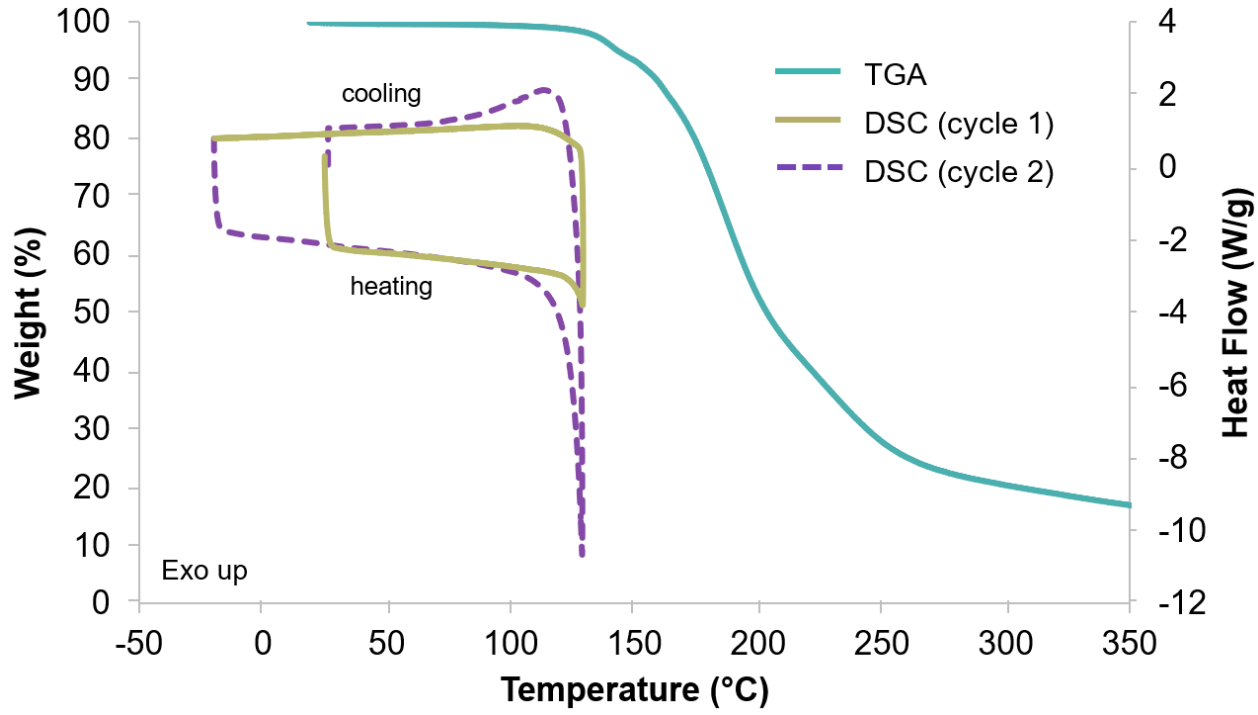

Figure S21. Thermal analysis results for **1b**. TGA trace shown in blue and DSC traces in yellow (cycle 1) and purple dashes (cycle 2).

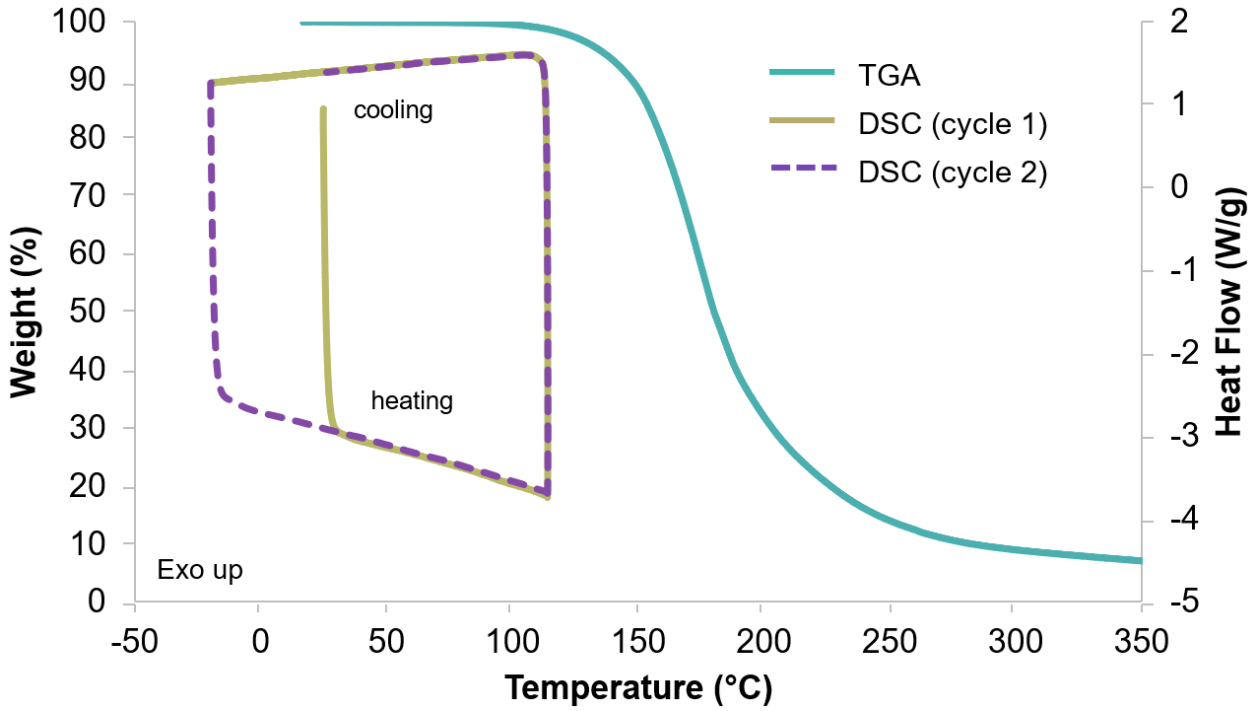

Figure S22. Thermal analysis results for **1c**. TGA trace shown in blue and DSC traces in yellow (cycle 1) and purple dashes (cycle 2).

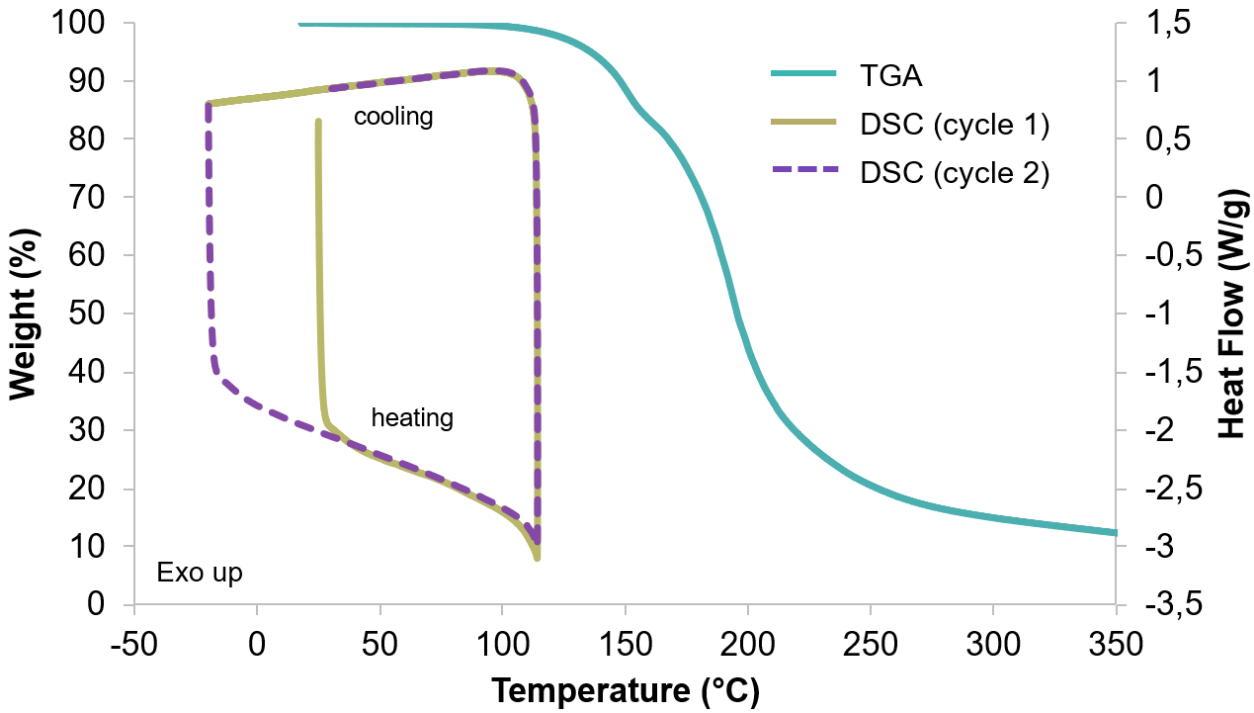

Figure S23. Thermal analysis results for the unknown co-crystal, **1d**. TGA trace shown in blue and DSC traces in yellow (cycle 1) and purple dashes (cycle 2).

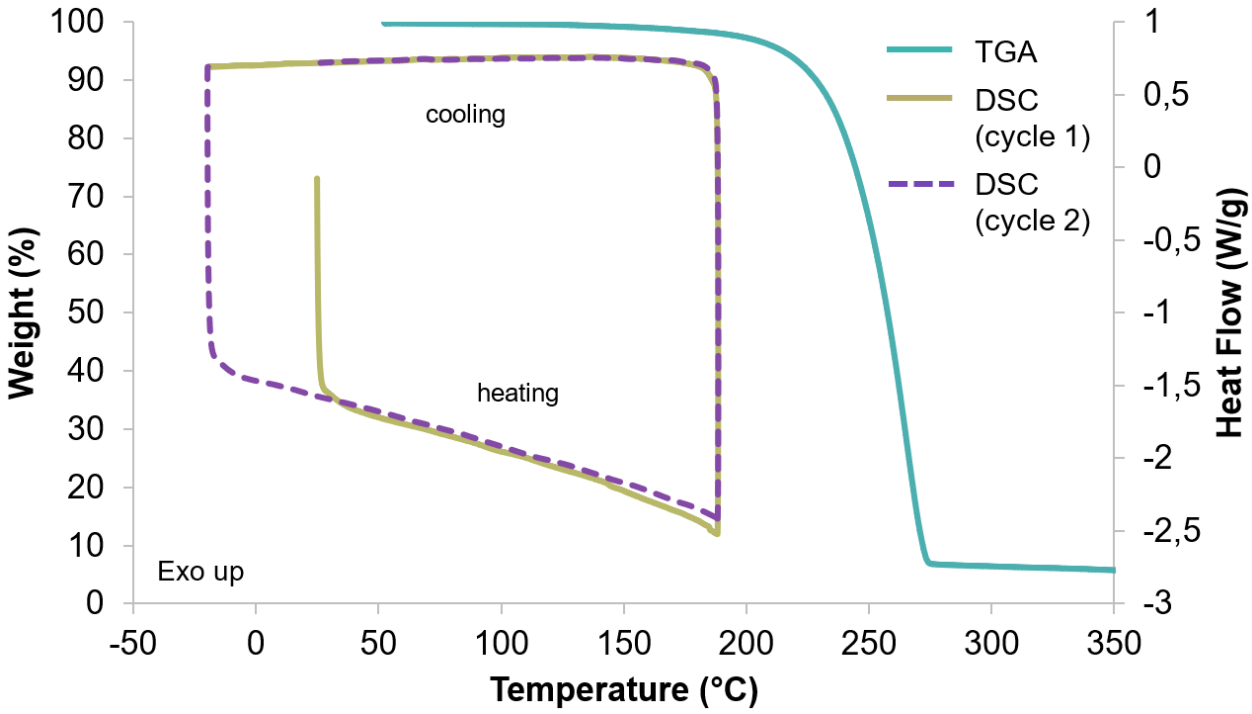

Figure S24. Thermal analysis results for **2a**. TGA trace shown in blue and DSC traces in yellow (cycle 1) and purple dashes (cycle 2).

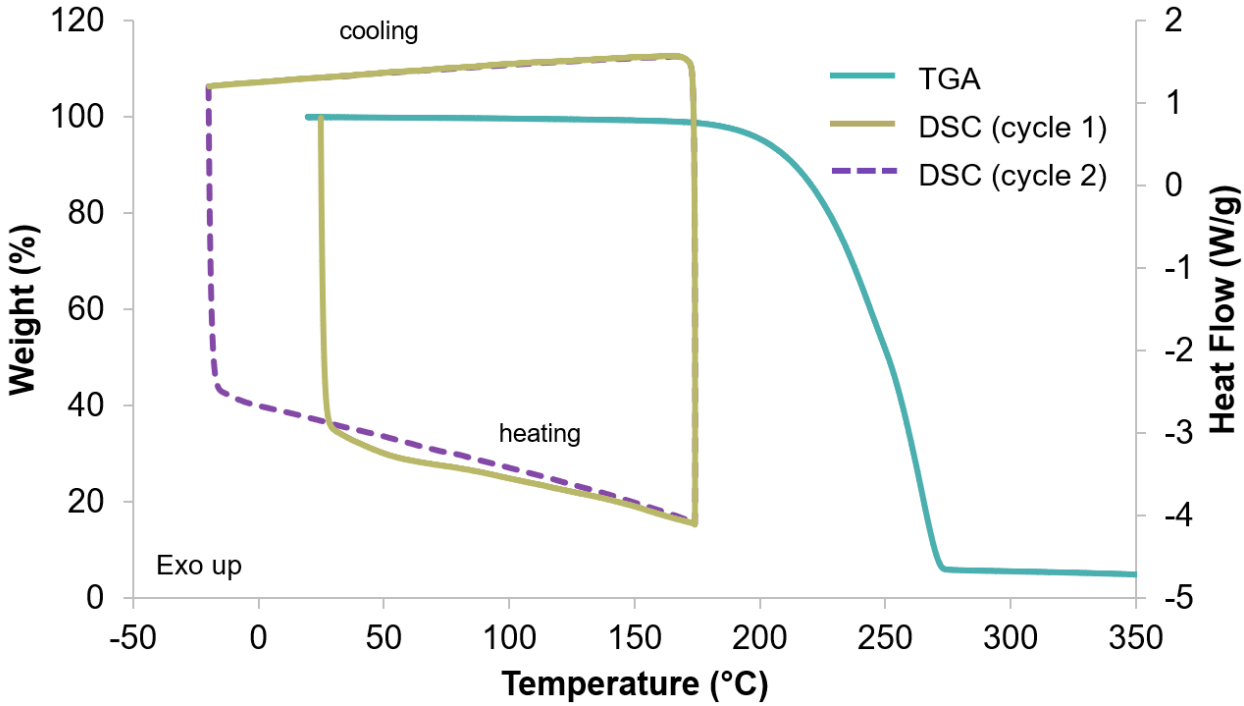

Figure S25. Thermal analysis results for **2b**. TGA trace shown in blue and DSC traces in yellow (cycle 1) and purple dashes (cycle 2).

FTIR

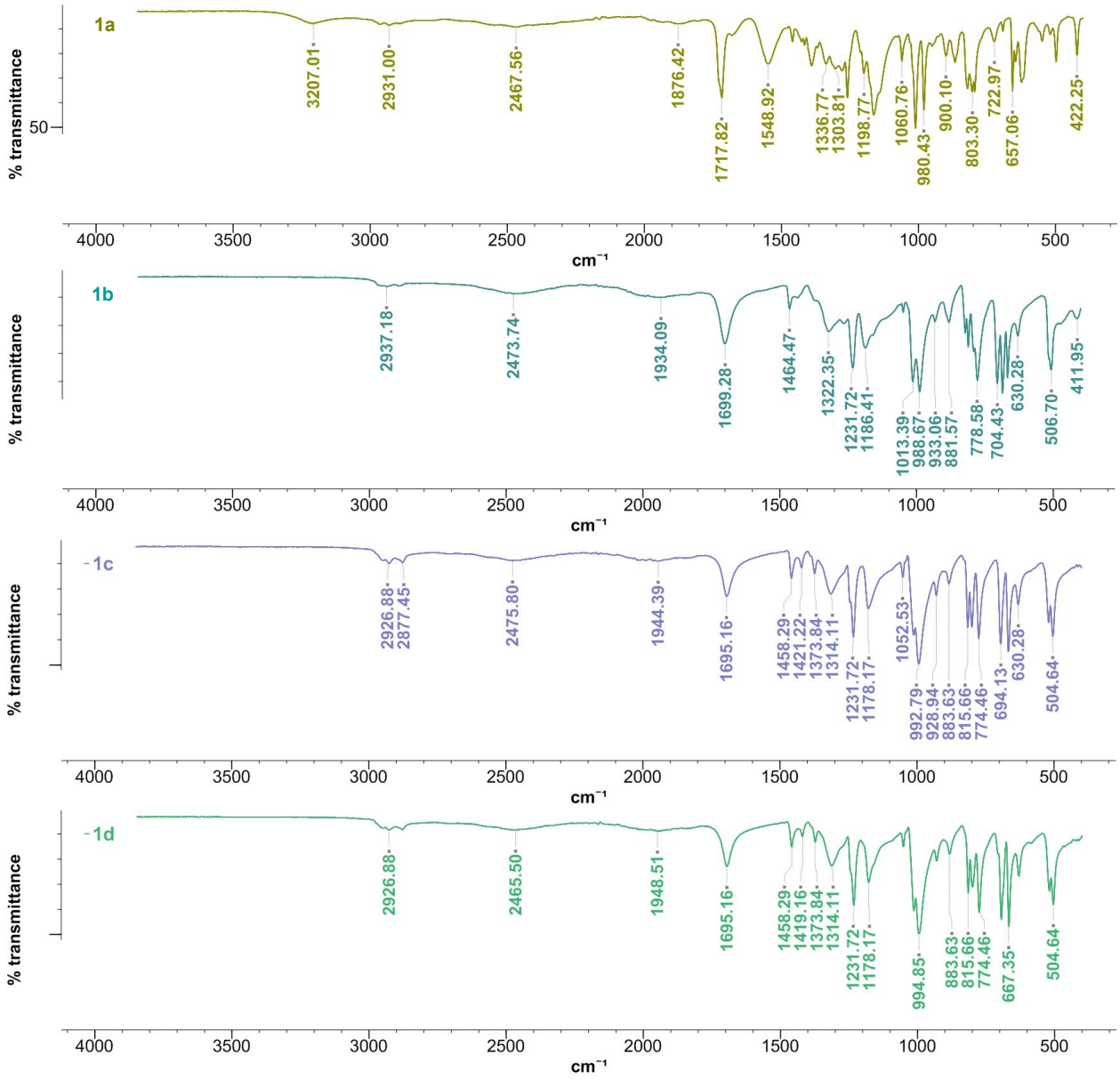

Figure S26. FTIR spectra for the salt, **1a**, and co-crystals, **1b**, **1c** and **1d**, formed from succinic acid and hexamethylenetetramine. For **1a**, the peak at 1717.82 cm^{-1} represents the carboxylic acid C=O stretching frequency, while the peak at 1548.92 cm^{-1} indicates the presence of a carboxylate group, as is expected for a salt. For the three co-crystals the peak at 1699.28 cm^{-1}/1695.16 cm^{-1} represents the carboxylic acid C=O stretching frequency for succinic acid. There is no carboxylate peak as **1b, 1c** and **1d** are co-crystals.

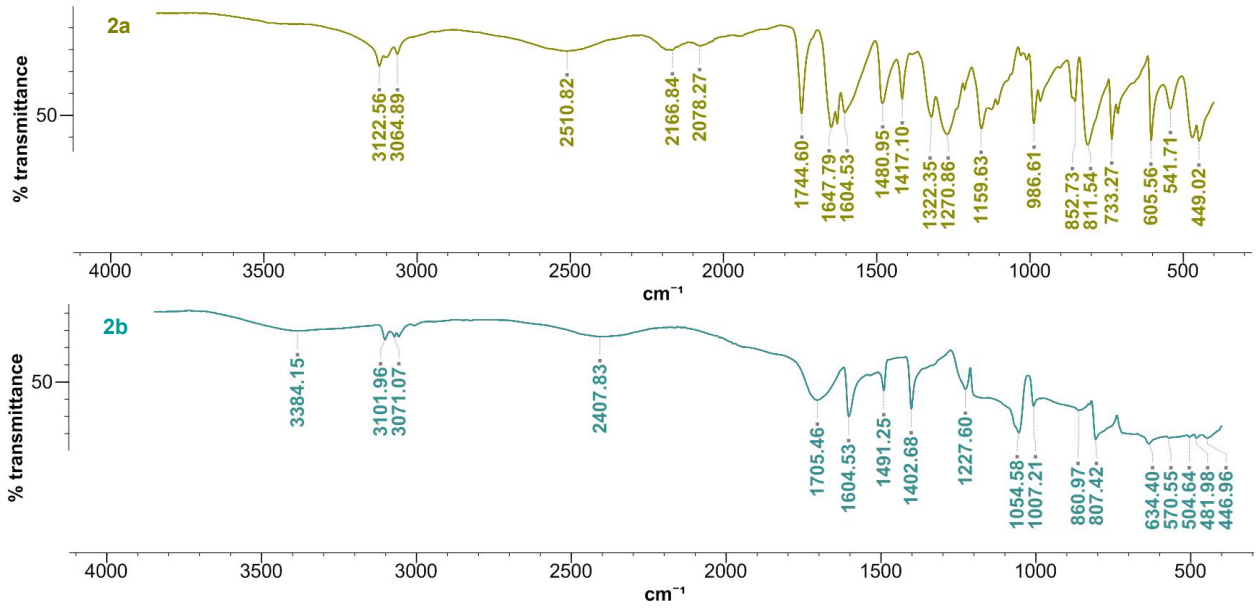

Figure S27. FTIR spectra for the salt and co-crystal formed from oxalic acid and 4,4'-bipyridine, **2a** and **2b**. For **2a**, the peak at 1744.60 cm^{-1} represents the carboxylic acid C=O stretching frequency, while the peaks around 1605 − 1648 cm^{-1} indicates the presence of a carboxylate group, as is expected for a salt. For **2b** the peak at 1705.46 cm^{-1} represents the carboxylic acid C=O stretching frequency, while the peak at 1604.53 cm^{-1} seems to indicate the presence of a carboxylate group, even though according to the literature this is a co-crystal. This carboxylate frequency could be due to small amounts of **2a** contaminant, as can be seen in the PXRD pattern (Figure S13).

Difference electron density maps

The position of acidic hydrogen atoms could be determined based on electron density.

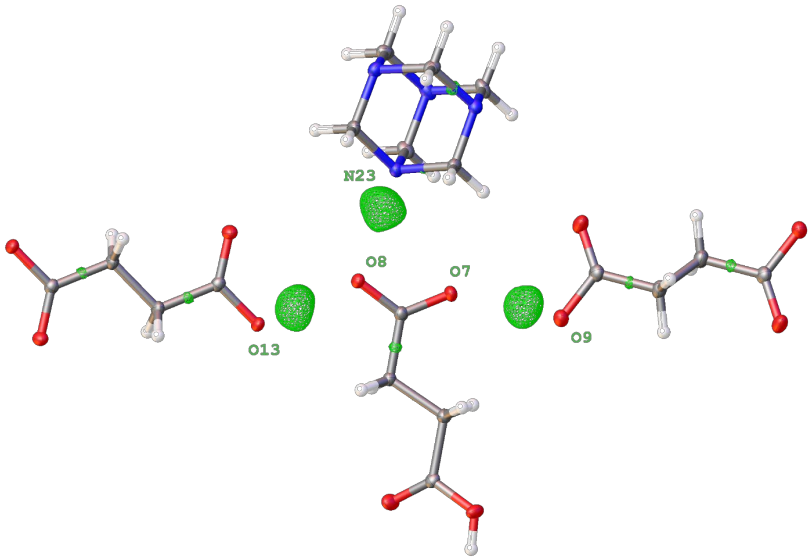

Figure S28. Electron density difference map for salt **1a** before the O–H and N–H hydrogen atoms were assigned.

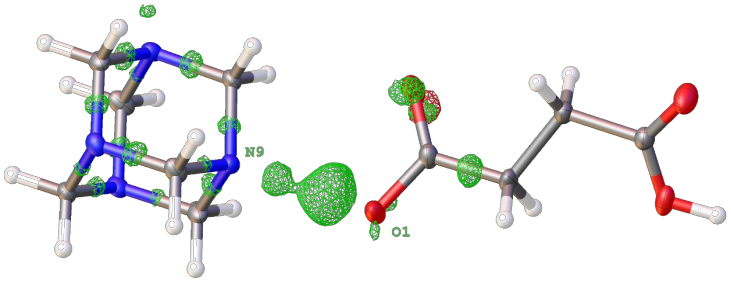

Figure S29. Electron density difference map for co-crystal **1b** before the O–H and N–H hydrogen atoms were assigned.

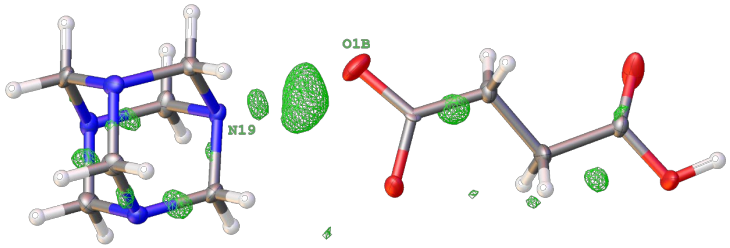

Figure S30. Electron density difference map for co-crystal **1c** before the O–H and N–H hydrogen atoms were assigned.

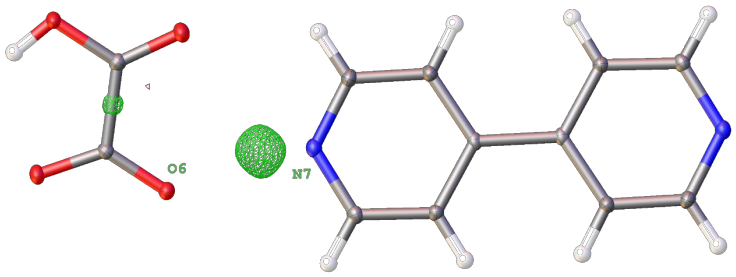

Figure S31. Electron density difference map for salt **2a** before the O–H and N–H hydrogen atoms were assigned.

MS

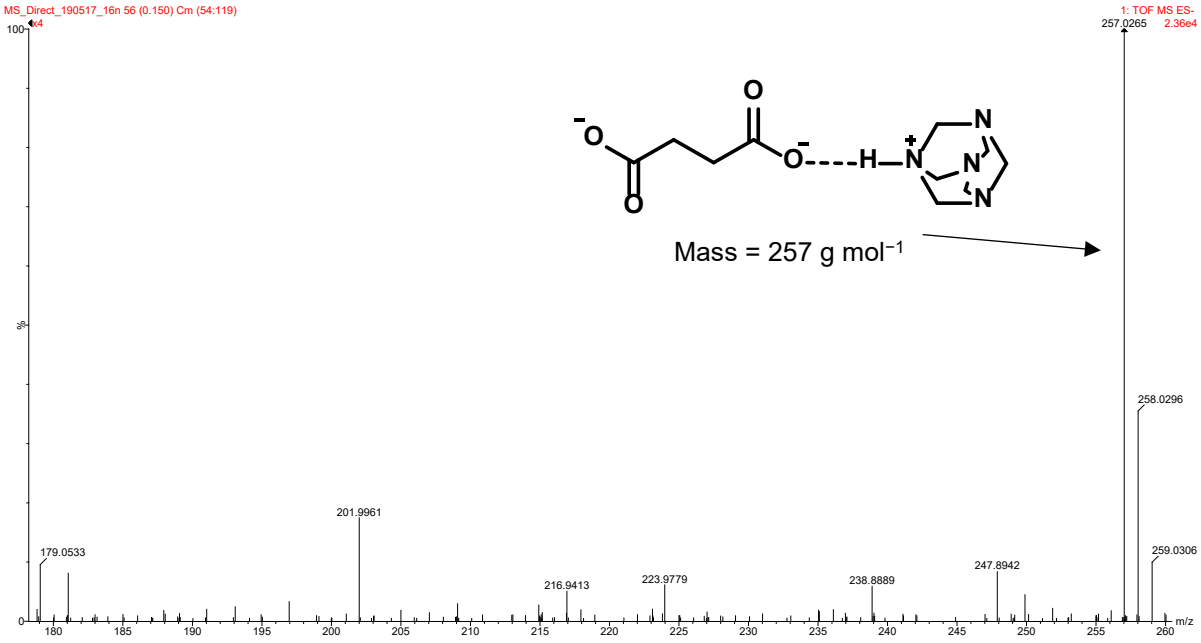

Figure S32. Mass spectrum for **1a** showing the presence of the hydrogen-bonded adduct SA–HMT at $m/z = 257$.

References

[1] *SAINT Data Reduction Software*, Version V7.99A; Bruker AXS Inc., Madison, WI, **2012**.

[2] *SADABS*, Version 2012/1; Bruker AXS Inc., Madison, WI, **2012**.

[3] Blessing, R. H. *Acta Crystallogr. Sect. A Found. Crystallogr.* **1995**, *51*, 33−38.

[4] Sheldrick, G. M. *Acta Crystallogr. Sect. A Found. Adv.* **2015**, *71* (1), 3−8.

[5] Atwood, J. L.; Barbour, L. J. *Cryst. Growth Des.* **2003**, *3* (3), 3−8.

[6] Barbour, L. J. *J. Supramol. Chem.* **2001**, *1* (189), 189−191.

[7] Sheldrick, G. M. *Acta Crystallogr. Sect. C Struct. Chem.* **2015**, *71* (1), 3−8.

[8] *POV-Ray for Windows*, Version 3.6; Persistence of Vision Pty. Ltd., Williamstown, Australia, **2004**.

[9] Dolomanov, O. V.; Bourhis, L. J.; Gildea, R. J.; Howard, J. A. K.; Puschmann, H. *J. Appl. Crystallogr.* **2009**, *42* (2), 339−341.

[10] Steiner, T.; Majerz, I.; Wilson, C. C. *Angew. Chem. Int. Ed.* **2001**, *40* (14), 2651−2654.

[11] Padmavathy, R.; Karthikeyan, N.; Sathya, D.; Jagan, R.; Mohan Kumar, R.; Sivakumar, K. *RSC Adv.* **2016**, *6* (72), 68468−68484.

[12] Androš, L.; Planinić, P.; Jurić, M. *Acta Crystallogr. Sect. C Cryst. Struct. Commun.* **2011**, *67* (9), o337−o340.

[13] Cowan, J. A.; Howard, J. A. K.; Puschmann H.; Williams, I. D. *Acta Crystallogr. Sect. E Struct. Reports Online.* **2007**, *63* (3), o1240−o1242.

CHAPTER 3

Competition between hydrogen- and halogen bonds: the effect of solvent volume

---

3.1 Article submitted to Crystal Growth and Design (unpublished)

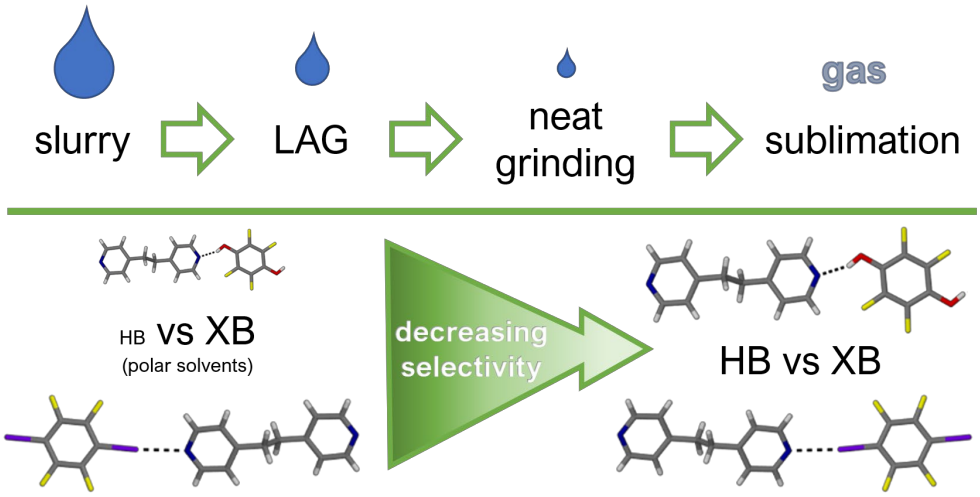

Contributions of the author:

- Design of project with co-authors
- Preparation of all co-crystals
- Competition experiments
- Collection of single-crystal X-ray data
- Solution and refinement of single-crystal X-ray structures
- Recording of PXRD patterns
- Recording of NMR spectra
- Calculation of interaction energies with Dewald P. van Heerden
- Interpretation of results with co-authors
- Writing the first draft of the article

COMPETITION BETWEEN HYDROGEN- AND HALOGEN BONDS: THE EFFECT OF SOLVENT VOLUME

Jean Lombard, Tanya le Roex and Delia A. Haynes[*]

Department of Chemistry and Polymer Science, University of Stellenbosch, P. Bag X1, Matieland, 7602, Republic of South Africa. E-mail: dhaynes@sun.ac.za

Abstract

The effect of crystallization method and solvent volume on the competition between hydrogen and halogen bond formation was investigated through co-crystallization experiments carried out by adding the common ditopic acceptor molecule, 1,2-bis(4-pyridyl)ethane, to both a halogen-bond donor molecule and a hydrogen-bond donor molecule simultaneously. The formation of a halogen-bonded co-crystal of 1,2-bis(4-pyridyl)ethane and 1,4-diiodotetrafluorobenzene (**1·3**) is compared to formation of three structurally similar hydrogen-bonded co-crystals of 1,2-bis(4-pyridyl)ethane and hydroquinone (**2a·3**), 2-fluorohydroquinone (**2b·3**), and 2,3,5,6-tetrafluorohydroquinone (**2c·3**). Different crystallization methods, including sonic slurry crystallization, neat grinding, liquid-assisted grinding, and co-sublimation, were chosen as they differ, amongst other things, in the amount of solvent that is used. We observe the known preference towards the halogen-bonded co-crystal when polar solvents are used, but the selectivity is much less pronounced as the amount of solvent is reduced. Competition experiments carried out by vacuum sublimation exclude all solvent, and all selectivity for one form over another is eliminated. The amount of solvent used, and not just its polarity, is therefore critical when co-crystallization is attempted.

Introduction

Co-crystals are constructed from organic molecules held together by relatively weak intermolecular interactions. Understanding these interactions and their hierarchical organization will help to develop real and practical design strategies for creating these materials. Perhaps the most well-known intermolecular interaction is the hydrogen bond (HB). However, some halogen bonds[1] (XBs) can be comparable in strength, and are very similar to HBs with respect to geometry and directionality.[2] The IUPAC has defined a hydrogen bond as "…an attractive interaction between a hydrogen atom from a molecule or a molecular fragment X–H in which X is more electronegative than H, and an atom or

a group of atoms in the same or a different molecule, in which there is evidence of bond formation"[3]. On the other hand, according to the IUPAC, a halogen bond "…occurs when there is evidence of a net attractive interaction between an electrophilic region associated with a halogen atom in a molecular entity and a nucleophilic region in another, or the same, molecular entity".[4] Therefore, both of these interactions can generally be considered as interactions between an electron-donating Lewis base (the XB or HB acceptor molecule) and an electron-deficient halogen or hydrogen atom, acting as the XB or HB donor molecule.[5] Hydrogen bonds and halogen bonds can co-exist in crystalline materials,[6,7] but often compete for the same interaction sites. Certain functional groups, such as pyridines, can accept hydrogen bonds and halogen bonds equally well.[2] Therefore, to compare the strength of these two types of interactions, and develop a type of supramolecular hierarchy, various co-crystal competition studies have been carried out over the years.[8–11]

Notably, Corradi *et al.* carried out competitive co-crystallization experiments by dissolving equimolar amounts of 1,2-bis(4-pyridyl)ethane, 1,4-diiodotetrafluorobenzene and hydroquinone in acetone and found that the halogen-bonded co-crystal containing the first two molecules is the favored product, and not the hydrogen-bonded co-crystal with hydroquinone.[12] Studies like these are based on the assumption that one interaction is simply stronger than the other, and do not take into account what role the solvent plays in crystallization, and that the selectivity observed is not just a factor of the strength of the interaction, but also of the technique and conditions that are employed.

Robertson *et al.* were the first to consider the effect of solvent polarity on the selective crystallization of halogen- and hydrogen-bonded co-crystals, by employing different solvents in a series of selectivity experiments.[13] They investigated a series of dihydroxy hydrogen-bond donor molecules, **2a**, **2b**, and **2c** (Chart 1) which form a series of similar co-crystals with the hydrogen-bond acceptor molecule 1,2-bis(4-pyridyl)ethane (**3**). The donor molecules range from strong (**2a**) to weak (**2c**) hydrogen-bond donors, which the authors determined experimentally.[13] A similar halogen-bonded co-crystal can be formed using the halogen-bond donor molecule 1,4-diiodotetrafluorobenzene (**1**). Robertson *et al*.[13] conducted competitive co-crystallization experiments using these analogous co-crystals. They combined the donor molecule, **3**, with both a hydrogen- and the halogen-bond donor molecule concurrently in solution to determine which co-crystal is produced, and what effect the choice of solvent, and its polarity, has on this outcome. They concluded that the halogen-bonded co-crystal is favored when polar solvents are used for crystallization, and that the hydrogen-bonded co-crystal is favored when less polar solvents are used. Exactly where division occurs depends on the strength of the hydrogen-bond donor molecule, with mixtures forming around the transition point. The reason for the selectivity is that the use of more polar solvents decreases the binding constant between the acceptor molecule and the hydrogen-bond donor molecule, thus

decreasing the likelihood of formation of the hydrogen-bonded co-crystal under these circumstances. Their work forms the basis for our study.

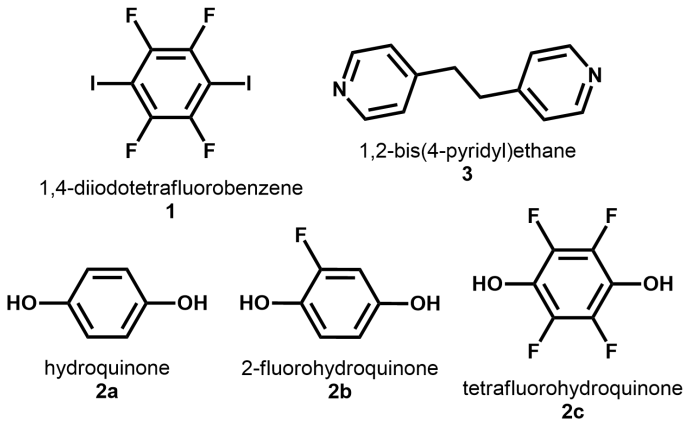

Chart 1. The donor molecules used in this study include the halogen-bond donor molecule 1,4-diiodotetrafluorobenzene (**1**) and the hydrogen-bond donor molecules hydroquinone (**2a**), 2-fluorohydroquinone (**2b**), and 2,3,5,6-tetrafluorohydroquinone (**2c**). Each of these are known to form a co-crystal with the same acceptor molecule, 1,2-bis(4-pyridyl)ethane (**3**).

Besides the type of solvent, the amount of solvent used could also influence co-crystallization outcome, as different interactions could be influenced in a dissimilar manner by the presence or absence of solvent molecules. Previous work has shown that the amount of solvent used can have a definitive effect on the polymorphic outcome of co-crystallization reactions.[14,15] In this study we wanted to gauge the effect of using varying amounts of solvents in co-crystal competition experiments analogous to those reported by Robertson *et al*. We have used different crystallization techniques, based on mechanochemistry and sublimation, in order to assess both the effect of the technique used and the effect of solvent volume on the competition between hydrogen and halogen bonding. Both hydrogen-bonded co-crystals[16] and salts,[17] and halogen-bonded co-crystals (first reported in 2011)[18], can be formed by co-sublimation, but to our knowledge no competitive studies have been carried out using sublimation. In the gas phase, where matrix effects are minimal, is there some specific preference for one type of interaction above another?

Results and discussion

Crystallization of the four co-crystals was first carried out using all techniques that would be employed for the competition experiments, to ensure that no form would particularly be favored or disfavored simply by the method used. Co-crystals **1**·**3**, **2a**·**3**, **2b**·**3**, and **2c**·**3** were obtained by neat grinding, liquid-assisted grinding (LAG), sonic slurry (SS), and co-sublimation under vacuum (0.6 mbar). Each form could be obtained with equal ease; the only differences came about during co-

sublimation. To form the co-crystals **1·3**, **2a·3** and **2b·3**, the starting components needed to be heated to at least 90 °C in order for the crystals to form. However, to crystallize **2c·3** a temperature of 110 °C was required.

Grinding experiments were also carried out in order to identify products other than the known co-crystals that might arise during competition experiments. The halogen-bond donor molecule, **1**, was combined with each variation of the hydrogen-bonding molecule, **2**. Different ratios of these, and the original donor-acceptor combinations, were used (1:1, 2:1 and 1:2). This lead to the discovery of one new co-crystal, a 1:3 co-crystal of **1** and **2a**. Co-crystal **1·2a** could also be formed by co-sublimation, although this was not very reproducible, and only small amounts could be isolated in this way. Attempts to crystallize **1·2a** from solution *via* slow evaporation lead to crystallization of the two components separately.

Two other new products were obtained during the competitive milling experiments. When **1**, **2a** and **3** were milled in a 2:2:1 ratio, a new powder X-ray diffraction pattern was obtained for the product, indicating the formation of a ternary co-crystal containing these three components (**1·2a·3**). A similar ternary co-crystal was observed when **1**, **2b** and **3** were combined (**1·2b·3**). No crystal structures could be obtained for either of these new materials; however, NMR confirmed that the three components were still present in the sample in each case, and that the molecules had not reacted with one another covalently (Figure S18, S19). The powder patterns for **1·2a·3** and **1·2b·3** are very similar to each other, indicating that these are probably isostructural materials (Figure S11).

Crystal structures

The crystal structures for the four analogous co-crystals have been previously reported, i.e. **1·3** (CSD refcode: MEKWOO)[19], **2a·3** (CSD refcode: MEKWUU)[19], **2b·3** (CSD refcode: RAXYAT)[13] and **2c·3** (CSD refcode: RAXYEX)[13]. The crystal structures for these co-crystals are very similar. Each one is comprised of infinite hydrogen-bonded (O–H···N) or halogen-bonded (C–I···N) chains of the two co-crystal components alternating down the chain (Figure 1). Neighboring chains are then held together by various weak interactions, including π-π interactions. Each co-crystal crystallizes in space group $P\bar{1}$. **2b·3** is the only co-crystal with disorder present in the structure, which is in the form of a 50:50 H/F disorder at positions 2- and 5- of the aromatic ring. While they are quite similar in structure, the powder pattern for the halogen-bonded co-crystal **1·3** is different, so that mixtures of halogen- and hydrogen-bonded co-crystals can easily be identified as such (Figure 2).

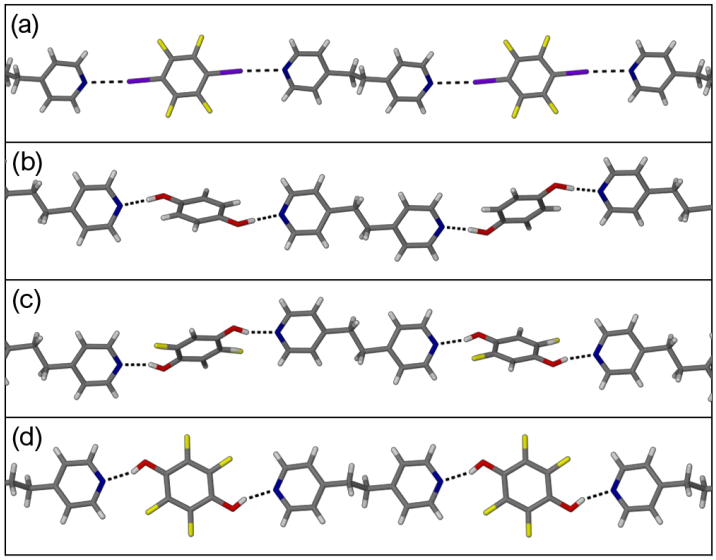

Figure 1. Infinite co-crystal chains of (a) **1**·**3**, (b) **2a**·**3**, (c) **2b**·**3** (note that the fluorine atoms are disordered over positions 2 and 5 of **2b**), and (d) **2c**·**3**. Images were generated from published crystal structures.[13,19]

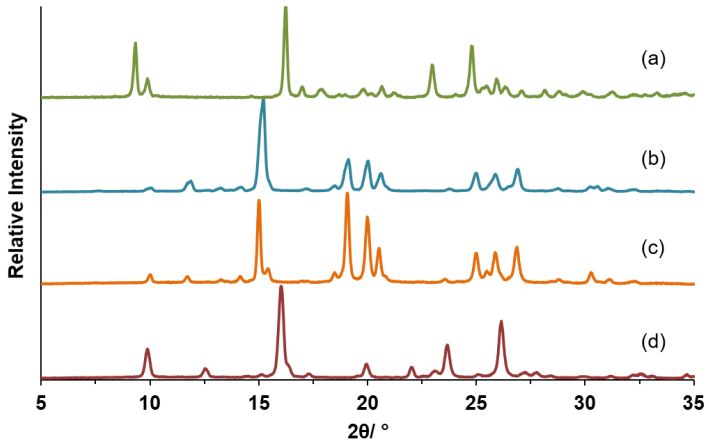

Figure 2. PXRD profiles for (a) **1**·**3**, (b) **2a**·**3**, (c) **2b**·**3**, and (d) **2c**·**3**.

Crystals for the new co-crystal, **1**·**2a**, were grown by sublimation. This co-crystal also crystallizes in the triclinic space group $P\bar{1}$, with half a molecule of **1** and three halves of hydroquinone in the asymmetric unit. The co-crystal therefore has a 1:3 ratio of **1**:**2a**. The molecules are interconnected in three dimensions by hydrogen bonds between the hydroxyl groups as well as halogen bonds between the lone pairs on the hydroxyl groups and the iodine atoms of **1** (Figure 3). Once it had been clearly established that all co-crystal combinations could easily be formed using all the methods, competition experiments were carried out.

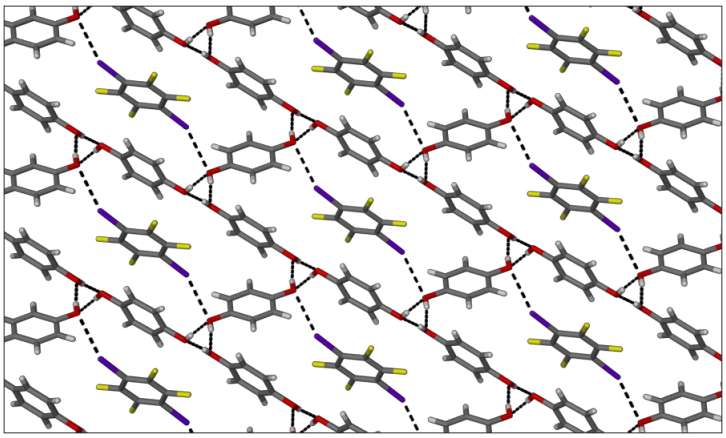

Figure 3. Packing diagram for **1**·**2a** viewed along [100].

Competition experiments by mechanochemistry

Selectivity experiments were carried out to determine whether the hydrogen-bonded or halogen-bonded co-crystal is preferred during competitive milling experiments, as well as the effect of solvent choice during milling. As in the previous work by Robertson *et al.*,[13] these experiments were carried out in three sets: a 1:1:1 ratio of acceptor molecule **3**, donor molecule **1** and either **2a** (System A), **2b** (System B) or **2c** (System C). Each system was milled for 20 minutes with the addition of one of seven different solvents, ranging from non-polar to polar (toluene, chloroform, dichloromethane, acetone, acetonitrile, 2-propanol or methanol). The resultant microcrystalline products were analyzed using Powder X-ray Diffraction (PXRD), and the results are summarized in Table 1.

For each system, experiments were repeated with 5 minutes and 60 minutes milling time, but no change in the results were observed, and thus the effect of milling time was not investigated further. To rule out that co-crystal formation occurs outside of the mill due to contact between the starting materials, some competition experiments were repeated with the inclusion of 24-hour waiting periods before and after milling, but this also had no effect on the observed product. Solvent amount was fixed at 20 µl for an 80 mg sample size ($\eta = 0.25$ µl mg^{-1}). Generally, all competition experiments were carried out at least twice. Finally, to probe the effect of not only the solvent choice, but also the solvent volume, competition experiments were carried out neat, as well as in a slurry of either a polar solvent (methanol) or an apolar solvent (chloroform) ($\eta = 6$ µl mg^{-1}). These changes affected the products formed; the results are included in Table 1.

For System A, the halogen bonded co-crystal was obtained most frequently, especially when higher polarity solvents were used. According to Robertson *et al.*,[13] **2a** is the weakest hydrogen-bond donor out of the three used. It is therefore not surprising that the halogen-bonded co-crystal is generally favored in System A. In polar solvents we only observed the halogen-bonded co-crystal **1**·**3**: it is likely that the solvent interacts with the hydrogen-bond donor molecule, making the

formation of **2a·3** even less likely. When lower-polarity solvents were used (e.g. $CHCl_3$ and DCM), the competing effect of the solvent interacting with **2a** was absent, which allowed for the hydrogen-bonded co-crystal, as well as the ternary co-crystal **1·2a·3**, to form. The exception to this is toluene: only **1·3** is formed when LAG was carried out in toluene. Similar results were obtained for the neat grinding experiments where no solvent was used at all – again we observed the formation of all three possible co-crystals. In the absence of solvent, selectivity was lost. In the sonic slurry experiments more solvent was used, and the selectivity observed is therefore more pronounced: the XB co-crystal was formed in both polar and non-polar solvent (probably because **2a** is such a weak HB donor).

It should be noted that PXRD has limited sensitivity. In the cases where only co-crystal **1·3** was observed, there was undoubtedly some of the relevant hydrogen-bond donor **2** left over as well. The amount by mass of unreacted **2** is small in comparison with the heavier halogen-containing **1·3**, and so its pattern is not distinguishable from the background noise.

Table 1. Summary of the results from the mechanochemical competition experiments. The halogen-bonded co-crystal is represented by a red dot, the hydrogen-bonded co-crystal by a blue dot, and the ternary co-crystals by green dots. Unreacted starting material **1** is represented by gray dots. Dot sizes allows for easy visualization of relative amounts – for System B, the PXRD peak at 9.3° 2θ is shown as an inset showing how the amounts were determined.

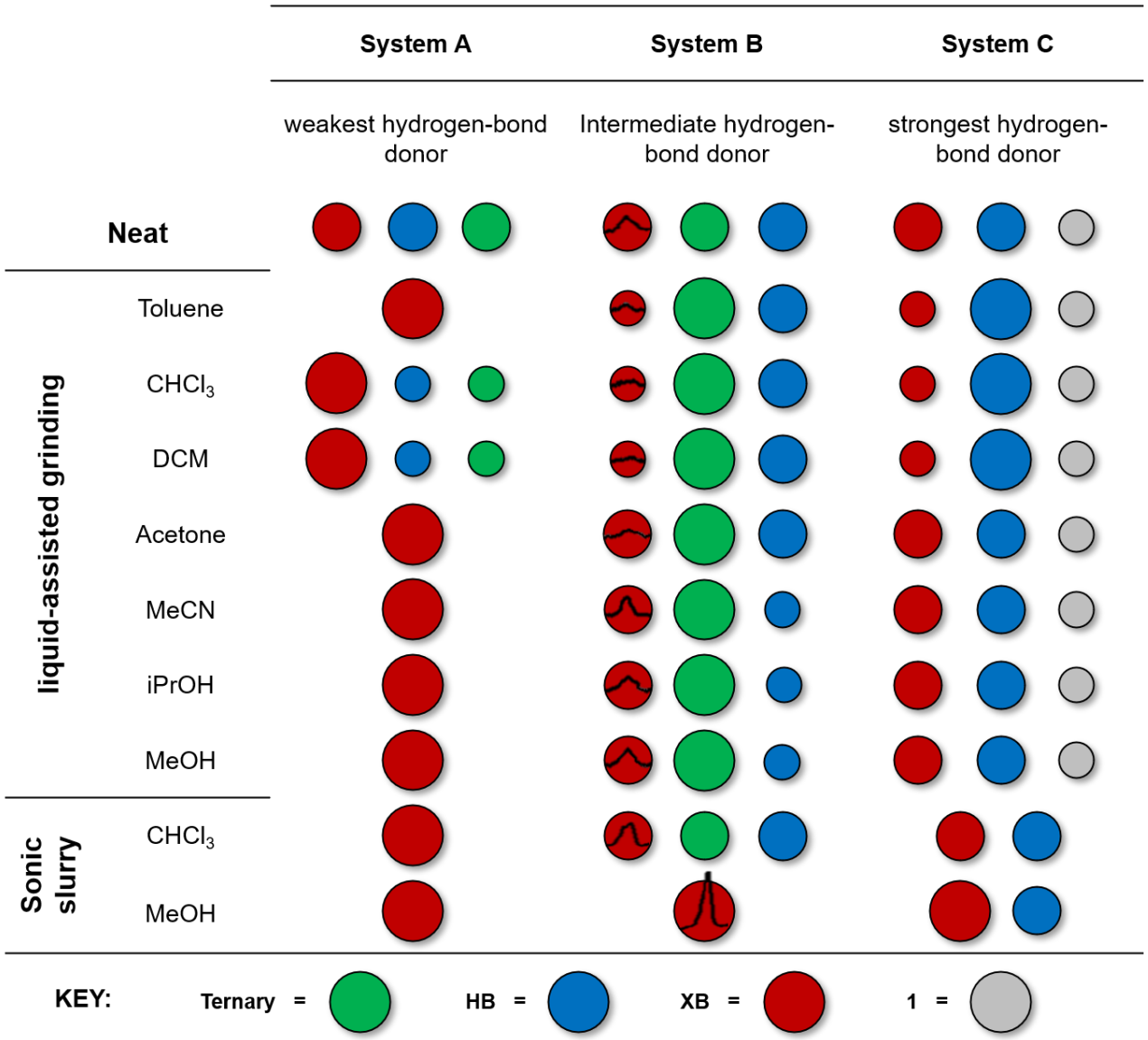

For System B, the suspected ternary co-crystal, **1·2b·3**, was the major product from milling in all cases, however both **1·3** and **2b·3** were also formed in small amounts. The solvent used during milling did not have a pronounced effect, but as the polarity of the solvent increased, the amount of **1·3** formed did increase somewhat, as can be seen from the powder patterns (Table 1, Figure S9 – the **1·3** peaks start to become more prominent). This is similar to what is observed in System A, i.e. polar solvents tend to interact with the hydrogen-bond donor molecule (here **2b**) and impede formation of the hydrogen-bonded co-crystal compared to the halogen-bonded co-crystal. This selectivity was

more pronounced in the slurry experiments where the use of a polar solvent lead to formation of only the halogen-bonded co-crystal. Clearly, the presence of solvent is essential for selectivity. The neat grinding experiment demonstrates this as well; here the PXRD pattern appears to be a roughly equal mixture of **1·3**, **2·3**, and the suspected ternary co-crystal (Figure S10). The abundance of ternary co-crystal in System B is also understandable, as hydrogen-bond donor **2b** is of intermediary strength, compared to **2a** and **2c**, and thus forming a ternary co-crystal containing both hydrogen-bonding and halogen-bonding interactions seems like a likely outcome.

In System C, for each solvent used, small amounts of both the halogen-bonded co-crystal (**1·3**) and the hydrogen-bonded co-crystal (**2c·3**) were formed, and a large amount of 1,4-diiodotetrafluorobenzene remained unreacted. Continuing the milling experiment for 60 minutes instead of the normal 20 minutes made no difference; milling for only 5 minutes made no difference either. We suspect that the hydrogen-bonded co-crystal **2c·3** is in actual fact the major product (as **2c** is the strongest HB donor molecule), and that some of **1** was therefore left unreacted. Because of the larger molar mass of the halogen-bond donor molecule, the actual mass of **1** used for these experiments was more than twice the amount of either of the other components. Therefore, even if only a small percentage of **1** is left over, the actual mass is quite a lot, and so its trace will dominate the powder pattern. Unfortunately, because the trace for **1** dominates the PXRD patterns, no clear trend can be seen in the relative amounts of the two co-crystals. This is a shortcoming of the analytical technique, with no obvious solution.

Unlike in System A and B, in System C no unknown product (ternary co-crystal) has been identified. However, some new peaks were observed when a 2:2:1 ratio of starting materials were milled, indicating that there may also be another crystalline product forming (Figure S14). In System C the solvent added had the smallest effect (compared to A and B). Even when more solvent was used, as for the SS experiments, the results remain practically unchanged (Figure S13). Small amounts of the hydrogen-bonded co-crystal could even be formed from a methanol slurry. However, this is consistent with **2c** being the strongest hydrogen-bond donor of those used, and thus more able to overcome the solvent-donor molecule interactions in order to form the hydrogen-bonded co-crystal in a polar environment. These results also echo the reported solution results where it was found that the hydrogen-bonded co-crystal was always formed, but in high polarity solvents the amount of **2c·3** formed would decrease (Table 2).

Table 2. Selected results from the different techniques showing increased selectivity as larger solvent volumes are used. The halogen-bonded co-crystal is represented by a red dot, the hydrogen-bonded co-crystal by a blue dot, and the ternary co-crystals by green dots. Unreacted starting material **1** is represented by a gray dot.

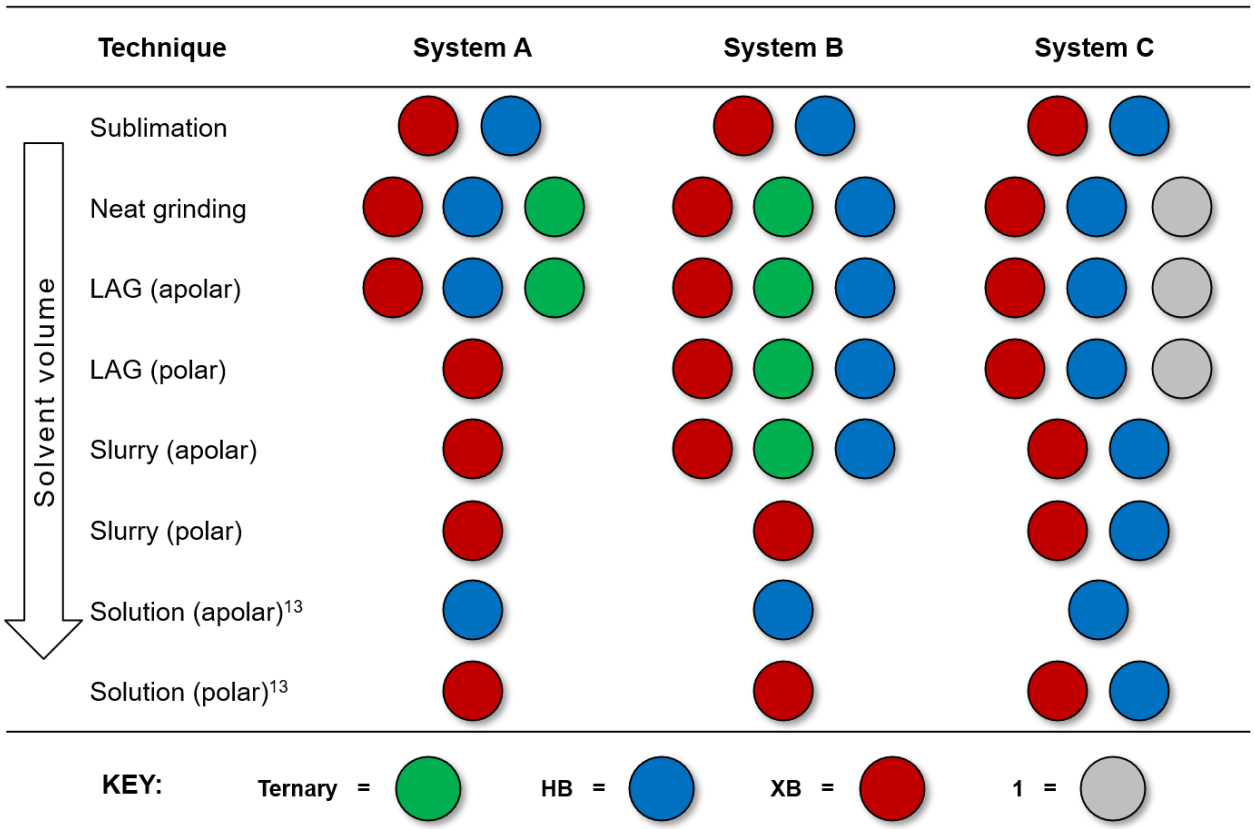

Generally, mechanochemistry shows the same trends in selectivity as the solution crystallization results of Robertson *et al.*,[13] but the effect is much less pronounced as less solvent is used. Neat grinding gives virtually no selectivity, but selectivity was amplified when slightly more solvent was used in the SS experiments. This proves that solvent plays a crucial role during crystallization, both in terms of the nature of the solvent, and also the amount used. It is interesting to note the formation of products *via* mechanochemical reaction that are not obtained during solution crystallization, i.e. the ternary co-crystals. This confirms the importance of using a variety of techniques in co-crystal screening. There are a number of other examples in the literature of the need for a multi-technique approach to finding different crystal forms.[20–21]

Competition experiments by co-sublimation

If solvent has such a large effect on selectivity, will all selectivity be lost when solvent is completely absent? Or will other factors start to play a more prominent role? To answer these questions, the same three sets of competition experiments were carried out by vacuum sublimation.

Each set of three starting materials were added to the bottom of a thin Schlenk tube which was heated overnight in an oil bath under static vacuum (0.6 mbar). Two different temperatures were used, 110 ˚C and 130 ˚C, but the change in temperature did not affect the results. Sublimation experiments were carried out on the same scale as the mechanochemical experiments, i.e. roughly 80 mg total mass, and products were identified using PXRD and single-crystal X-ray diffraction (SCXRD).

For System A, both co-crystals (**1·3** and **2a·3**) formed more or less simultaneously and crystallized in the same region within the sublimation tube, i.e. in a band right above the level of the oil bath. There is no notable selectivity between the two (Table 2). This was not unexpected, as both these co-crystals are very similar, and form at the same temperature when the pairs of starting materials are sublimed. The two co-crystals could not be separated from each other and the powder pattern obtained simply shows a mixture of the two products. In some cases, the **1·2a** co-crystal crystallized as well, but this co-crystal tends to form at a lower temperature, and crystallized higher up in the tube in very small amounts.

The results for System B are essentially identical to those of System A, although no equivalent co-crystal between the two donor molecules was observed. The two relevant co-crystals (**1·3** and **2b·3**) formed as a mixture in a band above the level of the oil bath.

For System C the results are slightly different as **2c·3** forms at a higher temperature during co-sublimation (110 °C) compared to the halogen-bonded co-crystal (90 °C). Both these co-crystals still formed at roughly the same time, but because of this slight difference, they crystallized as two distinct bands, one above the other, so that they could be separated and analyzed individually. Visually the amount of each co-crystal appeared equivalent.

It is clear that all selectivity is lost in the absence of solvent; both halogen- and hydrogen-bonded co-crystals form equally well by sublimation.

Intermolecular interaction energies

As the hydrogen- and halogen-bonded co-crystals form by sublimation with equal ease, we would expect the forces holding them together to be of equal strength. To gain further insight, density functional theory (DFT) was used to calculate the intermolecular interaction energies (E_{int}) between the donor and acceptor for each co-crystal (Table 3). The two relevant molecules were extracted from

the crystallographic information file and their atomic coordinates were allowed to optimize before the relevant gas-phase single-point energies were calculated. The halogen- and hydrogen bonds are the strongest interactions in each structure, so their formation would presumably drive formation of the co-crystals. The interaction energy is thus one measure of the likelihood of each co-crystal forming.

Table 3. Intermolecular interaction energies for each hydrogen-bonded or halogen-bonded pair of molecules as they form in each of the four co-crystals.

	E_{int} (kJ/mol)
1–**3**	−36.78
2a–**3**	−49.24
2b–**3**	−53.26
2c–**3**	−66.30

The results show that **2a** is indeed the weakest hydrogen bond donor molecule, and **2c** the strongest. Unexpectedly, the halogen-bonding interaction is much weaker than all hydrogen-bonding interactions. However, as previously discussed, we have observed that both HB and XB co-crystals form with equal ease from the gas phase, by sublimation. We conclude that the relative strength of the strongest interactions in a crystal is therefore not a very reliable method for comparing different co-crystals, especially those that contain different types of interactions. Oh *et al.* has reported two co-crystals containing the same molecules, in different stoichiometric ratios. The intermolecular interactions that can form are the same for both, however only one of the co-crystals contains the strong I···O halogen bond. This interaction does not form in the other co-crystal, where C−H···O hydrogen bonds direct the packing.[22] In this case, the strength of the interaction was not the determining factor either. Many weaker interactions can have a large cumulative stabilizing effect on crystal packing,[23] and all of the interactions that molecules have with each other in the gas phase contribute to the crystallization process.

One possible reason for the unexpected pervasiveness of the weakly-bonded halogen-bonded co-crystal is the lower sublimation temperature of **1** compared to **2a**, **2b** and **2c**. Sublimation of **1** starts at around 35 °C, while **2b** and **2c** start subliming around 60 °C, and **2a** only at 70 °C (donor molecule **3** has the highest sublimation temperature and starts subliming at about 75 °C). There would therefore be a higher concentration of **1** in the gas phase during the initial stages of co-sublimation, allowing **1·3** to form more quickly than the hydrogen-bonded co-crystal and thus allowing its formation alongside **2a·3**, **2b·3** and **2c·3** even though it contains weaker interactions.

Conclusion

In conclusion, we have shown that the amount and type of solvent used is an important consideration when carrying out co-crystal competition studies, as the solvent can interfere with intermolecular interactions between the co-formers. It is known that the solvent used can direct the outcome of co-crystal formation in that halogen-bonded co-crystals are more likely to form in polar solvents, while hydrogen bonding becomes favored when less polar solvents are used. We have shown that these effects persist when co-crystals are produced mechanochemically, but the amount of solvent used is critical in observing any selectivity effect. During LAG experiments, much of the selectivity is lost, but general trends in selectivity still hold. When the solvent amount is somewhat increased, as for SS experiments, selectivity becomes more prominent, and when solvent is removed in neat grinding experiments, all selectivity is lost. In the extreme case of gas-phase co-crystal formation by sublimation, all solvent is removed, and the co-crystals are allowed to form *in vacuo*. All selectivity is thus removed from the system and both halogen-bonded and hydrogen-bonded co-crystals form simultaneously and in similar amounts. We have further observed that co-sublimation can be influenced by many factors, including interaction strength, vapor pressure, and temperature, and definitely warrants further study. Simply comparing intermolecular interaction energies does not give an accurate representation of whether a co-crystal will form. It would be useful if the concentration of each molecule in the gas phase could be determined, but this will need to be investigated further.

In essence, we have shown that solvent, and the amount of solvent used, can significantly affect the outcome of co-crystallization reactions and thus careful choices regarding solvent can be used to selectively form a desired product. When carrying out experiments in the laboratory, the choice of which solvent to use, and how much, is not arbitrary and warrants some serious thought.

Experimental

All solvents and chemicals used were obtained from commercial sources and used without further purification.

Synthesis of the co-crystals

The halogen-bonded co-crystal (**1·3**) was made mechanochemically by milling 1,2-bis(4-pyridyl)ethane (**3**, 25 mg, 0.14 mmol) with 1,4-diiodotetrafluorobenzene (**1**, 55 mg, 0.14 mmol) for 20 min with 20 μl methanol ($\eta = 0.25$ μl mg^{-1}). An FTS1000 Shaker Mill from Form-tech Scientific was used for this purpose, operated at 20 Hz, equipped with two 15 ml stainless steel SmartSnap^{TM} grinding jars together with two 6 mm steel grinding balls each. Co-crystal **1·3** could also be made (on

the same scale) by neat grinding, or by suspending a sealed vial of the starting materials and 480 µl of methanol (η = 6 µl mg^{-1}) in a sonic water bath for a total of 5 minutes (in intervals of 30 seconds, with 30 seconds rest in between to prevent heating of the sample). The solid product was filtered immediately and analyzed, the solvent was not simply left to evaporate. Co-crystal **1·3** could additionally be crystallized by subliming these same starting materials in a thin Schlenk tube (14 mm diameter, 220 mm length) under static vacuum (0.6 mbar line pressure), for roughly 16 hours. The tube needed to be heated to at least 90 °C using an oil bath in order for the co-crystal to form.

Co-crystal **2a·3** was made mechanochemically by milling 1,2-bis(4-pyridyl)ethane (**3**, 50 mg, 0.27 mmol) with hydroquinone (**2a**, 30 mg, 0.27 mmol) for 20 min with 20 µl methanol (0.25 µl mg^{-1}). Like co-crystal **1·3**, this co-crystal could also be formed from neat grinding, slurry and sublimation, using the same procedures described above.

Co-crystal **2b·3** was made mechanochemically by milling 1,2-bis(4-pyridyl)ethane (**3**, 47 mg, 0.26 mmol) with 2-fluorohydroquinone (**2b**, 33 mg, 0.26 mmol) for 20 min with 20 µl methanol (0.25 µl mg^{-1}). In the same way as the abovementioned co-crystals, **2b·3** could also be made *via* neat grinding, sonic slurry, and sublimation co-crystallization at 90 °C.

Co-crystal **2c·3** was similarly made mechanochemically by milling 1,2-bis(4-pyridyl)ethane (**3**, 40 mg, 0.22 mmol) with tetrafluorohydroquinone (**2c**, 40 mg, 0.22 mmol) for 20 min with 20 µl methanol (0.25 µl mg^{-1}). This co-crystal could also be made from neat grinding and sonic slurry reaction. Co-crystal **2c·3** could also be made by subliming the relevant starting materials together in a Schlenk tube, but a temperature of 110 °C was required to afford crystals of the product.

Co-crystal **1·2a** was made mechanochemically by milling 1,4-diiodotetrafluorobenzene (**1**, 44 mg, 0.11 mmol) with hydroquinone (**2a**, 36 mg, 0.33 mmol) for 40 min with 20 µl acetone (0.25 µl mg^{-1}). Co-crystal **1·2a** could also be formed by subliming the two starting materials together in a Schlenk tube for 16 hours, at 70 °C or higher.

The ternary co-crystal **1·2a·3** was made mechanochemically by milling 1,4-diiodotetra-fluorobenzene (**1**, 73 mg, 0.18 mmol) with hydroquinone (**2a**, 20 mg, 0.18 mmol) and 1,2-bis(4-pyridyl)ethane (**3**, 17 mg, 0.092 mmol) for 40 min with 28 µl acetone (0.25 µl mg^{-1}). The ternary co-crystal **1·2b·3** was similarly made by milling 1,4-diiodotetrafluorobenzene (**1**, 71 mg, 0.18 mmol) with 2-fluorohydroquinone (**2b**, 23 mg, 0.18 mmol) and 1,2-bis(4-pyridyl)ethane (**3**, 16 mg, 0.087 mmol) for 40 min with 28 µl Acetone (0.25 µl mg^{-1}).

Methods of characterization

All products were crystalline. Analysis of products using PXRD was carried out on a Bruker D2 phaser benchtop powder diffractometer equipped with a copper source (1.54183 Å radiation). Data

were collected from 2θ = 4 to 40° at a speed of 0.5 seconds per scan (0.016° step size). SCXRD data for the co-crystal **1·2a** were collected using a Bruker DUO Apex II diffractometer. MoKα radiation (0.71073 Å) was used as generated by an Incoatec IμS microsource coupled with a multilayer mirror optics monochromator. The crystal was cooled to 100 K during the data collection using an Oxford Cryosystems Cryostat (700 Series Cryostream Plus). Data collection and reduction were carried out using the Bruker software package SAINT[24] through the Apex3 software, and subsequently corrected for absorption using SADABS.[25] The structure was solved by direct methods (SHELXT-18)[26] and refined (SHELXL-18)[27] through the graphical user interface XSeed.[28] Hydrogen atoms on sp^2-hybridised carbon atoms were placed in calculated positions using riding models, while O–H hydrogen atoms were placed on maxima in the electron density difference maps. Images were generated using POV-ray,[29] as visualized through XSeed.[28] A summary of the structure refinement parameters is provided in the ESI (Table S1). Crystal structures for **1·3**, **2a·3**, **2b·3** and **2c·3** have been previously reported and were not re-determined. Nuclear Magnetic Resonance (NMR) spectroscopy was carried out using a 300 MHz Agilent spectrometer. Samples were dissolved in $CDCl_3$ and filtered before analysis.

Calculations

The geometries of pairs of interacting molecules extracted from crystal structures were optimized using the DMol3 module[30] of DS BIOVIA Materials Studio 2019 v19.1.0.2353. The TPSS[31] m-GGA and DND basis set were employed along with Grimme's dispersion correction.[32] Frequency calculations confirmed attainment of minimum energy conformations and BSSE-corrected interaction energies were subsequently determined.

The interaction energies of the two disordered configurations of **2b** differed by only 0.2 kJ/mol and the average value is thus reported.

Associated content

Supporting Information

Full details of all experimental procedures and analysis of powder X-ray data. NMR spectroscopic data for **1·2a·3** and **1·2b·3** and single-crystal X-ray diffraction data for **1·2a**. The X-ray crystallographic file in CIF format are available. This material is available free of charge via the Internet at http://pubs.acs.org. CCDC 2019756 contains the supplementary crystallographic data for this paper. These data can be obtained free of charge from The Cambridge Crystallographic Data Centre via www.ccdc.cam.ac.uk/data_request/cif.

Author information

Corresponding Author

* Email: dhaynes@sun.ac.za

Acknowledgments

The authors would like to thank the Wilhelm Frank Scholarship Fund and Stellenbosch University for funding, as well as Dewald P. van Heerden for assistance with carrying out the calculations.

References

[1] Gilday, L. C.; Robinson, S. W.; Barendt, T. A.; Langton, M. J.; Mullaney, B. R.; Beer, P. D. Halogen Bonding in Supramolecular Chemistry. *Chem. Rev.* **2015**, *115* (15), 7118–7195.

[2] Metrangolo, P.; Meyer, F.; Pilati, T.; Resnati, G.; Terraneo, G. Halogen Bonding in Supramolecular Chemistry. *Angew. Chem. Int. Ed.* **2008**, *47* (33), 6114–6127.

[3] Arunan, E.; Desiraju, G. R.; Klein, R. A.; Sadlej, J.; Scheiner, S.; Alkorta, I.; Clary, D. C.; Crabtree, R. H.; Dannenberg, J. J.; Hobza, P.; Kjaergaard, H. G.; Legon, A. C.; Mennucci, B.; Nesbitt, D. J. Definition of the Hydrogen Bond (IUPAC Recommendations 2011). *Pure Appl. Chem.* **2011**, *83* (8), 1637–1641.

[4] Desiraju, G.; Ho, P. S.; Kloo, L.; Legon, A. C.; Marquardt, R.; Metrangolo, P.; Politzer, P.; Resnati, G.; Rissanen, K. Definition of the Halogen Bond (IUPAC Recommendations 2013). *Pure Appl. Chem.* **2013**, *85* (8), 1711–1713.

[5] Metrangolo, P.; Resnati, G. Halogen Versus Hydrogen. *Science* **2008**, *321* (5891), 918–919.

[6] Szell, P. M. J.; Dragon, J.; Zablotny, S.; Harrigan, S. R.; Gabidullin, B.; Bryce, D. L. Mechanochemistry and Cocrystallization of 3-Iodoethynylbenzoic Acid with Nitrogen-Containing Heterocycles: Concurrent Halogen and Hydrogen Bonding. *New J. Chem.* **2018**, *42* (13), 10493–10501.

[7] Goswami, A.; Garai, M.; Biradha, K. Interplay of Halogen Bonding and Hydrogen Bonding in the Cocrystals and Salts of Dihalogens and Trihalides with N,N′-Bis(3-Pyridylacrylamido) Derivatives: Phosphorescent Organic Salts. *Cryst. Growth Des.* **2019**, *19* (4), 2175–2188.

[8] Aakeröy, C. B.; Fasulo, M.; Schultheiss, N.; Desper, J.; Moore, C. Structural Competition between Hydrogen Bonds and Halogen Bonds. *J. Am. Chem. Soc.* **2007**, *129* (45), 13772–13773.

[9] Gamekkanda, J. C.; Sinha, A. S.; Desper, J.; Đaković, M.; Aakeröy, C. B. Competition between Hydrogen Bonds and Halogen Bonds: A Structural Study. *New J. Chem.* **2018**, *42* (13), 10539–10547.

[10] Kowalska, K.; Trzybiński, D.; Sikorski, A. Influence of the Halogen Substituent on the Formation of Halogen and Hydrogen Bonding in Co-Crystals Formed from Acridine and Benzoic Acids. *CrystEngComm* **2015**, *17* (37), 7199–7212.

[11] Takemura, A.; McAllister, L. J.; Karadakov, P. B.; Pridmore, N. E.; Whitwood, A. C.; Bruce, D. W. Competition and Cooperation: Hydrogen and Halogen Bonding in Co-Crystals Involving 4-Iodotetrafluorobenzoic Acid, 4-Iodotetrafluorophenol and 4-Bromotetrafluorophenol. *CrystEngComm* **2014**, *16* (20), 4254–4264.

[12] Corradi, E.; Meille, S. V.; Messina, M. T.; Metrangolo, P.; Resnati, G. Halogen Bonding versus Hydrogen Bonding in Driving Self-Assembly Processes. *Angew. Chem. Int. Ed.* **2000**, *39* (10), 1782–1786.

[13] Robertson, C. C.; Wright, J. S.; Carrington, E. J.; Perutz, R. N.; Hunter, C. A.; Brammer, L. Hydrogen Bonding vs. Halogen Bonding: The Solvent Decides. *Chem. Sci.* **2017**, *8* (8), 5392–5398.

[14] Hasa, D.; Miniussi, E.; Jones, W. Mechanochemical Synthesis of Multicomponent Crystals: One Liquid for One Polymorph? A Myth to Dispel. *Cryst. Growth Des.* **2016**, *16* (8), 4582–4588.

[15] Belenguer, A. M.; Lampronti, G. I.; Cruz-Cabeza, A. J.; Hunter, C. A.; Sanders, J. K. M. Solvation and Surface Effects on Polymorph Stabilities at the Nanoscale. *Chem. Sci.* **2016**, *7* (11), 6617–6627.

[16] Carstens, T.; Haynes, D. A.; Smith, V. J. Cocrystals: Solution, Mechanochemistry, and Sublimation. *Cryst. Growth Des.* **2020**, *20* (2), 1139–1149.

[17] Lombard, J.; Smith, V. J.; le Roex, T.; Haynes, D. A. Crystallisation of Organic Salts by Sublimation: Salt Formation from the Gas Phase. *Manuscript submitted*. **2020**.

[18] Davy, K. J. P.; McMurtrie, J.; Rintoul, L.; Bernhardt, P. V.; Micallef, A. S. Vapour Phase Assembly of a Halogen Bonded Complex of an Isoindoline Nitroxide and 1,2-Diiodotetrafluorobenzene. *CrystEngComm* **2011**, *13* (16), 5062–5070.

[19] Corradi, E.; Meille, S. V.; Messina, M. T.; Metrangolo, P.; Resnati, G. Halogen Bonding versus Hydrogen Bonding in Driving Self-Assembly Processes. *Angew. Chem. Int. Ed.* **2000**, *39* (10), 1782–1786.

[20] Friščić, T.; Trask, A. V.; Jones, W.; Motherwell, W. D. S. Screening for Inclusion Compounds and Systematic Construction of Three-Component Solids by Liquid-Assisted Grinding. *Angew. Chem. Int. Ed.* **2006**, *45* (45), 7546–7550.

[21] Eddleston, M. D.; Sivachelvam, S.; Jones, W. Screening for Polymorphs of Cocrystals: A Case Study. *CrystEngComm* **2013**, *15* (1), 175–181.

[22] Oh, S. Y.; Nickels, C. W.; Garcia, F.; Jones, W.; Friščić, T. Switching Between Halogen- and Hydrogen-bonding in Stoichiometric Variations of a Cocrystal of a Phosphine Oxide. *CrystEngComm* **2012**, *14* (19), 6110–6114.

[23] Calvo-Castro, J.; Morris, G.; Kennedy, A. R.; McHugh, C. J. Effects of Fluorine Substitution on the Intermolecular Interactions, Energetics, and Packing Behavior of N-Benzyl Substituted Diketopyrrolopyrroles. *Cryst. Growth Des.* **2016**, *16* (4), 2371–2384.

[24] SAINT *Data Collection Software*, Version V7.99A; Bruker AXS Inc., **2012**, Madison, WI.

[25] (a) SADABS, Version 2012/1; Bruker AXS Inc., Madison, WI, **2012**; (b) Blessing, R. H. An Empirical Correction for Absorption Anisotropy. *Acta Crystallogr. Sect. A Found. Crystallogr.* **1995**, *51*, 33–38.

[26] Sheldrick, G. M. SHELXT – Integrated Space-Group and Crystal-Structure Determination. *Acta Crystallogr. Sect. A Found. Adv.* **2015**, *71* (1), 3–8.

[27] Sheldrick, G. M. Crystal Structure Refinement with SHELXL. *Acta Crystallogr. Sect. C Struct. Chem.* **2015**, *71* (1), 3–8.

[28] (a) Barbour, L. J. X-Seed – A Software Tool for Supramolecular Crystallography. *J. Supramol. Chem* **2001**, *1* (189), 189–191; (b) Atwood, J. L.; Barbour, L. J. Molecular Graphics: From Science to Art. *Cryst. Growth Des.* **2003**, *3* (3), 3–8.

[29] *POV-Ray for Windows*, version 3.6; Persistence of Vision Pty. Ltd., Williamstown, Australia, **2004**.

[30] (a) Delley, B. An All-electron Numerical Method for Solving the Local Density Functional for Polyatomic Molecules. *J. Chem. Phys.* **1990**, *92* (1), 508–517; (b) Delley, B., From Molecules to Solids with the DMol3 Approach. *J. Chem. Phys.* **2000**, *113* (18), 7756–7764.

[31] Tao, J.; Perdew, J. P.; Staroverov, V. N.; Scuseria, G. E. Climbing the Density Functional Ladder: Nonempirical Meta-generalized Gradient Approximation Designed for Molecules and Solids, *Phys. Rev. Lett.* **2003**, *91* (14), 146401–146402.

[32] Grimme, S. Semiempirical GGA-type Density Functional Constructed with a Long-range Dispersion Correction. *J. Comput. Chem.* **2006**, *27* (15), 1787–1799.

3.2 Supporting information

Crystallographic information

Table S1. Crystallographic information for the co-crystal **1·2a**.

Structure	**1·2a**
Chemical formula	$C_{24}H_{18}F_4I_2O_6$
Formula weight /g mol^{-1}	732.18
Crystal system	triclinic
Space group	$P\bar{1}$
Temperature /K	100(2)
a /Å	6.1990(5)
b /Å	8.3411(6)
c /Å	12.5345(9)
α /°	83.353(1)
β /°	76.046(1)
γ /°	86.037(1)
Calc. density /g cm^{-3}	1.948
Volume /Å^3	624.19(8)
Z	1
Independent reflections	2324
R_{int}	0.0177
R_1 [I > 2σ(I)]	0.0135

Table S2. Hydrogen-bond lengths and angles for **1·2a** at 100 K.

Structure	D–H···A	D—H /Å	H···A /Å	D···A /Å	D—H···A /°	Symmetry code
1·2a	O7–H7···O11	0.74 (2)	1.99 (3)	2.723 (2)	171 (3)	x+1, y, z
	O11–H11···O15	0.76 (3)	1.92 (3)	2.667 (2)	172 (3)	
	O15–H15···O7	0.73 (3)	1.96 (3)	2.689 (1)	171 (2)	

Table S3. Halogen-bond lengths and angles for **1·2a** at 100 K.

Structure	Y–X···A	X—A /Å	Y—X···A /°	Symmetry code
1·2a	C4–I1···O11	3.212 (1)	157.09 (5)	x, y+1, z

General procedure: Mechanochemical competition experiments

System A

The acceptor molecule 1,2-bis(4-pyridyl)ethane (**3**, 21 mg, 0.11 mmol) was combined with equimolar quantities of the two donor molecules, 1,4-diiodotetrafluorobenzene (**1**, 46 mg, 0.11 mmol) and hydroquinone (**2a**, 13 mg, 0.11 mmol). The reactants were combined with 20 µl of the relevant solvent (η = 0.25 µl mg^{-1}) and milled for 20 minutes. The solvents used were toluene, chloroform, dichloromethane, acetone, acetonitrile, 2-propanol, and methanol. For the neat grinding experiments, no solvent was added. The resultant powder was analyzed by powder X-ray diffraction (PXRD).

Slurry experiments were carried out on the same scale as above, but the reactants were added to 0.48 ml of the solvent (η = 6 µl mg^{-1}). These were added to a small 8 ml glass vial which was capped and sealed with parafilm. The vial was then sonicated in a water bath for a total of 5 minutes (in intervals of 30 seconds, with 30 seconds rest in between to prevent heating of the sample). The solid product was filtered immediately and analyzed by PXRD, the solvent was not simply left to evaporate.

For the sublimation experiments the reagents were added to a thin Schlenk tube (14 mm diameter, 220 mm length) under static vacuum (~0.6 mbar line pressure), and then heated at 110 °C or 130 °C by suspension in an oil bath for 19 hours. Crystals formed on the sides of the glass tube in bands. Each band was removed separately for analysis by PXRD or single-crystal X-ray diffraction (SCXRD).

System B

The acceptor molecule 1,2-bis(4-pyridyl)ethane (**3**, 21 mg, 0.11 mmol) was combined with equimolar quantities of the two donor molecules, 1,4-diiodotetrafluorobenzene (**1**, 45 mg, 0.11 mmol) and 2-fluorohydroquinone (**2b**, 14 mg, 0.11 mmol). The reactants were combined with 20 µl of the relevant solvent (η = 0.25 µl mg^{-1}) and milled for 20 minutes. The solvents used were toluene, chloroform, dichloromethane, acetone, acetonitrile, 2-propanol, and methanol. For the neat grinding experiments, no solvent was added. The resultant powder was analyzed by PXRD.

Slurry experiments were carried out on the same scale as above, but the reactants were added to 0.48 ml of the solvent (η = 6 µl mg^{-1}). These were added to a small 8 ml glass vial which was capped and sealed with parafilm. The vial was then sonicated in a water bath for a total of 5 minutes (in intervals of 30 seconds, with 30 seconds rest in between to prevent heating of the sample). The solid product was filtered immediately and analyzed by PXRD, the solvent was not simply left to evaporate.

For the sublimation experiments the reagents were added to a thin Schlenk tube (14 mm diameter, 220 mm length) under static vacuum (~0.6 mbar line pressure), and then heated at 110 °C or 130 °C by suspension in an oil bath for 19 hours. Crystals formed on the sides of the glass tube in bands. Each band was removed separately for analysis by PXRD or SCXRD.

System C

Acceptor molecule 1,2-bis(4-pyridyl)ethane (**3**, 19 mg, 0.10 mmol) was combined with equimolar quantities of the two donor molecules, 1,4-diiodotetrafluorobenzene (**1**, 42 mg, 0.10 mmol) and 2,3,5,6-tetrafluorohydroquinone (**2c**, 19 mg, 0.10 mmol). The reactants were combined with 20 µl of the relevant solvent (η = 0.25 µl mg^{-1}) and milled for 20 minutes. The solvents used were toluene, chloroform, dichloromethane, acetone, acetonitrile, 2-propanol, and methanol. For the neat grinding experiments, no solvent was added. The resultant powder was analyzed by PXRD.

Slurry experiments were carried out on the same scale as above, but the reactants were added to 0.48 ml of the solvent (η = 6 µl mg^{-1}). These were added to a small 8 ml glass vial which was capped and sealed with parafilm. The vial was then sonicated in a water bath for a total of 5 minutes (in intervals of 30 seconds, with 30 seconds rest in between to prevent heating of the sample). The solid product was filtered immediately and analyzed by PXRD, the solvent was not simply left to evaporate.

For the sublimation experiments the reagents were added to a thin Schlenk tube (14 mm diameter, 220 mm length) under static vacuum (~0.6 mbar line pressure), and then heated at 110 °C or 130 °C by suspension in an oil bath for 19 hours. Crystals formed on the sides of the glass tube in bands. Each band was removed separately for analysis by PXRD or SCXRD.

PXRD

Synthesis of the co-crystals

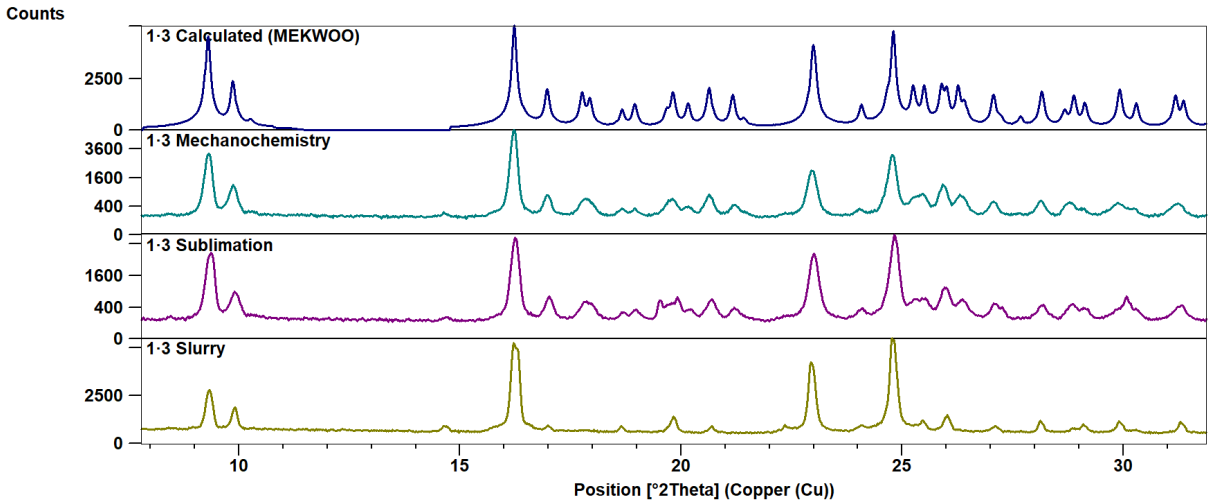

Figure S1. Comparison of the simulated powder pattern for the halogen-bonded co-crystal **1·3** with experimental patterns obtained when **1·3** is made mechanochemically, by sublimation, and from a slurry. There is good agreement between the patterns, indicative of the formation of pure products.

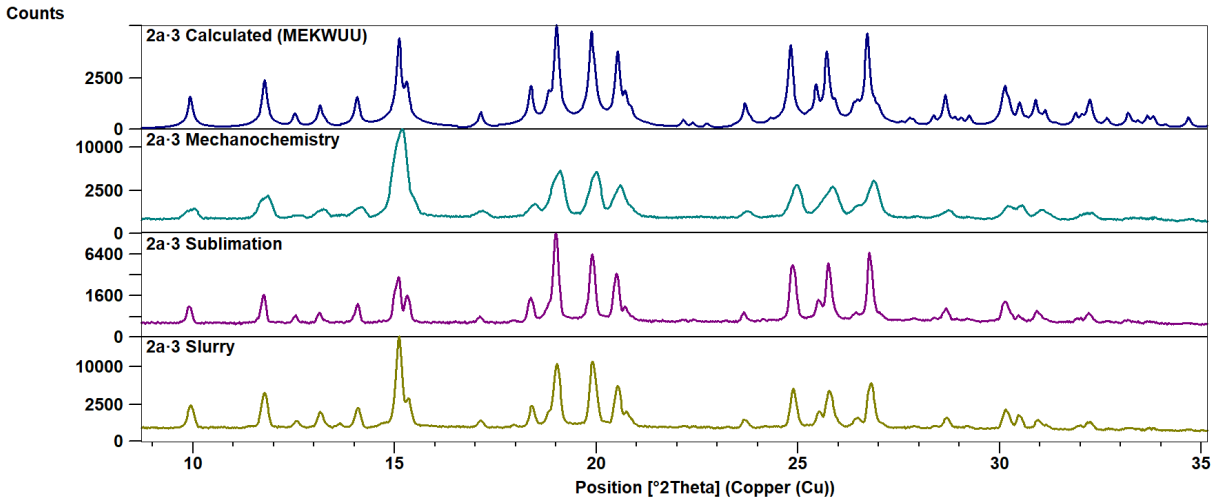

Figure S2. Comparison of the simulated powder pattern for the hydrogen-bonded co-crystal **2a·3** with experimental patterns obtained when **2a·3** is made mechanochemically, by sublimation, and from a slurry. There is good agreement between the patterns, indicative of the formation of pure products.

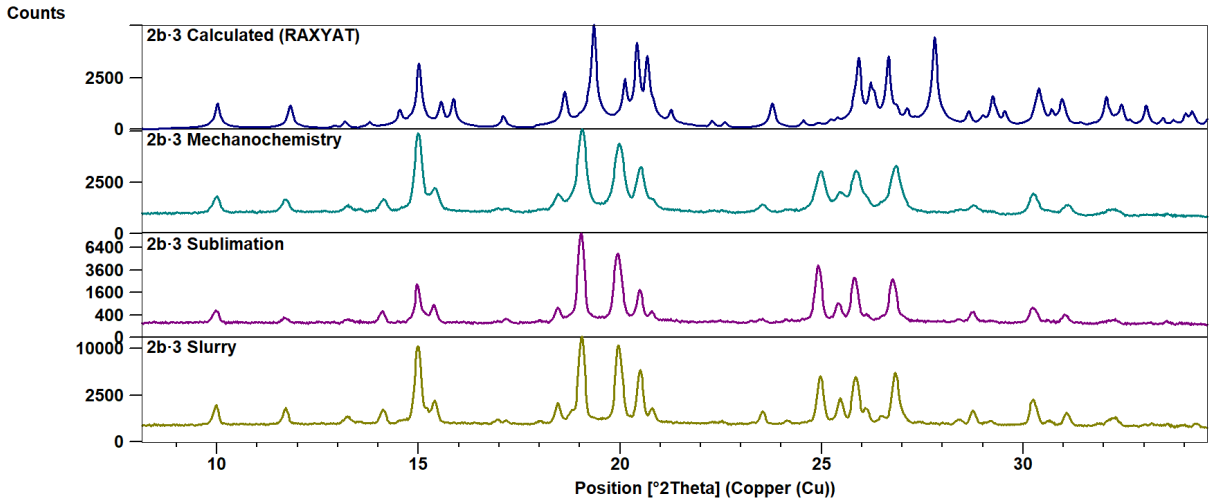

Figure S3. Comparison of the simulated powder pattern for the hydrogen-bonded co-crystal **2b·3** with experimental patterns obtained when **2b·3** is made mechanochemically, by sublimation, and from a slurry. There is good agreement between the patterns, indicative of the formation of pure products.

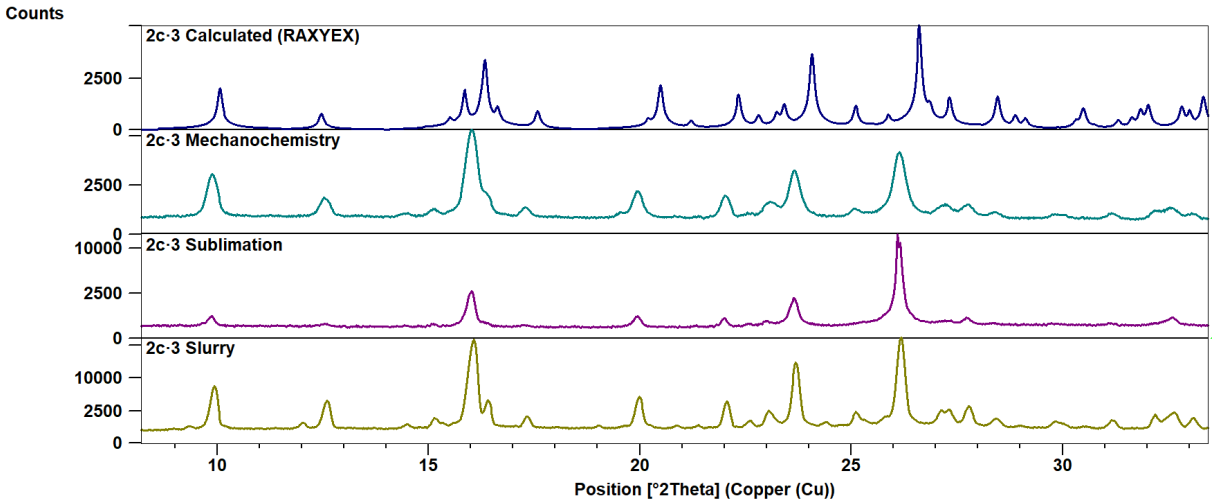

Figure S4. Comparison of the simulated powder pattern for the hydrogen-bonded co-crystal **2c·3** with experimental patterns obtained when **2c·3** is made mechanochemically, by sublimation, and from a slurry. There is good agreement between the patterns, indicative of the formation of pure products.

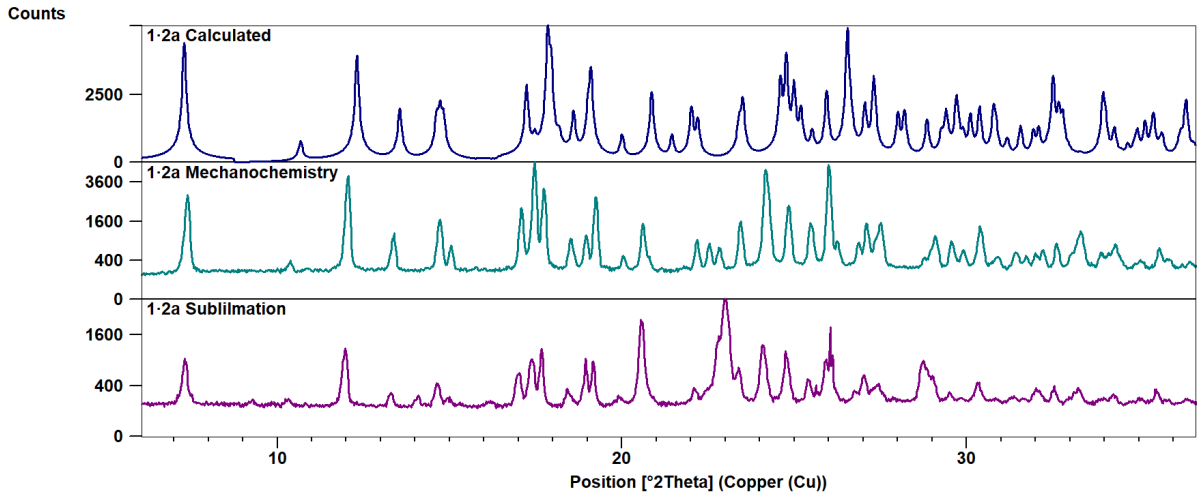

Figure S5. Comparison of the simulated powder pattern for the new co-crystal (**1·2a** at 100 K) with experimental patterns obtained when **1·2a** is made mechanochemically and by sublimation. There is good agreement between the patterns, indicative of the formation of pure products.

Selectivity Experiments: Mechanochemistry (System A)

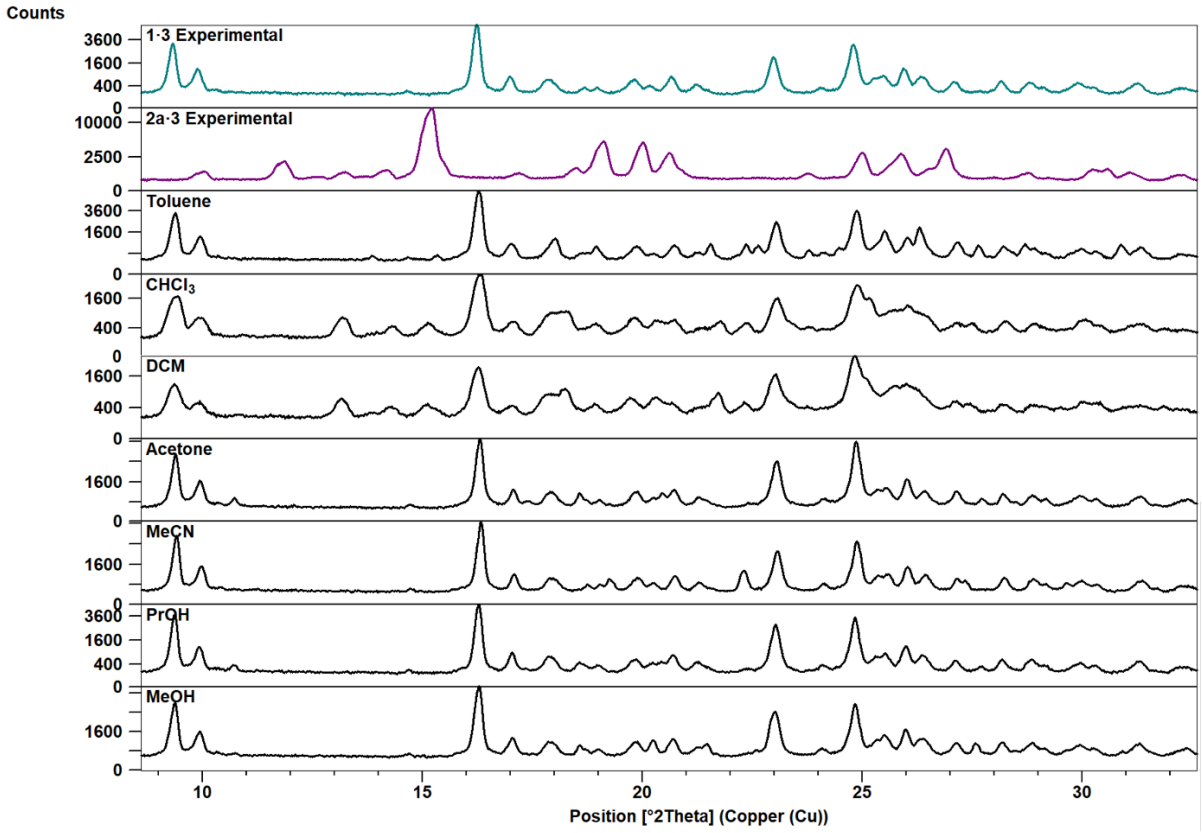

Figure S6. Comparison of LAG results, using seven different solvents, for System A. For each solvent used, the halogen-bonded co-crystal **1·3** is always formed. When chloroform or dichloromethane is used, additional peaks can be seen. Some of these weak peaks match the hydrogen-bonded co-crystal **2a·3** (e.g. at 15.2°), but a number of peaks do not match either co-crystal, these can be attributed to the ternary co-crystal **1·2a·3** (see also Figure S8).

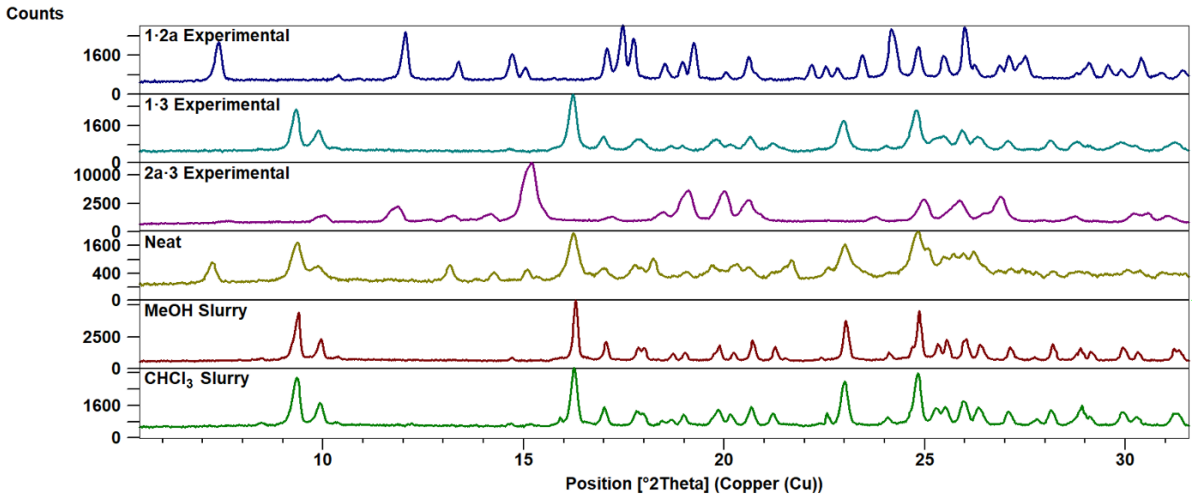

Figure S7. Comparison of neat grinding and slurry results for System A. Similar to the LAG results, the halogen-bonded co-crystal **1·3** is formed each time. When the three starting materials are milled without the addition of any solvent, the same pattern is obtained as with the DCM and $CHCl_3$ LAG experiments, i.e. containing **1·3**, **2a·3**, and the ternary co-crystal (see also Figure S8).

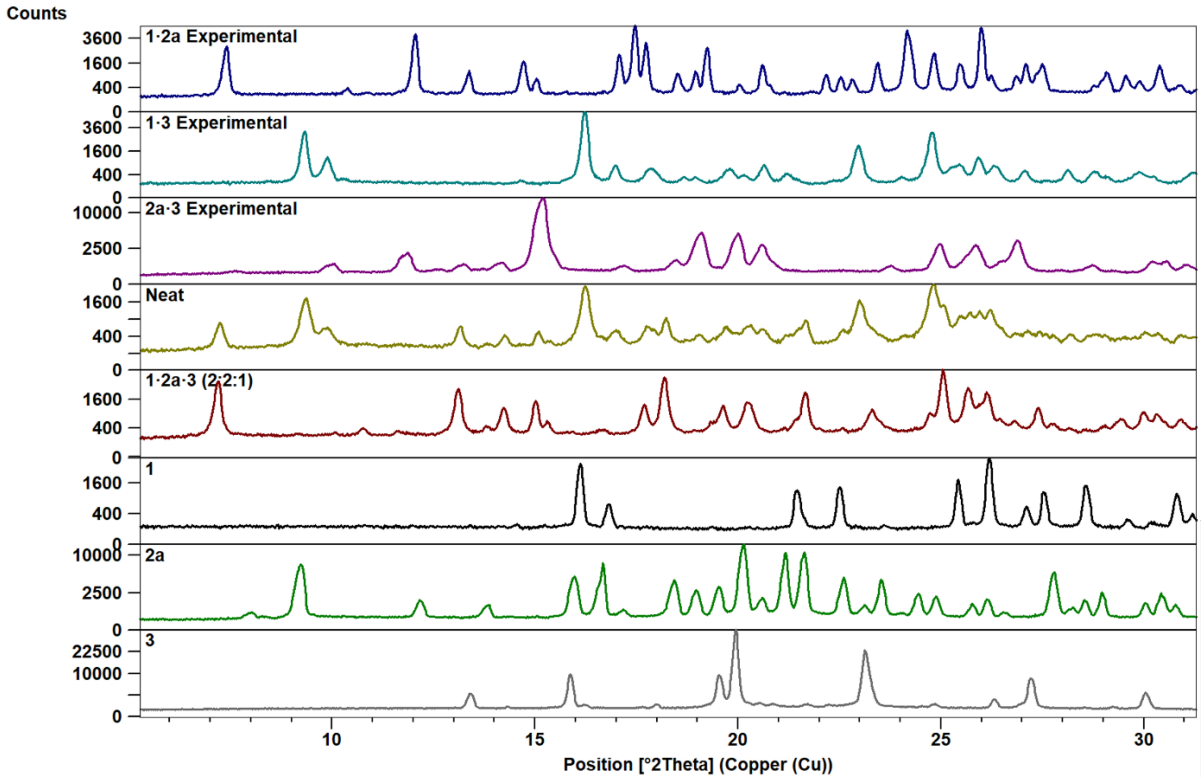

Figure S8. A closer look at one of the patterns containing the ternary co-crystal **1·2a·3** – the pattern obtained from neat grinding **1**, **2a** and **3** is used here as an example, shown in yellow (also contains **1·3** and **2a·3**). We suspect that the ternary co-crystal contains **1**, **2a**, and **3** in a 2:2:1 ratio. When the three starting materials are milled in this ratio, the pattern shown in red is obtained, which shows good correlation with peaks in the neat grinding trace that cannot be attributed to any of the binary co-crystals.

Selectivity Experiments: Mechanochemistry (System B)

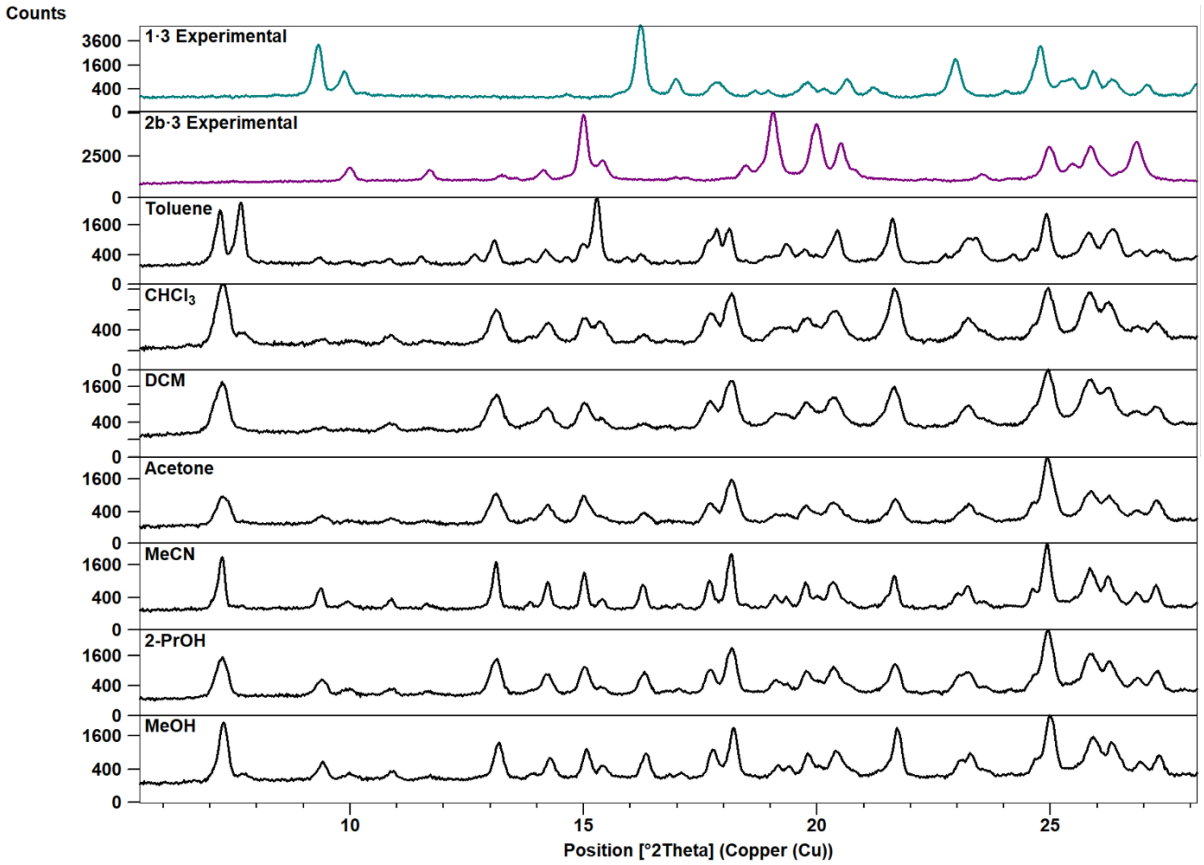

Figure S9. Comparison of LAG results for System B. For each solvent used, a small amount of both the halogen-bonded and hydrogen-bonded co-crystal is always formed, but mostly, peaks of an unknown product can be seen, which has been identified as a ternary co-crystal, **1·2b·3** (see also Figure S11). As expected, the more polar the solvent is, the more distinct the **1·3** peaks are.

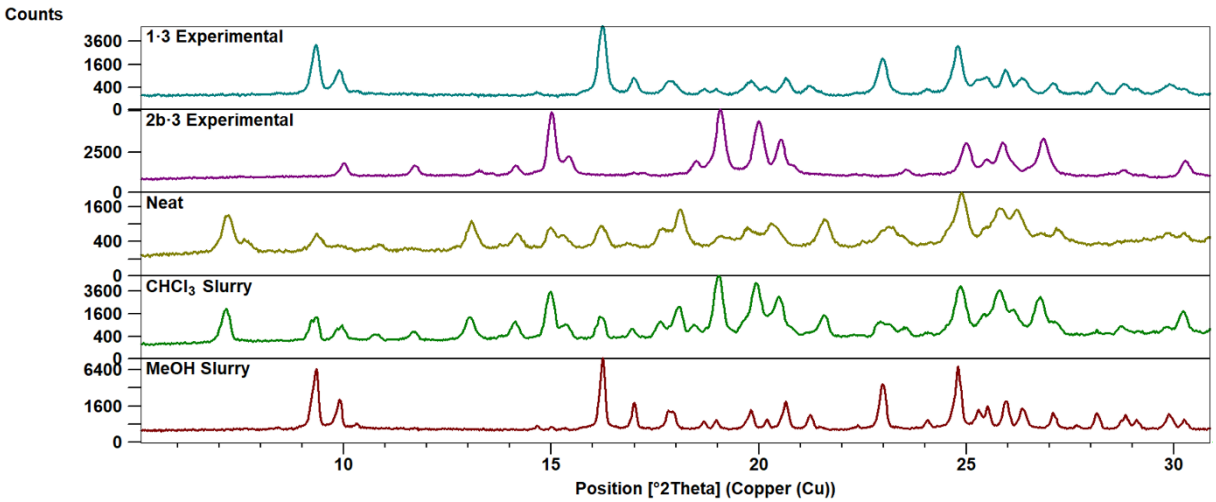

Figure S10. Comparison of neat grinding and slurry results for System B. When neat grinding is carried out, as well as after slurry experiments in chloroform, the ternary co-crystal is the major product (see also Figure S11), with small amounts of the two known co-crystals forming, similar to the LAG results. When slurry experiments are carried out in methanol, only the halogen-bonded co-crystal **1·3** is formed.

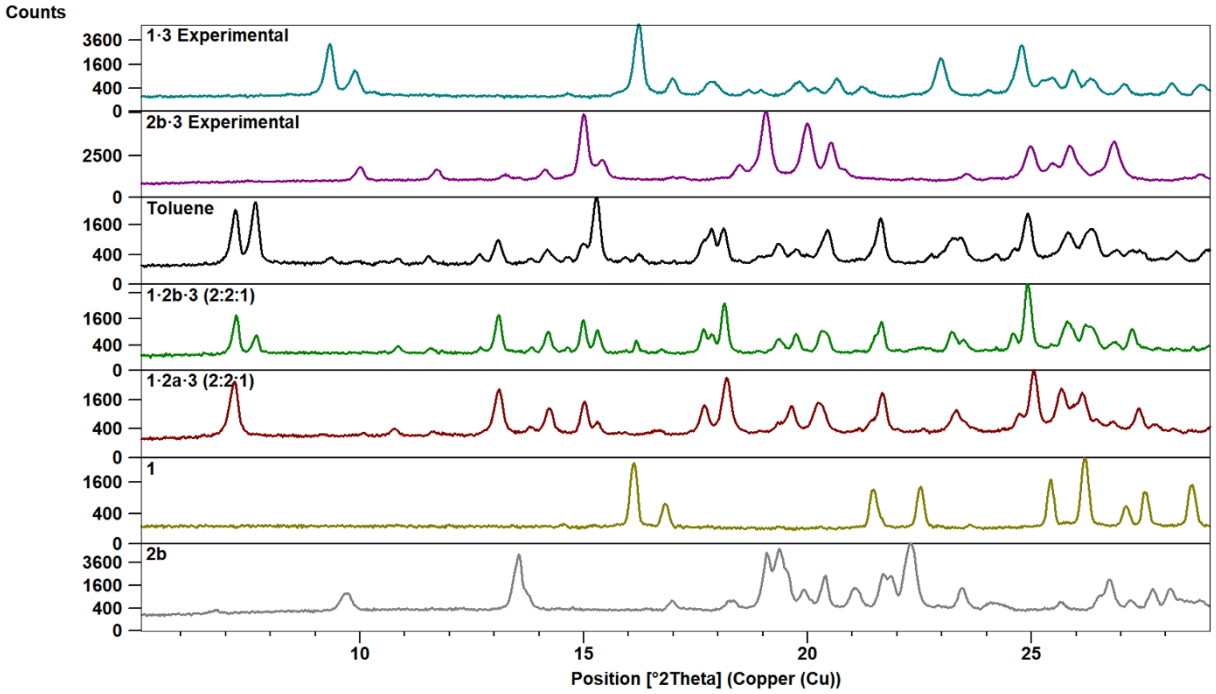

Figure S11. A closer look at one of the patterns containing the ternary co-crystal **1·2b·3** shows that there are many peaks that cannot be assigned to either **1·3** or **2b·3** – the pattern obtained from grinding **1**, **2b**, and **3** with toluene is used here as an example, shown in black (also contains **1·3** and **2b·3**). We suspect that the ternary co-crystal contains **1**, **2b**, and **3** in a 2:2:1 ratio. When the three starting materials are milled in this ratio, the pattern shown in red is obtained, which shows good correlation with the trace obtained from LAG. Furthermore, the pattern for this ternary co-crystal (red) matches the trace for the **1·2a·3** ternary co-crystal, indicating that these are likely isostructural materials.

Selectivity Experiments: Mechanochemistry (System C)

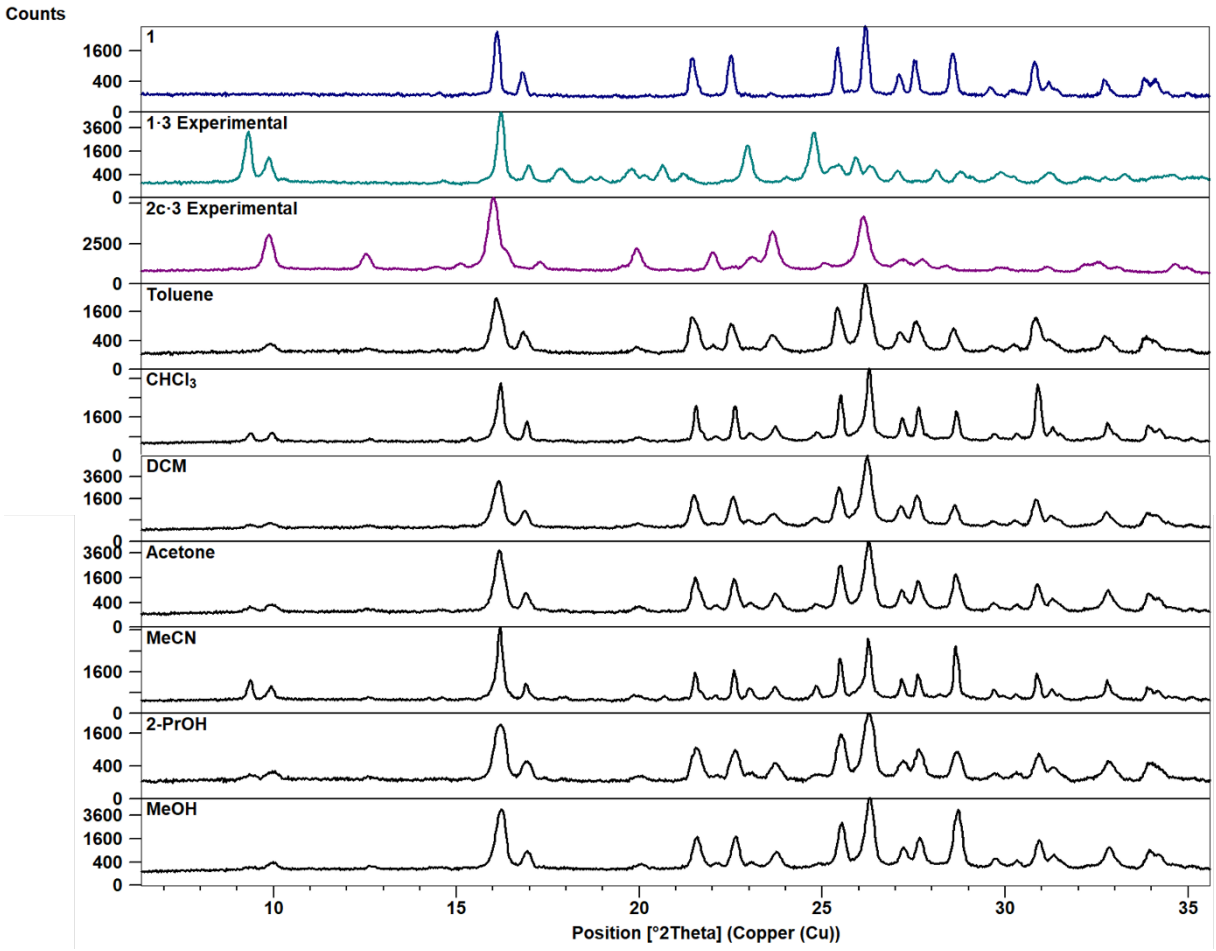

Figure S12. Comparison of LAG results, using seven different solvents, for System C. For each solvent used, small amounts of both the halogen bonded co-crystal (**1·3**) and the hydrogen-bonded co-crystal (**2c·3**) is formed, and a large amount of 1,4-diiodotetrafluorobenzene remains.

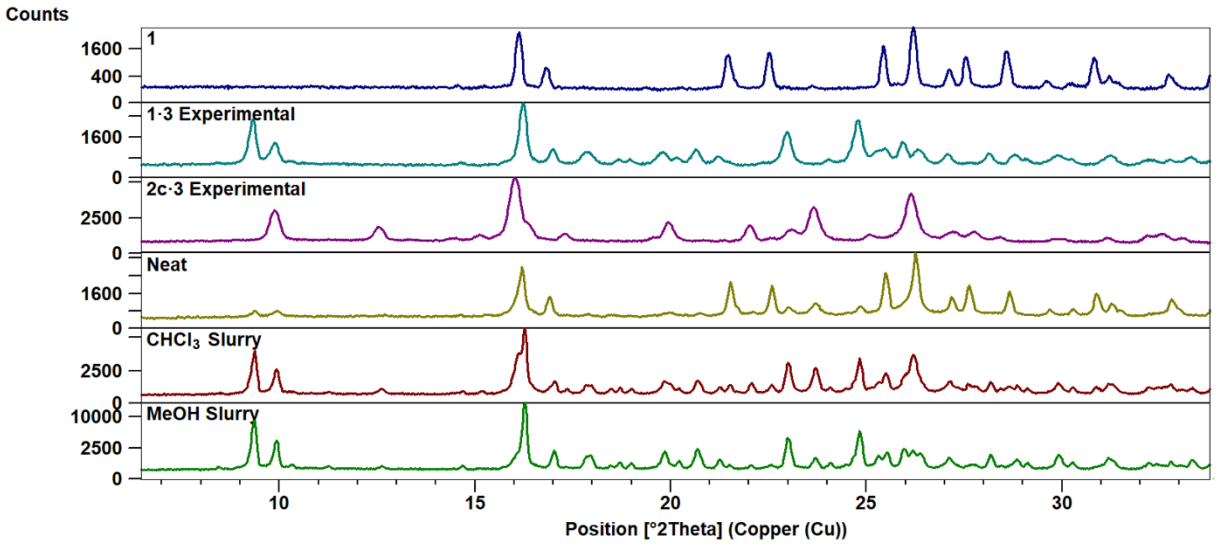

Figure S13. Comparison of neat grinding and slurry results for System C. When neat grinding is carried out, both **1**·**3** and **2c**·**3** is formed, along with **1** being left over, similar to the LAG results. When slurry experiments are carried out in methanol and chloroform, similar results are obtained, but the halogen-bonded co-crystal, **1**·**3**, becomes more prominent, and much less unreacted starting material remains. The peaks corresponding to **2c**·**3** similarly become more visible, e.g. around 12.6°.

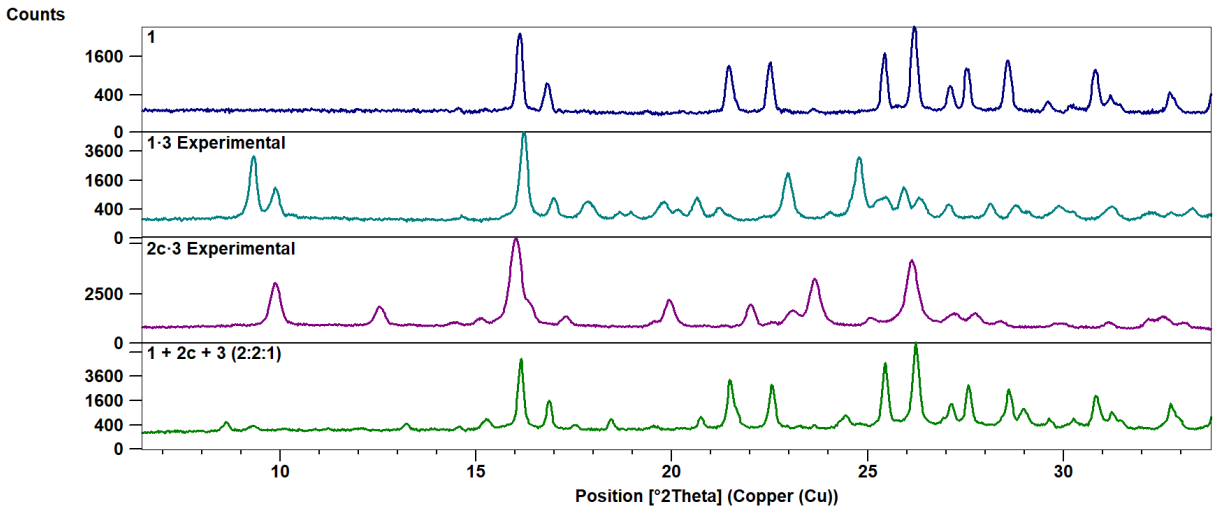

Figure S14. When a 2:2:1 ratio of **1**, **2c** and **3** are milled together, similar to what was done for Systems A and B, the trace is dominated by left-over starting material **1**. However, some new peaks do appear (e.g. peak at 8.6°), indicating another crystalline product that potentially exists.

Selectivity Experiments: Sublimation

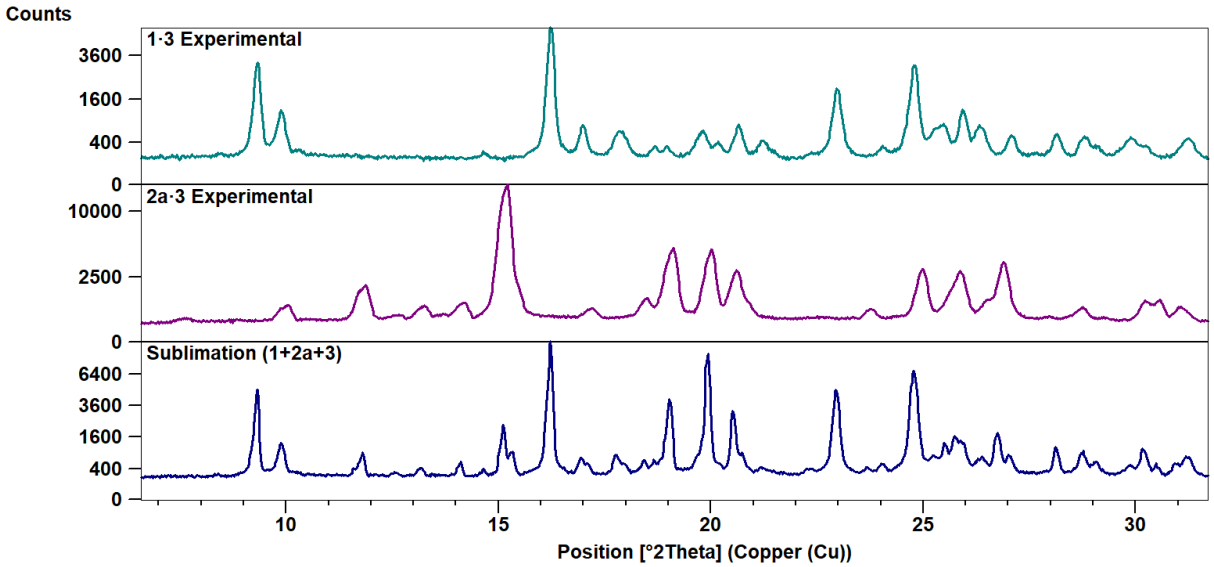

Figure S15. Results of selectivity tests by sublimation for System A. When a mixture of **1**, **2a**, and **3** is sublimed at 130 °C, a mixture of **1**·**3** and **2a**·**3** is formed.

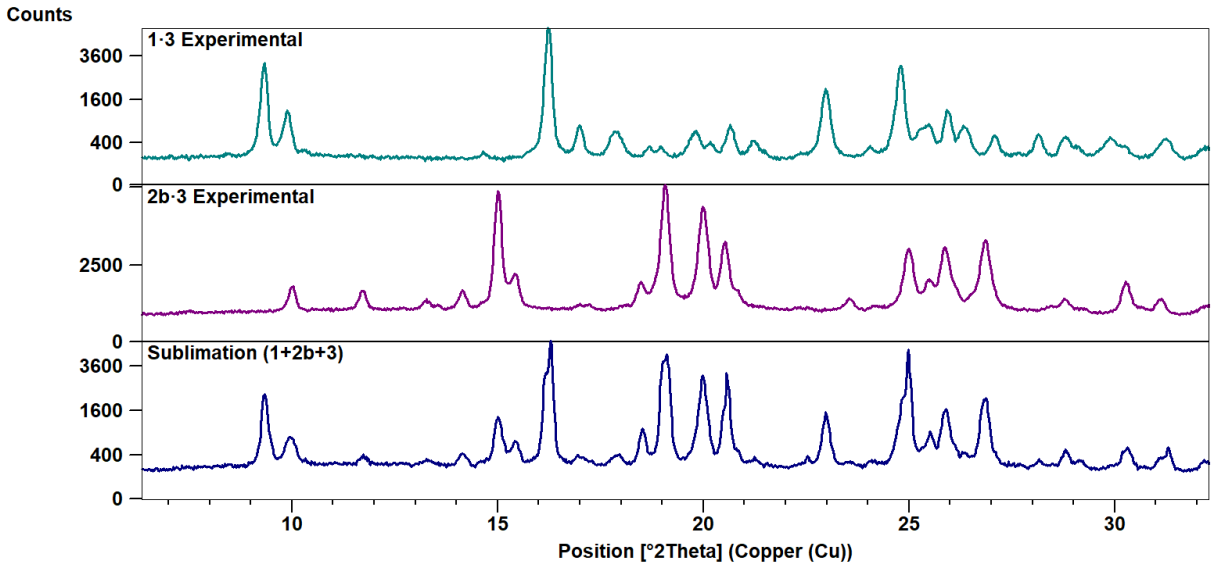

Figure S16. Results of selectivity tests by sublimation for System B. When a mixture of **1**, **2b**, and **3** is sublimed at 130 °C, a mixture of **1**·**3** and **2b**·**3** is formed.

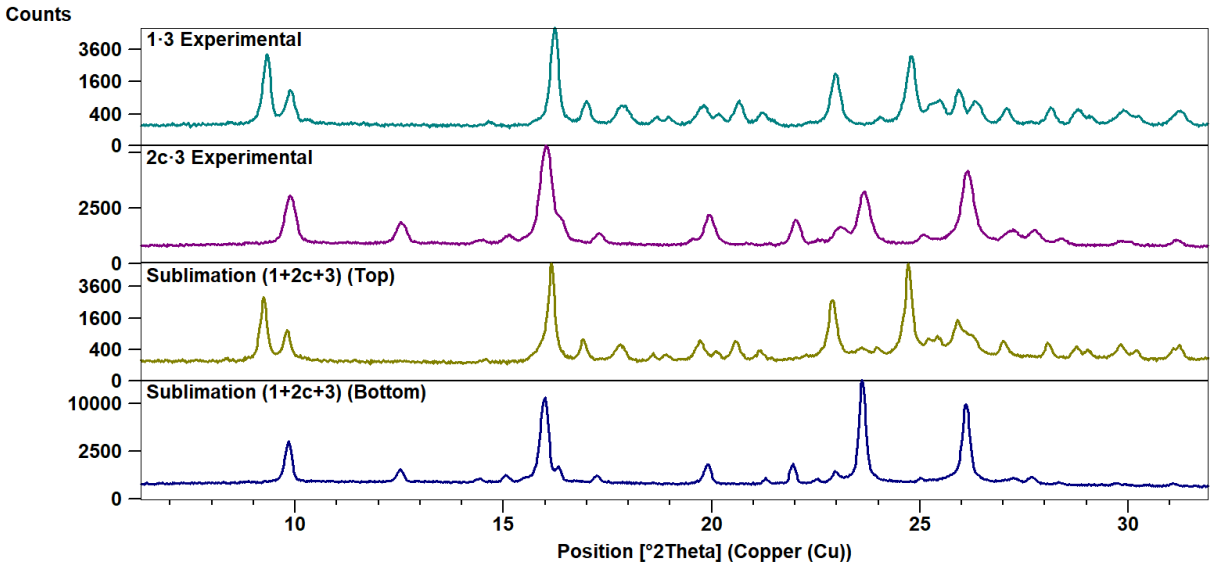

Figure S17. Results of selectivity tests by sublimation for System C. When a mixture of **1**, **2c**, and **3** is sublimed at 130 °C, separate bands of **1**·**3** and **2c**·**3** is formed. **1**·**3** crystallizes at the top, and **2c**·**3** forms below that.

NMR

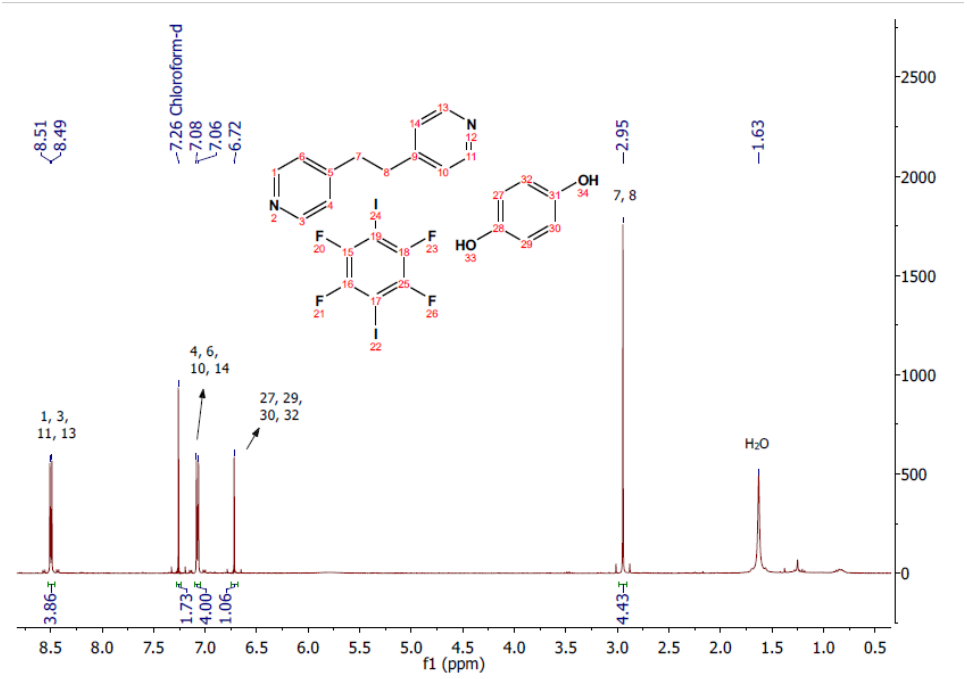

Figure S18. ^{1}H NMR spectrum (300 MHz) for the product obtained when a 2:2:1 mixture of **1**, **2a** and **3** was milled for 20 minutes, indicating that each individual molecule is still present in the product. Therefore, it can be concluded that no reaction occurred between the components. Peaks are referenced to the $CDCl_3$ peak at 7.26 ppm.

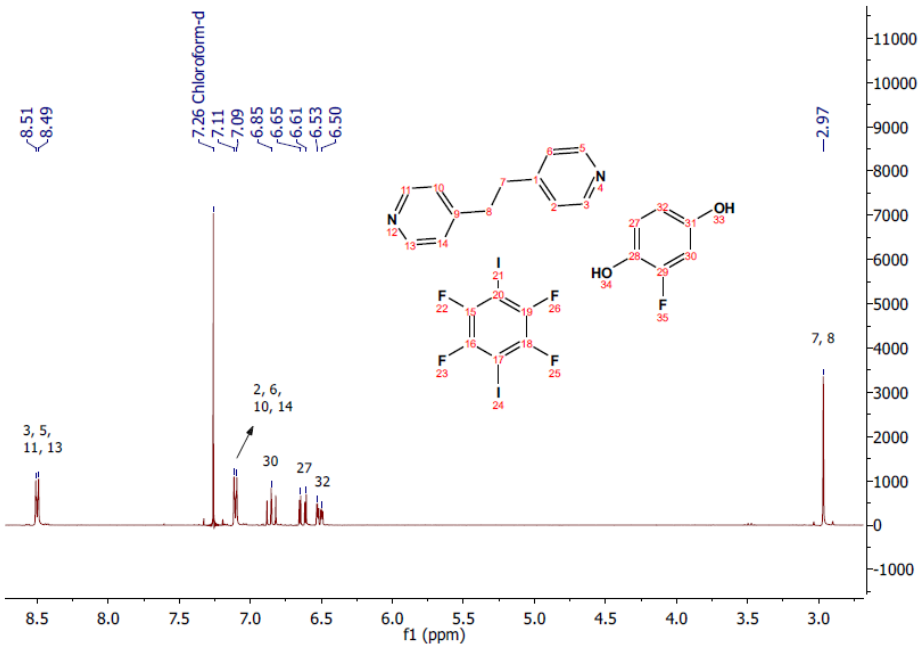

Figure S19. ^{1}H NMR spectrum (300 MHz) for the product obtained when a 2:2:1 mixture of **1**, **2b** and **3** was milled for 20 minutes, indicating that each individual molecule is still present in the product. Therefore, it can be concluded that no reaction occurred between the components. Peaks are referenced to the $CDCl_3$ peak at 7.26 ppm.

CHAPTER 4

Assessment of co-sublimation for the formation of multicomponent crystals

---

4.1 Article submitted to Crystal Growth and Design (unpublished)

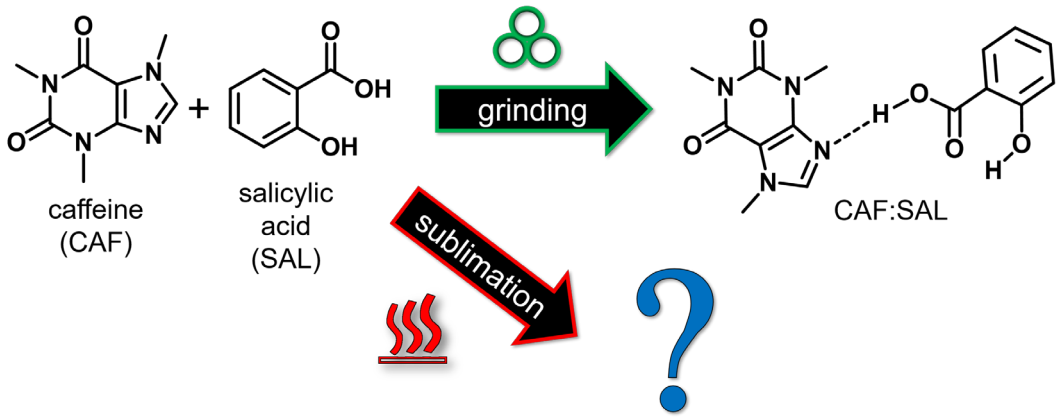

Contributions of the author:

- Design of project
- Preparation of all co-crystals, salts and co-crystal salts
- Collection of single-crystal X-ray data
- Solution and refinement of single-crystal X-ray structures with assistance from co-authors and Dr Leigh Loots
- Recording of PXRD patterns
- Recording of FTIR spectra
- Interpretation of results with co-authors
- Writing of the article and submission as corresponding author

ASSESSMENT OF CO-SUBLIMATION FOR THE FORMATION OF MULTICOMPONENT CRYSTALS

Jean Lombard[*]*, Tanya le Roex and Delia A. Haynes*

Department of Chemistry and Polymer Science, University of Stellenbosch, P. Bag X1, Matieland, 7602, Republic of South Africa. E-mail: jeanl@sun.ac.za

Abstract

The merits of co-sublimation and mechanochemistry as screening techniques for multicomponent crystal formation are compared. Several multicomponent crystals that can be formed both mechanochemically and by sublimation are investigated, allowing for a comparison between the relatively unknown technique of co-sublimation and a well-known, robust solid-state screening methodology. This work aims to determine the general utility and versatility of co-sublimation in the preparation of multi-component crystals. Co-crystals and salts, as well as their polymorphs have been investigated, and problems that can arise due to sublimation temperature differences, isomerization, and degradation are discussed. Co-sublimation is shown to be a valuable co-crystallization technique for the discovery and identification of new multicomponent materials.

Introduction

A multicomponent crystal forms when two or more different molecules or ions solidify together as a crystalline single-phase material. When such a material contains only neutral components in a stoichiometric ratio, it is called a co-crystal. When the components are charged, such as when a hydrogen atom shifts from an acid to a base, a salt is formed. Such an ion pair may also crystallize alongside the neutral conjugate form of either the acid or the base, in which case the material can be called a co-crystal salt.[1] Multicomponent crystals are of significant interest due to the potential improvement of physical properties they may offer over the single-component material.[2] A multicomponent material can have different mechanical properties,[3] optical properties,[4] thermal stability,[5] or reactivity[6] when compared to its constituent species. The discovery of new multicomponent forms is therefore an important step in the development of new materials.

In order to identify new multicomponent forms, a molecule of interest will often be co-crystallized with a large number of other organic molecules, called coformers. Such systematic multicomponent

screening tests need to be simple, fast, and efficient. Solution crystallization is perhaps the most widely-used co-crystallization methodology; however, mechanochemical grinding has been shown to require less time and effort[7] and be more effective when it comes to screening for multicomponent crystals.[8,9] To carry out mechanochemical screening the two components are either ground together by hand in a mortar and pestle, or milled mechanically. A small amount of solvent can be added to speed up the reaction (liquid-assisted grinding; LAG) and the transformation usually does not take longer than 30 minutes.

A number of other crystallization[10–12] and computational[13,14] techniques have been employed for the screening of potential multicomponent crystals; however, due to the large number of variables one can never be sure whether all solid forms have been identified. It is possible that multicomponent crystal forms exist that are not detected due to biases imposed by the techniques themselves. For instance, two coformers may not be soluble in the same solvents, which would inhibit their interaction and co-crystallization when solution-based techniques are used. It has also been shown that the solvent used can favor, or disfavor, specific types of intermolecular interactions.[15,16] Therefore, if all multicomponent forms are to be discovered, it is important that a variety of crystallization techniques are used.[9] This led us to study crystallization by sublimation as an alternative to the standard solution-based crystallization techniques.

Co-sublimation of neutral components to yield multicomponent crystals has not been studied in great depth, and when used it is often simply reported as an inconsequential detail – the general versatility and practicality of this technique has not been discussed. During co-sublimation, neutral components are simultaneously sublimed so that they may interact in the gas phase and crystallize as the multicomponent form. A limited number of co-crystals have been formed by co-sublimation,[17–21] and we have recently shown that molecular salts and co-crystal salts can easily be formed by sublimation as well.[18] We generally employ a very simple sublimation strategy: an evacuated Schlenk tube containing a mixture of starting materials is heated using an oil bath. The use of more sophisticated apparatus may improve the outcome of co-sublimation experiments and produce higher yields. However, our goal in this work was not to perfect the formation of a particular co-crystal, but rather to study a wide variety of systems so that some general observations can be made regarding the technique of co-sublimation itself.

In this study we report on the co-crystallization of 16 combinations of common organic molecules (Scheme 1, Table 1) by mechanochemistry (neat- and liquid-assisted grinding) and co-sublimation in order to determine how these techniques compare. Can sublimation compete with a robust screening technique such as mechanochemistry? Does crystallization by sublimation offer any advantage over

other methods? Common problems that can be encountered during co-sublimation will be discussed, as well as how they can potentially be overcome.

Table 1. Summary of the multicomponent crystals investigated, which includes the sample number used in this report, the coformers, stoichiometry and the classification in terms of ionization.

Code	Coformers		Classification	Code	Coformers		Classification
1	CAF	SAL	1:1 co-crystal	**9a**	SA	PIP	2:1 salt
2	CAF	OA	2:1 co-crystal	**9b**	SA	PIP	1:1 salt
3	THE	SAL	1:1 co-crystal	**10***	MA	PYR	1:1 salt
4	THE	OA	2:1 co-crystal	**11a**	FA	PYR	1:2 co-crystal
5	THE	INAM	1:1 co-crystal	**11b***	FA	PYR	1:1 co-crystal salt
6a	FA	23LUT	1:2 co-crystal	**12a**	FA	3PIC	1:2 co-crystal
6b	FA	23LUT	2:1 co-crystal salt	**12b***	FA	3PIC	1:1 co-crystal salt
6c*	FA	23LUT	2:1 co-crystal salt	**13**	NA	OA	1:1 salt
7a	NAM	BA	1:1 co-crystal	**14**	PYG	HMT	1:1 co-crystal
7b	NAM	BA	1:1 co-crystal	**15**	GA	4PP	1:1 salt
8	MA	BPY	2:1 salt	**16***	PYG	4PP	1:1 co-crystal

* These crystal structures are presented here for the first time.

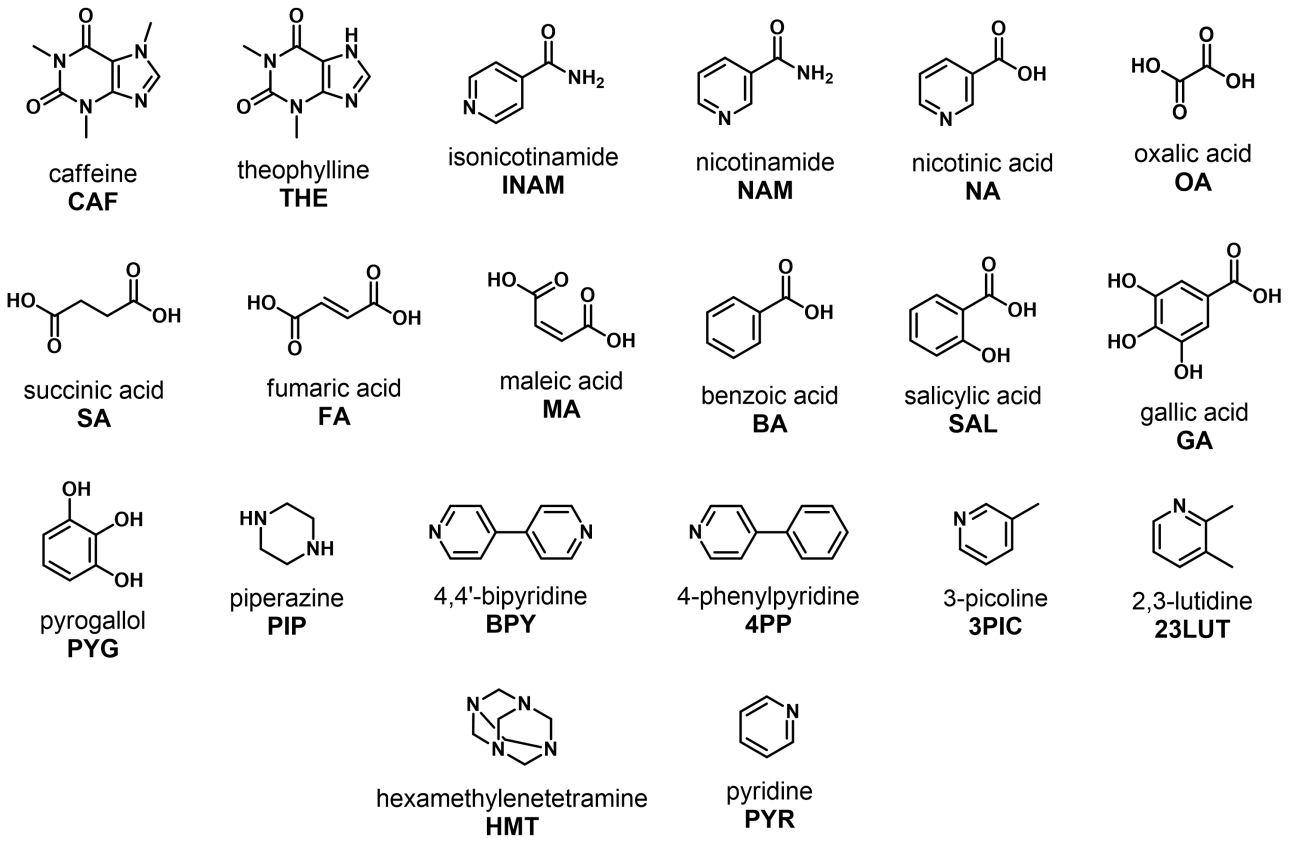

Scheme 1. Summary of the coformers used for the multicomponent crystallizations.

Experimental

Compounds were purchased from Sigma Aldrich and used without further purification (Scheme 1).

Mechanochemistry

A FTS1000 Shaker Mill from Form-tech Scientific was used for mechanochemical experiments, which were performed using two 15 ml stainless steel grinding jars each with two 6 mm steel balls as the milling medium. Milling was either carried out without any solvent (neat) or with the addition of a small amount of solvent ($\eta = 0.25$ µl mg^{-1}), added with a micropipette. Unless otherwise stated, samples were milled at room temperature for 20 minutes at 20 Hz.

Co-sublimation

Co-sublimation was carried out by simultaneously subliming the starting materials in a Schlenk tube, with a physical mixture of the starting materials placed together at the bottom of the tube. The sublimation tube was evacuated (0.6 mbar line pressure) and the end containing the coformers heated in an oil bath. In most cases a thin Schlenk tube (14 mm diameter, 220 mm length) was used so that a temperature gradient formed along the sides of the tube, along which crystals could deposit depending on their vapor pressure (usually within a few hours). This temperature gradient resulted in products crystallizing in separate bands, allowing for easy removal of pure materials. In some cases, sublimation was carried out using a larger Schlenk tube equipped with a water-cooled cold finger on which crystals could grow.

Re-sublimation

The term re-sublimation is used to describe the re-crystallization by sublimation of pre-formed multicomponent material. This is distinct from co-sublimation, where unreacted coformers are sublimed. Experimentally, re-sublimation was carried out in a similar manner to co-sublimation. Instead of unreacted neutral starting materials, the pre-formed multicomponent materials (formed by grinding) were added to the tube and sublimed to form crystals of the multicomponent materials.

Powder X-ray Diffraction

Powder X-ray diffraction (PXRD) was carried out at room temperature using a Bruker D2 Phaser benchtop diffractometer equipped with a copper radiation source ($\lambda = 1.54183$ Å) and operating at 30 kV and 10 mA. Powdered samples were loaded onto a zero-background holder and data collected in the range of $2\theta = 4$ to 40° at a speed of 0.5 seconds per scan (0.016° step size). Data analysis was carried out using X'Pert HighScore Plus.[22]

Single-Crystal X-ray Diffraction

Single-crystal X-ray diffraction (SCXRD) was carried out using a Bruker Duo diffractometer equipped with a CCD area detector and an Incoatec IμS microsource coupled with a multilayer mirror optics monochromator. Data were collected at room temperature or 100 K, with the temperature being controlled by an Oxford Cryosystems Cryostat (700 Series Cryostream Plus). Single crystals were irradiated (MoKα, λ = 0.71073 Å) and data collected and reduced using the Bruker software package SAINT,[23] operated through the Apex3 software. Data were subsequently corrected for absorption and other systematic errors using SADABS.[24,25] Crystal structures were solved using direct methods (SHELXT-18)[26] within the graphical user interface XSeed,[27,28] and then refined using SHELXL-18.[29] All atoms (except hydrogen atoms) were refined anisotropically. Hydrogen atoms bonded to carbon atoms were placed in calculated positions using riding models, while O–H and N–H hydrogen atoms were located using electron density maps and their positions allowed to refine. Images were created using POV-ray,[30] as visualized within XSeed.[27,28]

IR Spectroscopy

Fourier Transform Infrared spectroscopy (FTIR) was carried out using a Bruker Alpha P spectrometer with a Platinum ATR attachment.

Results and discussion

A number of multicomponent materials formed from small organic molecules were investigated (Table 1). Results are discussed below grouped according to either the type of multicomponent material or the type of molecules used. In all cases, co-crystallization was attempted by mechanochemical grinding using a ball mill, and by vacuum sublimation. Products were analyzed by PXRD and, where possible, SCXRD. The majority of the crystal structures have been reported previously; however, five new multicomponent materials were identified (Table 1), and their crystal structures determined. Full experimental details and information regarding these crystal structures are given in the Supplementary Information.

Simple co-crystals

A series of known co-crystals containing the xanthines caffeine (CAF) and theophylline (THE) were investigated (Figure 1). These co-crystals were straightforward to synthesize by both mechanochemistry and co-sublimation. The starting materials do not degrade, and their sublimation

temperatures are comparable, such that there exists a temperature at which both sublime at a similar rate, ensuring the coformers are in the gas phase simultaneously.

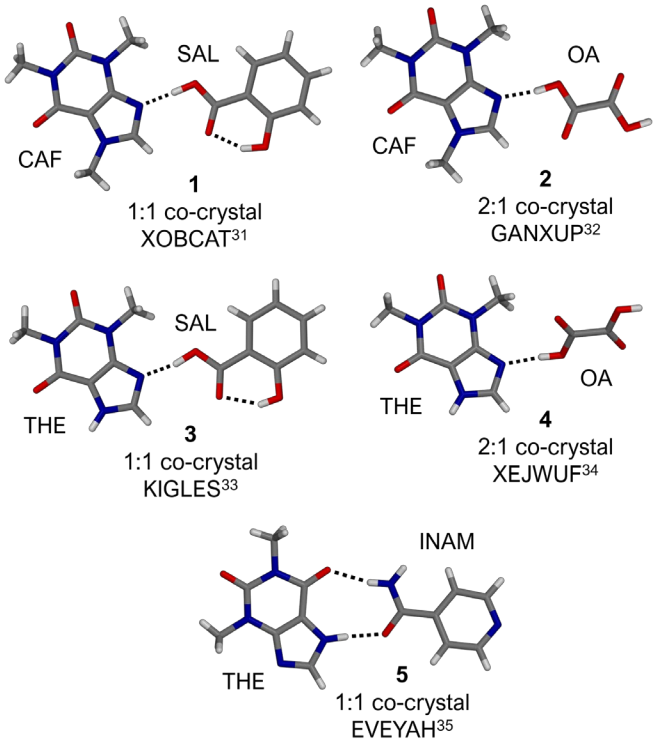

Figure 1. Hydrogen bonding between coformers in the crystal structures of co-crystals **1** – **5** formed by caffeine and theophylline. Images were generated from crystal structures deposited in the Cambridge Structural Database; refcodes are indicated with references to the literature.[31–35]

CAF and SAL

The combination of CAF and SAL produced a 1:1 co-crystal (**1**) in all experiments. Grinding a 1:1 molar ratio of caffeine and salicylic acid without the addition of solvent led to the formation of **1** in quantitative yield. Co-sublimation of the two starting materials (1:1 molar ratio) *in vacuo* in a Schlenk tube at 140 °C (a temperature at which both compounds sublime rapidly) yielded a powder of the co-crystal in between bands of CAF and SAL crystals (Figure 2). While the amount of **1** that formed was relatively small, the three crystallization zones did not overlap, and pure co-crystal powder could be collected for identification via PXRD.

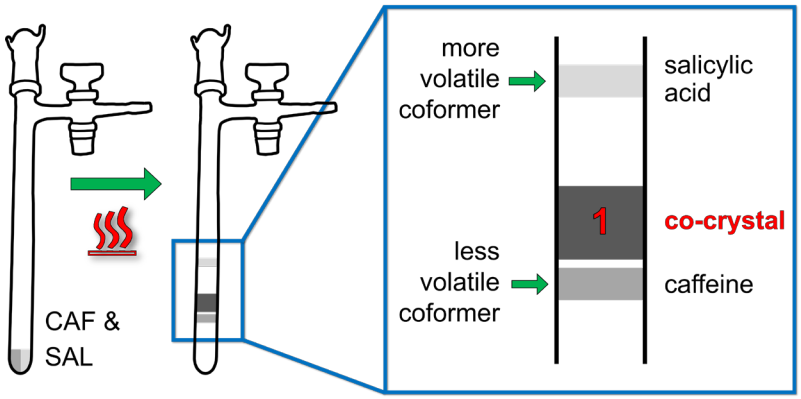

Figure 2. Schematic representation of the co-sublimation of CAF and SAL in a Schlenk tube, which yielded a powder of the co-crystal in between bands of CAF and SAL crystals.

CAF and OA

The combination of CAF and OA produced a 2:1 co-crystal (**2**) in all experiments. Grinding a 2:1 molar ratio of caffeine and oxalic acid, with the addition of a small amount of methanol, led to the formation of co-crystal **2**. Co-subliming CAF and OA (in a 1:1 molar ratio) at 120 °C led to the formation of fine crystals of **2**. A band of OA crystals also formed higher up in the sublimation tube and could be removed separately from the co-crystals. Additionally, water droplets condensed in the cap of the tube, as the dihydrate of OA was used as the starting material.

THE and SAL

The combination of THE and SAL produced a 1:1 co-crystal (**3**) in all experiments. Grinding theophylline and salicylic acid in a 1:1 molar ratio with a small quantity of methanol led to complete conversion to the co-crystal (**3**). Subliming a 1:1 molar ratio of THE and SAL at 140 °C led to the formation of polycrystalline **3**. SAL is more volatile than THE, and crystals of pure SAL were found to form in the cooler part of the sublimation tube (high in the tube). Conversely, THE crystallized at the bottom of the tube. The co-crystal formed just above the band of theophylline crystals, with slight overlap between these two bands.

THE and OA

The combination of THE and OA produced a 2:1 co-crystal (**4**) in all experiments. Grinding a 2:1 molar ratio of theophylline and oxalic acid (LAG using methanol) produced the co-crystal **4**. Co-subliming a mixture of THE and OA at 160 °C also produced pure **4** in between OA (top) and THE crystals (bottom).

THE and INAM

The combination of THE and INAM produced a 1:1 co-crystal (**5**) in all experiments. Grinding a 1:1 molar ratio of theophylline and isonicotinamide with a small amount of methanol produced the co-crystal **5**. Co-subliming a 1:1 molar ratio of THE and INAM at 120 °C produced **5** as a band of powder below a band of INAM (the more volatile coformer).

From these simple co-crystallizations we observe a general trend. When two starting materials are combined using co-sublimation the more volatile component crystallizes high up in the sublimation tube, in the coolest region. The least volatile component crystallizes lower down in the tube where it is warmer, and the co-crystal crystallizes between these two limits. The three crystallization zones do not usually overlap, allowing the collection of pure co-crystal from these experiments.

In the case of **1 – 5**, the co-crystals obtained by co-sublimation are equivalent to those formed mechanochemically. They were quick to form, and in each case, co-sublimation was successful on the first attempt, provided a suitable sublimation temperature, at which both components can sublime, was chosen.

Polymorphic systems

Molecules can often arrange in more than one way when they solidify, and thereby form polymorphs. Even though such polymorphs contain the same components, they can differ with regards to their physical properties.[36] Unfortunately, regulating which form is obtained is not always easy. It is possible to selectively isolate a particular polymorph of a pure- or multicomponent material when carrying out crystallizations in solution or mechanochemically, by altering variables such as the temperature and the solvent used.[37–39] It is also possible to selectively obtain polymorphs of molecular materials when using co-sublimation, particularly by using additives[40] and controlling the temperature of the area where de-sublimation occurs.[41,42] To our knowledge, the use of sublimation to selectively prepare a specific multicomponent crystal polymorph has not been reported. Two sets of multicomponent polymorphs will be presented here to compare their formation using solid-state and gas-phase techniques.

FA and 23LUT

The combination of fumaric acid and 2,3-lutidine is known to form a 1:2 co-crystal (**6a**) and a 2:1 co-crystal salt (**6b**) (CSD refcodes: RESFOL & RESFIF).[43] Using co-sublimation we discovered that a second polymorph of the co-crystal salt, **6c**, could also be produced. Due to the similarities between these materials, the crystal structures of **6a** and **6b** were re-determined along with that of **6c**.

The crystal structure of **6a** comprises hydrogen-bonded base-acid-base trimers, while the co-crystal salts (**6b** and **6c**) are made up of infinite hydrogen-bonded nets of FA and FA^- with pendant cations (Figure 3). In both **6b** and **6c**, each hydrogen fumarate ion forms an additional charge-assisted hydrogen bond with a lutidinium cation which is positioned inside each of the apertures in the nets (Figure 3). Two of these nets pair up to form a bilayer such that the apertures align. Each of these holes in the bilayers is then filled with two cations, one bonded to each net. The layers exist in both polymorphs, they are identical in this regard; however, the way in which the layers stack is slightly shifted in each form (Figure 3).

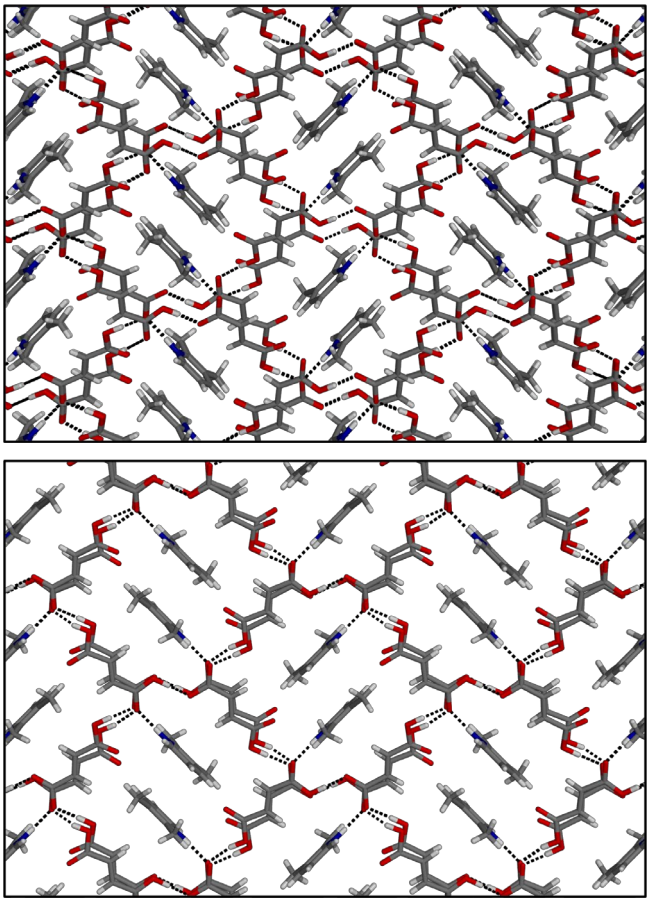

Figure 3. Packing diagram for **6b** (top) and **6c** (bottom), both viewed along [100]. Each polymorph is made up of identical layers that differ in how they stack.

All three crystal forms were produced mechanochemically, but not as pure materials. Co-crystal **6a** was obtained by milling a 1:2 ratio of FA and 23LUT; however, using a 2:1 ratio led to formation of both polymorphs **6b** and **6c** simultaneously (with the peaks for **6c** in the powder pattern being much less prominent) (Figure S8). Additionally, when ground, **6c** partially converted to **6b** – even during preparation of a powdered material for PXRD. This makes sense considering the polymorphs only

differ by a slight shift of the layers within their structures. However, the transformation did not proceed to completion; some **6c** remained even after 3 hours of milling.

Heating FA and 23LUT together under vacuum produced all three forms by sublimation. Different ratios of starting materials were used but this did not appear to have an effect on the product obtained, and co-sublimation of these molecules most often produced a mixture of **6b** and **6c**, as single crystals, irrespective of the ratios used. On occasion, these crystals were accompanied by a powder of **6a**. It should be noted that single crystals of all three forms were also obtained from solution, also as mixtures that mostly contained only **6b** and **6c** (crystals of **6a** were obtained only once). The same was observed during re-sublimation of pre-formed **6a**, **6b**, and **6c**, i.e. crystals of the two polymorphs formed, occasionally accompanied by the co-crystal.

NAM and BA

The combination of nicotinamide and benzoic acid is known to form two 1:1 co-crystal polymorphs (**7a** and **7b**) (CSD refcodes: GAZCES & GAZCES01).[44] Lukin *et al.* reported two further polymorphs that could be obtained mechanochemically; however, their structures have not been determined.[44] Polymorphs **7a** and **7b** are structurally similar – in each the carboxylic acid functional group of BA forms a hydrogen bond to the pyridine nitrogen atom of NAM. However, in **7a** the amide groups also hydrogen bond to form NAM dimers, while in **7b** the N−H and O of each amide interacts with two different NAM molecules (Figure 4).

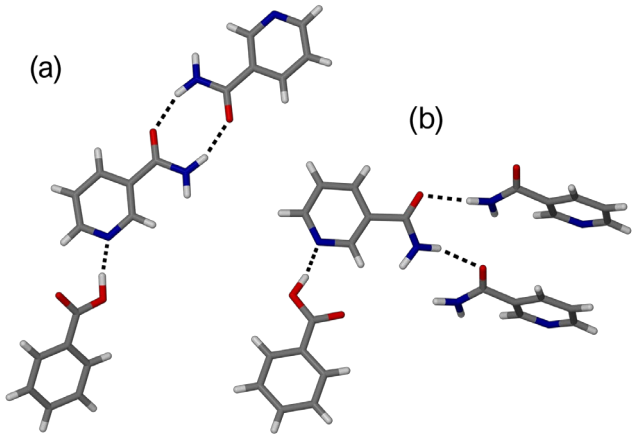

Figure 4. Hydrogen bonding in (a) **7a** and (b) **7b**. Images generated from published crystal structures.[44]

Co-subliming NAM and BA in a 1:1 molar ratio at 100 °C led to formation of polycrystalline **7a** and **7b**, as a mixture. BA and NAM crystallized above and below the multicomponent crystals respectively. Conversely, depending on the solvent used, grinding a 1:1 molar ratio of these starting materials produced either **7b** or a material with a PXRD pattern corresponding to a previously

reported material for which the crystal structure has not been determined.[44] In the published study more variables were explored (such as different solvent additives and milling duration) and the authors found that it was possible to form both **7a** and **7b** mechanochemically, and determined the crystal structures from powder diffraction data.

In general, we have observed that co-sublimation can be used for the formation of polymorphic multicomponent crystals, but not in a selective manner – mixtures of polymorphs are obtained. Sublimation apparatus which allows for more precise control over temperature may be useful in this regard. However, polymorphs that are not easily identified in an initial series of LAG screening experiments can be identified using co-sublimation. These may form as powders, but, as we see in the case of **6b** and **6c**, can also sublime as single crystals. Co-sublimation could therefore be useful both for the identification of polymorphs and for the determination of their crystal structures.

Co-crystallization when molecules have different sublimation temperatures

For multicomponent crystals to form by co-sublimation, the coformers need to encounter one another in the gas phase. However, the components to be co-sublimed need not have the same sublimation temperature for there to be enough of each present in the gas phase. Often, as in the previous examples, each coformer crystallizes separately from sublimation, with the multicomponent material crystallizing in between them. However, if one coformer has a much lower sublimation temperature than the other, it may sublime and crystallize as the molecular material completely separately from the other component.

Fortunately, it is possible to modify the amount of each component present in the gas phase to some extent. The simplest way to go about this is by changing the relative amounts of the starting materials used as this will influence the relative amounts of each coformer in the gas phase during the initial stages of co-sublimation. Technically, the amount of each component in the gas phase at equilibrium is only dependent on the vapor pressures of the solids, and not on the quantities used. However, because co-crystallization starts as soon as a sublimation experiment begins (as soon as heat is applied), the compound with the lower volatility may not reach equilibrium before co-crystallization occurs. Adding excess of the less volatile solid allows more of that coformer to enter the gas phase initially. Another possibility is to heat the coformers at two different temperatures, so that they sublime almost simultaneously, i.e. the vapor pressures of the two components are equalized. Such an example has been published recently where this technique was shown to be very effective.[21] It is also possible to control relative amounts of coformers in the gas phase by pre-forming the multicomponent material, with the desired stoichiometry, as a powder before sublimation is carried out. When this multicomponent material is re-sublimed under vacuum conditions, both coformers can

potentially enter the gas phase simultaneously, in the correct ratio. In this case sublimation has to be coupled with another technique, such as grinding, but it has the potential to form diffraction-quality single crystals. Three cases are reported here to demonstrate each of these approaches.

MA and BPY

The combination of maleic acid and 4,4'-bipyridine is known to form a 2:1 salt (**8**) from solution, the structure of which has been previously determined (CSD refcode: GIPQAX01).[45] This adduct was crystallized from solution; however, we observed that isomerization frequently occurred in solution so that a fumaric acid co-crystal formed instead. In our hands, salt **8** could be made mechanochemically by grinding a 2:1 ratio of MA and BPY, but when recrystallized from solution the FA co-crystal formed instead. The simplest way of obtaining single crystals of **8** turned out to be co-sublimation, even though the starting materials differ greatly with regards to sublimation temperature (BPY sublimation starts at 50 °C and MA at 100 °C). When a 2:1 ratio of starting materials was used, the salt did not form, as BPY is too volatile compared to MA, and the starting materials sublimed separately. However, when a 4:1 molar ratio of MA:BPY was used, co-sublimation at 100 °C was successful and single crystals of the salt formed within 4 hours. It is therefore possible for the gas phase coformer concentration during co-sublimation to be altered by changing stoichiometry and using an excess of the least volatile starting material.

FA and 23LUT

The formation of co-crystal **6a** and the co-crystal salt polymorphs **6b** and **6c** were described earlier in this paper; however, it is pertinent to mention them again at this stage as the two coformers have vastly different volatilities. In fact, 2,3-lutidine is a liquid at room temperature. Apparatus has been designed in our group that can be used to heat two compounds at two different temperatures under vacuum (Figure S15).[17] The apparatus consists of a U-shaped tube with a removable bulb at each end in which compounds are placed. The tube can be placed under vacuum and the bulbs suspended in adjacent oil baths or heating pockets so that each compound may be sublimed at the desired temperature. In this way, FA was sublimed at 200 °C while 23LUT was vaporized at 40 °C, so that both compounds entered the gas phase simultaneously. The crystals that formed in the connecting tube could be identified by PXRD and unit cell determinations as **6b** and **6c** (Figure S16). Heating coformers at different temperatures is therefore another useful method of obtaining multicomponent crystals when vapor pressures differ.

SA and PIP

The combination of succinic acid and piperazine is known to form a 2:1 salt (**9a**) and a 1:1 salt (**9b**) (CSD refcodes: IMEZIL[46] & BURWEQ[47]). Note that **9a** is classified as a co-crystal in the literature, but our structure determination indicates clearly that it is a salt: C−O bond lengths and FTIR indicate the presence of carboxylate groups. The crystal structures of **9a** and **9b** were re-determined for confirmation (Figure 5; details are given in the Supplementary Information).

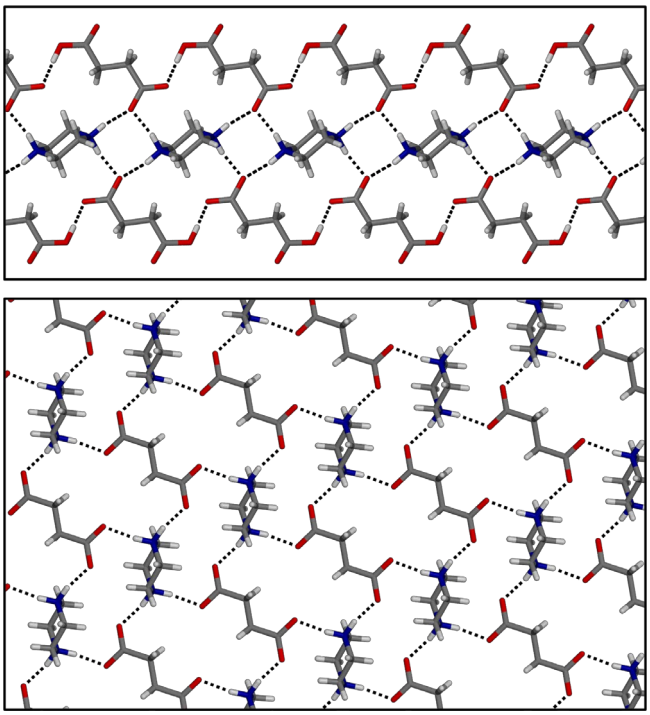

Figure 5. Top: Hydrogen-bonded ribbons in salt **9a** that run along the *a*-axis. Bottom: Hydrogen-bonded layer in salt **9b**, viewed along [101].

Grinding SA and PIP in a 2:1 molar ratio (neat- or liquid-assisted), led to complete conversion to the salt **9a**, while the use of a 1:1 ratio led to the formation of **9b**. However, subliming a number of different molar ratios of SA and PIP at 120 and 140 °C (1:1, 2:1 and 4:1) led to the formation of single crystals of **9b** only. This may be a result of the differences in vapor pressure of the two coformers. PIP is very volatile and will even slowly sublime at room temperature. On the other hand, SA only sublimes at 110−120 °C, which is why co-sublimation was carried out at a higher temperature. At 120 and 140 °C both compounds can sublime; however, PIP will always start to sublime faster than SA, with co-crystallization initiated before SA sublimation reaches equilibrium. This means that as soon as SA sublimes, it immediately crystallizes with the PIP already present in the gas phase to form the 1:1 product (**9b**) instead of staying in the gas phase until SA is concentrated enough to form the 2:1 product. In other words, it is easier for the 1:1 salt to form than for the 2:1 salt that requires two

SA molecules in the gas phase for every one molecule of PIP. Unfortunately, because the sublimation temperatures of the starting materials are so vastly different, using an excess of succinic acid did not rectify the problem.

Fortunately, both **9a** and **9b** were able to re-sublime if pre-formed by grinding (**9a** at 160 °C and **9b** at 140 °C). When re-sublimed, **9a** recrystallized as **9a**, and **9b** recrystallized as **9b**, with some starting materials crystallizing separately. During re-sublimation of a multicomponent crystal, the components can vaporize individually. However, it is also possible that both coformers sublime simultaneously in either a 1:1 or 2:1 ratio (in the case of **9a** and **9b**), so that either salt could in theory deposit again from the gas phase. In this case, the gas phase stoichiometry is defined by the starting salts, and the volatility differences experienced during co-sublimation are no longer a limiting factor. Our previous work has indicated that some molecules or ions remain hydrogen bonded when they enter the gas phase.[18] If pairs or clusters of molecules specific to a particular material are retained in the gas phase it would further drive crystallization of that material. This is possibly what is happening here too: we are not seeing interconversion between **9a** and **9b** in the gas phase, **9b** only re-sublimes as **9b**. Re-sublimation is therefore a viable alternative to co-sublimation if single crystals are desired.

Clearly, compound volatility and the compatibility of sublimation temperatures are important factors when growing multicomponent crystals by sublimation. Coformers need to be present in the gas phase in the correct stoichiometry for multicomponent crystals to form. Gas-phase concentrations can be manipulated to some extent by changing the ratio of starting material used, heating coformers at different temperatures, or by pre-forming multicomponent materials before sublimation so that the stoichiometry is predetermined.

Co-crystallization when coformers can isomerize

The formation of certain multicomponent crystals can be hindered by unwanted isomerization of the coformers.[48] For example, in solution maleic acid isomerizes to fumaric acid in the presence of a base (Figure 6). It has been reported that a co-crystal between maleic acid and pyridine could not be obtained, as pyridine catalyzes the transformation of maleic acid to fumaric acid.[48] Mohamed *et al.* reported that they could not form a co-crystal or a salt with MA and PYR as this isomerization happened within a few hours, while crystals took a week to form. Isomerization in the gas phase may proceed differently than in solution, and sublimation may thus present a new synthetic pathway for multicomponent materials containing these types of coformers. Additionally, crystal growth and nucleation generally occur much faster during co-sublimation. Crystals usually form within a few hours, and so it may be possible to form a co-crystal with maleic acid before isomerization can occur. We have already discussed a salt containing MA and BPY (**8**) – this salt was easily formed by co-

sublimation, while solution crystallization was often accompanied by a fumaric acid co-crystal due to isomerization. Here we report three new co-crystals that were discovered by co-sublimation involving maleic acid.

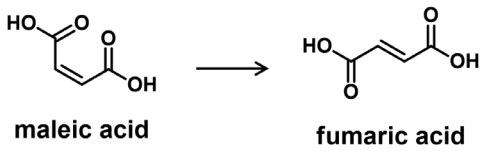

Figure 6. Maleic acid isomerizes to fumaric acid.

MA and PYR

As previously stated, no known multicomponent forms of maleic acid and pyridine have been reported. Milling different ratios of MA and PYR led to the formation of a material with a PXRD trace not matching either starting material. Single crystals of this material, a new 1:1 MA-PYR salt (**10**), were obtained by sublimation. Heating a 1:1 mixture of the two starting materials in a large Schlenk tube *in vacuo* at 120 °C yielded single crystals of **10** on the cold finger after a few hours, and its crystal structure could be determined. Unfortunately, these crystals formed concomitantly with two other types of crystals. These were a 1:2 co-crystal between fumaric acid and pyridine (**11a**, CSD refcode: GUKWOZ)[48] and a new 1:1 co-crystal salt, also containing fumaric acid and pyridine (**11b**). Re-sublimation of the MA-PYR salt obtained from grinding led to the same three multicomponent products crystallizing.

When MA and PYR were combined in solution (using a variety of common organic solvents and mild heating to aid dissolution) they reacted covalently to form a zwitterionic molecule (CSD refcode: SUCPYR)[49]. However, it was eventually also possible to crystallize **10** from solution when vials were placed in the refrigerator at 4 °C. Carrying out crystallizations at low temperature allowed crystals to form quickly (within 24 h), potentially trapping maleic acid before isomerization could occur.

FA and PYR

Grinding a 1:2 molar ratio of fumaric acid and pyridine led to crystallization of the new co-crystal salt that was mentioned above, **11b**. The co-crystal **11a** was never obtained from grinding; however, another unknown product was obtained when FA and PYR were milled in a 1:1 ratio. Sublimation of a 1:1 mixture of the two starting materials at 170 °C yielded a powder of this unknown product as well as single crystals of **11b**. It is interesting that crystals of **11a** (a fumaric acid:pyridine co-crystal) could be obtained when co-subliming MA and PYR, but not when subliming FA and PYR. The reason for this may be the significantly higher sublimation temperature of FA (~140 °C) compared to MA (~100 °C).

MA and 3PIC

There are no multicomponent forms of maleic acid and 3-picoline reported in the CSD. Milling different ratios of MA and 3PIC together led to the formation of a powder with an unknown PXRD trace. Crystallizing these starting materials from solution (using common organic solvents) led to the formation of another powdered material with a PXRD trace not matching either starting material, or the unknown obtained from grinding. Neither of these unknown materials have been identified, but single crystals of a third material were finally obtained by co-sublimation at 130 °C. The crystal structure was determined, which identified the crystals as a new 1:1 co-crystal salt of 3-picoline and fumaric acid (**12b**). In the CSD there is also a 1:2 co-crystal formed by FA and 3PIC (**12a**, refcode: MOGWAI)[50]. Interestingly, when FA is dissolved directly in 3PIC, crystals of **12a** are obtained after 24 hours, with no **12b** forming (similar to what was observed in the literature). When the powder pattern for **12b** was simulated, it did not correspond to either of the powdered materials obtained from mechanochemistry or solution crystallization of MA and 3PIC, and neither did **12a**. Thus far, **12b** has only been obtained by sublimation.

From these examples it is clear that co-sublimation can be very useful for obtaining new multicomponent crystals. While isomerization does occur in the gas phase and in solution, the crystallization mechanism appears to be faster, potentially leading to the formation of different materials. It is also clear that the materials formed by mechanochemistry are not always the same as those formed by sublimation.

Salts by co-sublimation

It seems unlikely that salts would form by sublimation, as ions would not be stable in the gas phase. However, our previous work has shown that salts can indeed crystallize by co-sublimation.[18] In this paper so far a number of salts produced by co-sublimation have been presented. Specifically, the salts **8**, **9a**, **9b** and **10**, and the co-crystal salts, **6b**, **6c**, **11b** and **12b** can all be obtained from co-sublimation of neutral coformers, and generally crystallize from sublimation as diffraction-quality single crystals. One further noteworthy example will be highlighted here.

NA and OA

Co-subliming a 1:1 molar ratio of nicotinic acid and oxalic acid for 7 hours at 120 °C led to crystallization of a 1:1 salt containing the two coformers (**13**, CSD refcode: HEWWAI[51]). The salt formed in quantitative yield, and no starting materials sublimed separately or remained unreacted. Grinding a 1:1 molar ratio of the starting materials together similarly produced **13** in quantitative yield. According to the literature, this salt can also be formed by crystallizing the coformers from

solution; however, our experiments prove that co-sublimation can definitely also be used for the efficient production of a molecular salt.

Co-crystallization using heat-sensitive molecules

Not all coformers are well suited for co-sublimation, as some compounds can degrade or melt during heating. For example, maleic acid starts to degrade above 100 °C. Despite this, we have demonstrated its use in co-sublimation (see above). Being aware of the heat sensitivity of coformers is crucial in co-sublimation experiments, so that appropriate measures can be taken to overcome any degradation. When forming salt **8**, which contains MA, the temperature of co-sublimation had to be restricted to 100 °C. Co-crystallization was achieved by using specific ratios of starting materials to ensure sufficient amounts of each coformer in the gas phase. Of course, this will not always work – some co-crystals and salts cannot be formed by co-sublimation at all. Another potential solution to this problem is to reduce the pressure in the system, which would allow for sublimation to occur at a lower temperature. Problems involving heat-sensitive coformers can thus potentially be solved by generating a stronger vacuum, although this was not explored in this study. Further examples concerning heat-sensitive coformers are discussed below.

SA and PIP

Consider again the case of succinic acid and piperazine. It was determined that salt **9b** re-sublimed at 140 °C while salt **9a** only re-sublimed at 160 °C. Additionally, during co-sublimation at 140 °C, salt **9b** was obtained while **9a** did not form. It is possible that **9a** would also be able to form if co-sublimation were carried out at 160 °C. However, it was not possible to use such a high temperature because SA would melt at this temperature. If co-sublimation could be carried out at a lower pressure, using a more powerful vacuum pump, it should be possible to prevent SA from melting before it sublimes, which could allow for **9a** to form by co-sublimation.

PYG and HMT

The combination of pyrogallol and hexamethylenetetramine is known to form a 1:1 co-crystal (**14**), the structure of which has previously been solved from powder diffraction data (CSD refcode: BINDIL).[52] Grinding a 1:1 molar ratio of the starting materials together produced **14** in quantitative yield. Co-sublimation of the two starting materials at 110-120 °C for 6 h afforded crystalline material with a powder pattern matching that of **14**. However, one additional peak was observed which corresponds to a co-crystal between 1,2-dihydroxybenzene and HMT. Unit cell determination of single crystals confirmed the presence of this co-crystal in the products of the co-sublimation

experiment (CSD refcode: CERXIH)[53]. Pyrogallol clearly partially degrades during sublimation (Figure 7), but not before the majority co-crystallizes with HMT.

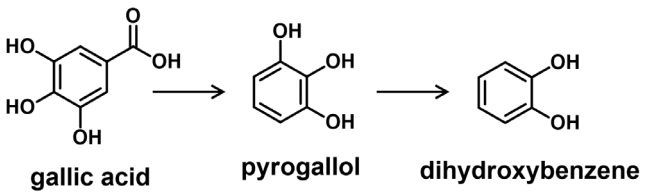

Figure 7. During sublimation, gallic acid can decarboxylate to form pyrogallol, and pyrogallol can similarly degrade into a dihydroxybenzene.

GA and 4PP

The combination of gallic acid and 4-phenylpyridine is known to form a 1:1 salt (**15**, CSD refcode: TICZIQ).[54] Salt **15** can easily be made by liquid-assisted grinding, but in this case GA degradation entirely prevents formation of **15** by co-sublimation. It was possible to sublime the gallic acid monohydrate starting material on its own to form an anhydrous polymorph of gallic acid (CSD refcode IJUMEG06), as reported in the literature.[55] However, GA also tends to decarboxylate and degrade at high temperatures (Figure 7). During co-sublimation with 4-phenylpyridine the gallate salt did not form; instead, powder diffraction shows the formation of products which do not match the salt or either starting material. We suspect that these are multicomponent materials containing GA decomposition products, such as pyrogallol or dihydroxybenzenes. It was possible to identify one such product by single-crystal diffraction, namely a pyrogallol:4-phenylpyridine co-crystal **16**, the structure of which is described in the Supplementary Information.

Coformer decomposition or melting can therefore be a major hindrance during sublimation. However, it is clear that there are some ways to overcome heat sensitivity (at least partially), such as carefully controlling temperature, pressure, and reagent ratios. Additionally, new multicomponent materials containing decomposition products may be discovered inadvertently.

Conclusion

We have shown that co-sublimation is an efficient crystallization technique for the formation of co-crystals, salts and the intermediate co-crystal salts. When two starting materials have similar sublimation rates and temperatures, co-sublimation can be a quick and easy way to determine whether a multicomponent crystal exists, and potentially to obtain single crystals of the material. In fact, even when sublimation temperatures differ, co-sublimation can still be successful. When this temperature difference is very large, the gas-phase coformer concentrations can be manipulated by changing

coformer stoichiometries, pre-forming multicomponent crystals by mechanochemistry, or by heating the starting materials at two different temperatures. In this way, even multiple polymorphic forms can be obtained by co-sublimation. Our simple sublimation apparatus did not allow for sufficiently precise temperature control to selectively form particular polymorphs, but a new polymorph of a known co-crystal salt was identified from single crystals obtained by co-sublimation (**6c**). Co-sublimation is more challenging when one of the coformers can isomerize or degrade during sublimation, but we have demonstrated how these problems can be overcome, and have successfully produced multicomponent crystals containing maleic acid by co-sublimation. When coformer decomposition could not be prevented, degradation products, as well as multicomponent crystals formed with them, could easily be identified by SCXRD.

Mechanochemistry is a rapid and efficient crystallization technique convenient for screening for multicomponent materials. Unfortunately, single crystals are not produced. On the other hand, co-sublimation successfully produced multicomponent crystals in most of the examples presented here, and often formed diffraction-quality single crystals. We also observed that the products formed during co-sublimation are not always the same as those obtained from mechanochemistry (or solution crystallization), which has allowed us to discover new multicomponent crystals (**10**, **11b** and **12b**), one of which has not been obtained using any other technique (**12b**). It would be interesting to attempt a number of failed co-grinding experiments by co-sublimation, but unfortunately these are rarely published. Further study into the mechanisms of gas-phase crystal growth is definitely warranted.

Co-sublimation is more laborious than mechanochemical grinding and will therefore not replace it as a routine technique. However, sublimation is clearly a valuable co-crystallization technique for the discovery and identification of new multicomponent materials. We encourage the incorporation of co-sublimation into screening protocols in addition to other crystallization methodologies, especially when working on complex or problematic systems. In our opinion, a multi-technique approach is always best.

Associated content

Supporting Information

Full details of all experimental procedures and analysis of powder X-ray data and FTIR spectra. Single-crystal X-ray diffraction data for **6a**, **6b**, **6c**, **8**, **9a**, **9b**, **10**, **11b**, **12b** and **16**. The X-ray crystallographic files in CIF format are available. This material is available free of charge via the Internet at http://pubs.acs.org. CCDC 2023387 – 2023396 contains the supplementary

crystallographic data for this paper. These data can be obtained free of charge from The Cambridge Crystallographic Data Centre via www.ccdc.cam.ac.uk/data_request/cif.

Author information

Corresponding Author

* Email: jeanl@sun.ac.za

Acknowledgements

The authors would like to thank the Wilhelm Frank Scholarship Fund and Stellenbosch University for funding, as well as Dr Leigh Loots for assistance regarding refinement of the crystal structure of **16**.

References

[1] Grothe, E.; Meekes, H.; Vlieg, E.; ter Horst, J. H.; de Gelder, R. Solvates, Salts, and Cocrystals: A Proposal for a Feasible Classification System. *Cryst. Growth Des.* **2016**, *16* (6), 3237–3243.

[2] Berry, D. J.; Steed, J. W. Pharmaceutical Cocrystals, Salts and Multicomponent Systems; Intermolecular Interactions and Property Based Design. *Adv. Drug Deliv. Rev.* **2017**, *117*, 3–24.

[3] Dey, S.; Das, S.; Bhunia, S.; Chowdhury, R.; Mondal, A.; Bhattacharya, B.; Devarapalli, R.; Yasuda, N.; Moriwaki, T.; Mandal, K.; Mukherjee, G. D.; Reddy, C. M. Mechanically Interlocked Architecture Aids an Ultra-Stiff and Ultra-Hard Elastically Bendable Cocrystal. *Nat. Commun.* **2019**, *10* (1), 3711–3721.

[4] Zheng, K.; Gao, S.; Chen, M.; Li, A.; Wu, W.; Qian, S.; Pang, Q. Color Tuning of an Active Pharmaceutical Ingredient through Cocrystallization: A Case Study of a Metronidazole–Pyrogallol Cocrystal. *CrystEngComm* **2020**, *22* (8), 1404–1413.

[5] Gamekkanda, J. C.; Sinha, A. S.; Aakeröy, C. B. Cocrystals and Salts of Tetrazole-Based Energetic Materials. *Cryst. Growth Des.* **2020**, *20* (4), 2432–2439.

[6] Friščić, T.; Elacqua, E.; Dutta, S.; Oburn, S. M.; MacGillivray, L. R. Total Syntheses Supramolecular Style: Solid-State Construction of [2.2]Cyclophanes with Modular Control of Stereochemistry. *Cryst. Growth Des.* **2020**, *20* (4), 2584–2589.

[7] Hasa, D.; Jones, W. Screening for New Pharmaceutical Solid Forms Using Mechanochemistry: A Practical Guide. *Adv. Drug Deliv. Rev.* **2017**, *117*, 147–161.

[8] Trask, A. V.; van de Streek, J.; Motherwell, W. D. S.; Jones, W. Achieving Polymorphic and Stoichiometric Diversity in Cocrystal Formation: Importance of Solid-State Grinding, Powder X-Ray Structure Determination, and Seeding. *Cryst. Growth Des.* **2005**, *5* (6), 2233–2241.

[9] Fucke, K.; Myz, S. A.; Shakhtshneider, T. P.; Boldyreva, E. V.; Griesser, U. J. How Good Are the Crystallisation Methods for Co-Crystals? A Comparative Study of Piroxicam. *New J. Chem.* **2012**, *36* (10), 1969–1977.

[10] Tanabe, Y.; Maeno, Y.; Ohashi, K.; Hisada, H.; Roy, A.; Carriere, J.; Heyler, R.; Fukami, T. Screening a Trace Amount of Pharmaceutical Cocrystals by Using an Enhanced Nano-Spot Method. *Eur. J. Pharm. Biopharm.* **2019**, *136*, 131–137.

[11] Park, B.; Yoon, W.; Yun, J.; Ban, E.; Yun, H.; Kim, A. Emodin-Nicotinamide (1:2) Cocrystal Identified by Thermal Screening to Improve Emodin Solubility. *Int. J. Pharm.* **2019**, *557*, 26–35.

[12] Nagapudi, K.; Umanzor, E. Y.; Masui, C. High-Throughput Screening and Scale-up of Cocrystals Using Resonant Acoustic Mixing. *Int. J. Pharm.* **2017**, *521* (1–2), 337–345.

[13] Shunnar, A. F.; Dhokale, B.; Karothu, D. P.; Bowskill, D. H.; Sugden, I. J.; Hernandez, H. H.; Naumov, P.; Mohamed, S. Efficient Screening for Ternary Molecular Ionic Cocrystals Using a Complementary Mechanosynthesis and Computational Structure Prediction Approach. *Chem. Eur. J.* **2020**, *26* (21), 4752–4765.

[14] Barbas, R.; Font-Bardia, M.; Paradkar, A.; Hunter, C. A.; Prohens, R. Combined Virtual/Experimental Multicomponent Solid Forms Screening of Sildenafil: New Salts, Cocrystals, and Hybrid Salt–Cocrystals. *Cryst. Growth Des.* **2018**, *18* (12), 7618–7627.

[15] Robertson, C. C.; Wright, J. S.; Carrington, E. J.; Perutz, R. N.; Hunter, C. A.; Brammer, L. Hydrogen Bonding vs. Halogen Bonding: The Solvent Decides. *Chem. Sci.* **2017**, *8* (8), 5392–5398.

[16] Lombard, J.; le Roex, T.; Haynes, D. A. Competition between Hydrogen- and Halogen Bonds : The Effect of Solvent Volume. *Manuscript Submitted* **2020**.

[17] Carstens, T.; Haynes, D. A.; Smith, V. J. Cocrystals: Solution, Mechanochemistry, and Sublimation. *Cryst. Growth Des.* **2020**, *20* (2), 1139–1149.

[18] Lombard, J.; Smith, V. J.; le Roex, T.; Haynes, D. A. Crystallisation of Organic Salts by Sublimation: Salt Formation from the Gas Phase. *Manuscript Submitted* **2020**.

[19] Zhang, T.; Yu, Q.; Li, X.; Ma, X. Preparation of 2:1 Urea-Succinic Acid Cocrystals by Sublimation. *J. Cryst. Growth* **2017**, *469*, 114–118.

[20] Szell, P. M. J.; Gabriel, S. A.; Caron-Poulin, E.; Jeannin, O.; Fourmigué, M.; Bryce, D. L. Cosublimation: A Rapid Route Toward Otherwise Inaccessible Halogen-Bonded Architectures. *Cryst. Growth Des.* **2018**, *18* (10), 6227–6238.

[21] O'Malley, C.; Erxleben, A.; Kellehan, S.; McArdle, P. Unprecedented Morphology Control of Gas Phase Cocrystal Growth Using Multi Zone Heating and Tailor Made Additives. *Chem. Commun.* **2020**, *56* (42), 4–7.

[22] *X'Pert HighScore Plus*; version 2.2e; PANalytical, Almelo, B. V., the Netherlands, **2009**.

[23] SAINT Data Collection Software, Version V7.99A; Bruker AXS Inc., **2012**, Madison, WI.

[24] *SADABS, Version 2012/1*; Bruker AXS Inc., Madison, WI, **2012**.

[25] Blessing, R. H. An Empirical Correction for Absorption Anisotropy. *Acta Crystallogr. Sect. A Found. Crystallogr.* **1995**, *51*, 33–38.

[26] Sheldrick, G. M. SHELXT – Integrated Space-Group and Crystal-Structure Determination. *Acta Crystallogr. Sect. A Found. Adv.* **2015**, *71* (1), 3–8.

[27] Atwood, J. L.; Barbour, L. J. Molecular Graphics: From Science to Art. *Cryst. Growth Des.* **2003**, *3* (3), 3–8.

[28] Barbour, L. J. X-Seed – A Software Tool for Supramolecular Crystallography. *J. Supramol. Chem* **2001**, *1* (189), 189–191.

[29] Sheldrick, G. M. Crystal Structure Refinement with SHELXL. *Acta Crystallogr. Sect. C Struct. Chem.* **2015**, *71* (1), 3–8.

[30] *POV-Ray for Windows*; version 3.6; Persistence of Vision Pty. Ltd., Williamstown, Australia, **2004**.

[31] Lu, E.; Rodríguez-Hornedo, N.; Suryanarayanan, R. A Rapid Thermal Method for Cocrystal Screening. *CrystEngComm* **2008**, *10* (6), 665–668.

[32] Trask, A. V.; Motherwell, W. D. S.; Jones, W. Pharmaceutical Cocrystallization: Engineering a Remedy for Caffeine Hydration. *Cryst. Growth Des.* **2005**, *5* (3), 1013–1021.

[33] Childs, S. L.; Stahly, G. P.; Park, A. The Salt−Cocrystal Continuum: The Influence of Crystal Structure on Ionization State. *Mol. Pharm.* **2007**, *4* (3), 323–338.

[34] Trask, A.; Motherwell, W.; Jones, W. Physical Stability Enhancement of Theophylline via Cocrystallization. *Int. J. Pharm.* **2006**, *320* (1–2), 114–123.

[35] Fischer, F.; Lubjuhn, D.; Greiser, S.; Rademann, K.; Emmerling, F. Supply and Demand in the Ball Mill: Competitive Cocrystal Reactions. *Cryst. Growth Des.* **2016**, *16* (10), 5843–5851.

[36] Braga, D.; Grepioni, F.; Maini, L.; Polito, M. Crystal Polymorphism and Multiple Crystal Forms. In *Molecular networks*; Hosseini, M. W., Ed.; Springer: Berlin, **2009**; pp 25–50.

[37] Hasa, D.; Miniussi, E.; Jones, W. Mechanochemical Synthesis of Multicomponent Crystals: One Liquid for One Polymorph? A Myth to Dispel. *Cryst. Growth Des.* **2016**, *16* (8), 4582–4588.

[38] Fischer, F.; Heidrich, A.; Greiser, S.; Benemann, S.; Rademann, K.; Emmerling, F. Polymorphism of Mechanochemically Synthesized Cocrystals: A Case Study. *Cryst. Growth Des.* **2016**, *16* (3), 1701–1707.

[39] Bevill, M. J.; Vlahova, P. I.; Smit, J. P. Polymorphic Cocrystals of Nutraceutical Compound p-Coumaric Acid with Nicotinamide: Characterization, Relative Solid-State Stability, and Conversion to Alternate Stoichiometries. *Cryst. Growth Des.* **2014**, *14* (3), 1438–1448.

[40] Kamali, N.; O'Malley, C.; Mahon, M. F.; Erxleben, A.; McArdle, P. Use of Sublimation Catalysis and Polycrystalline Powder Templates for Polymorph Control of Gas Phase Crystallization. *Cryst. Growth Des.* **2018**, *18* (6), 3510–3516.

[41] Karpinska, J.; Erxleben, A.; McArdle, P. 17β-Hydroxy-17α-Methylandrostano[3,2-c]-Pyrazole, Stanozolol: The Crystal Structures of Polymorphs 1 and 2 and 10 Solvates. *Cryst. Growth Des.* **2011**, *11* (7), 2829–2838.

[42] Kamali, N.; Erxleben, A.; McArdle, P. Unexpected Effects of Catalytic Amounts of Additives on Crystallization from the Gas Phase: Depression of the Sublimation Temperature and Polymorph Control. *Cryst. Growth Des.* **2016**, *16* (5), 2492–2495.

[43] Haynes, D. A.; Jones, W.; Motherwell, W. D. S. Cocrystallisation of Succinic and Fumaric Acids with Lutidines: A Systematic Study. *CrystEngComm* **2006**, *8* (11), 830–840.

[44] Lukin, S.; Stolar, T.; Tireli, M.; Blanco, M. V.; Babić, D.; Friščić, T.; Užarević, K.; Halasz, I. Tandem In Situ Monitoring for Quantitative Assessment of Mechanochemical Reactions Involving Structurally Unknown Phases. *Chem. Eur. J.* **2017**, *23* (56), 13941–13949.

[45] Bowes, K. F.; Ferguson, G.; Lough, A. J.; Glidewell, C. Salts of Maleic and Fumaric Acids with Organic Polyamines: Comparison of Isomeric Acids as Building Blocks in Supramolecular Chemistry. *Acta Crystallogr. Sect. B Struct. Sci.* **2003**, *59* (1), 100–117.

[46] Vizhi, R. E.; Vijayalakshmi, M. Bulk Growth and Characterization of Novel Organic Piperazinium (Bis) Hydrogen Succinate Single Crystals. *J. Cryst. Growth* **2016**, *452*, 204–212.

[47] Vanier, M.; Brisse, F. Structure of Piperazinium Succinate, $C_4H_4O_4^{2-}\cdot C_4H_{12}N_2^{2+}$. *Acta Crystallogr. Sect. C Cryst. Struct. Commun.* **1983**, *39* (7), 912–914.

[48] Mohamed, S.; Tocher, D. a; Vickers, M.; Karamertzanis, P. G.; Price, S. L. Salt or Cocrystal? A New Series of Crystal Structures Formed from Simple Pyridines and Carboxylic Acids. *Cryst. Growth Des.* **2009**, *9* (6), 2881–2889.

[49] Nelyubina, Y. V.; Antipin, M. Y.; Lyssenko, K. A. Hydrogen Bonds between Zwitterions: Intermediate between Classical and Charge-Assisted Ones. A Case Study. *J. Phys. Chem. A* **2009**, *113* (15), 3615–3620.

[50] Batisai, E.; Ayamine, A.; Kilinkissa, O. E. Y.; Báthori, N. B. Melting Point–Solubility–Structure Correlations in Multicomponent Crystals Containing Fumaric or Adipic Acid. *CrystEngComm* **2014**, *16* (43), 9992–9998.

[51] Athimoolam, S.; Natarajan, S. 3-Carboxypyridinium Hydrogen Oxalate. *Acta Crystallogr. Sect. E Struct. Reports Online* **2007**, *63* (2), o963–o965.

[52] Tremayne, M.; Glidewell, C. Direct-Space Structure Solution from Laboratory Powder Diffraction Data of an Organic Cocrystal: 1,2,3-Trihydroxybenzene–HMTA (1/1). *Chem. Commun.* **2000**, No. 24, 2425–2426.

[53] Daka, P.; Wheeler, K. A. Bis(1,2-Dihydroxybenzene) Hexamethylenetetramine. *Acta Crystallogr. Sect. E Struct. Reports Online* **2006**, *62* (12), o5477–o5479.

[54] Seaton, C. C.; Munshi, T.; Williams, S. E.; Scowen, I. J. Multi-Component Crystals of 4-Phenylpyridine: Challenging the Boundaries between Co-Crystal and Organic Salt Formation with Insight into Solid-State Proton Transfer. *CrystEngComm* **2013**, *15* (26), 5250–5260.

[55] Braun, D. E.; Bhardwaj, R. M.; Florence, A. J.; Tocher, D. A.; Price, S. L. Complex Polymorphic System of Gallic Acid—Five Monohydrates, Three Anhydrates, and over 20 Solvates. *Cryst. Growth Des.* **2013**, *13* (1), 19–23.

4.2 Supporting information

Materials

Coformer abbreviations: caffeine (CAF), theophylline (THE), nicotinamide (NAM), isonicotinamide (INAM), fumaric acid (FA), maleic acid (MA), benzoic acid (BA), nicotinic acid (NA), succinic acid (SA), salicylic acid (SAL), gallic acid monohydrate (GA), oxalic acid dihydrate (OA), pyridine (PYR), 4,4'-bipyridine (BPY), 4-phenylpyridine (4PP), 3-picoline (3PIC), 2,3-lutidine (23LUT), piperazine (PIP), hexamethylenetetramine (HMT), pyrogallol (PYG).

Simple co-crystals

CAF and SAL

The 1:1 co-crystal of caffeine and salicylic acid (**1**) was formed by grinding caffeine (0.047 g, 0.24 mmol) and salicylic acid (0.033 g, 0.24 mmol) together for 20 minutes in a ball mill (neat) (Figure S1).

Co-crystal **1** could also be formed by sublimation of a 1:1 molar ratio of the starting materials. Caffeine (0.035 g, 0.18 mmol) and salicylic acid (0.025 g, 0.18 mmol) were added to a thin Schlenk tube and heated in a 140 °C oil bath for 8 h under static vacuum. A 2:1 or 1:2 ratio could also be used.

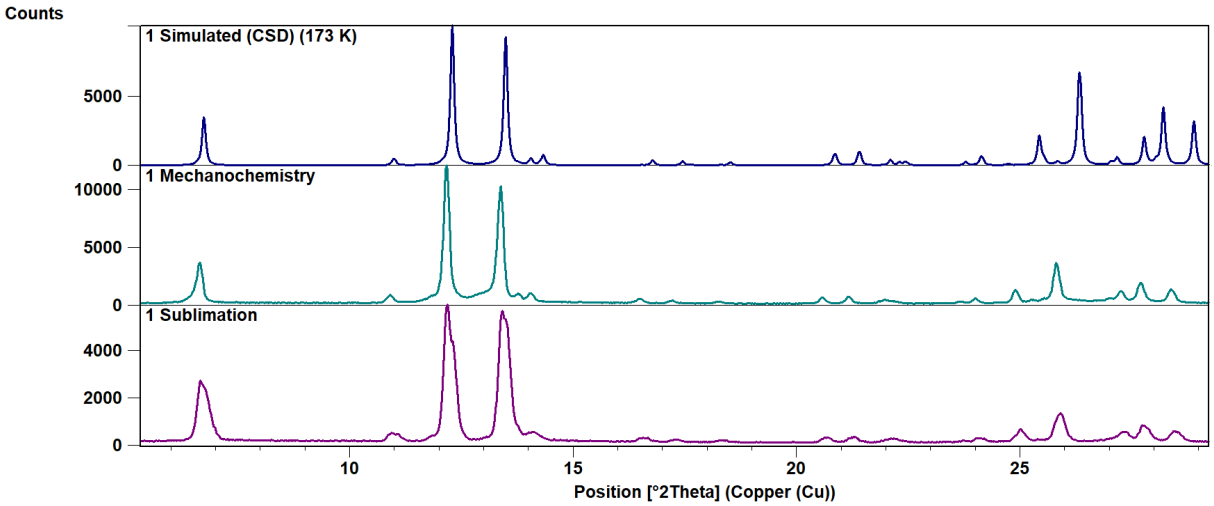

Figure S1. Comparison of the experimental powder patterns of **1** (obtained from neat grinding and co-sublimation) to the pattern simulated from single-crystal data obtained from the CSD (refcode XOBCAT)[1].

CAF and OA

The 2:1 co-crystal of caffeine and oxalic acid (**2**) was made by grinding caffeine (0.060 g, 0.31 mmol), oxalic acid dihydrate (0.020 g, 0.16 mmol) and 20 µl methanol together for 20 minutes in a ball mill (Figure S2).

Co-crystal **2** could also be formed by sublimation of a 2:1 molar ratio of the starting materials. Caffeine (0.045 g, 0.23 mmol) and oxalic acid dihydrate (0.015 g, 0.12 mmol) were added to a thin Schlenk tube and heated in a 120 °C oil bath for 24 h under static vacuum. A 1:1 or 1:2 ratio could also be used.

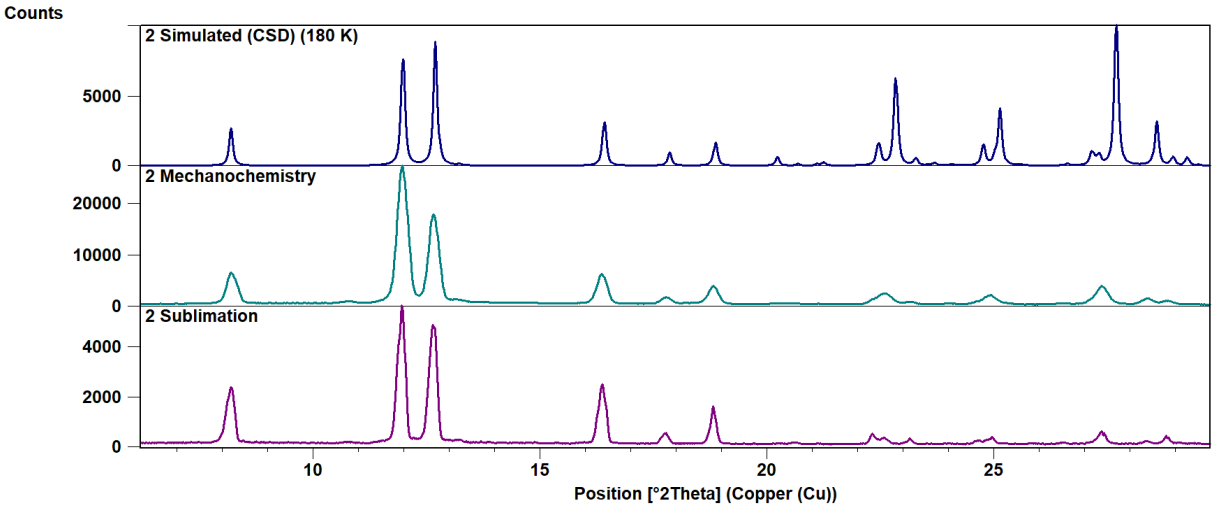

Figure S2. Comparison of the experimental powder patterns of **2** (obtained from LAG and co-sublimation) to the pattern simulated from single-crystal data obtained from the CSD (refcode GANXUP)[2].

THE and SAL

The 1:1 co-crystal of theophylline and salicylic acid (**3**) was made by grinding theophylline (0.045 g, 0.25 mmol), salicylic acid (0.035 g, 0.25 mmol) and 20 µl methanol together for 20 minutes in a ball mill (Figure S3).

Co-crystal **3** could also be formed by sublimation of a 1:1 molar ratio of the starting materials. Theophylline (0.034 g, 0.19 mmol) and salicylic acid (0.026 g, 0.19 mmol) were added to a thin Schlenk tube and heated in a 140 °C oil bath for 15 h under static vacuum. A 2:1 or 1:2 ratio could also be used.

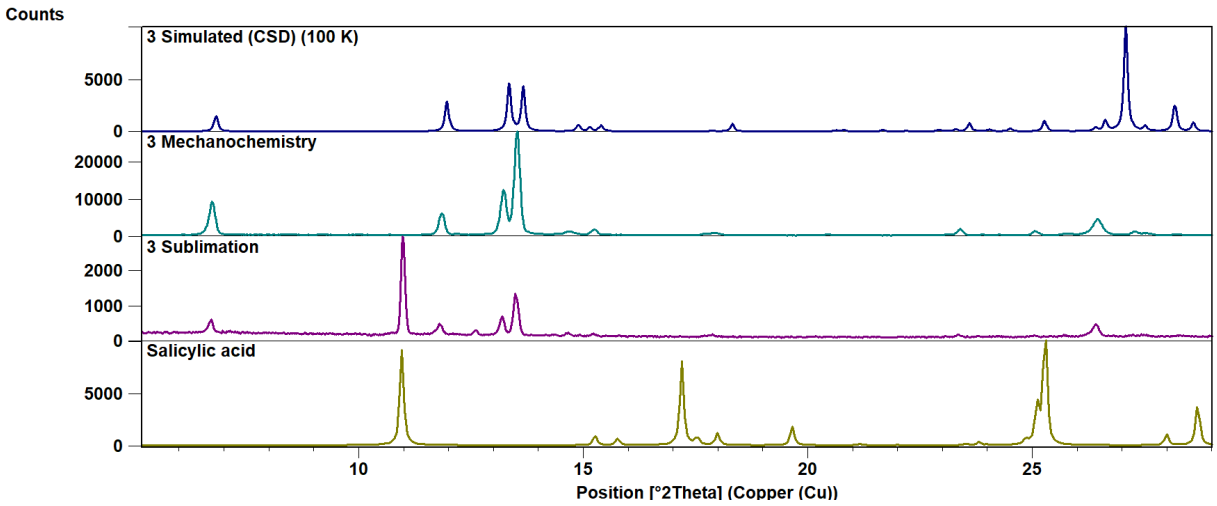

Figure S3. Comparison of the experimental powder patterns of **3** (obtained from LAG and co-sublimation) to the pattern simulated from single-crystal data obtained from the CSD (refcode KIGLES)[3]. The product obtained from sublimation also contains salicylic acid.

THE and OA

The 2:1 co-crystal of theophylline and oxalic acid (**4**) was made by grinding theophylline (0.059 g, 0.33 mmol), oxalic acid dihydrate (0.021 g, 0.16 mmol) and 20 µl methanol together for 20 minutes in a ball mill (Figure S4).

Co-crystal **4** could also be formed by sublimation of a 2:1 molar ratio of the starting materials. Theophylline (0.044 g, 0.24 mmol) and oxalic acid dihydrate (0.015 g, 0.12 mmol) were added to a thin Schlenk tube and heated in a 160 °C oil bath for 24 h under static vacuum.

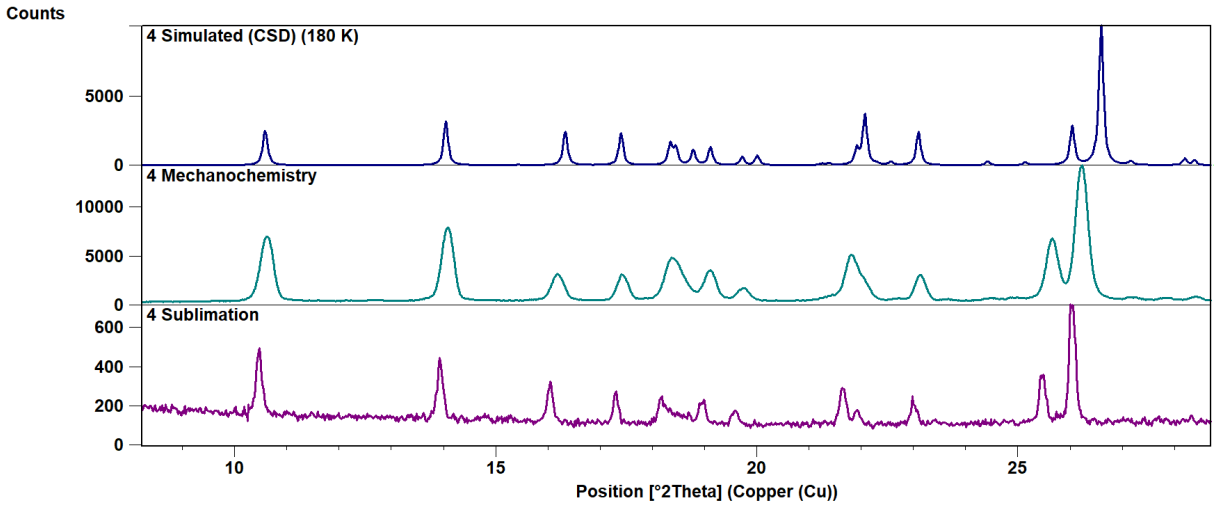

Figure S4. Comparison of the experimental powder patterns of **4** (obtained from LAG and co-sublimation) to the pattern simulated from single-crystal data obtained from the CSD (refcode XEJWUF)[4].

THE and INAM

The 1:1 co-crystal of theophylline and isonicotinamide (**5**) was made by grinding theophylline (0.060 g, 0.33 mmol), isonicotinamide (0.040 g, 0.33 mmol) and 25 µl methanol together for 20 minutes in a ball mill (Figure S5).

Co-crystal **5** could also be formed by sublimation of a 1:1 molar ratio of the starting materials. Theophylline (0.080 g, 0.44 mmol) and isonicotinamide (0.054 g, 0.44 mmol) were added to a thin Schlenk tube and heated in a 120 °C oil bath for 8 h under static vacuum.

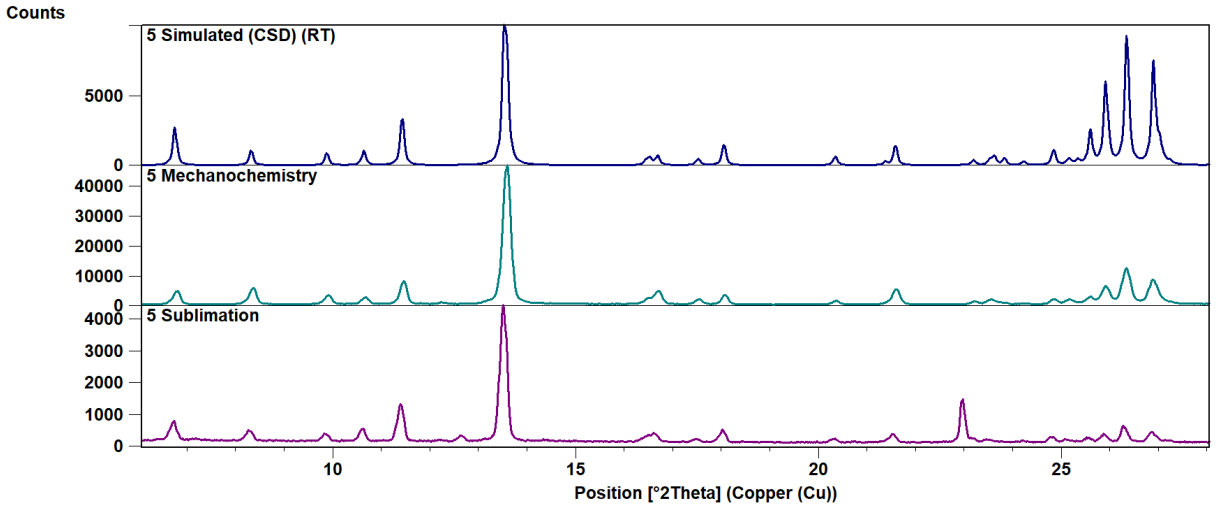

Figure S5. Comparison of the experimental powder patterns of **5** (obtained from LAG and co-sublimation) to the pattern simulated from single-crystal data obtained from the CSD (refcode EVEYAH)[5].

Polymorphic systems

FA and 23LUT

The 1:2 co-crystal of fumaric acid and 2,3-lutidine (**6a**) was made by grinding FA (0.035 g, 0.30 mmol) and 23LUT (69 µl, 0.60 mmol) together for 20 minutes in a ball mill (neat) (Figure S6). The 2:1 co-crystal salt polymorphs of fumaric acid and 2,3-lutidine (**6b** and **6c**) were made as a mixture by grinding FA (0.069 g, 0.59 mmol) and 23LUT (34 µl, 0.30 mmol) together for 20 minutes in a ball mill (neat) (Figure S8).

The new polymorph (**6c**) could be obtained by heating FA (0.040 g, 0.34 mmol) and 23LUT (39 µl, 0.34 mmol) together for 2 hours in a test tube at 125 °C.

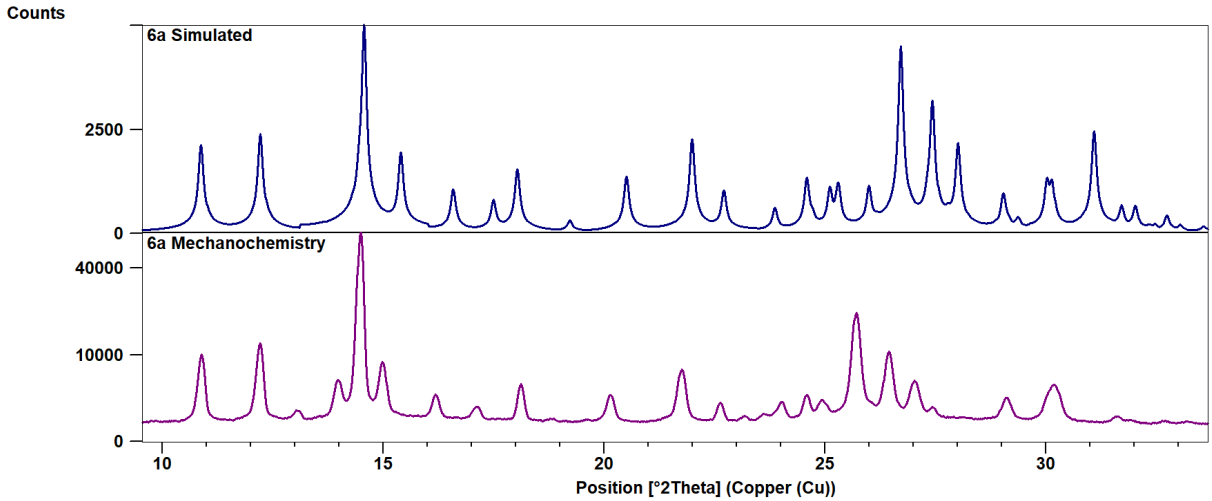

Figure S6. Comparison of the experimental powder pattern of **6a**, obtained from neat grinding, to the pattern simulated from single-crystal data obtained from the CSD (refcode RESFOL)[6].

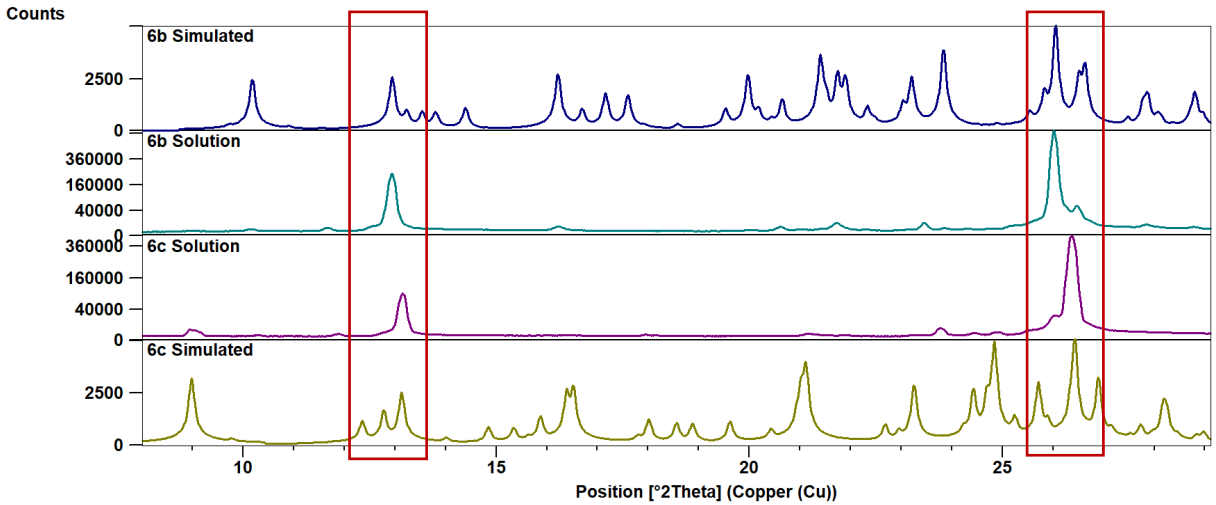

Figure S7. PXRD patterns for **6b** and **6c** obtained from solution. It is challenging to distinguish between **6b** and **6c** due to facial selectivity – samples cannot be ground before analysis as the polymorphs interconvert in the process. The indicated peaks are used primarily to distinguish between the two forms.

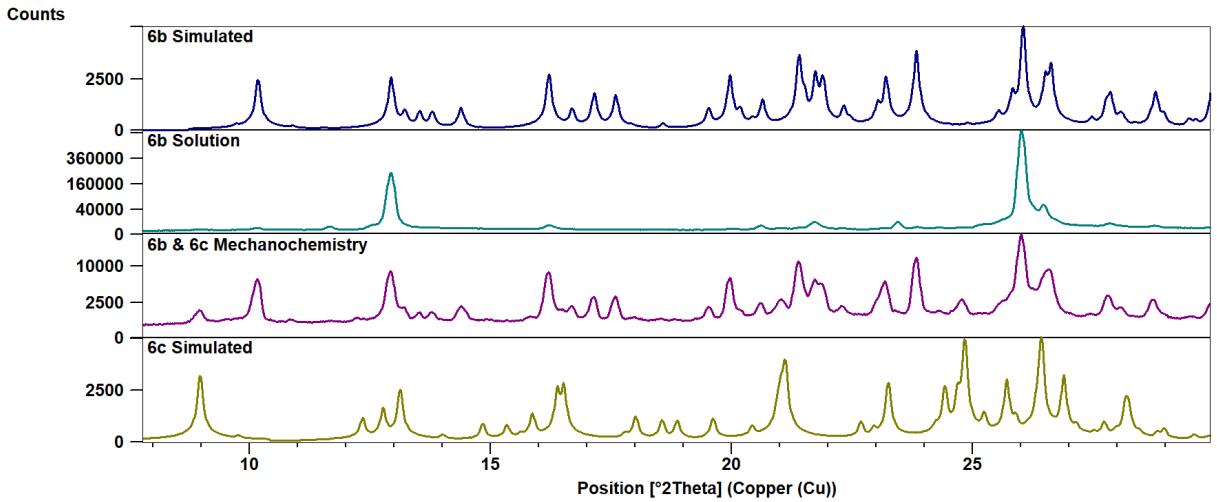

Figure S8. Comparison of the experimental powder pattern, obtained from grinding FUM and 23LUT, to the simulated powder patterns shows that the formation of **6b** mechanochemically is always accompanied by the formation of **6c**.

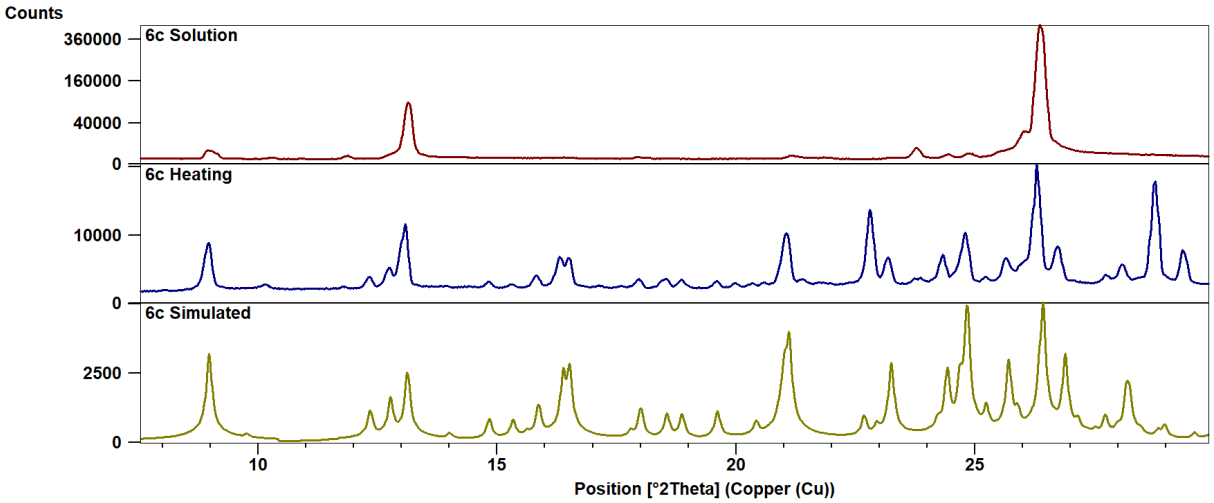

Figure S9. Comparison of the experimental powder patterns of **6c** (obtained from solution crystallization or heating the starting materials together) to the pattern simulated from single-crystal data collected for this study.1

All three multicomponent crystals (**6a**, **6b**, **6c**) could also be formed by sublimation of a 2:1 molar ratio of the starting materials. FA (0.069 g, 0.59 mmol) and 23LUT (34 µl, 0.30 mmol) were added to a large Schlenk tube and heated in a 140 °C oil bath for 24 h under static vacuum. Crystals of **6b** and **6c** formed alongside polycrystalline **6a**.

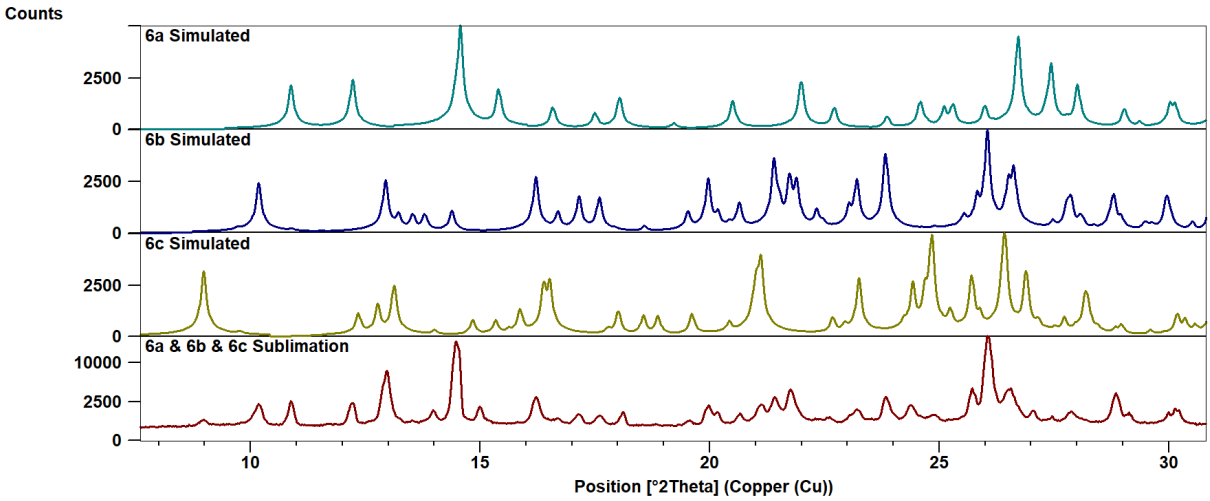

Figure S10. When crystallized by sublimation, a mixture of **6a**, **6b**, and **6c** is often formed.

Table S1. Crystallographic data for the co-crystal **6a** and the co-crystal salts **6b** and **6c**.

Structure	**6a**	**6b**	**6c**
Chemical formula	$C_{18}H_{22}N_2O_8$	$C_{15}H_{17}NO_8$	$C_{15}H_{17}NO_8$
Formula weight /g mol^{-1}	330.37	339.29	339.29
Crystal system	monoclinic	monoclinic	monoclinic
Space group	$P2_1/n$	$P2_1/n$	$P2_1/n$
Temperature /K	100(2)	100(2)	100(2)
a /Å	9.897(2)	9.025(1)	7.4340(7)
b /Å	7.088(1)	18.151(2)	18.131(2)
c /Å	12.239(2)	9.665(1)	11.656(1)
α /°	90	90	90
β /°	96.786(3)	90.509(2)	95.628(1)
γ /°	90	90	90
Calc. density /g cm^{-3}	1.287	1.424	1.441
Volume /Å^3	852.5(3)	1583.0(3)	1563.5(3)
Z	2	4	4
Independent reflections	1981	3691	3866
R_{int}	0.0297	0.0407	0.0242
R_1 [I > 2σ(I)]	0.0436	0.0426	0.0432

Table S2. Hydrogen bond lengths and angles for **6a**, **6b** and **6c** at 100 K.

Structure	D–H···A	D—H /Å	H···A /Å	D···A /Å	D—H···A /°	Symmetry codes
6a	O1–H1···N5	1.17 (3)	1.38 (3)	2.551 (2)	175 (2)	
6b	O1–H1···O9	0.98 (3)	1.52 (3)	2.495 (2)	174 (3)	
	O8–H8···O2	1.03 (3)	1.59 (3)	2.613 (2)	171 (2)	*x−1/2, −y+3/2, z−1/2*
	O16–H16···O10	0.98 (2)	1.63 (2)	2.613 (2)	176 (2)	*x+1/2, −y+1/2, z+1/2*
	N20B–H20B···O10	0.88	1.90	2.769 (5)	169	
	N25A–H25A···O10	0.97 (3)	1.78 (3)	2.748 (6)	176 (2)	
6c	O1–H1···O7	0.95 (2)	1.65 (2)	2.601 (1)	175 (2)	*x+1/2, −y+3/2, z+1/2*
	O16–H16···O9	0.96 (3)	1.66 (3)	2.608 (1)	167 (2)	*x−1/2, −y+1/2, z−1/2*
	O10–H10···O8	0.98 (3)	1.52 (3)	2.501 (1)	178 (3)	
	N17A–H17A···O7	0.88	1.83	2.706 (2)	178	
	N25B–H25B···O7	0.88	1.99	2.857 (2)	167	

NAM and BA

The 1:1 co-crystals of nicotinamide and benzoic acid (polymorphs **7a** and **7b**) were made by subliming NAM (0.070 g, 0.57 mmol) and BA (70 g, 0.57 mmol) in a thin Schlenk heated at 100 °C for 6 hours under static vacuum (Figure S11). A 1:2 ratio could also be used. Grinding a 1:1 ratio of NAM and BA with the addition of 25 µl of acetonitrile or water produced **7b**, while using 25 µl of methanol does not yield either polymorph.

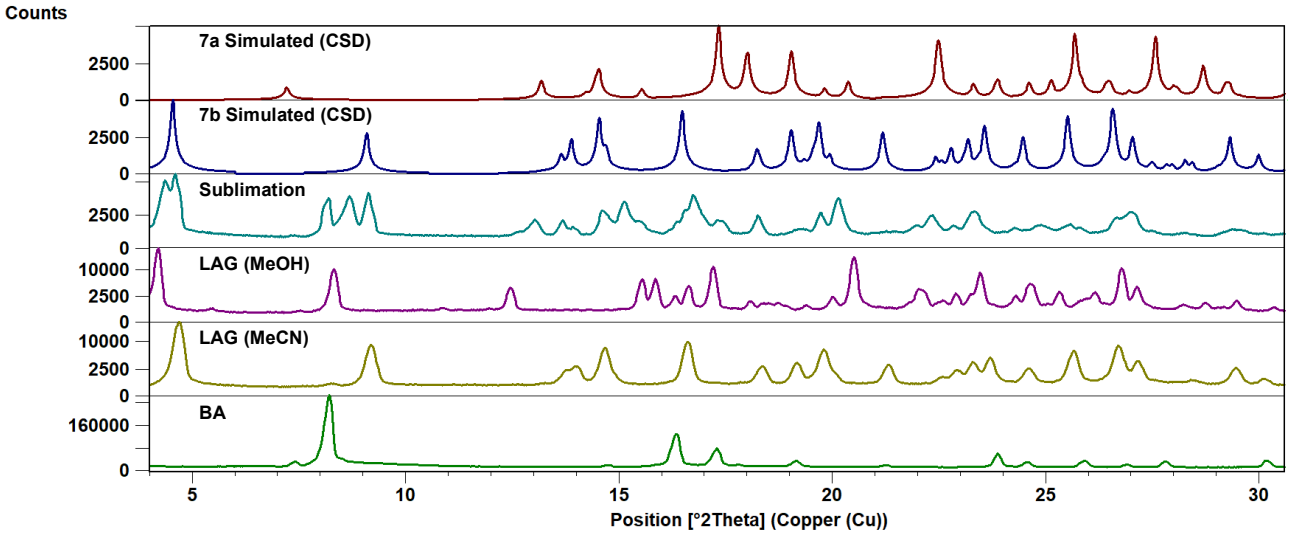

Figure S11. Comparison of the simulated powder patterns of **7a** and **7b** (obtained from the CSD)[7] to the patterns of the products obtained from co-sublimation and co-grinding. Sublimation and MeOH LAG traces contain residual BA. The pattern of the product obtained from sublimation has peaks that can be ascribed to **7a** and **7b**, while the pattern of the product obtained from LAG using acetonitrile matches **7b**.

Co-crystallization when molecules have different sublimation temperatures

MA and BPY

The 2:1 salt of maleic acid and 4,4'-bipyridine (**8**) was made by grinding MA (0.060 g, 0.51 mmol), BPY (0.040 g, 0.25 mmol), and 25 µl THF together for 20 minutes in a ball mill (Figure S12). Methanol or water could also be used, or no solvent at all.

Single crystals of **8** could also be formed by sublimation of a 4:1 molar ratio of the starting materials. MA (0.035 g, 0.30 mmol) and BPY (0.012 g, 0.077 mmol) were added to a thin Schlenk tube and heated in a 100 °C oil bath for 4 h under static vacuum.

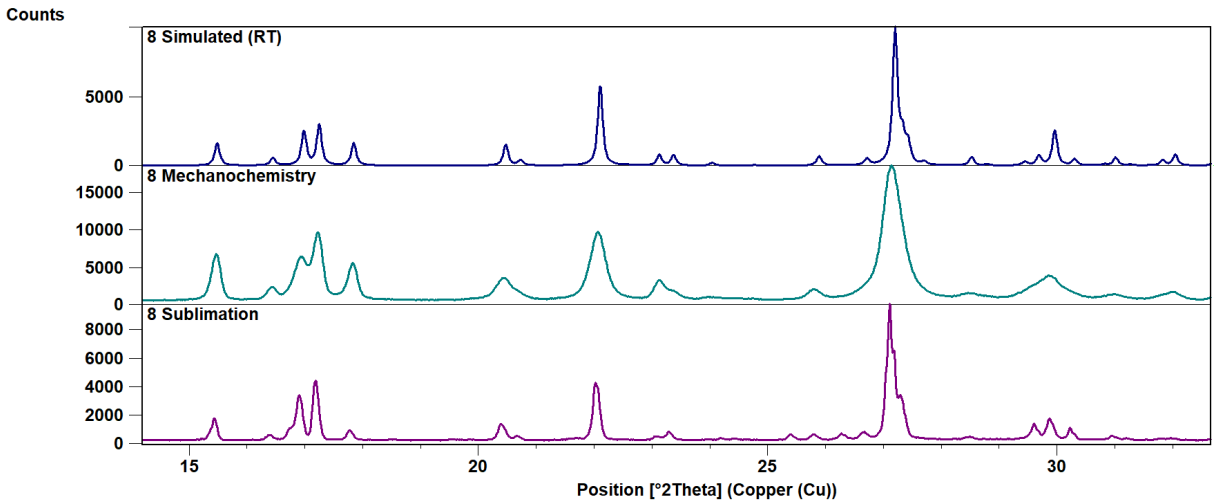

Figure S12. Comparison of the experimental powder patterns of **8** (obtained from LAG and co-sublimation) to the pattern simulated from single-crystal data collected at room temperature.

Single-crystal data for **8** was collected to confirm its classification as a salt, along with FTIR data (Figure S14). Salt **8** crystallizes in the monoclinic spacegroup *C*2/*c* with one hydrogen maleate ion and one half of a bipyridinium ion in the ASU. The monoanion, MA, forms a short intramolecular hydrogen bond between the carboxylic acid group and the carboxylate, with the latter also forming a charge-assisted hydrogen bond (CAHB) with BPY. Each end of the BPY cation has this interaction, so that acid-base-acid trimers are formed. The trimers pack together via various weak interactions to form the 3D structure (Figure S13).

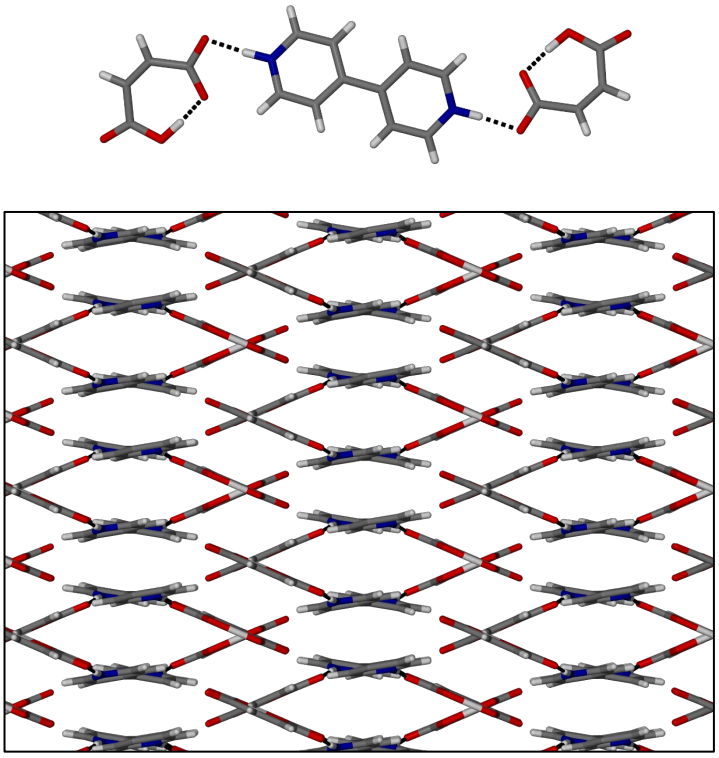

Figure S13. Hydrogen-bonded trimer of **8** (top) and the packing diagram for **8** viewed along [001] (bottom).

Table S3. Crystallographic data for the salt **8**.

Structure	**8**
Chemical formula	$C_{18}H_{16}N_2O_8$
Formula weight /g mol^{-1}	388.33
Crystal system	monoclinic
Space group	*C*2/*c*
Temperature /K	298(2)
a /Å	23.997(2)
b /Å	6.8777(7)
c /Å	11.446(1)
α /°	90
β /°	116.127(1)
γ /°	90
Calc. density /g cm^{-3}	1.521
Volume /Å^3	1696.1(3)
Z	4
Independent reflections	2101
R_{int}	0.0322
R_1 [I > 2σ(I)]	0.0439

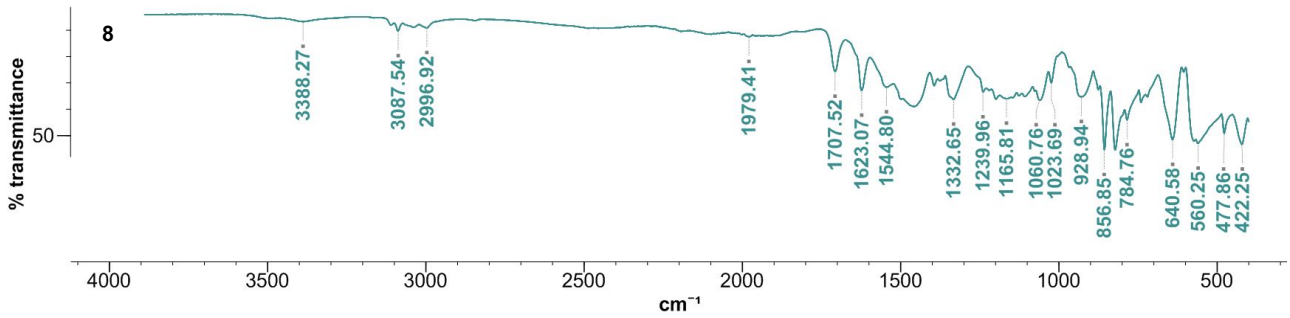

Figure S14. FTIR spectrum for salt **8** as obtained from LAG. The peaks at 1708 cm^{-1} and 1623 cm^{-1} indicate the presence of both carboxylic acid and carboxylate groups, which confirms that **8** is a salt.

FA and 23LUT

The 2:1 co-crystal salt polymorphs of fumaric acid and 2,3-lutidine (**6b** and **6c**) were made as a mixture by subliming FA (0.150 g, 1.29 mmol) while vaporizing 23LUT (147 µl, 1.29 mmol) using in-house developed glassware. FA was heated at 200 °C and 23LUT at 40 °C. A few single crystals of **6b** and **6c** formed; however, to ensure accuracy the experiment was carried out multiple times and crystals identified with PXRD and unit cell determinations.

Figure S15. Apparatus for the sublimation of compounds at two different temperatures.

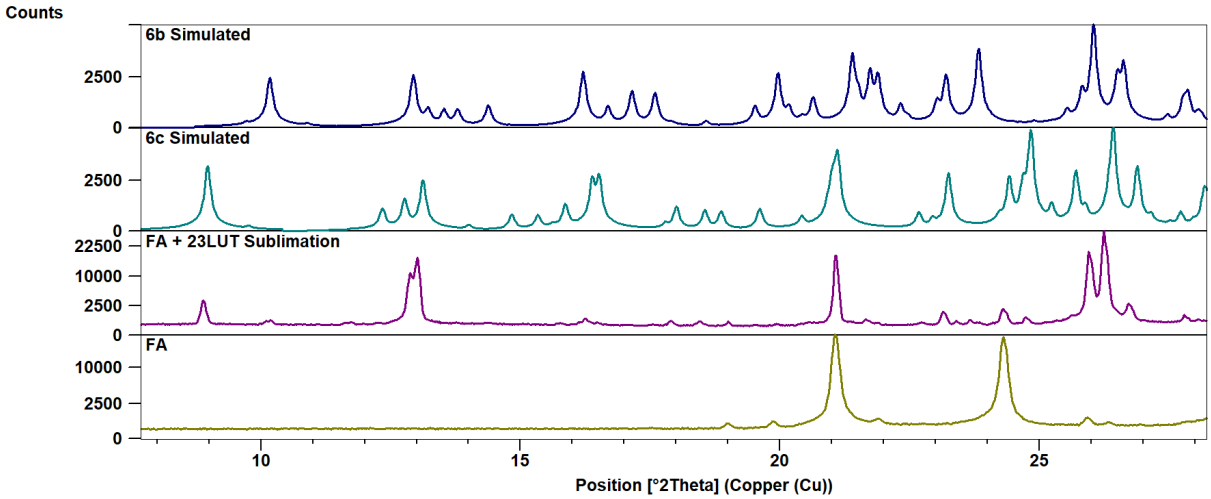

Figure S16. Comparison of the pattern obtained from sublimation using specialized glassware to the simulated powder patterns for **6b** and **6c**. The experimental trace contains both these polymorphs as well as some residual fumaric acid starting material. Poor pattern quality can be attributed to the small sample size and the fact that the sample consisted of single crystals, instead of powder (**6c** converts to **6b** on grinding).

SA and PIP

The 2:1 salt of succinic acid and piperazine (**9a**) was made by grinding SA (0.074 g, 0.63 mmol) and PIP (0.027 g, 0.32 mmol) together for 20 minutes in a ball mill (neat or with the addition of methanol, THF or water). The 1:1 salt of succinic acid and piperazine (**9b**) was made by grinding SA (0.058 g, 0.49 mmol) and PIP (0.042 g, 0.49 mmol) together for 20 minutes in a ball mill (neat or with the addition of methanol, THF or water).

Co-crystal **9b** could also be formed by sublimation of a 1:1 molar ratio of the starting materials. SA (0.045 g, 0.38 mmol) and PIP (0.033 g, 0.38 mmol) were added to a thin Schlenk tube and heated in a 140 °C oil bath for 2 h under static vacuum. A 2:1 or 4:1 ratio could also be used.

Crystals of **9a** could also be obtained from solution crystallization. SA (0.040 g, 0.34 mmol) and PIP (0.015 g, 0.17 mmol) were dissolved in 2 ml ethanol and 0.5 ml water at 70 °C. The solution was left at room temperature and crystals formed after 24 hours. Crystals of **9b** could similarly be obtained by dissolving SA (0.040 g, 0.34 mmol) and PIP (0.029 g, 0.34 mmol) in 4 ml dimethylformamide and 2 ml water at 70 °C. Crystals formed at room temperature after 24 hours.

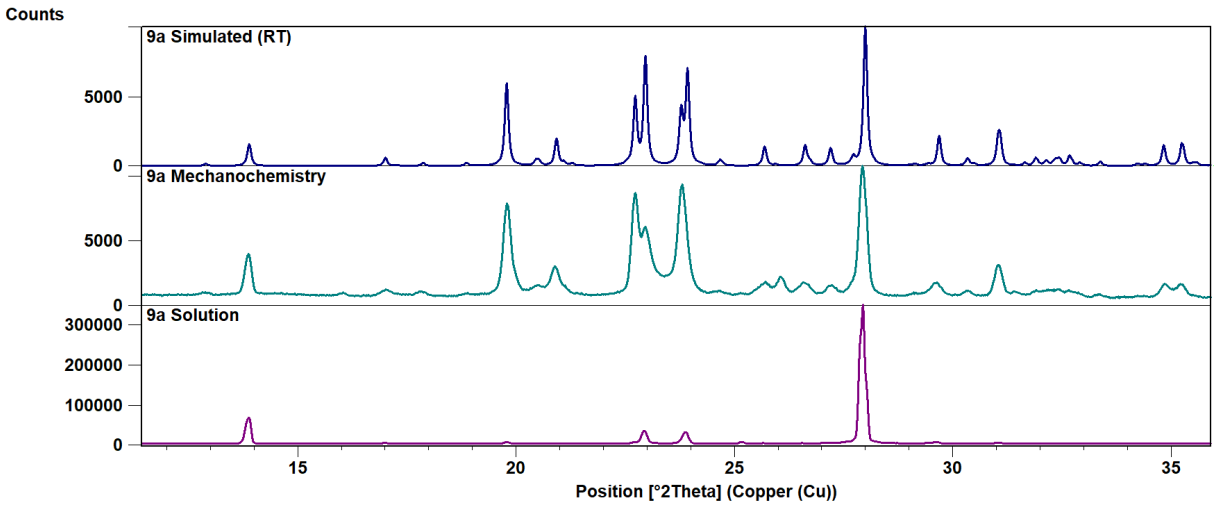

Figure S17. Comparison of the experimental powder patterns of **9a** (obtained from grinding and solution crystallization) to the pattern simulated from single-crystal data collected at room temperature.

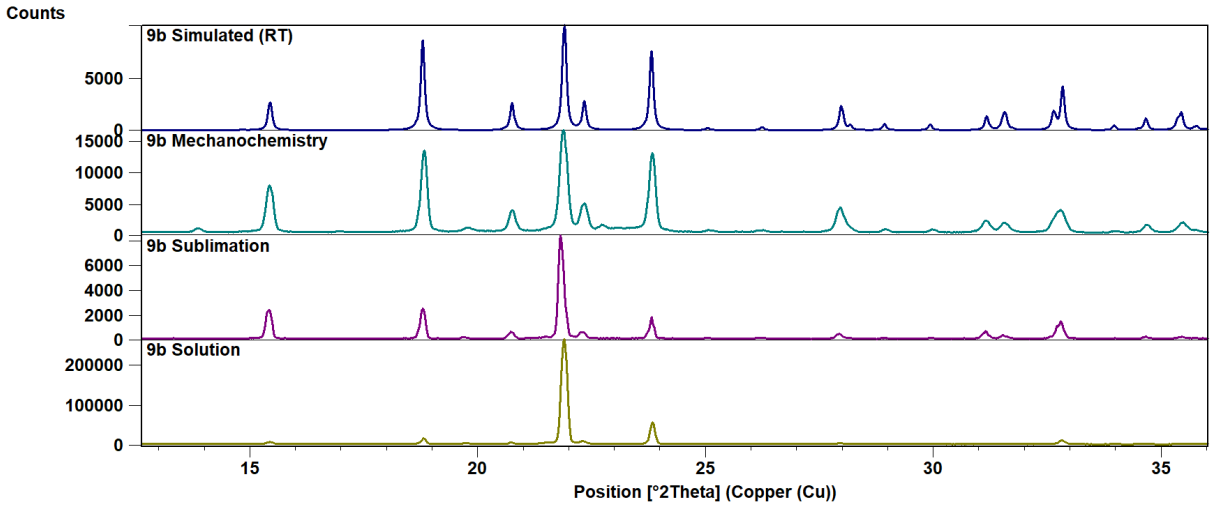

Figure S18. Comparison of the experimental powder patterns of **9b** (obtained from grinding, co-sublimation and solution crystallization) to the pattern simulated from single-crystal data collected at room temperature. The first peak in the trace obtained for mechanochemistry (at roughly 14°) is due to a small amount of **9a** present in the sample.

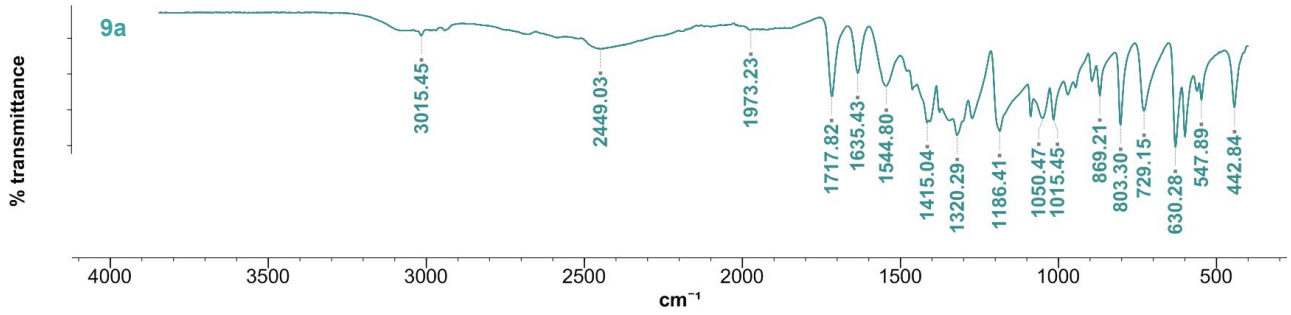

Figure S19. FTIR pattern for **9a**. The peaks at 1718 cm^{-1} and 1635 cm^{-1} indicate the presence of both carboxylic acid and carboxylate groups (as can be seen in the crystal structure), which confirms that **9a** is a salt.

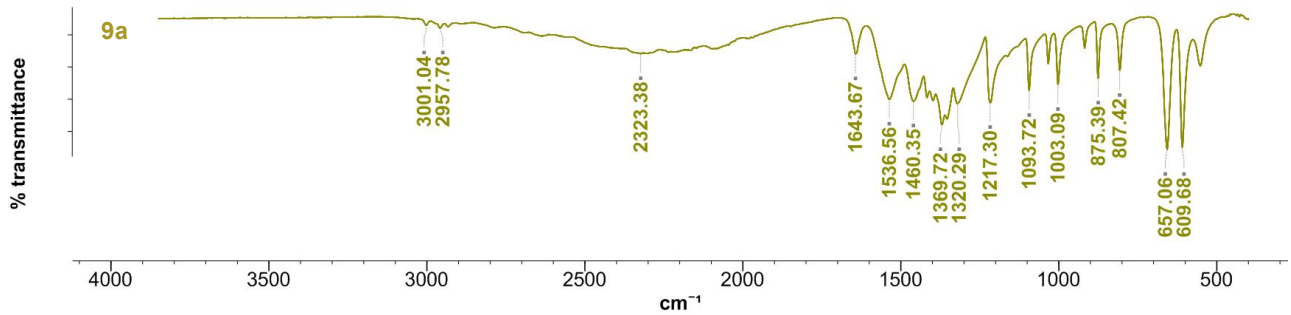

Figure S20. FTIR pattern for **9b**. The peak at 1644 cm^{-1} indicate the presence of carboxylate groups (as can be seen in the crystal structure), which confirms that **9b** is a salt.

Salt **9a** crystallizes in the triclinic spacegroup $P\bar{1}$, with two hydrogen succinate ions and two half PIP cations in the ASU. The SA anions hydrogen bond to each other forming zig-zag chains. Two such chains are held together by PIP cations linking to two carboxylate groups in each chain to form ribbons (Figure 4 in the paper). There are two types of ribbons that pack together to form the 3D structure – they differ with respect to the exact intermolecular distances.

Salt **9b** crystallizes in the triclinic spacegroup $P\bar{1}$ with half a SA anion and half a PIP cation. Each succinate dianion forms four CAHBs to four different cations, and similarly, each PIP cation forms four CAHBs to four different anions so that hydrogen-bonded sheets are formed (Figure 4) that stack with bases overlapping acids, to give a layered structure.

Table S4. Crystallographic data for the salts **9a** and **9b**.

Structure	**9a**	**9b**
Chemical formula	$C_{24}H_{44}N_4O_{16}$	$C_8H_{16}N_2O_4$
Formula weight /g mol^{-1}	644.63	204.23
Crystal system	triclinic	triclinic
Space group	$P\bar{1}$	$P\bar{1}$
Temperature /K	298(2)	298(2)
a /Å	6.5440(5)	5.828(1)
b /Å	8.6135(6)	6.007(1)
c /Å	12.7894(9)	6.910(1)
α /°	92.0020(1)	94.993(2)
β /°	94.0400(1)	99.339(2)
γ /°	101.9450(1)	93.730(2)
Calc. density /g cm^{-3}	1.523	1.431
Volume /Å^3	702.63(9)	237.05(8)
Z	1	1
Independent reflections	3480	1178
R_{int}	0.0234	0.0234
R_1 [I > 2σ(I)]	0.0414	0.0425

Table S5. Hydrogen bond lengths and angles for **9a** and **9b** at room temperature.

Structure	D–H···A	D—H /Å	H···A /Å	D···A /Å	D—H···A /°	Symmetry codes
9a	O7–H7···O2	0.94 (3)	1.61 (3)	2.541 (2)	171 (2)	*x+1, y, z*
	O15–H15···O10	0.94 (3)	1.60 (3)	2.535 (2)	172 (2)	*x+1, y, z*
	N17–H17A···O9	0.93 (2)	2.12 (2)	2.907 (2)	142 (2)	*−x+1, −y+2, −z+1*
	N17–H17B···O9	0.95 (2)	1.79 (2)	2.722 (2)	168 (2)	
	N20–H20A···O1	0.90 (2)	2.06 (2)	2.852 (2)	148 (2)	*−x+1, −y+1, −z*
	N20–H20B···O1	0.94 (2)	1.83 (2)	2.749 (2)	165 (2)	
9b	N5–H5A···O1	0.93 (2)	1.80 (2)	2.730 (1)	172 (2)	*x, y+1, z*
	N5–H5B···O1	0.96 (2)	1.73 (2)	2.659 (2)	165 (2)	

Co-crystallization when coformers can isomerize

MA and PYR

The 1:1 salt of maleic acid and pyridine (**10**) was made by grinding MA (0.048 g, 0.41 mmol) and pyridine (34 µl, 0.41 mmol) together for 20 minutes in a ball mill (Figure S21). A 1:2 molar ratio could also be used.

Salt **10** could also be formed by sublimation of a 1:1 molar ratio of the starting materials. MA (0.120 g, 1.0 mmol) and PYR (83 µl, 1.0 mmol) were added to a large Schlenk tube and heated in a 120 °C oil bath for 5 h under static vacuum. A lower temperature of 100 °C could also be used. Single crystals were obtained that were used to determine the crystal structure by single-crystal diffraction. Crystals of **11a** and **11b** formed alongside crystals of **10** on the coldfinger.

Salt **10** could also be formed by dissolving MA (150 mg) in PYR (5 ml) at 50 °C. The vial was capped and placed in the refrigerator at 4 °C. Crystals formed within 24 hours.

Crystals of the zwitterion could be formed by dissolving MA (0.040 g, 0.34 mmol) and PYR (28 µl, 0.34 mmol) in 2 ml methanol at 60 °C. Vials were capped and left undisturbed until crystals formed a few days later. Other solvents such as ethanol, acetone or THF could also be used, and MA could also be replaced with FA.

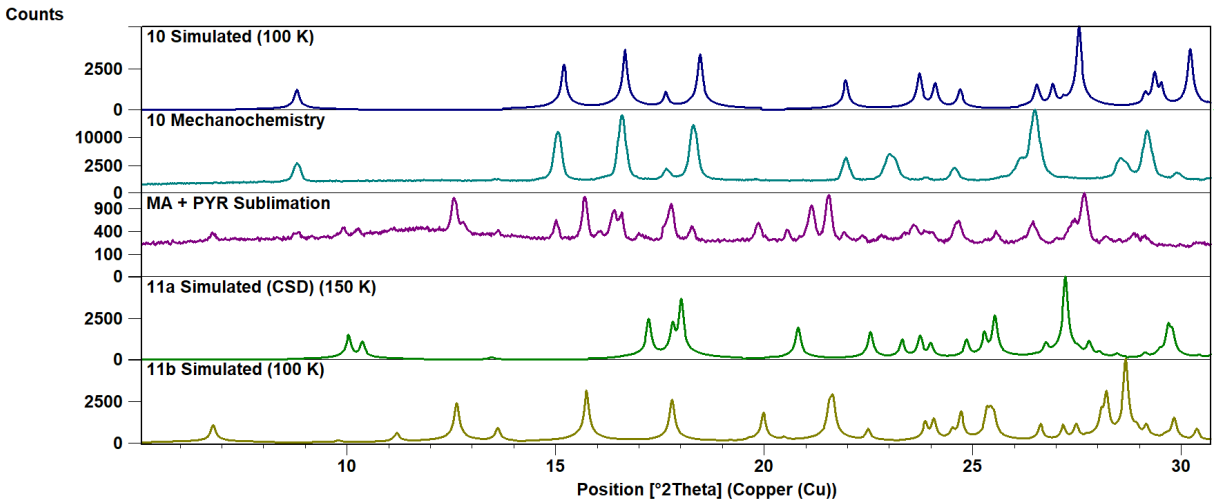

Figure S21. Comparison of the experimental pattern for **10** obtained from grinding to the pattern simulated from single crystal data. The experimental pattern obtained from sublimation of MA and PYR shows that **10**, **11a**, and **11b** is formed simultaneously.

Salt **10** crystallizes in the triclinic spacegroup, *P*1 (Table S6), with one pyridinium ion and one intramolecularly hydrogen-bonded hydrogen succinate in the asymmetric unit. The cation interacts with the anion via a charge-assisted hydrogen bond and these dimers stack via π-π interactions. The structure has been checked for higher symmetry, and the assigned space group is correct

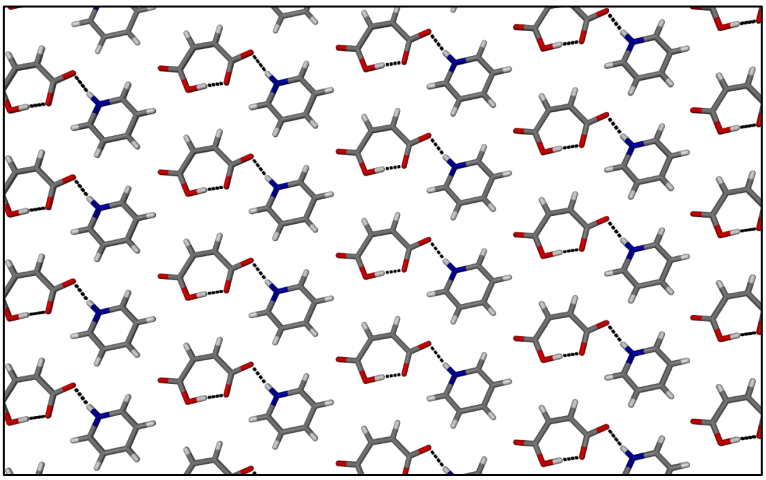

Figure S22. Packing diagram for salt **10** viewed along [100].

FA and PYR

The 1:1 co-crystal salt, **11b**, was made by grinding FA (0.043 g, 0.37 mmol) and PYR (60 µl, 0.74 mmol) together for 20 minutes in a ball mill. An unknown product was obtained by grinding FA (0.060 g, 0.52 mmol) and PYR (42 µl, 0.52 mmol) in a 1:1 molar ratio.

Single crystals of **11b** (as well as a powder of the unknown product) could also be formed by sublimation of FA and PYR. FA (0.12 g, 1.0 mmol) and PYR (83 µl, 1.0 mmol) were added to a large Schlenk tube and heated in a 170 °C oil bath for 15 hours under static vacuum.

Crystals of **11a** and **11b** could also be formed by dissolving FA (150 mg) in PYR (5 ml) at 50 °C. The vial was capped and placed in the refrigerator at 4 °C. Crystals formed within 24 hours.

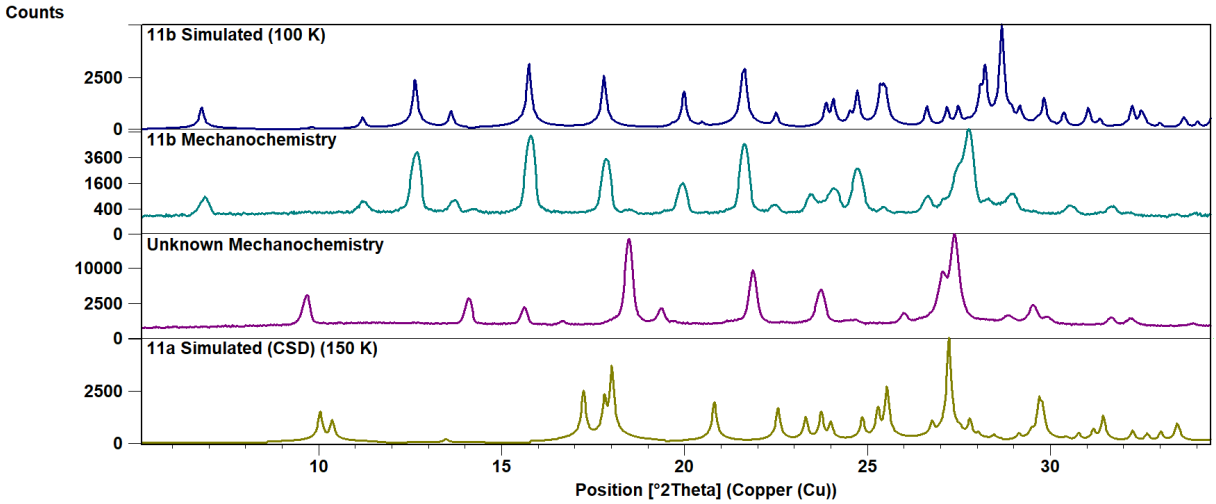

Figure S23. Comparison of the experimental pattern for **11b** obtained from grinding to the pattern simulated from single crystal data. An unknown pattern was also obtained mechanochemically, which does not match either **11a** or **11b**.

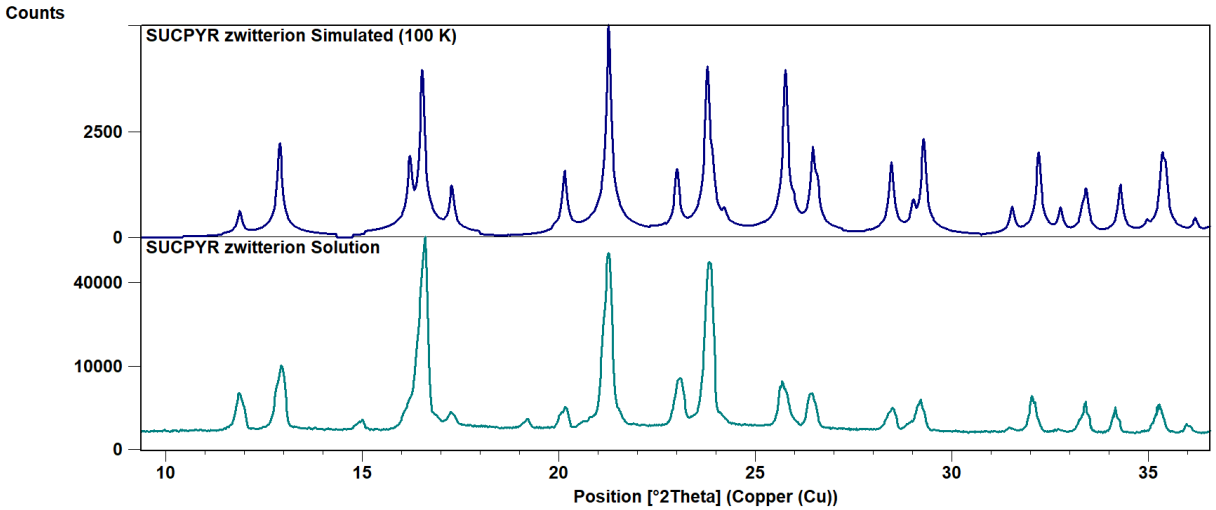

Figure S24. Comparison of the experimental pattern for the SUCPYR zwitterion obtained from solution crystallization to the pattern simulated from single crystal data.

The co-crystal salt **11b** crystallizes in the triclinic spacegroup, $P\bar{1}$ (Table S6), with one pyridinium ion, one half of a fumaric acid molecule and one half of a fumarate anion in the asymmetric unit. FA and FA^{2-} form hydrogen-bonded zig-zag chains, with each carboxylate functional group forming an

additional charge-assisted hydrogen bond with a pyridinium cation. These chains stack via π-π interactions.

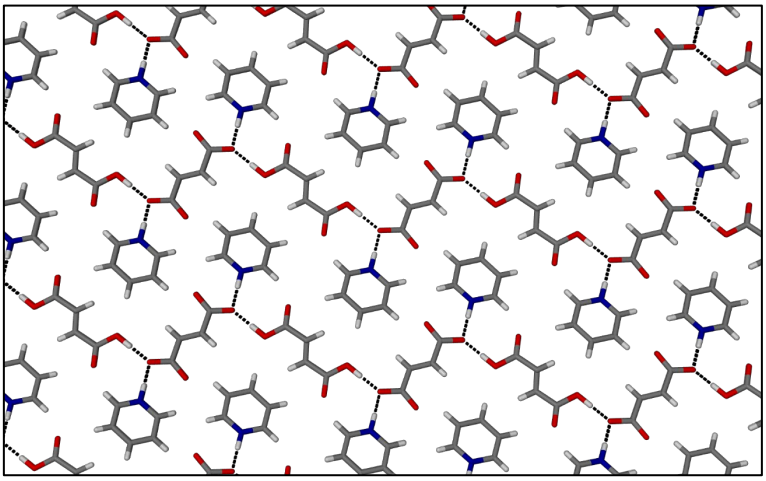

Figure S25. Packing diagram for **11b** viewed along [100].

Table S6. Crystallographic data for **10**, **11b** and **12b**.

Structure	**10**	**11b**	**12b**
Chemical formula	$C_9H_9NO_4$	$C_{18}H_{18}N_2O_8$	$C_{20}H_{22}N_2O_8$
Formula weight /g mol^{-1}	195.17	390.34	418.39
Crystal system	triclinic	triclinic	triclinic
Space group	*P*1	*P*$\bar{1}$	*P*$\bar{1}$
Temperature /K	100(2)	100(2)	100(2)
a /Å	3.8035(2)	3.7446(5)	3.8504(6)
b /Å	5.9008(3)	9.2066(1)	8.9317(1)
c /Å	10.2405(5)	13.1148(2)	14.638(2)
α /°	82.498(1)	96.994(3)	80.664(3)
β /°	81.078(1)	91.568(2)	82.913(3)
γ /°	84.150(1)	98.886(2)	80.197(3)
Calc. density /g cm^{-3}	1.445	1.464	1.426
Volume /Å^3	224.33(2)	442.89(6)	487.12(1)
Z	1	1	1
Independent reflections	2232	1562	1742
R_{int}	0.0141	0.0185	0.0236
R_1 [I > 2σ(I)]	0.0256	0.0285	0.0378

MA and 3PIC

Single crystals of the 1:1 co-crystal salt of maleic acid and 3-picoline (**12b**) were obtained by co-subliming MA (0.045 g, 0.39 mmol) and 3PIC (38 µl, 0.39 mmol) in a large Schlenk tube heated to 130 °C for 5 hours under static vacuum.

Grinding MA (0.045 g, 0.39 mmol) and 3PIC (38 µl, 0.39 mmol) together for 30 minutes in a ball mill (neat or with THF) lead to the formation of an unknown product. Dissolving MA (0.089 g, 0.77 mmol) and 3PIC (75 µl, 0.77 mmol) in 5 ml acetone or methanol (or 3PIC) at 60 °C lead to the formation of another unknown powder.

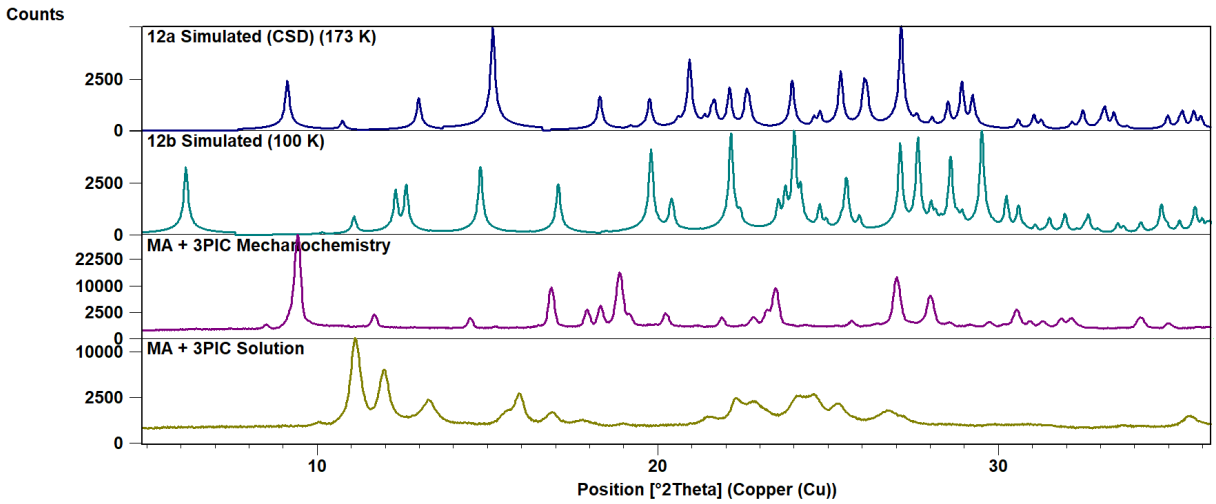

Figure S26. Simulated powder patterns for **12a** and **12b** compared to the unknown patterns obtained from mechanochemistry and solution crystallization.

The new co-crystal salt, **12b**, crystallizes in the triclinic spacegroup P$\bar{1}$ with one 3-methylpyridinium cation, one half fumaric acid molecule and one half of a fumarate anion. Similar to **11b**, FA and FA^{2-} form hydrogen-bonded chains, with each carboxylate functional group forming an additional charge-assisted hydrogen bond with the cation. These chains stack via π-π interactions.

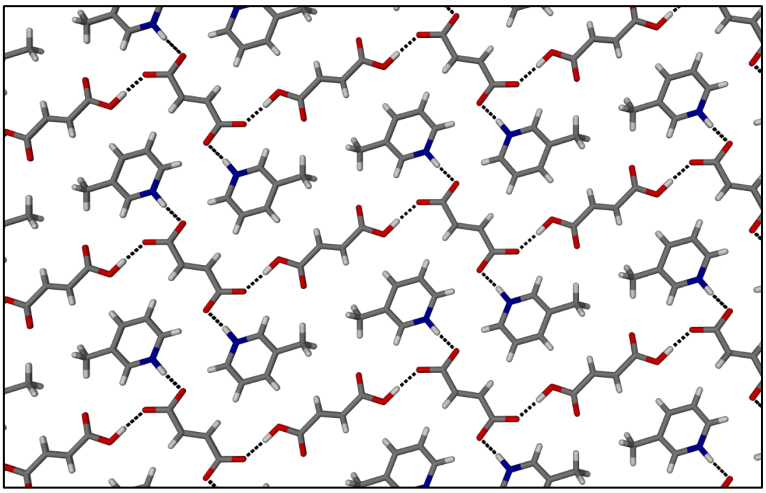

Figure S27. Packing diagram for **12b** viewed along [100].

Salts by co-sublimation

NA and OA

The 1:1 salt of nicotinic acid and oxalic acid (**13**) was made by adding NA (0.035 g, 0.28 mmol) and OA (0.036 g, 0.28 mmol) to a thin Schlenk tube and placing it under static vacuum. The mixture was heated at 120 °C for 7 hours after which all starting materials had converted to the salt.

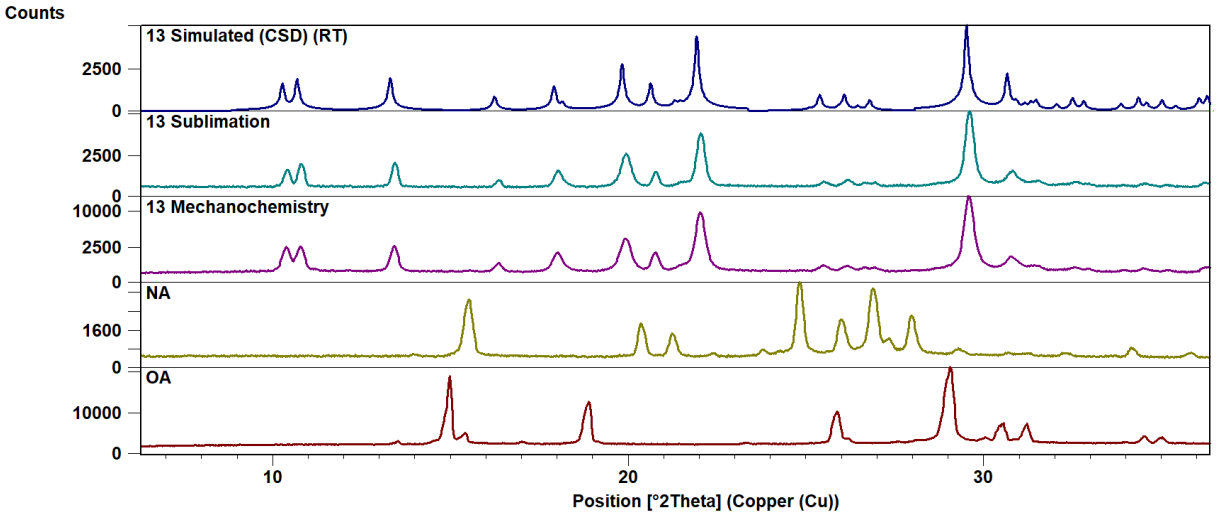

Figure S28. Comparison of the experimental powder patterns of **13** (obtained from co-sublimation and grinding) to the pattern simulated from single-crystal data obtained from the CSD (refcode HEWWAI)[8].

Co-crystallization using heat-sensitive molecules

PYG and HMT

The 1:1 co-crystal of pyrogallol and hexamethylenetetramine (**14**) was made by grinding PYG (0.047 g, 0.37 mmol), HMT (0.052 g, 0.37 mmol), and methanol (25 µl) together for 20 minutes in a ball mill (Figure S29).

Co-crystal **14** could also be formed by sublimation of a 1:1 molar ratio of the starting materials. PYG (0.070 g, 0.56 mmol) and HMT (0.078 g, 0.56 mmol) were added to a thin Schlenk tube and heated in a 110 °C or 120 °C oil bath for 6 h under static vacuum. HMT crystals formed higher up in the tube as well, in a separate band.

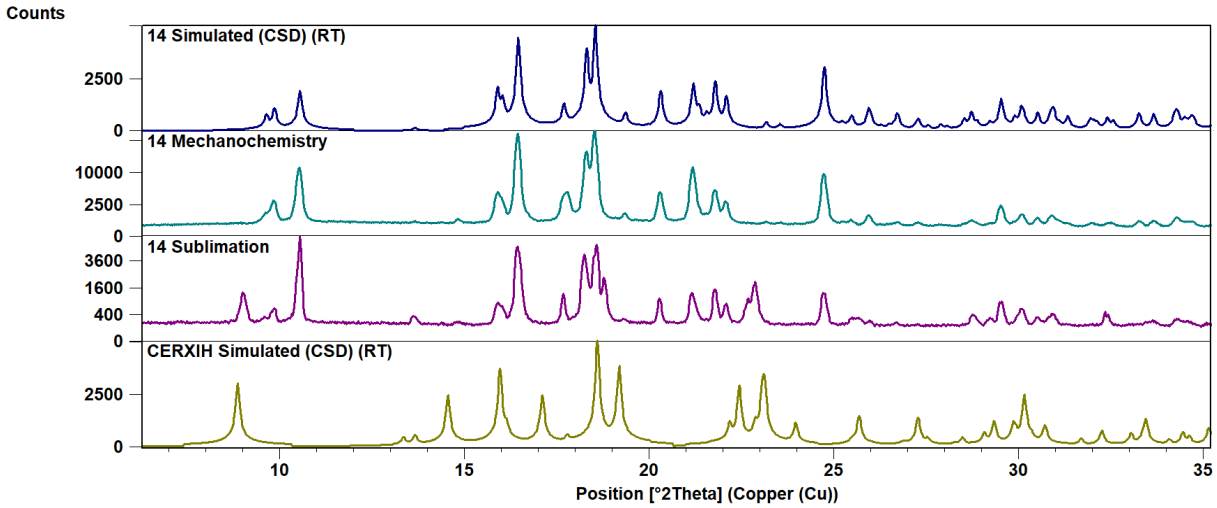

Figure S29. Comparison of the experimental powder patterns of **14** (obtained from LAG and co-sublimation) to the pattern simulated form single-crystal data obtained from the CSD (refcode BINDIL)[9]. The material obtained from co-sublimation also contains some of the dihydroxybenzene-HMT co-crystal (CSD refcode CERXIH).

GA and 4PP

The 1:1 salt of gallic acid and 4-phenylpyridine (**15**) was made by grinding GA (0.055 g, 0.32 mmol) and 4PP (0.045 g, 0.32 mmol) together for 20 minutes in a ball mill (25 µl of methanol, THF or water could also be added). When subliming these starting materials, GA decarboxylated to form pyrogallol, which co-crystallized with 4PP to give a new co-crystal (**16**). Specifically, GA (0.055 g, 0.32 mmol) and 4PP (0.045 g, 0.32 mmol) were added to a thin Schlenk tube and heated under vacuum at 190 °C for 2 hours.

Co-crystal **16** crystallizes in the monoclinic spacegroup $P2_1/n$ with two molecules PYG and two molecules 4PP in the ASU. The 4PP molecules are disordered over two positions in an approximately 60:40 ratio such that the nitrogen atom can be at either end of the molecule (Figure S30). The 4PP molecules hydrogen bond to pyrogallol forming curved chains which pack together via PYG-PYG hydrogen bonds and π-π interactions to give the 3D structure.

However, each disordered 4PP molecule naturally only forms a hydrogen bond at one end (via the nitrogen atom). At the other end there is a phenyl group which does not hydrogen bond to pyrogallol. This means that the hydroxyl hydrogen atom of pyrogallol (that is involved in hydrogen bonding to the other disordered part of 4PP) needs to occupy another position when the phenyl group is pointing towards it. The positions of these partially occupied hydrogen atoms could not be determined. Some additional constraints were also needed to model the disorder in the structure.

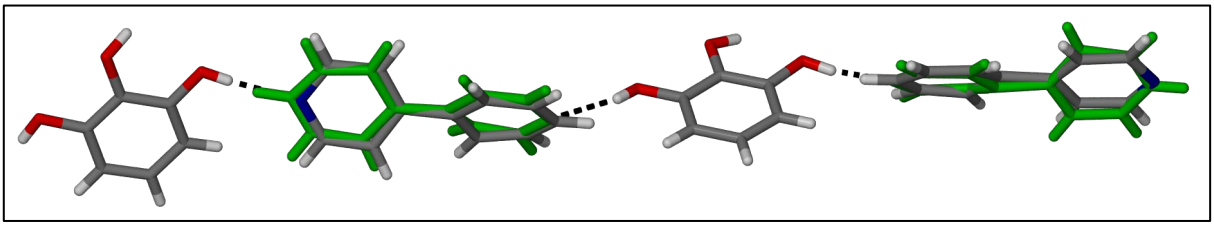

Figure S30. Asymmetric unit for the co-crystal between pyrogallol and 4-phenylpyridine (**16**). 4PP is disordered over two positions (50:50 occupancy) – one of the positions is indicated in green.

Table S7. Crystallographic data for co-crystal **16**.

Structure	**16**
Chemical formula	$C_{34}H_{30}N_2O_6$
Formula weight /g mol^{-1}	562.60
Crystal system	monoclinic
Space group	$P2_1/n$
Temperature /K	298(2)
a /Å	13.1236(6)
b /Å	15.0024(7)
c /Å	14.4778(7)
α /°	90
β /°	106.4680(1)
γ /°	90
Calc. density /g cm^{-3}	1.362
Volume /Å^3	2733.5(2)
Z	4
Independent reflections	5221
R_{int}	0.0490
R_1 [I > 2σ(I)]	0.0610

References

[1] Lu, E.; Rodríguez-Hornedo, N.; Suryanarayanan, R. *CrystEngComm* **2008**, *10* (6), 665–668.

[2] Trask, A. V.; Motherwell, W. D. S.; Jones, W. *Cryst. Growth Des.* **2005**, *5* (3), 1013–1021.

[3] Childs, S. L.; Stahly, G. P.; Park, A. *Mol. Pharm*. **2007**, *4* (3), 323–338.

[4] Trask, A.; Motherwell, W.; Jones, W. *Int. J. Pharm.* **2006**, *320* (1–2), 114–123.

[5] Fischer, F.; Lubjuhn, D.; Greiser, S.; Rademann, K.; Emmerling, F. *Cryst. Growth Des.* **2016**, *16* (10), 5843–5851.

[6] Haynes, D. A.; Jones, W.; Motherwell, W. D. S. *CrystEngComm* **2006**, *8* (11), 830–840.

[7] Lukin, S.; Stolar, T.; Tireli, M.; Blanco, M. V.; Babić, D.; Friščić, T.; Užarević, K.; Halasz, I. *Chem. Eur. J.* **2017**, *23* (56), 13941–13949.

[8] Athimoolam, S.; Natarajan, S. *Acta Crystallogr. Sect. E Struct. Reports Online* **2007**, *63* (2), o963–o965.

[9] Tremayne, M.; Glidewell, C. *Chem. Commun.* **2000**, No. 24, 2425–2426.

CHAPTER 5

Summary and concluding remarks

The aim of this thesis was to demonstrate how deliberate control of crystallisation methodology can lead to the selective formation of a particular multicomponent product. A crystalline material is usually obtained from a saturated solution after the relevant compounds have been dissolved in a chosen solvent. The focus generally lies on the material that is obtained; however, it would be a mistake to disregard the role played by the solvent during crystallisation, even when it is not included into the final product. Instead, a clear and unbiased view of chemical reactions and processes (of which crystallisation is one) may be obtained if the influence of the surrounding solvent medium is removed. For this reason, efforts were focussed on crystallisation processes that involve much less, or absolutely no solvent, namely mechanochemistry and sublimation. We believe that unexplored areas of the crystal form landscape may be reached if we broaden the scope of techniques commonly used in the laboratory. We were interested in using these techniques to study multicomponent materials in particular, as these often crystallise in more than one form, with different forms displaying different properties. Therefore, it is of interest to be able to selectively crystallise a particular multicomponent form. A number of multicomponent systems have been examined and discussed in three publications which have been presented as Chapters 2 – 4. A brief summary of each chapter outlining the most important findings will follow, as well as discussions regarding potential areas for further study.

The formation of molecular, organic salts and co-crystals was examined in **Chapter 2**. Two sets of molecules were used as model systems, namely succinic acid with hexamethylenetetramine and oxalic acid with 4,4'-bipyridine. These pairs are of interest as they are both able to form both salts (**1a** and **2a**) and co-crystals (**1b**, **1c**, **1d** and **2b**). The objective was to see what effect the crystallisation methodology had on the ionisation state of the product. Forming these materials from solution and mechanochemically was straightforward; however, we hypothesised that salt formation from the gas phase would not be possible without a solvent medium to promote proton transfer. We therefore anticipated the preferential formation of co-crystals (which does not require proton transfer) from crystallisations following sublimation. However, this hypothesis was disproven, and we were able to

report the first crystals of salts formed by co-subliming neutral molecular components. In fact, we have since shown (see Chapter 4) that many salts are similarly able to form by sublimation. Both salts and co-crystals are also able to re-sublime (i.e. re-crystallise by sublimation). These results seem to suggest that proton transfer to form these salts may be able to occur in the gas phase, where ions are consequently present. However, this intuitively seems unlikely and will need further experimental proof.

We postulate that ions may be able to exist in the gas phase if they are present as pairs or clusters of ions having an overall neutral charge. This could stabilise the ions and allow for proton transfer between molecules within the cluster. An attempt was made to prove this experimentally using mass spectrometry. Unfortunately, we were unable to directly analyse the gas phase after sublimation. Instead, a solution of salt **1a** was analysed, and showed that a hydrogen-bonded adduct of the acid and the base is stable enough to exist in the gas phase inside the spectrometer. Another possibility is that the gas phase contains only neutral molecules and that the proton transfer needed to form the salt only takes place after deposition from the gas phase, and similarly before re-sublimation. The latter case was tested experimentally using an environmental gas cell mounted on a single-crystal diffractometer to observe a salt crystal up until the point at which it sublimes. Proton migration was not observed and so it appears as if ions do indeed enter the gas phase. However, it may be possible that the changes in ionisation are only occurring right before sublimation (and therefore cannot be observed) or that changes are only occurring on the surface of the crystal. If this is true, and the gas phase only contains neutral molecules, it raises another question about why we observe both salts and co-crystals forming simultaneously from a homogenous gas. Is it possible that ionisation is not something that drives crystallisation, but rather a consequence of a material crystallising with a particular stoichiometry? In each of our examples the salt and co-crystal differ in terms of stoichiometry as well as ionisation. Could it be that as the one form crystallises it changes the concentration of molecules in the gas phase, which then preferentially forms the other crystal form (which may or may not be charged depending on crystal packing and the proximity of other molecules in the structure). It would be interesting to carry out a similar study with salts and co-crystals that have the same stoichiometry. Although we have no definitive answers to these questions at this stage, we hope that our work will promote further study and scientific discussion on the subject of gas-phase hydrogen bonding and proton transfer.

Other experiments that could be carried out include various analyses on the contents of the gas phase during sublimation. If it were possible to carry out IR- or NMR spectroscopy on a sublimed sample, it could be possible to discern between hydrogen-bonded adducts and individual molecules. The challenge here lies in keeping the sample under vacuum and thus vaporised throughout the

analysis. Another interesting variation on these experiments could be to change the pressure inside the sublimation vessel (potentially by using a stronger vacuum pump). Could it be that higher concentrations of molecules in the gas phase are more likely to form clusters (where proton transfer is possible) and can therefore more easily crystallise as a salt? Quantum mechanical calculations are also routinely carried out to model molecules and ions in the gas phase, and could be used to gauge the stability of various gas-phase clusters. Calculations could be carried out to determine the size of a cluster that would allow for the transfer of a proton from an acid to a base, as well as the energy barrier that would need to be crossed for this to happen. For each of the salts it could also be possible to compare the stability of pairs of interacting ions with their theoretical neutral counterparts to try and discern why they are charged instead of neutral within the crystals.

The second study examines the role that solvent plays during crystallisation by systematically removing it from a system. A competition study between hydrogen-bonded and halogen-bonded co-crystals formed from solution was previously published, in which it was discovered that polar solvents promoted halogen bonding, while apolar solvents encouraged the formation of hydrogen bonds.[1] The objective of the study described in **Chapter 3** was to determine whether this selectivity would hold when considerably less solvent is used, and what the consequences would be if all solvent were removed.

The competitive crystallisation of four analogous co-crystals was studied. Each co-crystal contained the molecule 1,2-bis(4-pyridyl)ethane (**3**), as pyridyl groups can accept halogen bonds and hydrogen bonds equally well. The second coformer was either a halogen-bond donor molecule (1,4-diiodotetrafluorobenzene, **1**) or a hydrogen-bond donor molecule (hydroquinone, **2a**; 2-fluorohydroquinone, **2b**; or 2,3,5,6-tetrafluorohydroquinone, **2c**). Three different hydrogen-bond donor molecules were used as they differ in strength, with **2a** being the weakest and **2c** the strongest. For each competition experiment acceptor **3** was combined with both **1** and either **2a**, **2b**, or **2c**. After crystallisation, the relative amounts of products were determined using powder X-ray diffraction. In the literature these competitive crystallisations were carried out in solution, but here the volume of solvent used was reduced in a stepwise manner, starting with slurry crystallisation. This was followed by liquid-assisted grinding and then neat grinding which (in terms of solvent) is only influenced by atmospheric moisture. Remarkably, the same trends in selectivity were observed when less solvent was used; however, the selectivity was greatly reduced. Interestingly, when less solvent was used, we also discovered some new ternary co-crystals which presumably contain both of these interactions. Lastly, the competition studies were carried out in a vacuum by co-sublimation. When no solvent was used, no selectivity was observed, and hydrogen bonds and halogen bonds formed equally well, proving that solvent does indeed play a central role in selectivity.

This study also leads us to reconsider what we know about hydrogen and halogen bonds. How much of what we know is influenced by the solvents that are used in the literature? Density functional theory was used to calculate the interaction energies between the hydrogen-bonded and halogen-bonded molecules in the gas phase to try and explain their formation by co-sublimation. Surprisingly, the interactions in the halogen-bonded co-crystal (**1·3**) were found to be weaker than all of the hydrogen-bonding interactions even though **1·3** crystallises from the gas phase as readily as the hydrogen-bonded co-crystals. Consequently, we question the ability of such simple calculations to accurately predict which product would crystallise preferentially, even from the gas phase. Could it be that hydrogen bonds and halogen bonds are fundamentally too different in terms of electronics, size, etc. to analyse them using the same method? Or do all of the weaker interactions that contribute to crystal packing play too big a role to be ignored? Of course, it is also possible that the calculations are correct, but how then can we explain the formation of both types of co-crystals in similar amounts? Perhaps co-sublimation is not as non-selective as it appears, while it is not affected by competing solvent interactions, both coformers are still not equally available to crystallise from the gas phase. Different coformers sublime at different temperatures and at different rates, which affects their existence in the gas phase; the concentrations of each coformer in the gas phase is not known. It appears as if removing solvent does not necessarily mean removing all bias.

However, the fact remains that the type and volume of solvent used can significantly affect co-crystallisation reactions and cannot be ignored. Thoughtful choices about the solvent used during crystallisation, using whichever technique, can be used to obtain selectivity, and consequently a desired product. In the future it would be interesting to observe the effect of using more sterically bulky solvents or solvents containing other functional groups, as they may influence other types of intermolecular interactions. The formation of co-crystals containing both halogen- and hydrogen bonds could also be manipulated in interesting ways by changing the solvent, particularly in terms of polymorphism. Lastly, we would be interested to know if the selectivity observed in this study may be regained during co-sublimation if polar additives, salts, or solvent drops were added to the vessel, or even polar gases such as SO_2.

In Chapters 2 and 3, some interesting observations about solid-state and gas-phase techniques were made, but how robust are these techniques really? Should they be routinely used or are they ineffectual? Mechanochemistry is known to be a reliable multicomponent crystallisation technique, but sublimation is rarely used for the formation of such materials. In the third study (**Chapter 4**) several systems containing a variety of small organic molecules were examined. The crystallisation of simple systems was studied, but also more complex and polymorphic systems. We looked at cases where coformers have similar sublimation temperatures, and where they are very different; where

molecules are stable, and where they degrade or isomerise on heating. While co-sublimation does not always work, we have shown how most problems can be overcome by controlling the sublimation temperature or starting material composition to ensure that both coformers are present in the gas phase simultaneously. Sublimation even led to the discovery of some new crystal forms, one of which has not been formed using other methods. Sublimation has also been observed to occur at a different rate than solution crystallisation, which can have interesting consequences when using coformers that can isomerise over time, and generally means that sublimation can be a quick way to obtain crystals. While not as routine a technique as mechanochemistry or solution crystallisation, co-sublimation definitely deserves a place in the crystallographer's toolbox as part of a multi-technique approach to selectively obtaining desired products.

A very simple sublimation setup was used in all of these studies, which has generally been adequate; however, in certain instances products crystallised as mixtures which could not be separated. More precise control over the outcome of co-sublimation as well as improved yields may be obtained by designing sublimation apparatus more meticulously. Future work should include designing an apparatus with different temperature zones or specific temperature gradients for vaporisation, but also for deposition. This could be done by using a multi-zone heating furnace or flexible heating tapes which could be wrapped around sublimation tubes. In that way it should be possible to separate different products more efficiently. It would also be interesting to see what the effect is of attempting sublimation under a flow of nitrogen gas instead of under vacuum (this has previously been reported for purification purposes).

In general, these studies have exposed us to a new area of research with a host of unanswered questions. For example, it would be interesting to explore the effect of additives during sublimation. Can crystals of a particular difficult-to-obtain multicomponent product or polymorph be obtained by adding seeds or additives during sublimation? Are there materials that can only form by co-sublimation, and not by other methods? It is not yet clear whether the same polymorph is always obtained from sublimation as is formed by mechanochemistry. Is it possible that sublimation is more inclined to produce the more thermodynamically stable product? What is the relevance of kinetics in sublimation crystallisation? In other words, what would happen if the timescale of sublimation is changed, or the temperature gradient in the sublimation vessel? The temperature of the cold finger could easily be changed. Would we be able to isolate different products by changing these parameters? We have shown that a multicomponent crystal of a particular molecule sublimes at a different temperature compared to the molecule on its own. Could this be used as a way to modify sublimation temperatures to ensure the desired molecules are entering the gas phase at the desired temperatures? We have also observed that starting materials sometimes crystallise as their hydrated

form after sublimation, can we similarly form hydrated multicomponent crystals by co-sublimation? It should be possible for water molecules to be included during sublimation if they form hydrogen bonds to other molecules within the crystal. Similarly, the formation of solvates and ternary co-crystals can also be attempted, as well as products involving organic reactions, such as [2+2] cycloaddition (none of which has been attempted before). Clearly, there is an abundance of research possibilities surrounding sublimation.

In its entirety, this study highlights the interesting discoveries that can be made when one explores different crystallisation techniques. Controlling the crystallisation technique used can allow us to selectively form a desired multicomponent product, but we believe that this may be true for other areas of chemistry as well. Solid-state and gas-phase techniques are not competitors for standard solution-based methods, instead they complement each other. As we know, a story is best told from multiple perspectives.

5.1 References

[1] Robertson, C. C.; Wright, J. S.; Carrington, E. J.; Perutz, R. N.; Hunter, C. A.; Brammer, L. *Chem. Sci.* **2017**, *8* (8), 5392–5398.

APPENDIX

The following supplementary data files are attached:

Chapter 2

- CIF and CheckCIF reports
  - Salt **1a** (298 K and 100 K)
  - Co-crystal **1b** (298 K and 100 K)
  - Co-crystal **1c** (298 K and 100 K)
  - Salt **2a** (298 K and 100 K)
  - Co-crystal **2b** (298 K and 100 K)

Chapter 3

- CIF and CheckCIF reports
  - Co-crystal **1·2a**

Chapter 4

- CIF and CheckCIF reports
  - Co-crystal **6a**
  - Co-crystal salt **6b**
  - Co-crystal salt **6c**
  - Salt **8**
  - Salt **9a**
  - Salt **9b**
  - Salt **10**
  - Co-crystal salt **11b**
  - Co-crystal salt **12b**
  - Salt **16**